筋収縮系におけるメカノケミカルカップリングの画像化と顕微解析

(研究課題番号　04402053)

平成４年度～平成６年度科学研究費補助金（一般研究Ａ）

研究成果報告書

平成１０年８月

研究代表者　石　渡　信　一

(早稲田大学理工学部物理学科教授)

はしがき

この報告書は、平成４年度から平成６年度にわたる３年間で行われた文部省科学研究費一般研究Ａ「筋収縮系におけるメカノケミカルカップリングの画像化と顕微解析」（課題番号０４４０２０５３）の研究成果をまとめたものである。

初年度に４０００万円近い高額の補助を得たことによって、位相差・蛍光同時画像化用倒立顕微鏡、レーザー光ピンセット装置（赤外 YLF レーザー（1W)、赤外光を導入するために特注した光ファイバー導入装置を含む)、Double(W)-view 光学系、画像処理コンピューター、超高感度テレビカメラ、２波長励起装置などの、特注装置を含むユニークなタンパク質分子操作・顕微解析用の装置を組み上げることが出来た。これと併せて、単一の筋原線維を操作し、発生張力を計測すると同時に内部構造を観察・記録することのできる顕微装置を組み上げた。前者の装置はその後、高速度カメラ・画像解析装置などを装備することによって性能を向上させ、次に続く研究に活用することが出来た。1998 年 8 月現在でも、この装置は直径 1μm のプラスチックビーズを 70pN の力で捕捉し、サブ nm の空間分解能と、2ms の時間分解能を持った顕微解析装置として、単一分子モーター（ミオシン、キネシンなど）の機能解析や、タンパク質間相互作用の１分子解析の研究に活躍している。後者の装置も蛍光装置を装備し、本研究の目的の一つである単一筋原線維の構造・機能連関の顕微解析に用いられている。

本研究の主な目的は、研究課題にあるように、“メカノケミカルカップリング（力学過程と化学過程との関係)”を顕微画像化することであった。そのために我々は、ATP 加水分解に伴って放出される H^+により pH が減少することに着目し、pH 感受性蛍光色素を通じて ATP 加水分解過程を画像化することを目指した。特に、アクチンフィラメントに選択的に結合する茸毒のファロイジン(Phalloidin)に pH 感受性蛍光色素を結合した色素を合成し、アクチンフィラメント近傍における局所的な pH 変化を時空間画像化することを試みた。我々はまず、当時慶大・理工学部・木下研に滞在した G.Marriott 氏〔現、Max Planck Inst.〕の協力を得て、SNAFL-Phalloidin(Ph)を合成した。この色素を筋原線維中のアクチンフィラメントに結合した上で溶液の pH を制御したところ、pH 変化に伴う蛍光スペクトルの変化を画像化することができた。しかしこの色素は、励起スペクトルが pH によって変化するという特性を持っているために、２波長励起をする必要があった。こうして、購入した２波長励起装置を用いて 0.2s 程度の時間遅れで pH 画像を録画することができたが、厳密な意味での pH の同時画像は取れなかった。その結果、時間分解能は高々１ｓ程度であり、当初の目的には不十分であった。すなわち、SNAFL-Ph でラベルした筋原線維の、ATP 分解特性に伴う pH の減少を画像化することを試みたが、時間分解能が不十分であるために、

はっきりした結論を得ることが出来なかった。

W-view 装置を活用して時間分解能を上げるためには、蛍光スペクトルが pH 感受性をもつ蛍光色素をどうしても手に入れる必要があった。そこでこの特性を持つ蛍光色素 SNARF を SNAFL と同じ手法で Ph に共有結合することを我々の手で試みた。しかし、SNAFL の場合と比べて合成のためのステップ数が多く、この試みは残念ながら不成功に終わった。こうして最終的には、この合成を Molecular Probe 社に依頼、特注することとなった。こうして手にした SNARF-Ph を筋原線維にラベルし、溶液の pH 変化に応じた画像化を、W-view 装置を用いて行うことができた。これを活用して、収縮、弛緩のみならず、SPOC（ATP だけでなく、ADP と無機リン酸（Pi）共存、Ca イオン非存在下で発生する自励振動現象）に応用し、各筋節ごとの化学・力学変化の画像化を行った。その結果、収縮時に pH の低下を示す画像が得られることもあったが、その再現性に問題があった。従って本研究は、pH 画像化の精度を上げる一方で、研究目的に適した実験系の開発を行うべく、現在も研究を継続している。

ここで開発した顕微解析装置は、以下のような in vitro 滑り運動系の研究に応用することが出来た。1）低濃度の ATP 存在下でアクチンフィラメントに発生するミオシン分子モーターによる滑り力と、1個の ATP 分子の加水分解に伴うミオシン分子のステップサイズとを、光ピンセットを活用して計測した。その結果、滑り力は最大捕捉力の下で約 3pN であり、ステップサイズは約 10nm であった。一方、2）ATP 非存在（硬直条件）下で、アクチンフィラメントと1個のミオシン（HMM）分子との間に形成された硬直結合の破断力を計測し、平均 9.2pN という値を得た。これはアクチン・ミオシン分子間結合の1分子結合力として初めて得られた値である。また、同時に得られた張力－歪み曲線の最大傾斜から求めた HMM 分子の弾性率は、約 0.5pN/nm であり、筋線維系で見積もられていた値とほぼ一致した。このような分子モーターの力学特性に関する1分子計測については、その後も研究を続けている。

本報告書については、研究の終了年度末である平成７年３月に取りまとめるべきであった。ところが、本研究を通じて開発した顕微装置を用いて、いくつかの副産物的研究成果は得られたが、当初計画した研究目的については未だ６０%程度しか達成されていないと判断し、報告書の作成を先延ばしにして今日に至った。その間、メカノケミカルカップリングの画像化については、蛍光性 ATP 分子や無機リン酸結合性のタンパク質分子などを用いた研究がいくつかのグループによって行われた。我々が採用した、pH 感受性色素によるタンパク質近傍の局所的 pH 変化の画像化、という方向での研究は一歩遅れを取っているというのが正直な評価であろう。しかし、ゆっくりとした歩みではあるが、今後もこの方向での研究を進めていく所存である。本研究でその芽を作った研究課題を、今後とも地道に発展させて行きたい。添付論文は、Abstract を除いて、平成４年４月から平成７年３月の、研究期間内に刊行されたものに限った。

なお本研究の主要なテーマは、当研究室の大学院生であった西坂崇之（D3,PDF：現、CREST)、加藤宏一（M2：現、日立基礎研)、染谷一行（M2 修了)、川瀬誠（M2 修了)、藤田英明（現、D3)、藤木保武（M2：現、王子製紙)、進泉（M2：現、ホロン)、多田隈尚史（現、D2）と、卒業生の安田賢二（M2：現、日立基礎研）の諸君を中心に行われた。骨格筋の筋（原）線維中でのアクチンフィラメントの再構成に関する研究は、卒業生の船津高志氏（現、早稲田大学・理工学部)、穴沢隆氏（M2：現、日立中研）らを中心に行われた。また、アクチンフィラメントの超らせん形成は、田中裕一郎氏（本田技研）らとの協同研究の成果である。そして、慶應義塾大学・理工学部・物理学科の木下一彦研究室とは常日頃からの研究交流を通じて、様々な面でお世話になった。記して感謝します。

平成１０年８月　　研究代表者　　石渡　信一

研　究　組　織

研究代表者

石渡　信一　（早稲田大学・理工学部・物理学科・教授）

研　究　経　費

平成４年度	３８，３００千円
平成５年度	２，６００千円
平成６年度	３，１００千円
計	４４，０００千円

研　究　業　績

研究成果の概要については、「はしがき」で述べたのでここでは改めてまとめない。

研究業績については、以下に添付した発表論文と、いくつかのアブストラクトによってそれに代える。

研　究　発　表

1．学会誌等

1)Shimizu,H., Fujita,T. and Ishiwata,S. (1992) : *Biophys.J.* 61, 1087-1098.
"Regulation of tension development by MgADP and Pi without Ca^{2+}. Role in spontaneous tension oscillation of skeletal muscle."

2)Anazawa,T., Yasuda,K. and Ishiwata,S. (1992) : *Biophys.J.* 61, 1099-1108.
"Spontaneous oscillation of tension and sarcomere length in skeletal myofibrils. Microscopic measurement and analysis."

3)Tanaka,Y.,Ishijima,A. and Ishiwata,S. (1992) : *Biochim.Biophys.Acta* 1159, 94-98.
"Super helix formation of actin filaments in an in vitro motile system."

4)西坂崇之、池田光洋、中村真、石渡信一 (1992) :
日本物理学会誌 47, No.12, 991-992.
" 筋タンパク質繊維を用いたブラウン運動の観察. "

5)Fujime,S., Miyamoto,S., Funatsu,T. and Ishiwata,S. (1992) : *SPIE* 1922, 337-346.
"A dynamic light scattering study on changes in mobility of chromaffin granules in actin network with its assembly and Ca^{2+}-dependent disassembly by gelsolin."

6)Nishizaka,T., Yagi,T., Tanaka,Y. and Ishiwata,S. (1993) : *Nature* 361, 269-271.
"Right-handed rotation of an actin filament in an in vitro motile system."

7)Funatsu,T., Kono,E., Higuchi,H., Kimura,S., Ishiwata,S., Yoshioka,T., Maruyama,K. and Tsukita,S. (1993) : *J.Cell Biol.* 120, 711-724.
"Elastic filaments in situ in cardiac muscle: Deep-etch replica analysis in combination with selective removal of actin and myosin filaments."

8)Miyamoto,S., Funatsu,T., Ishiwata,S. and Fujime,S. (1993) :
Biophys.J. 64, 1139-1149.

and Ca^{2+}-dependent disassembly by gelsolin."

9)Ishiwata,S. and Yasuda,K. (1993) : *Phase Transitions* 45, 105-136.
"Mechano- chemical coupling in spontaneous oscillatory contraction of muscle."

10)Miyata,H., Hakozaki,H., Yoshikawa,H., Suzuki,N., Kinosita,Jr.,K., Nishizaka,T. and Ishiwata,S. (1994) : *J.Biochem.* 115, 644-647.
"Stepwise motion of an actin filament over a small number of heavy meromyosin molecules is revealed in an in vitro motility assay."

11)Funatsu,T., Anazawa,T. and Ishiwata,S. (1994) :
J. Muscle Res. Cell Motil. 15, 158-171.
"Structural and functional reconstitution of thin filaments in skeletal muscle."

12)Yasuda,K., Fujita,H., Fujiki,Y. and Ishiwata,S. (1994) :
Proc.Jap.Acad. 70, Ser.B.151-156.
"Length regulation of thin filaments without nebulin."

13)Yasuda,K., Anazawa,T. and Ishiwata,S. (1995) : *Biophys.J.* 68, 598-608.
"Microscopic analysis of the elastic properties of nebulin in skeletal myofibrils."

2．口頭発表

1)Ishiwata,S. : Mechano-chemical coupling in muscle as suggested by spontaneous oscillatory contraction.
Alpbach workshop, Austria（1992年4月）

2)石渡信一：筋フィラメントの格子構造と筋収縮機構.
第8回高分子ゲル研究会，東京（1992年6月）

3)Moriyama,Y., Yasuda,K., Ishiwata,S. & Asai,H. :
Ca^{2+}-induced tension development of the stalks of glycerol-treated Volticella sp.
3rd Asian Conference on Ciliate Genetics Cell Biology and Molecular Biology, Shenzhen (China)（1992年7月）

4)Suzuki,N., Hakozaki,H., Nishizaka,T., Miyata,H., Ishiwata,S. & Kinosita,Jr.,K. :
Nanometer／piconewton analysis of the sliding of bead-tailed actin filaments on a myosin-coated surface.
第5回国際細胞生物物理学会，Madrid（1992年7月）

5)Nishizaka,T., Yagi,T., Ishijima,A., Tanaka,Y., Ishiwata,S. :
An evidence for rotation of an actin filament sliding in an in vitro motile system.
第4回生物物理学及びシンクロトロン放射光国際会議，筑波（1992年8月）

6)Yasuda,K.. Ishiwata,S. : Elastic properties of nebulin as a scaffold protein of actin filament in skeletal muscle.
第4回生物物理学及びシンクロトロン放射光国際会議，筑波（1992年8月）

7)Suzuki,N., Hakozaki,H., Nishizaka,T., Miyata,H., Ishiwata,S. & Kinosita,Jr.,K. :
Piconewton force analysis in in an vitro motility assay using bead-tailed F-actin and optical tweezers.
第4回生物物理学及びシンクロトロン放射光国際会議，筑波（1992年8月）

8)Fujime,S., Miyamoto,S., Funatsu,T. & Ishiwata,S. :
A dynamic light scattering study on changes in motility of chromaffin granules in actin network with its assembly and Ca^{2+}-dependent disassembly by gelsolin.

第4回 Laser Application in Life Sciences 国際会議（1992年9月）

9)染谷一行、G. Marriott、木下一彦、石渡信一：
pH感受性色素を用いたアクトミオシンATPase活性の研究.
日本生物物理学会第30回年会，豊中（1992年11月）

10)石渡信一、川瀬誠、福田賢司、安田賢二：
筋収縮系の自励振動（SPOC）とメカノケミカルカップリング.
日本生物物理学会第30回年会，豊中（1992年11月）

11)西坂崇之、鈴木直哉、箱崎博之、宮田英威、石渡信一、木下一彦：
低濃度HMMでのin vitro滑り運動系における光ピンセット法を用いたアクチンフィラメントの滑り力の計測Ⅰ.
日本生物物理学会第30回年会，豊中（1992年11月）

12)箱崎博之、鈴木直哉、宮田英威、西坂崇之、石渡信一、木下一彦：
低濃度HMMでのin vitro滑り運動系における光ピンセット法を用いたアクチンフィラメントの滑り力の計測Ⅱ.
日本生物物理学会第30回年会，豊中（1992年11月）

13)宮本茂昭、船津高志、石渡信一、藤目智：
アクチンネットワークの形成および解消に伴う分泌小胞の移動度の変化.
日本生物物理学会第30回年会，豊中（1992年11月）

14)安田賢二、石渡信一：ネブリンの力学的特性と機能.
日本生物物理学会第30回年会，豊中（1992年11月）

15)忠重純子、西坂崇之、石渡信一：
一本のアクチンフィラメント上での重合・脱重合ダイナミクスの直視.
日本生物物理学会第30回年会，豊中（1992年11月）

16)NishizakaT., Suzuki,N., Hakozaki,H., Miyata,H., IshiwataS. & Kinosita,Jr.,K. :
Measurement of sliding force generated on an actin filament under various concentrations of HMM in an in vitro motile system.
細胞運動研究会，東京／J. Muscle Res.Cell Motil.vol.14（1992年12月）

17)Hakozaki,H., Miyata,H., Nishizaka,T., Suzuki,N., IshiwataS. & Kinosita,Jr.,K. :
Sliding force between a small number of HMM molecules and a single actin filament under optical tweezers
細胞運動研究会，東京／J. Muscle Res.Cell Motil.vol.14（1992年12月）

18)箱崎博之、鈴木直哉、 宮田英威、西坂崇之、石渡信一、木下一彦：
数分子のHMMとF-アクチンによって発生する力の、光ピンセットを用いた測定.
生体運動合同班会議、名古屋（1993年1月）

19)西坂崇之、鈴木直哉、 箱崎博之、宮田英威、石渡信一：
光ピンセット法により測定した単一アクチンフィラメントの滑り力とその揺らぎ.
生体運動合同班会議、名古屋（1993年1月）

20)忠重純子、西坂崇之、石渡信一：
一本のアクチンフィラメント上での重合ダイナミクスの直視.
生体運動合同班会議、名古屋（1993年1月）

21)石渡信一，安田賢二：高次筋収縮系の化学・力学特性.
第3回バイオメカニクスカンファランス，東京（1993年1月）

22) Ishiwata,S., Anazawa,T.,& Yasuda, K. :
Mechano-chemical coupling in spontaneous oscillation
第11回国際生物物理学会，Budapest（1993年7月）

23)Nishizaka,T., Suzuki,N., Hakozaki,H., Miyata,H., Ishiwata,S., & Kinosita,Jr.,K. :
Properties of sliding force generated on an actin filament by a few HMM molecules
第11回国際生物物理学会，Budapest（1993年7月）

24)Miyata,H., Hakozaki,H., Suzuki,N., Kinosita,Hr.K.,Nishizaka,T.& Ishiwata,S. :
Piconewton, nanometer measurement of motile force of actin in an in vitro motility Assay.
第11回国際生物物理学会，Budapest（1993年7月）

25)川瀬誠、西坂崇之、石渡信一：等尺性条件下における筋原線維の収縮特性の顕微解析.
日本生物物理学会第31回年会，名古屋（1993年9月）

26)石渡信一：アクチン／ゲルゾリン溶液にみられる非等方的負性比粘度.
日本生物物理学会第 31 回年会，名古屋（1993 年 9 月）

27)西坂崇之、宮田英威、石渡信一、木下一彦：
光ピンセット法を用いたミオシン 1 分子とアクチンフィラメント間に働く力の測定.
日本生物物理学会第 31 回年会，名古屋（1993 年 9 月）

28)吉川博、宮田英威、箱崎博之、西坂崇之、石渡信一、木下一彦：低濃度 ATP in vitro 滑り運動系での光ピンセットを用いた HMM 1 分子による滑り力の測定（Ⅰ）.
日本生物物理学会第 31 回年会，名古屋（1993 年 9 月）

29)宮田英威、箱崎博之、西坂崇之、石渡信一、木下一彦：低濃度 ATP in vitro 滑り運動系での光ピンセットを用いた HMM 1 分子による滑り力の測定（Ⅱ）.
日本生物物理学会第 31 回年会，名古屋（1993 年 9 月）

30)木下一彦、宮田英威、石渡信一、西坂崇之、箱崎博之、吉川博、鈴木直哉、池上明：
アクトミオシン・モーターの動作原理の光ピンセットによる解析.
日本生物物理学会第 31 回年会，名古屋（1993 年 9 月）

31)福田賢司、新保剛司、伊賀隆志、石渡信一：
骨格筋・心筋繊維の SPOC 状態の研究—制御タンパク質の除去と再構成の影響.
日本生物物理学会第 31 回年会，名古屋（1993 年 9 月）

32)Kinosita,Jr.,K., Miyata,H., Hakozaki,H., Suzuki,N., Nishizaka,T. and Ishiwata,S. :
Nanometer／piconewton analysis of the actomyosin sliding.
第 19 回谷口シンポジウム（生物物理）（1993 年 12 月）

33)Fukuda,K., Shinpo,K., Iga,T. & Ishiwata,S. :
Effects of removal and reconstitution of myosin light chain 2 and troponin C on ADP-induced tension of single glycerinated skeletal muscle fibers.
細胞運動研究会，東京／J. Muscle Res.Cell Motil.vol.15（1993 年 12 月）

34)Miyata,H., Hakozaki,H., Nishizaka,T., Ishiwata,S. & Kinosita,Jr.,K. :
Stepwise motions of actin filaments sliding over glass-bound heavy meromyosin.
細胞運動研究会，東京／J. Muscle Res.Cell Motil.vol.15（1993 年 12 月）

35)吉川博、箱崎博之、西坂崇之、 宮田英威、石渡信一、木下一彦：
光ピンセット法による少数個のアクトミオシン分子モーターのステップ状変位の測定.
生体運動合同班会議，東京（1994年1月）

36)西坂崇之、吉川博、 宮田英威、石渡信一、木下一彦：
アクチンーミオシン間に働く滑り力・結合力の顕微測定.
生体運動合同班会議，東京（1994年1月）

37)加藤宏一、川瀬誠、西坂崇之、石渡信一：
pH感受性蛍光色素を用いた筋原線維内メカノケミカルカップリングの画像化.
生体運動合同班会議，東京（1994年1月）

38)石渡信一：分子エンジン集合体の運動特性.
第46回日本動物学会関東支部大会，東京（1994年3月）

39)石渡信一：収縮装置を組み立てる.
科学技術放談会，筑波（1994年3月）

40)Nishizaka,T., Miyata,H., Yoshikawa,H., Ishiwata,S. & Kinosita,Jr.,K. :
Microscopic measurement of the binding and sliding force between muscle protein. with optical tweezers
OWLSⅢ，東京（1994年4月）

41)Kinosita,Jr.,K., Miyata,H., Hakozaki,H., Nishizaka,T. & Ishiwata,S., :
Nanometer／piconewton analysis of the mechanism of the actomyosin motor.
OWLSⅢ，東京（1994年4月）

42)Nishizaka,T., Yoshikawa,H., Miyata,H., Kinosita,Jr.,K. & Ishiwata,S. : Microscopic study of mechanical properties of a single crossbridge with optical tweezers.
39th Yamada Conference，東京（1994年4月）

43)石渡信一：生体運動システムにみる物理法則.
第5回計測連合シンポジウム，東京（1994年4月）

44)Nishizaka,T., Yoshikawa,M., Miyata,H., Kinosita,Jr.,K. & Ishiwata,S. :
Binding and sliding force in single motor protein of muscle : Microscopic

measurement with optical tweezers.
1st East Asian Conference of Biophysics, 姫路（1994年5月）

45)Yoshikawa,H., Haokozaki,H., Yasuda,R., Suzuki,N., Nishizaka,T., Kinosita,Jr.,K., Miyata,H. & Ishiwata,S. : Stepwise motion of the acto-myosin motor as revealed by the use of optical trap in an in vitro motility assay.
1st East Asian Conference of Biophysics, 姫路（1994年5月）

46)石渡信一：筋タンパク質モーターの構造と機能を探る新しい光学顕微鏡システム.
第3回浜松医大メディカルホトニクスワークショップ, 浜松（1994年8月）

47)本多元、加来千織、羽鳥晋由、石渡信一、松野孝一郎：
F-アクチンによる二次元縞模様の形成.
日本生物物理学会第32回年会, 横浜（1994年9月）

48)加藤宏一、川瀬誠、西坂崇之、石渡信一：
pH感受性蛍光色素による筋原線維内メカノケミカルカップリングの画像化.
日本生物物理学会第32回年会, 横浜（1994年9月）

49)西坂崇之、吉川博、宮田英威、石渡信一、木下一彦：
クロスブリッジの破断力と硬さの顕微計測.
日本生物物理学会第32回年会, 横浜（1994年9月）

50)安田賢二、高倉達、石渡信一：筋原線維における静的・動的力学特性の顕微解析.
日本生物物理学会第32回年会, 横浜（1994年9月）

51)石渡信一、加藤宏一、西坂崇之、木下一彦：
筋収縮系におけるメカノケミカル過程の顕微画像化.
日本生物物理学会第32回年会, 横浜（1994年9月）

52)藤田英明、新津茂彦、安田賢二、石渡信一：
心筋筋線維における細いフィラメントの構造と機能の再構築.
日本生物物理学会第32回年会, 横浜（1994年9月）

53)吉川博、宮田英威、安田涼平、箱崎博之、西坂崇之、石渡信一、木下一彦：
低濃度in vitro滑り運動系での光ピンセットを用いたアクトミオシン・モーターの

ステップ状変位の測定.
日本生物物理学会第 32 回年会，横浜（1994 年 9 月）

54)藤崎久雄、近藤洋行、永田浩、高橋進一、大関尚夫、杉崎克己、加藤宏一、石渡信一：
軟 X 線照射による生体試料の損傷.
日本生物物理学会第 32 回年会，横浜（1994 年 9 月）

55)木下一彦、宮田英威、吉川博、安田涼平、西坂崇之、石渡信一：
分子モーターの動作機構のナノメーター・ピコニュートン画像解析.
日本生物物理学会第 32 回年会，横浜（1994 年 9 月）

56)吉川博、安田涼平、西坂崇之、宮田英威、石渡信一、木下一彦：
アクトミオシン分子モーターの画像解析による力ー変位測定.
第 3 回日本バイオイメージング学会，東京（1994 年 10 月）

57)Ishiwata,S. : Structural and functional reconstitution of thin filaments in skeletal and cardiacmuscle.
BBRI, Seminar, Boston（1994 年 10 月）

58)Miyata,H., Yoshikawa,H., Kinosita,Jr.,K.,Nishizaka,T. & Ishiwata,S. :
Mechanical measurement of single actomyosin motor force.
第 7 回米国生物物理学会討論集会，Airlie（1994 年 10 月）

59)Nishizaka,T., Yoshikawa,H., Kinosita,Jr.,K., Nishizaka,T. & Ishiwata,S. :
Microscopic measurement of binding force in single motor protein of muscle.
第 7 回米国生物物理学会討論集会，Airlie（1994 年 10 月）

60)Kato,H., Kawase,M., Nishizaka,T., Someya,K., Marriott, G., Kinosita,Jr.,K. & Ishiwata,S. : Imaging of mechanochemical coupling of muscle contractile system. by pH-sensitive fluorescent dyes
細胞運動研究会，東京／J. Muscle Res.Cell Motil.vol.16（1994 年 12 月）

61)Miyata,H., Yoshikawa,H., Yasuda,R., Nishizaka,T., Ishiwata,S. & Kinosita,Jr.,K. : Stepwise force-displacement measurement of actomyosin motor at extremely low ATP concentrations.
細胞運動研究会，東京／J. Muscle Res.Cell Motil.vol.16（1994 年 12 月）

62)吉川博、安田涼平、西坂崇之、 宮田英威、石渡信一、木下一彦：
光ピンセット法を用いた極少数個のアクトミオシン分子モーターのユニタリーステップの大きさとATP濃度依存性の測定.
生体運動合同班会議，大阪（1995年1月）

63)西坂崇之、吉川博、 宮田英威、石渡信一、木下一彦：
単一クロスブリッジの破断力の顕微測定.
生体運動合同班会議，大阪（1995年1月）

64)藤田英明、新津茂彦、安田賢二、石渡信一：
心筋筋線維における細いフィラメントの構造と機能の再構築.
生体運動合同班会議，大阪（1995年1月）

65)木下一彦、宮田英威、佐瀬一郎、吉川博、安田涼平、西坂崇之、石渡信一：
"Imaging and manipulating single molecules at work"
第2回浜松国際会議，浜松（1995年2月）

66)木下一彦、 宮田英威、佐瀬一郎、安田涼平、西坂崇之、石渡信一：
"Imaging and manipulating single molecules at work"
国際ワークショップ，和光（1995年2月）

67)高倉達、安田賢二、新藤嘉明、石渡信一：
顕微解析法を用いた筋原線維の静的・動的力学特性の研究.
物理学会春季年会，横浜（1995年3月）

68)増井一郎、忠重純子、西坂崇之、石渡信一：
単一アクチンフィラメントの重合過程の顕微解析.
物理学会春季年会，横浜（1995年3月）

69)Kato,H., Fujiki,Y., Kawase,H., Nishizaka,T., Kinosita,Jr.,K. & Ishiwata,S. :
Fluorescence imaging of mechanochemistry in muscle contractile system.
Int. Symp. on Cell Motil. and Cytogenesis，東京（1995年3月）

70)Ishiwata,S. : Microscopic analysis of mechanochemical properties of a single actomyosin motor and its assemblage.

Int. Symp. on Cell Motil. and Cytogenesis, 東京（1995年3月）

71)Nishizaka,T., Miyata,H., Yoshikawa,H., Ishiwata,S. & Kinosita,Jr.,K. :
Microscopic measurement of intermolecular forces between single myosin molecule and an actin filament.
Int. Symp. on Cell Motil. and Cytogenesis, 東京（1995年3月）

72)Ishiwata,S., Nishizaka,T., Miyata,H., Yoshikawa,H. & Kinosita,Jr.,K. :
Mechanical properties of single muscle protein motor studied by optical tweezers.
第2回日英生理学会シンポジウム, 岡崎（1995年3月）

3．出版物

1)石渡信一(1992)：「マイクロマシン技術による製品小型化・知能化事典」産業調査会事典出版センター pp.427-430.“筋肉”

2)Kinosita,Jr.,K., Suzuki,N., Ishiwata,S., Nishizaka,T., Itoh,H., Hakozaki,H., Marriott, G. and Miyata,H. (1993)：*In* Mechanism of myofilament sliding in muscle contraction. (ed. by H.Sugi & G.H.Pollack) Plenum Pub.Corp. pp.321-329.
"Orientation of actin monomers in moving actin filaments."

3)Ishiwata,S., Anazawa,T., Fujita,T., Fukuda,N., Shimizu,H. and Yasuda,K. (1993)：*ibid.* pp.545-556.
"Spontaneous tension oscillation (SPOC) of muscle fibers and myofibrils. Minimum requirements for SPOC."

4)Ishiwata,S. ed.(1993)：Rhythm, Oscillation and Phase Transitions「Phase Transitions」vol.45,No.2+3. Gordon & Breach

5)石渡信一 編(1993)：実験生物物理「Maruzen Adv.Tech. シリーズ」丸善

6)Nishizaka,T., Miyata,H., Yoshikawa,H., Ishiwata,S. and Kinosita,Jr.,K. (1994)：*In* Optical methods in biomedical and environmental sciences. (ed. by H.Ohzu,& S.Komatsu) Elsevier Sci.,B.V. pp.195-198.
"Microscopic measurement of the sliding and binding force between muscle proteins with optical tweezers."

Regulation of tension development by MgADP and Pi without Ca^{2+}

Role in spontaneous tension oscillation of skeletal muscle

Hideharu Shimizu, Takashi Fujita, and Shin'ichi Ishiwata

Department of Physics, School of Science and Engineering, Waseda University, Okubo, Shinjuku-ku, Tokyo 169, Japan

ABSTRACT The length of sarcomeres in isolated myofibrils fixed at both ends spontaneously oscillates when MgADP and Pi coexist with MgATP in the absence of Ca^{2+} (Okamura, N., and S. Ishiwata, 1988. *J. Muscle Res. Cell. Motil.* 9:111–119). Here, we report that MgADP and Pi function as an activator and an inhibitor, respectively, of tension development of single skeletal muscle fibers in the absence of Ca^{2+} and the coexistence of MgADP and Pi with MgATP induces spontaneous tension oscillation. First, the isometric tension sharply increased when the concentration of MgADP became higher than ~3× that of MgATP and saturated at ~90% of the tension obtained under full Ca^{2+} activation; in parallel with this sigmoidal increase of tension, MgATPase activity appeared. The inhibition of contraction by the regulatory system seems to be desuppressed by the allosteric effect of actomyosin-ADP complex, similarly to so-called rigor complex. The ADP-induced tension was decreased along a reversed sigmoidal curve by the addition of Pi; actomyosin-ADP-Pi complex, which has no desuppression function, may be formed by exogenous Pi; accompanying the decline of tension, spontaneous oscillations of tension and sarcomere length appeared. It is suggested that the length oscillation of each (half) sarcomere would occur through the transition of cross-bridges between force-generating (on) and non-force-generating (off) states, which may be regulated by the mechanical states (strain) of cross-bridges and/or thin filaments.

INTRODUCTION

Muscle contraction occurs as a result of mutual sliding of actin (thin) and myosin (thick) filaments with the consumption of chemical energy liberated from ATP hydrolysis. So, current studies on the molecular mechanism of muscle contraction have been focused on (*a*) mechanical (structural) properties, (*b*) enzymatic (thermodynamic) properties and (*c*) mechano-chemical coupling, i.e., the connection between the molecular mechanism of force generation and the mechanism of ATP hydrolysis, in actin and myosin complexes. The molecular mechanism of regulation is still unclear, although it has been established that the first event in triggering contraction is the binding of Ca^{2+} to regulatory proteins (Ebashi and Endo, 1968; Weber and Murray, 1973).

Recently, much effort has been made to connect the mechanical changes of muscle fibers with the kinetics of ATP hydrolysis by actomyosin complex. The leading theory is that cross-bridges can be classified into two types, i.e., a weakly-binding state with ATP or ADP-Pi which hardly contributes to tension and a strongly-binding state with ADP or without nucleotides which is responsible for tension development (Eisenberg and Hill, 1985; Goldman and Brenner, 1987; Goldman, 1987; Brenner, 1990). The regulation by Ca^{2+} occurs through the change of kinetic constant(s) at some step(s) between the weakly- and strongly-binding states, and/or within the weakly- and/or strongly-binding states, but not through the association and dissociation step of actin and myosin (Chalovich et al., 1981; Millar and Homsher, 1990). Based on such results, a detailed kinetic scheme for actomyosin ATPase has been proposed and analyzed by computer simulation (e.g., Pate and Cooke, 1989). Further, the effects of ADP and Pi on contraction have been studied (Hibberd and Trentham, 1986; Schoenberg and Eisenberg, 1987); MgADP potentiates isometric tension obtained in the presence of Ca^{2+} (Cooke and Pate, 1985; Kawai and Halvorson, 1989), whereas Pi depresses the tension (Rüegg et al., 1971; Herzig et al., 1981; Altringham and Johnston, 1985; Cooke and Pate, 1985; Hibberd et al., 1985; Kawai, 1986; Nosek et al., 1987; Cooke et al., 1988; Chase and Kushmerick, 1988; Kawai and Halvorson, 1991). Those results support the above scheme, implying that actomyosin(AM)-ADP complex is in a strongly binding state, whereas AM-ADP-Pi complex is in a weakly-binding state. Also, there is a report showing that even in the absence of Ca^{2+}, tension is developed to some extent upon the addition of MgADP (Hoar et al., 1987). It should be noted, however, that in spite of these various studies, both the effects of high concentrations of MgADP and the synergistic effects of MgADP and Pi in the absence of Ca^{2+} have not yet been examined.

Several years ago, we found a new phenomenon in

Address correspondence to Dr. Ishiwata.

Biophys. J. © Biophysical Society
Volume 61 May 1992 1087–1098
0006-3495/92/05/1087/12 $2.00

skeletal myofibrils, i.e., spontaneous oscillatory contraction, named SPOC, and clarified the conditions for oscillation, which seems to reflect an essential aspect of dynamical coupling between the mechanical and chemical properties of the contractile system composed of actin, myosin and regulatory proteins (Okamura and Ishiwata, 1988). That is, when high concentrations of MgADP and Pi coexist with MgATP and without Ca^{2+}, the lengths of all sarcomeres in isolated myofibrils fixed at both ends spontaneously oscillate, exhibiting a rapid lengthening phase and a slow shortening phase with a period of one to several seconds, where the oscillation of sarcomeres is usually out of phase to each other. The SPOC conditions, requiring the coexistence of MgADP and Pi with MgATP but not requiring Ca^{2+}, strongly suggest that not only the molecular mechanism of tension development but also its regulatory mechanism are involved in the oscillation mechanism.

Several reports have already been published on spontaneous oscillation of chemically or mechanically skinned fibers or fibrils of vertebrate striated muscle (Goodall, 1956; Lorand and Moos, 1956; Armstrong et al., 1966; Fabiato and Fabiato, 1978; Brenner, 1979; Iwazumi and Pollack, 1981; Stephenson and Williams, 1982; Onodera and Umazume, 1984; Onodera, 1990; Sweitzer and Moss, 1990). However, the conditions are apparently different from those of SPOC, e.g., submicromolar concentrations of free Ca^{2+} for skeletal (Iwazumi and Pollack, 1981; Stephenson and Williams, 1982) or cardiac muscle (Fabiato and Fabiato, 1978; Sweitzer and Moss, 1990) and high pH in the absence of Ca^{2+} for skeletal muscle (Onodera and Umazume, 1984; Onodera, 1990). These conditions for oscillation are apparently different from each other; besides the above two types of oscillations are limited to a narrow range of free Ca^{2+} concentrations or pH value, whereas the SPOC occurs over a wide range of concentrations of MgADP and Pi. In spite of these differences, there is one important point in common; all the conditions produce partial activation with a low level of tension, so that the state of oscillating fibers appears to be located in an intermediate state between contraction and relaxation. Therefore, the fluctuation between contraction and relaxation which occurs in each (half) sarcomere depending on the mechanical and chemical states of the contractile system may be an essential feature of all the types of spontaneous oscillations reported so far. The present work represents a first step towards examining this possibility and getting an insight into not only the mechanism of spontaneous oscillation but also the molecular mechanism of contraction and regulation of muscle.

MATERIALS AND METHODS

Solvent conditions

Solvent conditions for the measurement of developed tension of fibers and for the observation of states of myofibrils were as follows: ~120 mM K^+, 1 or 4 mM EGTA, 0.1 mM P^1,P^5-di(adenosine-5')pentaphosphate (AP_5A; Lienhard and Secemski, 1973) and 10 or 20 mM 3-(*N*-morpholino)propanesulfonic acid (MOPS). The pH value was adjusted to 6.5–8.2 for each solvent by the addition of KOH or HCl at 25°C. Appropriate concentrations of ATP, ADP, K_2HPO_4, KH_2PO_4, $MgCl_2$, and $CaCl_2$ were added. The ionic strength (I.S.) was maintained at 0.15 M by adjusting the concentration of KCl. In the case of fibers, the concentration of free Mg^{2+} was maintained at 2 mM by adjusting the total concentration of $MgCl_2$. The concentrations of the above chemicals were determined by computer calculation using the published values for stability constants (cf Horiuti, 1986). When it was necessary to maintain the concentration of MgATP in fibers constant, 1 mg/ml creatine phosphokinase (CPK) and 20 mM creatine phosphate (CP) were added. CPK and CP were purchased from Sigma Chemical Co. (St. Louis, MO); ATP, ADP and AP_5A were from Boehringer Mannheim GmbH (Mannheim, Germany). MOPS was purchased from Dojindo (Kumamoto, Japan). Other chemicals were of reagent grade.

Preparation of muscle fibers and myofibrils

Rabbit psoas glycerinated muscle fibers were prepared as described previously (Ishiwata et al., 1985). The glycerinated fibers were used after storage at −20°C for between three weeks and three months; within this period, the mechanical properties of the fibers reported here were unchanged. Single glycerinated fibers (~5 mm long, ~40 μm thick) were carefully prepared from a bundle of fibers immersed in 50% (*v*/*v*) glycerol solution on a cold bench under a stereo microscope. Then, one end of each single fiber was fixed to a thin tungsten wire attached to a tension transducer, of which characteristic frequency was ~40 Hz (UL-2GR, Nippon Denkei Co. Ltd., Tokyo) and the other end to a thin tungsten wire attached to a micromanipulator with enamel; this work was done in air at room temperature without removal of glycerol solution from the fibers except at both ends, where the enamel was smeared. The fibers thus fixed were first stored in a rigor solution (solution A with Triton X-100) containing 60 mM KCl, 5 mM $MgCl_2$, 10 mM Tris-maleate buffer (pH 6.8), 1 mM EGTA and 1% (*v*/*v*) Triton X-100, for 20 min at 25°C. The following treatment and all the experiments were done at 25°C. The fibers were then transferred to a relaxing solution (110 mM KCl, 6 mM $MgCl_2$ (free Mg^{2+} = 2 mM), 4 mM ATP (MgATP = 3.5 mM), 10 mM MOPS (pH 7.0), 4 mM EGTA and 0.1 mM AP_5A), in which the sarcomere length of fibers was estimated by means of laser light diffraction (He-Ne laser, type GLS 5110, NEC Inc., Tokyo, Japan; cf Ishiwata et al., 1985) and adjusted to 2.3–2.5 μm with a micromanipulator. Oscillation of sarcomeres in muscle fibers was detected by monitoring the fluctuation of the fine structure of the first-order diffraction lines. Even if the tension oscillation was not observable, the fine structure fluctuated maintaining the average position of the diffraction lines, which reflects the unorganized oscillation of sarcomere lengths.

Myofibrils were prepared by gently homogenizing glycerinated fibers under a rigor condition (solution A) at 2°C and the states of myofibrils were observed under a phase-contrast microscope at 25°C as described previously (Ishiwata and Funatsu, 1985).

Measurement of tension

The isometric tension generated by single fibers was measured by using a tension transducer according to the following procedure. First, the fibers immersed in a relaxing solution were transferred to a certain standard solution and the tension (P_0) was measured. After relaxing them again, the tension (P) was measured in an assay solution. Then, the measurement of tension (P_1) was repeated under the above standard condition. An example of typical records is shown in Fig. 3, which was recorded by a chart recorder having a cut-off frequency of 0.5 Hz (VP-6533A, Matsushita Communication Industrial Co. Ltd., Yokohama, Japan). Thus, the relative tension was estimated from the ratio of P to the average of P_0 and P_1. A single data point was obtained from each fiber. The volume of solution was ~0.3 ml; the solution was stirred with a miniature magnetic stirrer.

Measurement of ATPase activity

ATPase activity of fibers was estimated as follows. The concentration of Pi released from four single fibers into 0.3 ml of solution during 10 min after the addition of ADP was measured by a modified malachite green method (Lanzetta et al., 1979; Kodama et al., 1986; Ohno and Kodama, 1991). The ATPase activity was expressed in a unit of (number of released Pi)/(number of myosin heads)/s, with the assumption that myosin accounts for 50% (w/w) of total protein content in fibers. The amount of proteins of fibers was determined by a modified Lowry method (Ohnishi and Barr, 1978).

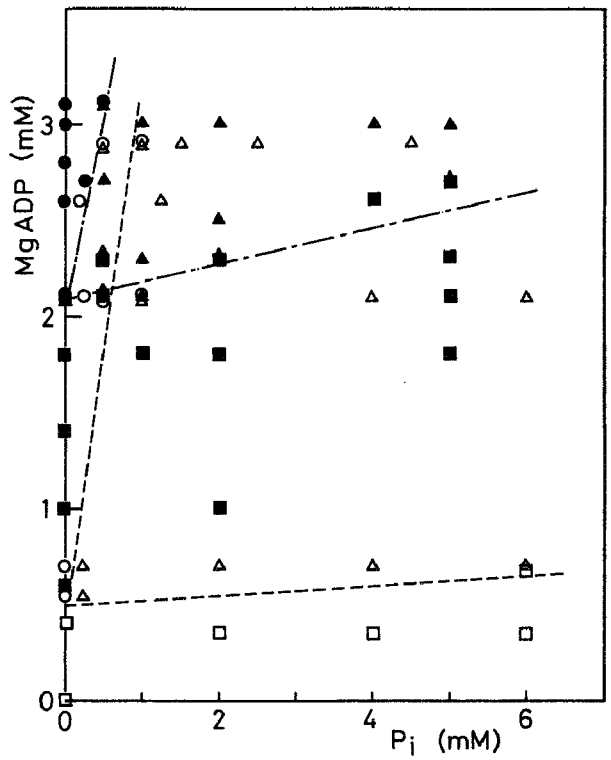

FIGURE 1 State diagram showing states of myofibrils, i.e., contraction (○, ●; myofibrils shorten without oscillation), relaxation (□, ■) and SPOC (△, ▲) at different concentrations of MgATP (0.2 mM, *open symbols;* 1 mM, *closed symbols*). The states of myofibrils were observed under a phase-contrast microscope. Ordinate and abscissa, the concentrations of MgADP (calculated) and Pi (added), respectively. Other solvent conditions, 4 mM $MgCl_2$, 10 mM MOPS (pH 7.0), 4 mM EGTA and 0.1 mM AP_5A. Ionic strength (I.S.) was adjusted with KCl to be 0.15 M. Temperature, 25°C.

RESULTS

Spontaneous oscillatory contraction (SPOC) characterized by microscopic observation of myofibrils

We have previously obtained a state diagram showing three states of myofibrils, i.e., spontaneous oscillation (SPOC), relaxation and contraction without oscillation, which are induced by adding various concentrations of ADP and Pi in the presence of 0.2 mM ATP and the absence of Ca^{2+} (Okamura and Ishiwata, 1988; Ishiwata et al., 1991). Here, we have refined the state diagram by controlling the concentrations of MgATP (0.2 or 1.0 mM) and MgADP, i.e., true substrates of actomyosin ATPase, and the ionic strength. The states of myofibrils, of which both ends were attached to a glass surface, were observed under a phase-contrast microscope as described in detail previously. The characteristics of the state diagram thus obtained were essentially the same as those found previously (Fig. 1; cf Okamura and Ishiwata, 1988; Ishiwata et al., 1991). That is, the SPOC region appeared between the contraction and relaxation regions; myofibrils which are relaxed in the absence of MgADP and Pi (corresponding to the origin of the diagram) were transformed into the contraction state by adding MgADP (along the ordinate) and then started to oscillate spontaneously on further addition of Pi (in parallel with the abscissa). Across the boundaries shown by dashed or once-broken lines, the state of myofibrils changed gradually and reversibly. There appears to be a triple point on the ordinate around which the three states of myofibrils merge. Across the triple point along the ordinate, the state of myofibrils gradually changed from relaxation to contraction; between the triple point and the origin on the ordinate, myofibrils may be partially activated and generate tension, though it seems that the tension was so small that myofibrils attached to a glass surface could not shorten appreciably (cf the text dealing with Fig. 4). So, we regard the concentration of MgADP at the triple point as a good measure to indicate a "critical MgADP concentration" above which ADP-induced contraction occurs. As described in the previous paper (Okamura and Ishiwata, 1988), the shortening velocity of myofibrils under the condition of ADP-induced contraction was low, about one tenth of the standard velocity of no-load shortening.

It should also be noted in Fig. 1 that on increasing the concentration of MgATP the SPOC region shifted

upward to the region of high concentrations of MgADP, suggesting that MgADP competes with MgATP for binding to actomyosin complex. To further clarify this point, we examined the relationship between the critical MgADP concentration and the concentration of MgATP. Fig. 2 shows that the critical MgADP concentration increases nearly in proportion to the concentration of added MgATP. The slope of the straight line was ~3, suggesting that the ratio of the apparent association constant of MgATP to that of MgADP with actomyosin complex was ~3. Fig. 2 is a state diagram in the sense that the straight line showing the relationship between the critical MgADP concentration and the concentration of MgATP corresponds to a boundary across which the state of myofibrils changes reversibly. When the concentration of MgATP is very low, lower than ~0.1 mM, myofibrils contracted without the addition of ADP, probably due to the activation by rigor complex (cf Bremmel and Weber, 1972; Weber and Murray, 1973).

Effects of MgADP on isometric tension of single fibers

We have measured the isometric tension generated by the ADP-induced contraction by using single glycerinated fibers. Fig. 3 is an example of record showing the reversibility and reproducibility of tension development with the change of concentration of MgADP. This isometric tension induced by MgADP in the absence of Ca^{2+} reached nearly 90% of that induced normally by the addition of Ca^{2+} instead of MgADP (see below). Fig. 4 summarizes these results, showing that the tension is generated with the addition of MgADP in the absence of Ca^{2+}; in the presence of 1 mM MgATP, the tension was abruptly increased at ~3 mM MgADP and almost saturated at ~10 mM MgADP. This concentration of 3 mM MgADP exactly corresponds to the critical MgADP concentration defined above. Such a sigmoidal curve of tension development and the presence of critical MgADP concentration indicate that MgADP functions as an allosteric effector and induces cooperative interaction between thin and thick filaments.

Next, we examined the effects of MgADP on the isometric tension under a contracting condition in the presence of Ca^{2+}. As summarized in Fig. 5, in the presence of 1 mM MgATP, the tension increased by ~10%, reached a plateau at ~3 mM MgADP and decreased on further increase in the concentration of MgADP. On the other hand, in the presence of 2 mM MgATP, the increase of tension was much larger, to nearly the same extent as reported before (cf Cooke and Pate, 1985; Kawai and Halvorson, 1989) and reached a

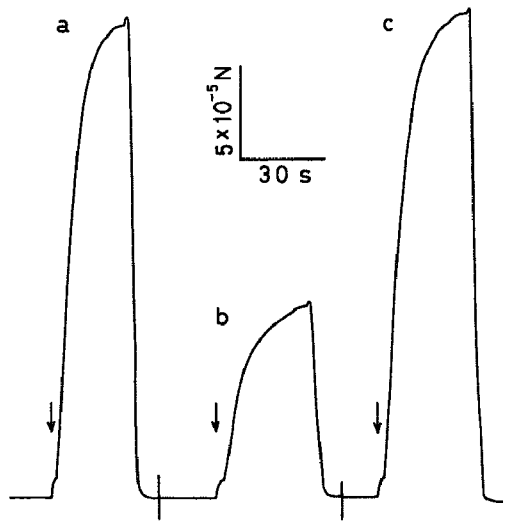

FIGURE 3 Recordings of tension development of a single fiber. Solvent conditions: 1 mM MgATP, 15 mM MgADP (*a* and *c*) or 5 mM MgADP (*b*), 2 mM Mg^{2+} (free), 4 mM EGTA, 10 mM MOPS (pH 7.0), 0.1 mM AP_5A, concentration of free Mg^{2+} maintained at 2 mM with $MgCl_2$ and I.S. maintained at 0.15 M with KCl. Temperature, 25°C. Tension was measured in sequence from *a* to *c*. Throughout the present work, the tension under a certain standard condition was measured before (*a*) and after (*c*) the measurement under the assay condition (*b* in this example). At each arrow, relaxing solution (1 mM MgATP, 2 mM Mg^{2+} (free), 4 mM EGTA, 10 mM MOPS (pH 7.0), 0.1 mM AP_5A and I.S. = 0.15 M) was exchanged with the above solution containing MgADP. Vertical and horizontal bars indicate 5×10^{-5} N and 30 s, respectively.

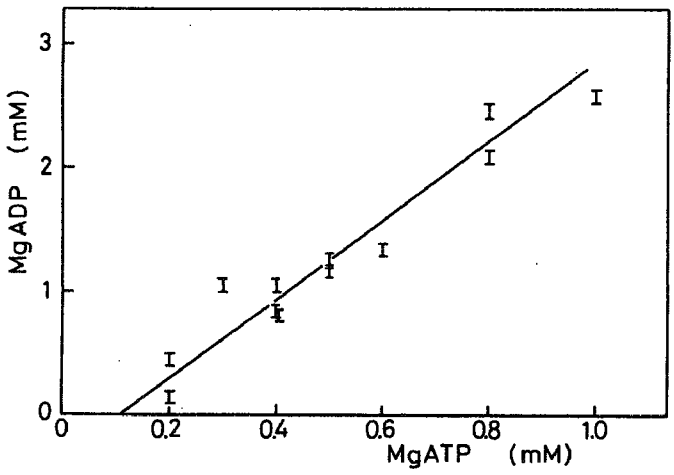

FIGURE 2 Critical concentrations of MgADP at various concentrations of MgATP without Pi. The critical concentration of MgADP, above which contraction of myofibrils started to occur, was determined under a phase-contrast microscope by stepwise increasing MgADP concentration along the ordinate in Fig. 1 at each concentration of MgATP (calculated). Other conditions, the same as in Fig. 1 except that Pi was absent.

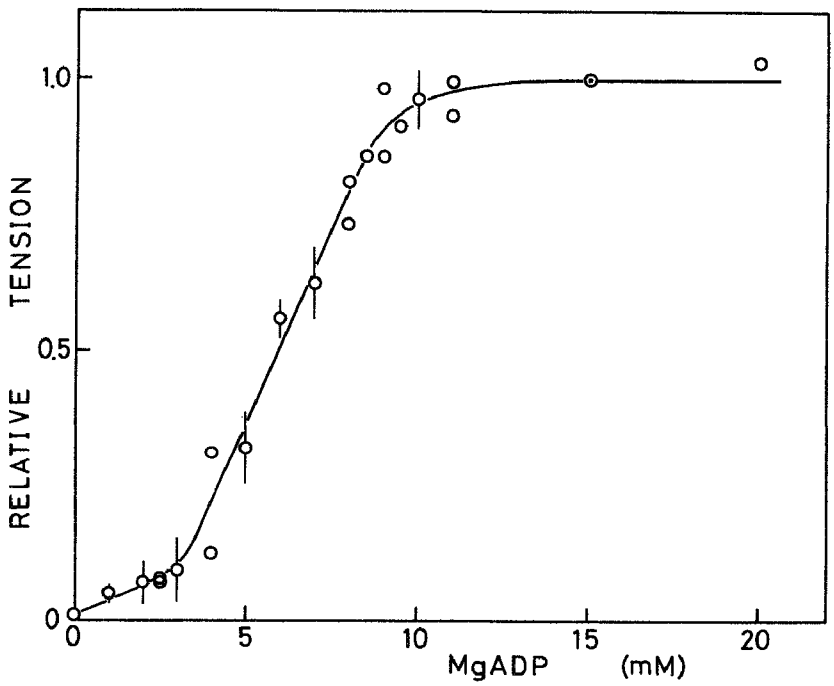

FIGURE 4 Effect of MgADP on tension development of single fibers in the presence of ATP and the absence of Ca^{2+}. Solvent conditions: the same as in Fig. 3 except that the concentration of MgADP was changed. Temperature, 25°C. Tension was normalized with respect to that at 15 mM MgADP (◉). Vertical bars, SD when more than three data points were obtained at each MgADP concentration.

plateau at ~7 mM MgADP. Thus, MgADP functions as a potentiator for the tension development irrespective of the presence or absence of Ca^{2+}; however, MgADP of much higher concentrations functions as a suppressor, probably due to competitive binding to an actomyosin complex with respect to MgATP, as already suggested above.

Data in Fig. 5 were normalized for the tension generated under the condition where MgADP was removed by adding an ATP-regenerating system. The slight increase of tension upon removal of the ATP-regenerating system (see the tension on the ordinate in Fig. 5) may be ascribed to the accumulation of MgADP in lattice spaces of the fiber.

Finally, we compared the tension generated in the presence (Fig. 5) and the absence (Fig. 4) of Ca^{2+} with 1 mM MgATP and 15 mM MgADP using the same fibers. The tension induced by MgADP in the absence of Ca^{2+} was 87 ± 2% (SD calculated from five experiments) of that in the presence of Ca^{2+}.

Activation of MgATPase of fibers by the addition of MgADP in the absence of Ca^{2+}

Although we have confirmed that the tension induced by MgADP in the absence of Ca^{2+} attained nearly 90% of

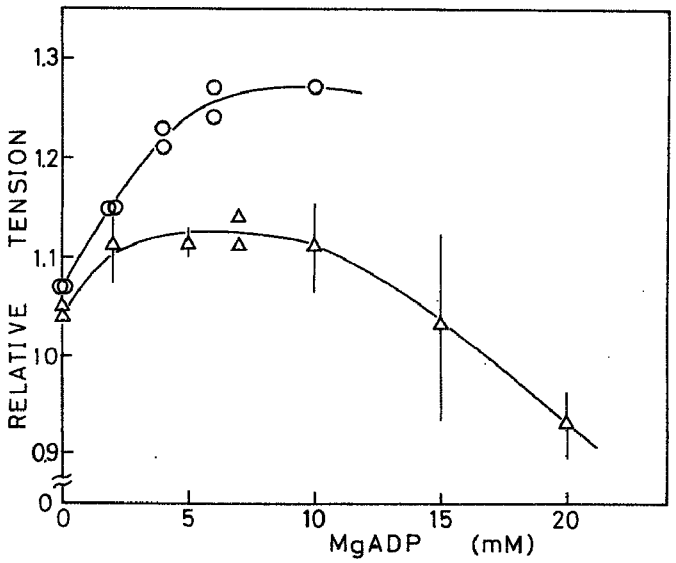

FIGURE 5 Effect of MgADP on tension development of single fibers in the presence of ATP and Ca^{2+}. Solvent condition: 1 mM (△) or 2 mM (○) MgATP, 2 mM Mg^{2+} (free), 1 mM EGTA (pCa adjusted to be 5.0 with $CaCl_2$), 20 mM MOPS (pH 7.0), 0.1 mM AP_5A and I.S. = 0.15 M. Temperature, 25°C. Tension was normalized with respect to that obtained in the presence of 1 mM MgATP and with the addition of 1 mg/ml of creatine phosphokinase and 20 mM creatine phosphate to suppress ADP contamination. Vertical bars, SD of more than three data points.

that in the presence of Ca^{2+}, there was a possibility that the tension is similar to rigor tension attained without ATP hydrolysis. So, we examined the ATPase activity of fibers by measuring the concentration of released Pi. Fig. 6 shows that accompanying the addition of MgADP, ATPase activity appeared and finally reached about 0.85 (Pi/myosin head/s). Thus, we conclude that the ADP-induced contraction generates active tension which is accompanied by ATP hydrolysis. It should be noted that the ATPase activity appears at slightly lower MgADP concentration than that required for tension development (cf Figs. 4 and 6).

Effects of Pi on isometric tension in the presence or absence of MgADP

Referring to the results of Figs. 1 and 4, we examined the effects of Pi on the tension induced by MgADP, i.e., the tension under SPOC conditions. Fig. 7 shows that the tension was decreased on increasing the concentration of Pi; first, in the presence of 15 mM MgADP and 1 mM MgATP where the ADP-induced tension was saturated (Fig. 4), the drop of tension occurred after some lag phase, along a reversed sigmoidal curve (~2 mM Pi at the point of inflection of the curve) and the extent of the tension drop was about 70% at 5 mM Pi. On the other hand, in the presence of 8 mM MgADP and 1 mM MgATP, where the ADP-induced tension was just before the saturation point (Fig. 4), the tension decreased monotonously without a lag phase (~1 mM Pi at the midpoint of the tension drop) and reached ~20% of the original value. In this respect, the result in the presence of 2 mM MgATP with 10 mM MgADP at pH 7.0 (cf *insert*, Fig. 10 *a*) was similar to that in the presence of 1 mM MgATP with 8 mM MgADP but not to that with 15 mM MgADP, although the extent of the tension drop was large.

We have noticed that the tension of single fibers start to oscillate spontaneously when the concentration of Pi is > 1–2 mM, i.e., on the right-hand side region of the descending phase of the tension drop in Fig. 7. A typical record is shown in Fig. 8. The wave form of the tension

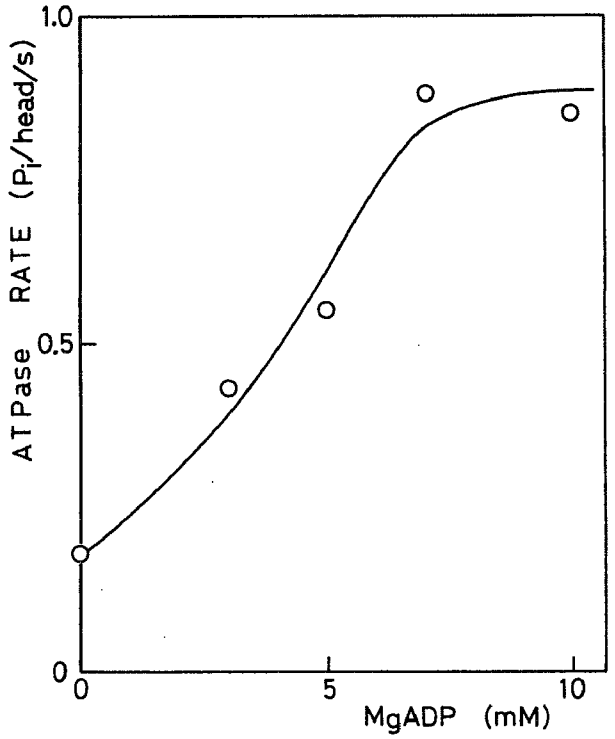

FIGURE 6 ATPase activity of single fibers on increasing MgADP concentration in the presence of ATP and absence of Ca^{2+}. Solvent conditions: 1 mM MgATP, 2 mM Mg^{2+} (free), 4 mM EGTA, 10 mM MOPS (pH 7.0), 0.1 mM AP_5A and I.S. = 0.15 M. ATPase rate is represented in a unit of (number of released Pi)/(number of myosin heads)/s. The concentration of myosin heads in fibers was assumed to be 0.2 mM. Temperature, 25°C.

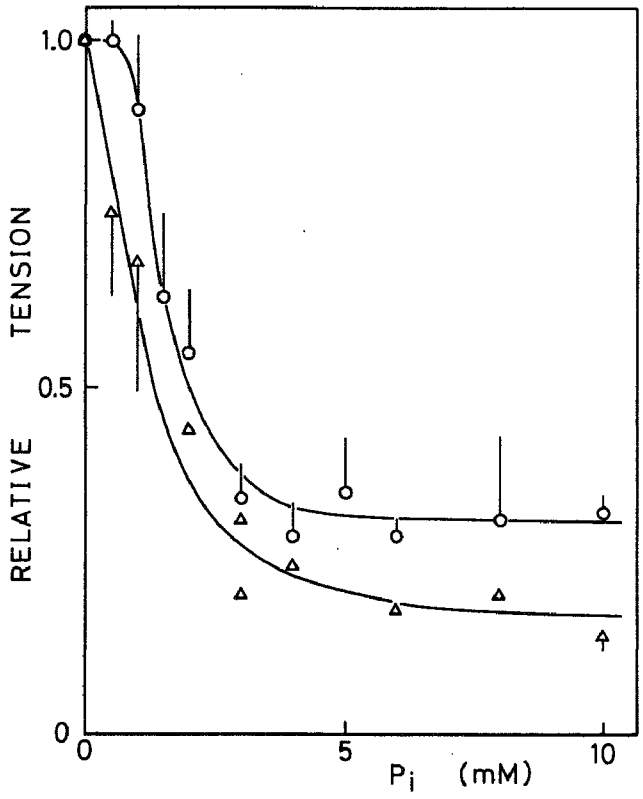

FIGURE 7 Effect of Pi on tension of single fibers induced by MgADP in the presence of ATP and absence of Ca^{2+}. Solvent conditions: (○, △), 1 mM MgATP and either 8 (△) or 15 (○) mM MgADP. Other conditions, 2 mM Mg^{2+} (free), 4 mM EGTA, 10 mM MOPS (pH 7.0), 0.1 mM AP_5A and I.S. = 0.15 M. Temperature, 25°C. Tension was normalized with respect to that obtained without Pi at each condition. When the tension oscillated as shown in Fig. 8, the initial peak tension was plotted. Vertical bars, SD of more than three data points.

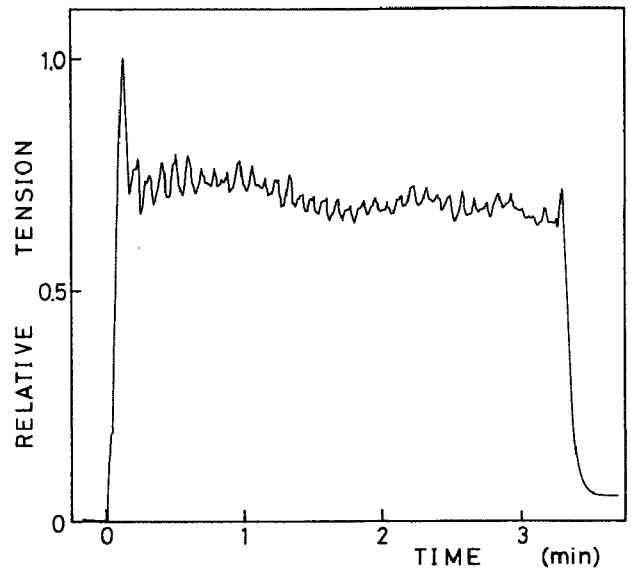

FIGURE 8 Example of tension oscillation of a single fiber observed under the SPOC condition. Solvent conditions: 1 mM MgATP, 15 mM MgADP, 1 mM Pi, 2 mM Mg^{2+} (free), 4 mM EGTA, 10 mM MOPS (pH 7.0), 0.1 mM AP_5A and I.S. = 0.15 M. Temperature, 25°C.

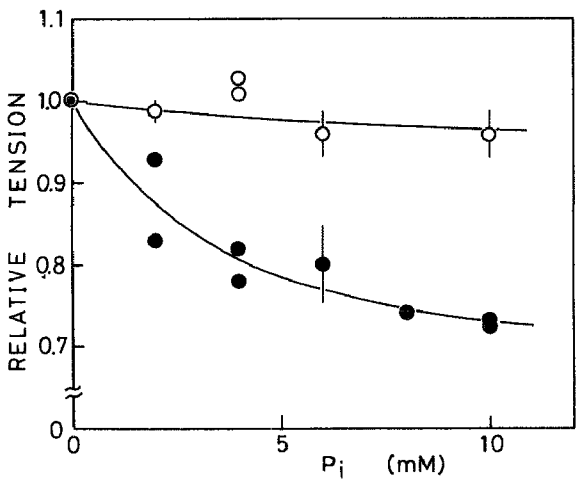

FIGURE 9 Effect of Pi on tension of single fibers developed in the presence of ATP and Ca^{2+} with or without ADP. Solvent conditions: 3.5 mM MgATP (●) or 1 mM MgATP and 15 mM MgADP (○) with 2 mM Mg^{2+} (free), 1 mM EGTA (pCa adjusted to be 5.0 with $CaCl_2$), 20 mM MOPS (pH 7.0), 0.1 mM AP_5A and I.S. = 0.15 M. Temperature, 25°C. Tension was normalized with respect to that obtained without Pi under each condition. Vertical bars, SD of three data points.

oscillation was not simple, but there appears to be some period of oscillation, ~11 s in this example. Accompanying this tension oscillation, propagation of the SPOC wave, i.e., the propagation of the rapid lengthening phase of sarcomeres (cf Okamura and Ishiwata, 1988; Ishiwata et al., 1991), was observed here and there along the long axis of fibers under a phase-contrast microscope. Even when the tension became negligibly small with the addition of Pi (cf *insert,* Fig. 10 *a*), the intensity fluctuation of the fine structure of laser light diffraction lines indicated that the sarcomere lengths spontaneously oscillated.

Next, we examined the effects of Pi on the tension generated under contraction conditions with Ca^{2+} and with or without MgADP (Fig. 9). The results under a standard contracting condition were similar to those reported previously (Cooke and Pate, 1985; Kawai, 1986; Kawai et al., 1987); the extent of the tension drop was as much as 30% at 10 mM Pi. On the other hand, the tension hardly decreased in the presence of 15 mM MgADP, which is in contrast to the results in the absence of Ca^{2+} (Fig. 7).

Effects of pH on isometric tension in the presence of MgADP and Pi

Finally, we examined the effects of pH on the ADP-induced tension in the presence of Pi and the absence of Ca^{2+}. In the pH range of 6.5–8.2, the higher the pH value, the larger the tension. The midpoint of pH was ~7.6 (Fig. 10 *a*); in other words, on increasing the pH, the midpoint of tension drop with the addition of Pi was shifted to higher concentrations of Pi (*insert,* Fig. 10 *a*). Next, we replotted the relative tension against the estimated concentrations of diprotonated Pi (Fig. 10 *b*) or protonated Pi (*insert,* Fig. 10 *b*). Fig. 10 *b* clearly shows that the tension decreases in proportion to the concentration of diprotonated Pi, irrespective of whether it is changed by the pH value or the total concentration of added Pi. On the other hand, there was no correlation between the tension drop and the concentration of protonated Pi (*insert,* Fig. 10 *b*).

DISCUSSION

Concentrations of ATP, ADP and Pi inside fibers

In the present study on muscle fibers, the concentration of MgATP was kept low, mostly 1 mM (2 mM in some cases), to examine the competitive action of MgADP. Therefore, when the ATPase activity was high, the MgATP concentration in the center of fibers may have become quite low. The MgATP concentration under a steady state was calculated based on the diffusion equation (cf Cooke and Pate, 1985) by assuming that the fibers are cylinders of radius 20 μm and the ATPase activity inside the fibers is uniform and 0.85/myosin head/s), which is the maximum value obtained under the conditions without Ca^{2+} in the present work. When

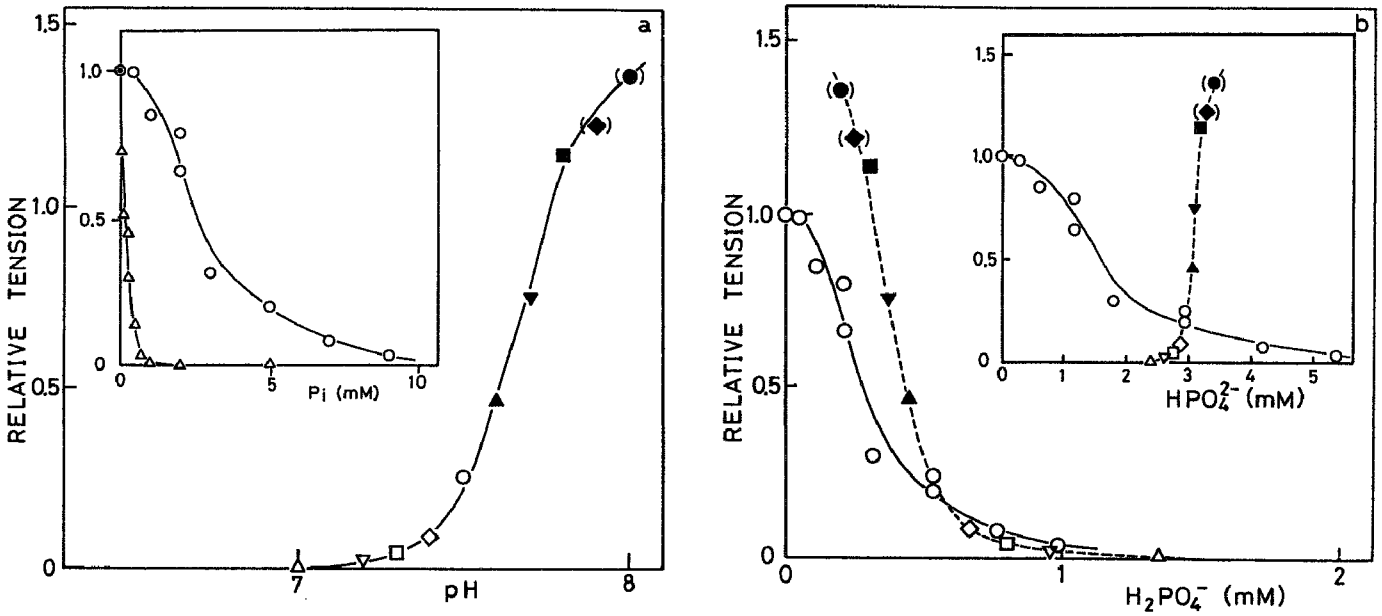

FIGURE 10 Effect of Pi at different pH values on tension of single fibers induced by MgADP in the presence of ATP and absence of Ca^{2+}. Solvent conditions: 2 mM MgATP (different from 1 mM used in Fig. 7), 10 mM MgADP, 2 mM Mg^{2+} (free), 5 mM Pi, 4 mM EGTA, 10 mM MOPS, 0.1 mM AP_5A and I.S. = 0.15 M (*a*); note that the concentrations of MgATP and MgADP used in Fig. 7 are 1 mM and either 8 or 15 mM, respectively. The pH value was adjusted for each solution by the addition of HCl or KOH. The effect of Pi concentration was examined at pH 7.0 (△) and 7.5 (○) (*insert* in *a*). Temperature, 25°C. The tension was normalized with respect to that (standard tension) obtained without Pi at pH 7.5 (◎, *insert* in *a*) according to the same procedure as described in Fig. 3. Two parentheses indicate that the standard tension obtained after the measurement of tension under the assay condition became < 80% of the initial standard tension; this tended to occur when large tension was developed at high pH. Relative tension was replotted against the concentration of diprotonated Pi, $H_2PO_4^-$ (*b*) or protonated Pi, HPO_4^{2-} (*insert* in *b*). The concentration of each Pi species was calculated by using published values for stability constants (cf Materials and Methods). Symbols correspond to those in *a*.

the concentration of MgATP outside the fibers was 1 (or 2) mM, the concentration of MgATP at the center of the fibers was estimated to be 0.15 (or 1.15) mM or 0.86 (or 1.86) mM for a value of the diffusion coefficient of ATP of either 2×10^{-7} (MgATP; Mannherz, 1968) or 1.2×10^{-6} cm^2/s (ATP^{3-}; Kushmerick and Podolsky, 1969), respectively. Thus, the concentration of MgATP inside the fibers may have become a half of that outside the fibers when the ATPase activity was high. It should be noted, however, that this is the case only for the core region of the fibers; in the broader outer region, the concentration of MgATP would have been much closer to that outside the fibers.

The reported values of ATPase activity in muscle fibers in the presence of Ca^{2+} are scattered in the range of 0.9 to 3.2/myosin head/s (Chaen et al., 1981; Cooke and Pate, 1985; Sleep, 1984; Webb et al., 1986). When the MgATP concentration outside the fibers is as low as 1 (or 2) mM, the threshold of ATPase activity above which the MgATP concentration at the core of muscle is exhausted may be ~1 (or 2)/myosin head/s. The ATPase activity, however, should be lowered with the addition of MgADP in the presence of Ca^{2+}, so that only a part of the conditions within the range examined in the present work may have met the above threshold of ATPase activity.

Conversely, the concentrations of MgADP and Pi inside the fibers will increase in proportion to the ATPase activity. Thus, the effective concentrations of such substances will be modified as considered above.

In summary, the data presented here appear to be quantitatively correct under conditions where the tension level (ATPase activity) is low, but we should keep in mind that the data obtained at high tension are less quantitative.

Activation of fibers with ADP

Both isometric tension and ATPase activity of muscle fibers sigmoidally increased with the addition of MgADP under the relaxing condition (Figs. 4 and 6). Fig. 2 suggests that the added MgADP competes with MgATP for the binding site and that relaxed muscle is activated when some fraction of myosin heads is occupied by MgADP. Thus, the SPOC region is determined by the

ratio of the concentrations of MgADP and MgATP but not by the MgADP concentration.

If MgADP is a simple competitor for MgATP, ATPase activity is considered to be suppressed. In fact, the ATPase activity of muscle fibers was decreased by the addition of MgADP under a contracting condition (Hoar et al., 1987). In the present work, behavior of MgADP as a simple competitor was observed in the decreasing phase of tension obtained with increasing concentration of MgADP under a contracting condition (Fig. 5).

On the other hand, under a relaxing condition, MgADP functioned as a competitive activator (Fig. 4). The most probable interpretation for this is that AM-ADP complexes (AM, actomyosin complex), which become predominant with the addition of MgADP, function as a desuppressor, i.e., a suppressor of the inhibitory function of regulatory proteins, similarly to so-called rigor complex (Bremmel and Weber, 1972; Weber and Murray, 1973; Greene and Eisenberg, 1980); probably, the step of Pi release and/or some step(s) of isomerization of AM-ADP-Pi complex, which are suppressed in the absence of Ca^{2+} (Chalovich et al., 1981), may be released allosterically and cooperatively through the conformational change of thin filaments by the formation of AM-ADP complex, so that the ATPase activity appears. Judging from the large tension (Fig. 4) and high ATPase activity (Fig. 6) attained, the suppression seems to be nearly fully released.

Even under a contracting condition with Ca^{2+}, the addition of ADP slightly elevated the isometric tension (Fig. 5; Cooke and Pate, 1985; Kawai, 1986). This fact suggests that although the suppression imposed by the regulatory system is released by Ca^{2+}, MgADP may have an extra function as an activator; this does not necessarily mean, however, that the step of ATPase reaction that is regulated by an AM-ADP complex is different from that regulated by Ca^{2+}. The decrease in tension observed with further addition of MgADP (Fig. 5) may be ascribed to the competitive binding of MgADP to the binding site of MgATP as mentioned above; this phenomenon is probably similar to that observed when the concentration of MgATP is lowered to $< \sim 20$ μM, where a rigor complex instead of the AM-ADP complex may play a key role as an allosteric regulator (Cooke and Bialek, 1979).

Deactivation of fibers with Pi

Several reports have shown that muscle fibers under a contracting condition are deactivated by the addition of Pi (Rüegg et al., 1971; Herzig et al., 1981; Altringham and Johnston, 1985; Cooke and Pate, 1985; Kawai, 1986; Nosek et al., 1987; Cooke et al., 1988; Chase and Kushmerick, 1988; Kawai and Halvorson, 1991). We confirmed that the addition of 10 mM Pi monotonously decreased the isometric tension under a contracting condition by ~30% (Fig. 9), whereas we found that the decrease in tension was not observed if a high concentration of MgADP coexisted in the presence of Ca^{2+} (Fig. 9). The effect of Pi on the ADP-induced tension in the absence of Ca^{2+} was peculiar; with the increase of Pi concentration the tension decreased along a reversed sigmoidal curve (Fig. 7; *insert*, Fig. 10 *a*); besides, the tension drop was as much as 70% or more in the presence of 1 mM MgATP (Fig. 7), and nearly 100% in the presence of 2 mM MgATP (*insert*, Fig. 10 *a*). As discussed above, the data obtained in the presence of 2 mM MgATP are considered to be more quantitative, so that we can conclude that the ability of Pi to suppress the tension is extraordinarily strong for the ADP-induced activation in the absence of Ca^{2+}.

Such features can be simply interpreted according to the kinetic scheme of actomyosin ATPase (cf the following review articles; Hibberd and Trentham, 1986; Goldman, 1987; Goldman and Brenner, 1987; Brenner, 1990; Homsher and Millar, 1990; Geeves, 1991) as follows. Under the condition of ADP-induced contraction in the absence of Ca^{2+}, myosin heads will be mostly (> 50%) in an AM-ADP complex, which is in a strong binding state and functions as an allosteric desuppressor of the inhibition, as pointed out repeatedly above. If Pi binds to this key complex and transforms it to an AM-ADP-Pi complex that is in a weak binding state having no desuppression function, the fibers will be easily deactivated again. If this is the case, as the Pi concentration is increased, the tension will decrease along a sigmoidal curve of tension vs MgADP concentration (Fig. 4) in an opposite direction, so that the decrease of tension occurs along either a reversed sigmoidal curve or a monotonous curve depending on the concentration of coexisting MgADP, or to be more precise, on the ratio of the concentrations of MgADP and MgATP (Figs. 7 and 10 *a*).

Now, Pi is considered to be a mixture of diprotonated form ($H_2PO_4^-$) and monoprotonated form without (HPO_4^{2-}) and with potassium ($KHPO_4^-$), and so on. There is a debate as to whether the diprotonated form (Dawson et al., 1986; Nosek et al., 1987) or all the species of Pi (Chase and Kushmerick, 1988) are responsible for the force reduction under a usual contracting condition with Ca^{2+}. Our results summarized in Fig. 10 *b* suggest that, at least under a SPOC condition, the diprotonated form is responsible. Although the relative tension curve obtained by changing the pH value at 5 mM Pi was slightly different from that obtained by

changing the Pi concentration at pH 7.0 (Fig. 10 *b*), this can be ascribed to the direct effect of pH on tension.

Synergistic effects of ADP and Pi

When both MgADP and Pi over critical concentrations, which depend on the concentration of MgATP, were added to the relaxing solution, spontaneous tension oscillation (SPOC) of muscle fibers was observed (Fig. 8). As far as we examined, the tension oscillation was not developed by the addition of either MgADP or Pi alone in the presence of MgATP and irrespective of the concentration of Ca^{2+}. Although the tension oscillation was not observed on a chart recorder, the intensity fluctuation of the fine structure of laser light diffraction lines, which originates from unorganized SPOC of sarcomeres, was clearly seen when MgADP alone was added (this phenomenon was not observed upon addition of Pi alone); this does not mean, however, that Pi is not needed for SPOC because submillimolar concentrations of Pi will be easily accumulated inside the fibers. So, until complete removal of Pi becomes possible, we can not reach a conclusion as to whether SPOC is induced by the addition of MgADP alone under the relaxing condition. It is true, in any case, that the coexistence of MgADP and Pi with MgATP is most suitable to induce stable SPOC.

The effects of MgADP and Pi on tension with Ca^{2+} (Figs. 5 and 9) are apparently similar to those without Ca^{2+} (Figs. 4 and 7). However, it is considered that the effects are qualitatively different from each other; in the presence of Ca^{2+}, MgADP and Pi may change the fraction of strong binding and weak binding states through direct interaction with myosin, whereas in the absence of Ca^{2+}, they may modulate the state of thin filaments, either the on-state or the off-state, in an allosteric and cooperative fashion through an AM-ADP (-Pi) complex similarly to rigor complex (Bremmel and Weber, 1972). We believe that this difference is essential to SPOC. Why is SPOC observed only in the latter condition but not in the former one, even under a similarly low level of tension? The key to this question must lie in the above difference.

Role of elastic components in SPOC

Here, we have neglected the contribution of the parallel elastic components composed of connectin (titin) (Maruyama, 1986; Wang, 1985), which are responsible for the resting tension (Funatsu et al., 1990). The reason is that SPOC can occur even at very short sarcomere lengths of ~ 2.0 μm, at which the extension of the parallel elastic components will be negligibly small; also, the dynamic feature of SPOC is unchanged by treatment with trypsin, to which connectin (titin) is very sensitive, until the destruction of the ordered structure of myofibrils becomes clear under an optical microscope (data not shown).

Mechanochemical coupling essential to the mechanism of SPOC

We infer that during SPOC each (half-)sarcomere cycles through turned-on and turned-off states, which are induced by stretch activation and/or release deactivation, i.e., activation during yielding and deactivation due to release caused by yielding of an adjacent (half-) sarcomere. Here, we suggest the following two types of regulatory mechanisms, where the key point is that the enzymic activity of actomyosin is modulated by the mechanical strain. First, the myosin(cross-bridge)-linked regulation: this is probable because the kinetic constant of some step(s), not only the step of Pi release but also the isomerization step of AM-ADP-Pi and/or AM-ADP complexes, may depend on the strain imposed on cross-bridges (cf Goldman, 1987; Danzig and Goldman, 1989). Second, the actin-linked regulation: the flexibility of reconstituted thin filaments is regulated by the concentration of free Ca^{2+} (Ishiwata and Fujime, 1972) and the flexibility change with Ca^{2+} is amplified by the interaction with myosin (Ishiwata and Fujime, 1971; Oosawa et al., 1973); conversely, the binding of myosin to reconstituted thin filaments increases the binding affinity of Ca^{2+} (Weber and Murray, 1973). From these properties, we infer that the strain of thin filaments induced by imposed stress may modify the functional state of thin filaments, so that the binding affinity and the state of cross-bridges are regulated. Other aspects of the molecular mechanism of SPOC will be discussed in the subsequent paper (Anazawa et al., 1992).

Physiological meaning of SPOC

It should be noted that the mechanochemical coupling essential to the mechanism of SPOC discussed above may play some role even under normal conditions. But, SPOC itself may not take place in vivo, because such high concentrations of MgADP as are required for SPOC will not be accumulated in living skeletal muscle, however severe muscle fatigue is.

On the other hand, some kinds of muscle may have the properties more suitable for SPOC. For example, cardiac myofibrils have more than ten times higher binding affinity to MgADP compared with skeletal muscle (Johnston and Adams, 1984). In practice, we found that SPOC of glycerinated cardiac muscle was observed in a lower concentration range of MgADP (Fukuda et al., 1991, and manuscript in preparation).

Cardiac muscle is not tetanizable while SPOC is observed under steady state. But, it may be important for the function of cardiac muscle that the contractile system has intrinsically such oscillatory properties.

Flight muscle, another example of which the physiological function is oscillation, needs activation by stretch in addition to Ca^{2+} to generate large tension; but the stretch is not needed if a low concentration of ADP is present (Pringle, 1967, 1978). It is inferred that the suppression, which may not be fully released by Ca^{2+}, is released by stretching of the muscle or the attachment of ADP to cross-bridges, which activates the muscle probably through the feed-back and allosteric regulation of transition between strong and weak-binding states of cross-bridges. Also, flight muscle is deactivated by quick release. In flight muscle, tension spontaneously oscillates without oscillation of membrane potential, i.e., the oscillation of free Ca^{2+} concentration, that is, the contractile system itself has oscillatory properties. In such muscle, feed-back regulation of tension through the tension-dependent (probably strain-dependent) change of state of cross-bridges as suggested in the above section may play a key role in its functioning. Thus, the molecular mechanism of oscillation of flight muscle may be essentially the same as that of SPOC.

This work was supported in part by Grants-in-Aid for Scientific Research (No. 61580226) and for Scientific Research on Priority Areas from the Ministry of Education, Science and Culture of Japan.

Received for publication 23 August 1991 and in final form 16 December 1991.

REFERENCES

Altringham, J. D., and I. A. Johnston. 1985. Effects of phosphate on the contractile properties of fast and slow muscle fibers from an antarctic fish. *J. Physiol. (Lond.).* 368:491–500.

Anazawa, T., K. Yasuda, and S. Ishiwata. 1992. Spontaneous oscillation of tension and sarcomere length in skeletal myofibrils. Microscopic measurement and analysis. *Biophys. J.* 61:1099–1108.

Armstrong, C. F., A. F. Huxley, and F. J. Julian. 1966. Oscillatory responses in frog skeletal muscle fibers. *J. Physiol. (Lond.).* 186:26–27.

Bremmel, R. D., and A. Weber. 1972. Cooperative behavior within the functional unit of the actin filament in vertebrate skeletal muscle. *Nature (Lond.).* 238:97–101.

Brenner, B. 1979. An indirect proof of stretch-induced Ca^{++} release from the sarcoplasmic reticulum in glycerinated skeletal and heart muscle preparations. *Basic Res. Cardiol.* 74:177–202.

Brenner, B. 1990. Muscle mechanics and biochemical kinetics. *In* Molecular mechanisms in muscular contraction. J. M. Squire, editor. The Macmillan Press Ltd. London. 77–149.

Chaen, S., K. Kometani, T. Yamada, and H. Shimizu. 1981. Substrate concentration dependences of tension, shortening velocity and ATPase activity of glycerinated fibers. *J. Biochem. (Tokyo).* 90:1611–1621.

Chalovich, J. M., P. B. Chock, and E. Eisenberg. 1981. Mechanism of action of troponin-tropomyosin. *J. Biol. Chem.* 256:575–578.

Chase, P. B., and M. J. Kushmerick. 1988. Effects of pH on contraction of rabbit fast and slow skeletal muscle fibers. *Biophys. J.* 53:935–946.

Cooke, R., and W. Bialek. 1979. Contraction of glycerinated muscle fibers as a function of the ATP concentration. *Biophys. J.* 28:241–258.

Cooke, R., and E. Pate. 1985. The effects of ADP and phosphate on the contraction of muscle fibers. *Biophys. J.* 48:789–798.

Cooke, R., K. Franks, G. B. Luciani, and E. Pate. 1988. The inhibition of rabbit skeletal muscle contraction by hydrogen ions and phosphate. *J. Physiol. (Lond.).* 395:77–97.

Danzig, J. A., and Y. E. Goldman. 1989. Photolysis of caged ATP in muscle fibers with negatively strained cross-bridges indicates that relaxation in the presence of MgADP is highly strain dependent. *Biophys. J.* 55:260*a*. (Abstr.)

Dawson, M. J., S. Smith, and D. R. Wilkie. 1986. The $[H_2PO_4^{-1}]$ may determine cross-bridge cycling rate and force reduction in living fatiguing muscle. *Biophys. J.* 49:268*a*. (Abstr.)

Ebashi, S., and M. Endo. 1968. Calcium ions and muscle contraction. *Prog. Biophys. Mol. Biol.* 18:123–183.

Eisenberg, E., and T. L. Hill. 1985. Muscle contraction and free energy transduction in biological systems. *Science (Wash. DC).* 227:999–1006.

Fabiato, A., and F. Fabiato. 1978. Myofilament-generated tension oscillations during partial calcium activation and activation dependence of the sarcomere length-tension relation of skinned cardiac cells. *J. Gen. Physiol.* 72:667–699.

Fukuda, N., T. Fujita, and S. Ishiwata. 1991. Effects of ADP, inorganic phosphate and calcium on spontaneous tension oscillation of glycerinated cardiac muscle. *J. Muscle Res. Cell Motil.* 12:304*a*. (Abstr.)

Funatsu, T., H. Higuchi, and S. Ishiwata. 1990. Elastic filaments in skeletal muscle revealed by selective removal of thin filaments with plasma gelsolin. *J. Cell Biol.* 110:53–62.

Geeves, M. A. 1991. The dynamics of actin and myosin association and the cross-bridge model of muscle contraction. *Biochem. J.* 274:1–14.

Goldman, Y. E. 1987. Kinetics of the actomyosin ATPase in muscle fibers. *Annu. Rev. Physiol.* 49:637–654.

Goldman, Y. E., and B. Brenner. 1987. Special topic: molecular mechanism of muscle contraction. *Annu. Rev. Physiol.* 49:629–636.

Goodall, M. C. 1956. Auto-oscillations in extracted muscle fibre systems. *Nature (Lond.).* 177:1238–1239.

Greene, L. E., and E. Eisenberg. 1980. Cooperative binding of myosin subfragment-1 to the actin-troponin-tropomyosin complex. *Proc. Natl. Acad. Sci. USA.* 77:2616–2620.

Herzig, J. W., J. W. Peterson, J. C. Rüegg, and R. J. Solaro. 1981. Vanadate and phosphate ions reduce tension and increase cross-bridge kinetics in chemically skinned heart muscle. *Biochim. Biophys. Acta.* 672:191–196.

Hibberd, M. G., J. A. Dantzig, D. R. Trentham, and Y. E. Goldman. 1985. Phosphate release and force generation in skeletal muscle fibers. *Science (Wash. DC).* 228:1317–1319.

Hibberd, M. G., and D. R. Trentham. 1986. Relationships between chemical and mechanical events during muscular contraction. *Annu. Rev. Biophys. Biophys. Chem.* 15:119–161.

Hoar, P. E., C. W. Mahoney, and W. G. L. Kerrick. 1987. $MgADP^-$ increases maximum tension and Ca^{2+} sensitivity in skinned rabbit soleus fibers. *Pfluegers Arch. Eur. J. Physiol.* 410:30–36.

Homsher, E., and N. C. Millar. 1990. Caged compounds and striated muscle contraction. *Annu. Rev. Physiol.* 52:875–896.

Horiuti, K. 1986. Some properties of the contractile system and sarcoplasmic reticulum of skinned low fibres from *Xenopus* muscle. *J. Physiol. (Lond.).* 373:1–23.

Ishiwata, S., and S. Fujime. 1971. Effect of Ca^{2+} on dynamic properties of muscle proteins studied by quasielastic light scattering. *J. Phys. Soc. Japan.* 31:1601.

Ishiwata, S., and S. Fujime. 1972. Effect of calcium ions on the flexibility of reconstituted thin filament of muscle studied by quasielastic scattering of laser light. *J. Mol. Biol.* 68:511–522.

Ishiwata, S., and T. Funatsu. 1985. Does actin bind to the ends of thin filaments in skeletal muscle? *J. Cell Biol.* 100:282–291.

Ishiwata, S., K. Muramatsu, and H. Higuchi. 1985. Disassembly from both ends of thick filaments in rabbit skeletal muscle fibers. An optical diffraction study. *Biophys. J.* 47:257–266.

Ishiwata, S., N. Okamura, H. Shimizu, T. Anazawa, and K. Yasuda. 1991. Spontaneous oscillatory contraction (SPOC) of sarcomeres in skeletal muscle. *Adv. Biophys.* 27:227–235.

Iwazumi, T., and G. H. Pollack. 1981. The effect of sarcomere nonuniformity on the sarcomere length-tension relationship of skinned fibers. *J. Cell. Physiol.* 106:321–337.

Johnston, R. E., and P. E. Adams. 1984. ADP binds similarly to rigor muscle myofibrils and to actomyosin-subfragment one. *FEBS (Fed. Eur. Biochem. Soc.) Lett.* 174:11–14.

Kawai, M. 1986. The role of orthophosphate in cross-bridge kinetics in chemically skinned rabbit psoas fibres as detected with sinusoidal and step length alterations. *J. Muscle Res. Cell Motil.* 7:421–434.

Kawai, M., K. Guth, K. Winnikes, C. Haist, and J. C. Rüegg. 1987. The effect of inorganic phosphate on ATP hydrolysis rate and the tension transients in chemically skinned rabbit psoas fibers. *Pfluegers Arch. Eur. J. Physiol.* 408:1–9.

Kawai, M., and H. R. Halvorson. 1989. Role of MgATP and MgADP in the cross-bridge kinetics in chemically skinned rabbit psoas fibers. *Biophys. J.* 55:595–603.

Kawai, M., and H. R. Halvorson. 1991. Two step mechanism of phosphate release and the mechanism of force generation in chemically skinned fibers of rabbit psoas muscle. *Biophys. J.* 59:329–342.

Kodama, T., K. Fukui, and K. Kometani. 1986. The initial phosphate burst in ATP hydrolysis by myosin and subfragment-1 as studied by a modified malachite green method for determination of inorganic phosphate. *J. Biochem. (Tokyo).* 99:1465–1472.

Kushmerick, M. J., and R. J. Podolsky. 1969. Ionic mobility in muscle cells. *Science (Wash. DC).* 166:1297–1298.

Lanzetta, P. A., L. J. Alvarez, P. S. Reinach, and O. A. Candia. 1979. An improved assay for nanomole amounts of inorganic phosphate. *Anal. Biochem.* 100:95–97.

Lienhard, G. E., and I. I. Secemski. 1973. P^1,P^5-Di(adenosine-5′)pentaphosphate, a potent multisubstrate inhibitor of adenylate kinase. *J. Biol. Chem.* 248:1121–1123.

Lorand, L., and C. Moos. 1956. Auto-oscillations in extracted muscle fibre systems. *Nature (Lond.).* 177:1239.

Mannherz, G. M. 1968. ATP-spaltung und ATP-diffusion in oscillierenden extrahierten muskelfasern. *Pfluegers Arch. Eur. J. Physiol.* 303:230–248.

Maruyama, K. 1986. Connectin, an elastic filamentous protein of striated muscle. *Int. Rev. Cytol.* 104:81–114.

Millar, N. C., and E. Homsher. 1990. The effect of phosphate and calcium on force generation in glycerinated rabbit skeletal muscle fibers. A steady-state and transient kinetic study. *J. Biol. Chem.* 265:20234–20240.

Nosek, T. M., K. Y. Fender, and R. E. Godt. 1987. It is diprotonated inorganic phosphate that depresses force in skinned skeletal muscle fibers. *Science (Wash. DC).* 236:191–193.

Ohnishi, S. T., and Barr, J. K. 1978. A simplified method of quantitating protein using the biuret and phenol reagents. *Anal. Biochem.* 86:193–200.

Ohno, T., and T. Kodama. 1991. Kinetics of adenosine triphosphate hydrolysis by shortening myofibrils from rabbit psoas muscle. *J. Physiol. (Lond.).* 441:685–702.

Okamura, N., and S. Ishiwata. 1988. Spontaneous oscillatory contraction of sarcomeres in skeletal myofibrils. *J. Muscle Res. Cell Motil.* 9:111–119.

Onodera, S., and Y. Umazume. 1984. Periodic contraction of skinned muscle fiber under high pH. *Biophys., Suppl. (Jpn.).* 24:S84*a*. (Abstr.)

Onodera, S. 1990. Oscillatory contraction waves in skinned skeletal muscle at high-pH without Ca^{2+}. *Jikeikai Med. J.* 37:447–455.

Oosawa, F., S. Fujime, S. Ishiwata, and K. Mihashi. 1973. Dynamic property of F-actin and thin filament. *Cold Spring Harbor Symp. Quant. Biol.* 37:277–286.

Pate, E., and R. Cooke. 1989. A model of cross-bridge action: the effects of ATP, ADP and Pi. *J. Muscle Res. Cell Motil.* 10:181–196.

Pringle, J. W. S. 1967. The contractile mechanism of insect fibrillar muscle. *Prog. Biophys. Mol. Biol.* 17:1–60.

Pringle, J. W. S. 1978. Stretch activation of muscle: function and mechanism. *Proc. R. Soc. Lond. B.* 201:107–130.

Rüegg, J. C., M. Schadler, G. J. Steiger, and G. Muller. 1971. Effects of inorganic phosphate on the contractile mechanism. *Pfluegers Arch. Eur. J. Physiol.* 325:359–364.

Schoenberg, M., and E. Eisenberg. 1987. ADP binding to myosin cross-bridges and its effect on the cross-bridge detachment rate constants. *J. Gen. Physiol.* 89:905–920.

Sleep, J. 1984. The adenosine-triphosphatase activity of muscle-fibers. *J. Physiol. (Lond.).* 326:5*a*. (Abstr.)

Stephenson, D. G., and D. A. Williams. 1982. Effects of sarcomere length on the force-pCa relation in fast- and slow-twitch skinned muscle fibres from the rat. *J. Physiol. (Lond.).* 333:637–653.

Sweitzer, N. K., and R. L. Moss. 1990. The effect of altered temperature on Ca^{2+}-sensitive force in permeabilized myocardium and skeletal muscle. *J. Gen. Physiol.* 96:1221–1245.

Wang, K. 1985. Sarcomere-associated cytoskeletal lattices in striated muscle: reviews and hypothesis. *In* Cell and Muscle Motility. Vol. 6. J. W. Shay, editor. Plenum Publishing Corp., New York. 315–369.

Webb, M. R., M. G. Hibberd, Y. E. Goldman, and D. R. Trentham. 1986. Oxygen exchange between Pi in the medium and water during ATP hydrolysis mediated by skinned fibers from rabbit skeletal muscle: Evidence for Pi binding to a force-generating state. *J. Biol. Chem.* 261:15557–15564.

Weber, A., and J. M. Murray. 1973. Molecular control mechanisms in muscle contraction. *Physiol. Rev.* 53:612–673.

Spontaneous oscillation of tension and sarcomere length in skeletal myofibrils

Microscopic measurement and analysis

Takashi Anazawa, Kenji Yasuda, and Shin'ichi Ishiwata
Department of Physics, School of Science and Engineering, Waseda University, Okubo, Shinjuku-ku, Tokyo 169, Japan

ABSTRACT We have devised a simple method for measuring tension development of single myofibrils by micromanipulation with a pair of glass micro-needles. The tension was estimated from the deflection of a flexible needle under an inverted phase-contrast microscope equipped with an image processor, so that the tension development is always accompanied by the shortening of the myofibril (auxotonic condition) in the present setup. The advantage of this method is that the measurement of tension (1/30 s for time resolution and about 0.05 μg for accuracy of tension measurement; 0.05 μm as a spatial resolution for displacement of the micro-needle) and the observation of sarcomere structure are possible at the same time, and the technique to hold myofibrils, even single myofibrils, is very simple. This method has been applied to study the tension development of glycerinated skeletal myofibrils under the condition where spontaneous oscillation of sarcomeres is induced, i.e., the coexistence of MgATP, MgADP and inorganic phosphate without free Ca^{2+}. Under this condition, we found that the tension of myofibrils spontaneously oscillates accompanied by the oscillation of sarcomere length with a main period of a few seconds; the period was lengthened and shortened with stretch and release of myofibrils. A possible mechanism of the oscillation is discussed.

INTRODUCTION

The molecular mechanism of muscle contraction and tension generation has been studied in detail for several decades by using intact, or mechanically or chemically skinned single fibers (a few tens of μm in diameter) (cf Cooke, 1986; Goldman and Brenner, 1987; Pollack, 1990). However, such an approach has several disadvantages for the study of structure and function of muscle; first, it is difficult to change quickly or even to maintain the internal chemical environment because of slow diffusion of chemical substances. Second, it is difficult to analyze the fine structure of sarcomeres, e.g., the optical properties of constituent proteins, with high spatial resolution under an optical microscope. Although the former problem has been partly overcome by the recent introduction of caged compounds (Goldman and Brenner, 1987; Homsher and Miller, 1990), it will be difficult to resolve the latter one.

Recently, Kishino and Yanagida (1988) succeeded in measuring the tension (of the order of one ng) imposed on a single actin filament by using a pair of glass micro-needles and an optical system which detects a displacement of the needle with a spatial resolution of 0.1 nm under an optical microscope (Kamimura, 1987; Iwazumi, 1987*a*). This system and such an in vitro reconstituted system (e.g., Chaen et al., 1989) are undoubtedly powerful techniques to elucidate the function and the mechanism of a minimum motile unit consisting of actin and myosin molecules.

On the other hand, from a physiological point of view, a single myofibril is considered to be the minimum structural and functional unit of muscle. This implies that the physiological function of myofibrils may not be a simple summation of the function of each motile unit; to elucidate the molecular mechanism of contraction and force generation, we will finally need to investigate the structure and function of motile units in an organized contractile system of muscle, i.e., a myofibril.

Here, we have devised a simple method appropriate for investigating both the mechanical properties, i.e., active or resting tension or stiffness, of myofibrils and their fine structure at the same time under an inverted optical microscope equipped with a micromanipulator. It seems that our method is simpler than the previous ones (Borejdo and Schweitzer, 1977; Iwazumi, 1987*a* and *b*; Bartoo et al., 1988).

We applied this technique and setup to measure the generated tension of single myofibrils and small bundles of myofibrils having a width of 1–10 μm, especially under conditions where the length of every sarcomere spontaneously oscillates (so-called SPOC condition, in which high concentrations of MgADP and Pi coexist with MgATP; Okamura and Ishiwata, 1988; Ishiwata et al., 1991). It was recently found that the tension spontaneously oscillates in single fibers under the SPOC condition (see the preceding paper; Shimizu et al., 1992). However, in the fiber system, not only is the wave form

Address correspondence to Dr. Ishiwata.

Biophys. J. © Biophysical Society
Volume 61 May 1992 1099–1108
0006-3495/92/05/1099/10 $2.00

of tension oscillation complicated, but also it is difficult to measure the oscillation of sarcomere lengths under an optical microscope. The present study has demonstrated that those difficulties can be overcome. A preliminary report of this work has been presented (Anazawa et al., 1990).

MATERIALS AND METHODS

Solutions

Rigor solution, 60 mM KCl, 5 mM $MgCl_2$, 10 mM Tris-maleate (pH 6.8) and 1 mM EGTA; relaxing solution, 0.12 M KCl, 4 mM $MgCl_2$, 4 mM ATP, 20 mM 3-(*N*-morpholino)propanesulfonic acid (MOPS, pH 7.0) and 4 mM EGTA; contracting solution, 0.12 M KCl, 4 mM $MgCl_2$, 4 mM ATP, 20 mM MOPS (pH 7.0), 2 mM EGTA, and 1.9 mM $CaCl_2$; SPOC solution, 0.12 M KCl, 4 mM $MgCl_2$, 0.2 mM ATP, 4 mM ADP, 4 mM K-Pi, 20 mM MOPS (pH 7.0), and 4 mM EGTA. The pH value was adjusted for each preparation of solution. ATP and ADP were purchased from Boehringer Mannheim GmbH (Mannheim, Germany); MOPS was from Dojindo (Kumamoto, Japan). Other chemicals were of reagent grade.

Preparation of myofibrils

Single myofibrils and small bundles of myofibrils were prepared by gently homogenizing rabbit psoas glycerinated muscle fibers as described previously (Ishiwata and Funatsu, 1985), except that 1 mM leupeptin was added to 50% (*v*/*v*) glycerol, 0.5 mM $NaHCO_3$, and 5 mM EGTA to suppress the proteolysis of parallel elastic components during glycerination (Funatsu et al., 1990). Glycerol and undissolved large aggregates in the suspension of myofibrils were removed by low-speed centrifugation in the rigor solution at 2°C. The protein concentration of the suspension of myofibrils was estimated by means of the biuret reaction.

Perfusion chamber and manipulation of myofibrils

The main part of the perfusion chamber with a size of 24 × 60 × 1 mm was made of Lucite (Fig. 1). The open base of the chamber was sealed with a cover slip (24 × 60 mm), of which the outer part was fixed to the Lucite with Vaseline. A suspension of myofibrils was allowed to settle in the chamber, then a pair of glass micro-needles were put down and the upper surface of the solution was covered with a cover slip (22 × 22 mm), which is indispensable for obtaining a clear image by phase-contrast microscopy. The solution, of which the effective volume in the chamber was 50 μl, was exchanged by continuously sucking it up from an outlet through a peristaltic pump and adding fresh solution from an inlet with a micropipette; because of the small space between the upper cover slip and the outlet (or inlet), the volume of solution (~50 μl) in the space under the cover slip remained nearly constant even if the solution was strongly sucked up; because only the solution that overflowed from the space was sucked up, steady exchange of solution was made possible. Because the micro-needles moved slightly during flow of the solution, the exchange of solution was not performed during experiments.

A pair of glass micro-needles were fixed with epoxy resin to glass rods of which the thickness at the tip was ~0.3 mm. The size of the micro-needles was 5–15 μm thick and 0.3–1.5 mm long, depending on the required stiffness. The glass rods were each connected to a micromanipulator, i.e., the one with a flexible micro-needle was coupled to a water-pressure-controlled 3-D-micromanipulator (WR-90, Narishige, Tokyo; its drift with time is much smaller than that of an oil-pressure-controlled one, within one pixel on a TV monitor [~50 nm] in 1 min irrespective of imposed load) and the other with a stiffer micro-needle to an oil-pressure-controlled 3-D-micromanipulator (MO-188, Narishige). Myofibrils which are sticky to glass surface were attached to a pair of glass micro-needles, perpendicularly to the micro-needles, as shown in the enlarged figure in Fig. 1 and as described in the Results section. The stiffness (Hooke's elastic constant) of glass micro-needles used in the present work was determined under an optical microscope to be ~300 μg/μm for a stiffer needle by direct measurement and 1.06 μg/μm for a flexible needle by cross-calibration (Kishino and Yanagida, 1988; Ishijima et al., 1991). We confirmed that the deflection of the flexible micro-needle disappeared without oscillation (over-damping) within 1/30 s, indicating the characteristic frequency of the needle was larger than 30 Hz, which is the limit of time resolution in our system.

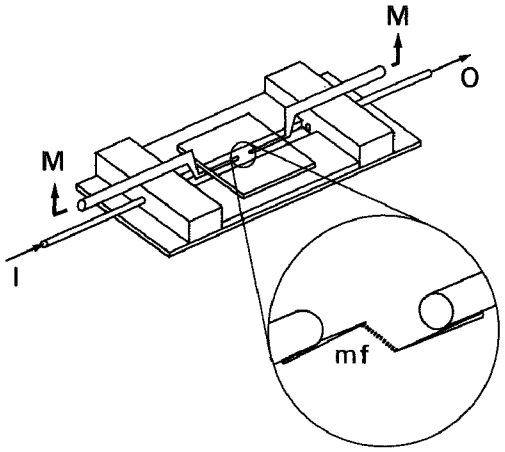

FIGURE 1 Schematic view of a perfusion chamber and a pair of glass micro-needles holding a myofibril (*mf*). Solution is put in through an inlet (*I*) and sucked up through an outlet (*O*). Both micro-needles are attached to micromanipulators (*M*). For details, see Materials and Methods.

The perfusion chamber was set on the stage of an inverted microscope (DIAPHOT-TMD, Nikon Co., Ltd., Tokyo), on which the micromanipulators were mounted. For holding myofibrils, a dry type of phase-contrast objective lens (Plan 40 × DM, Nikon) was used and for measuring tension, an oil immersion type of phase-contrast objective lens (Plan Apo 60 × oil DM, NA = 1.40, Nikon) was used to obtain a higher spatial resolution.

Measurement of tension and sarcomere length

A schematic diagram showing the system for microscopic analysis of myofibrils is shown in Fig. 2. A single myofibril or a small bundle of myofibrils was held by a pair of glass micro-needles as described in Results and the image was monitored by a CCD camera (C3077, Hamamatsu Photonics K.K., Hamamatsu, Japan) equipped with a TV zoom lens (0.9 – 2.25×, Nikon, Tokyo); a stiffer needle was used for the manipulation, i.e., stretching and imposing a load on myofibrils, and a flexible one was used for tension measurement. The displacements of both needles were measured by use of a double-channel position detector (Width analyzer C3161, Hamamatsu Photonics K.K.); to increase the accuracy of the measurement, the positions of

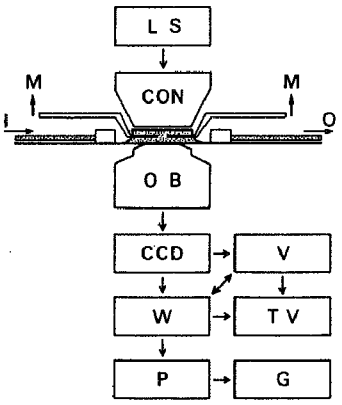

FIGURE 2 Schematic diagram showing a system for microscopic analysis of myofibrils. A cross-section of a perfusion chamber is illustrated. (*LS*) light source; (*CON*) condenser lens; (*OB*) objective lens; (*CCD*) CCD camera; (*V*) videotape recorder; (*W*) width analyzer; (*TV*) TV monitor; (*P*) personal computer; (*G*) graphic display; (*M*, *I*, and *O*) the same as in Fig. 1. For details, see Materials and Methods.

the edge of the needle were averaged along the needle within the window (cf Fig. 4 *b*). When the objective lens of 60× was used, the spatial resolution was ~50 nm (distance between adjacent pixels). The time resolution was 1/30 s. Data were analyzed in real time with a personal computer (PC-9801, NEC Inc., Tokyo) to obtain the developed tension (= [displacement of the flexible needle from an equilibrium position] × [Hooke's elastic constant of the needle]) and the average sarcomere length (= [total length of myofibril, i.e., the distance between the two micro-needles]/[number of sarcomeres]). In the present work, the accuracy of tension measurement was ~0.5 μg (= 0.05 μm [distance between adjacent pixels] × 1.06 μg/μm (Hooke's elastic constant of the flexible needle)). Images stored on a video tape (S-VHS; recorder HV-V1000, Mitsubishi Electric Co., Ltd., Tokyo) can also be analyzed afterwards through the width analyzer and computer (cf Fig. 2), though the spatial resolution is halved (~0.1 μm).

Analysis of oscillation wave of tension

The wave form of tension oscillation with time was analyzed by FFT and the power spectrum was obtained. Data were accumulated every 30 ms for ~31 s (total of 1,024 data points) under each experimental condition. The major peak at the lowest frequency region was considered to correspond to the fundamental period of oscillation. Practically, we determined the fundamental period (T) as the inverse of the weighted average of frequencies in the peak zone located at the lowest frequency region of power spectra, i.e., $1/T = (\Sigma_i$ amplitude × frequency$)/(\Sigma_i$ amplitude), where the summation was taken over the frequencies of which the amplitudes were > 30% of the largest amplitude in the peak.

RESULTS

How to hold both ends of myofibrils

A suspension of myofibrils (~0.1 mg/ml) in rigor solution was put in the chamber and washed with the rigor solution; this washing did not shift myofibrils attached to the glass surface, but floating myofibrils which would disturb the manipulation of the micro-needles were removed. Then, a pair of glass micro-needles were slowly inserted into the solution vertically to the stage and placed at ~100 μm above the glass surface. The upper surface of the solution was covered with a cover slip (24 × 24 mm).

Myofibrils suitable for experiments, i.e., those in which striated structure looks regular with sharp *Z*-lines but neither distorted nor twisted and only one end was attached to a glass surface whereas the other end was detached, were selected by moving the stage of the optical microscope. We can use any size of myofibrils for experiments, even a single myofibril thinner than 1 μm if it is observable.

A single myofibril or a small bundle of myofibrils thus selected was held by a pair of glass micro-needles according to the procedure schematically shown in Fig. 3. First, one of the micro-needles (*L*) was inserted beneath the floating end of the myofibril and slightly drawn up; because myofibrils adhere to glass, the end of the myofibril was loosely attached to the needle by this procedure. Another micro-needle (*R*) was touched onto the other end of the myofibril from above (Fig. 3 *a*). Then, the needle *L* was carefully moved along the arrow without slackening but without over-stretching the myofibril; it has been pointed out that there is a possibility

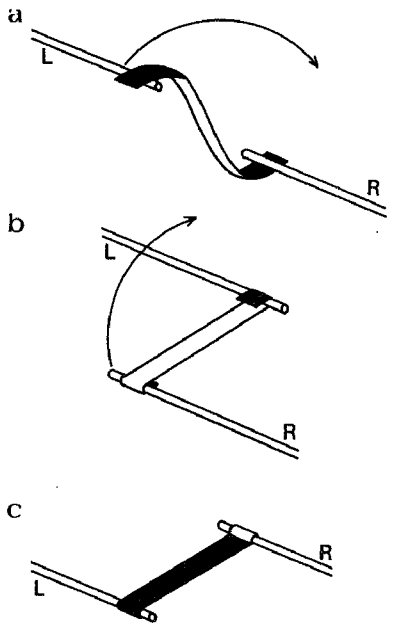

FIGURE 3 Schematic illustration showing the procedure (*a* to *c*) of holding both ends of myofibrils with a pair of micro-needles (*L* and *R*) under an inverted phase-contrast microscope. For details, see the text.

that myofibrils are damaged by over-stretching (Iwazumi, 1987*b*). The same procedure was repeated once more for the needle *R* (Fig. 3 *b*). The myofibril was thus twined around a pair of micro-needles (Fig. 3 *c*); this procedure is similar to that used to hold the ends of smooth muscle (cf Warshaw and Fay, 1983). Finally, both needles were placed at > 10 μm above the bottom glass surface and set so as to make the myofibril parallel to the optical stage and perpendicular to both needles. A phase-contrast micrograph of a single myofibril held by needles is shown in Fig. 4. The ordered structure of sarcomeres appears to be intact, extending over the whole myofibril (Fig. 4 *a*).

Measurement of tension development

The tension generated by myofibrils was measured by detecting the displacement of the flexible micro-needle by means of image processing (see Fig. 4 *b*). Fig. 5 is an

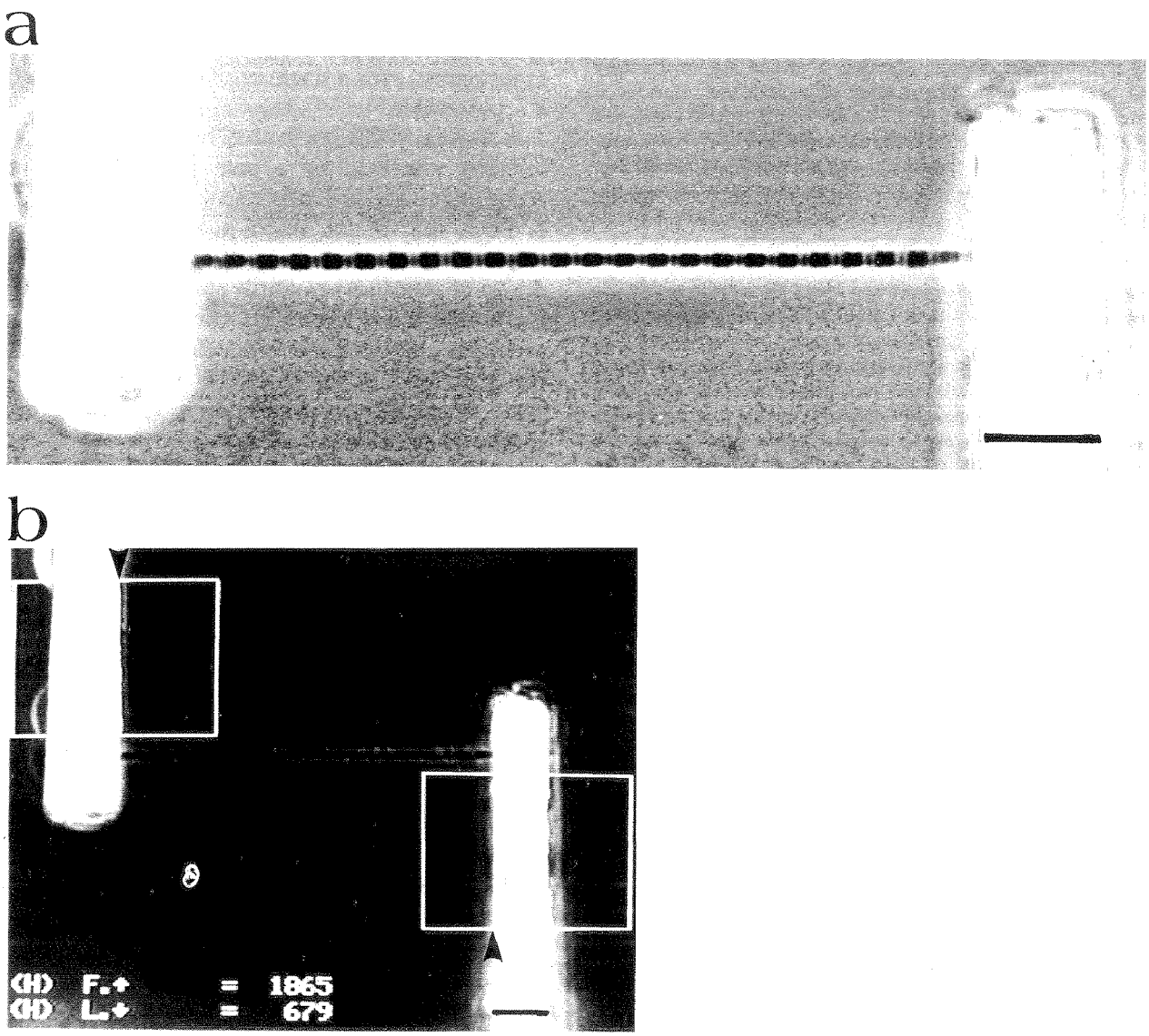

FIGURE 4 Optical micrograph of a single myofibril mounted in the perfusion chamber in rigor solution. (*a*) Phase-contrast micrograph of a single myofibril of which both ends were fixed to a pair of glass micro-needles, taken on Kodak Plus-X 35 mm photographic film. Scale bar, 10 μm. (*b*) The image of *a* taken by a CCD camera and processed by the width analyzer was displayed on a TV monitor (PVM-1442Q, Sony, Tokyo). The positions of the two micro-needles, i.e., the right-hand edge (*L*, *downward arrowhead*) of the left needle and the left-hand edge (*F*, *upward arrowhead*) of the right needle, were detected by setting a threshold for brightness in two windows. In the windows, black-and-white pictures are superimposed on a phase-contrast image. The positions of *F* and *L* are also indicated by the use of 2560 pixels (1280 pixels for a video tape image) on the monitor after averaging the position of the edge for each needle. Scale bar, 10 μm. For more details, see Materials and Methods.

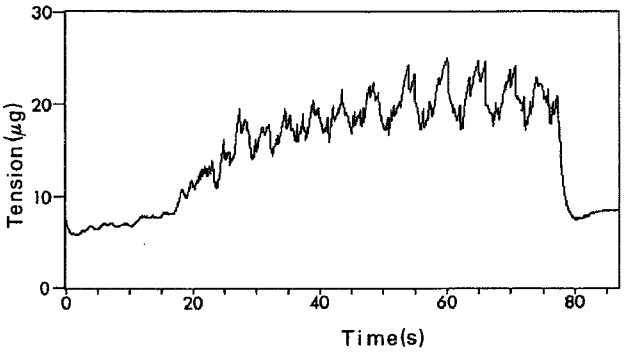

FIGURE 5 Time course of tension development under a SPOC condition. At time zero, injection of SPOC solution was started into the perfusion chamber in place of relaxing solution; after the steady SPOC was attained, relaxing solution was injected again. There was a lag time of ~3 s for exchanging solutions. A small bundle of myofibrils, ~3 μm thick and 36 sarcomeres long, was used. The average sarcomere length changed between 2.4 μm and 2.0 μm. For conditions, see Materials and Methods.

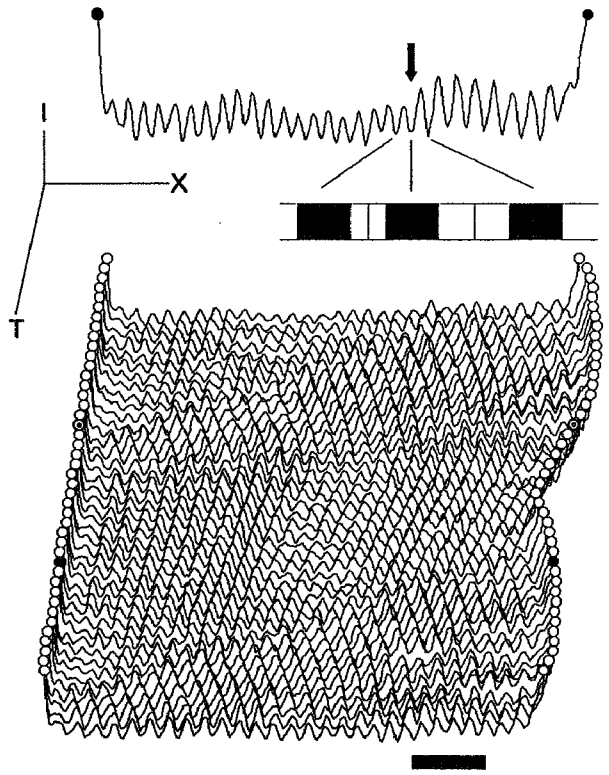

FIGURE 6 Time course of image profile of myofibrils showing propagation of a SPOC wave. *T*, *X*, and *I* axes, respectively, represent time course of SPOC, position along a myofibril and brightness of the phase-contrast image. Two circles at both sides correspond to the edges of the micro-needles. Serial images (every 1/15 s from top to bottom) show that the lengthening phase of (half) sarcomeres propagates with time from right to left along the long axis of the myofibril (see from the side). It can be seen that all the sarcomeres entered a shortening phase at a moment indicated by two double circles. In this example, a small bundle of myofibrils (~5 μm thick, 31 sarcomeres long) composed of several single myofibrils was used to obtain a typical organized state of SPOC. The needle at the left-hand side is stiff, so that the developed tension is represented by movement of the flexible needle on the right-hand side. An image profile of a myofibril corresponding to that with two filled circles is shown at the top of the figure as a typical example where the lengthening phase and shortening phase coexist, the boundary between them being indicated by an arrow; a peak and a valley of the image profile, respectively, correspond to the *I*-band and the *A*-band of the sarcomere as schematically shown, where the degree of lengthening and shortening of sarcomeres is exaggerated. Scale bar, 10 μm.

example of the time course of tension development under a SPOC condition. Myofibrils developed oscillatory tension, and the sarcomere lengths also oscillated; even at the very early stage before the tension was appreciably developed, the length of sarcomeres had already started to oscillate (see the small tension fluctuation at the initial lag phase of Fig. 5). It should also be noted that sarcomere lengths spontaneously oscillate even under an isometric condition, as previously reported (cf Okamura and Ishiwata, 1988). The lengthening phase of a (half) sarcomere propagated to adjacent sarcomere successively (SPOC wave). Usually, this SPOC wave propagated over a few to several sarcomeres along myofibrils but not over the whole length of myofibrils; SPOC waves appeared here and there, not at definite places but at random, and disappeared when two waves collided with each other; the travelling distance of a SPOC wave was usually restricted. Correspondingly, the tension oscillated with small amplitudes containing high-frequency components as shown in Fig. 5.

Organized state of SPOC

In some cases, a SPOC wave steadily and repeatedly propagated from one end to the other of myofibrils consisting of more than 10 sarcomeres (we call this an "organized" state of SPOC hereafter). A typical example is shown in Fig. 6 (corresponding tension records are shown in Fig. 7); a quick lengthening phase of the (half) sarcomere appeared from the right end of the myofibril and propagated to the left end with a nearly constant velocity (~70 μm/s in this example); after a lengthening phase of the order of 0.1 s, the sarcomeres started to shorten again slowly. The first sarcomere at the right end continued to shorten whereas the SPOC wave propagated through the myofibril, during which time the developed tension of the myofibril gradually decreased. Even after the last sarcomere at the left end had started to shorten (see the profile indicated by two double circles in Fig. 6), the first sarcomere kept on shortening for a while, very slowly; during this process, the devel-

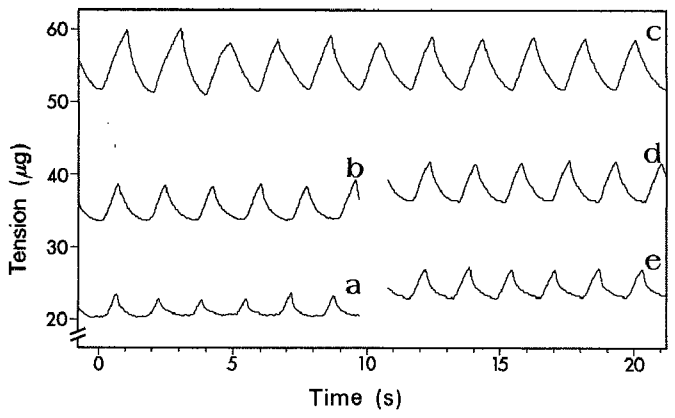

FIGURE 7 Reversible change with load (average tension) of the wave form of tension oscillation of myofibrils under an organized state of SPOC. A load imposed on the myofibril was stepwise increased from *a* to *c* and reversibly decreased from *c* to *e*. A sample is the same as in Fig. 6. For detailed analysis, see Figs. 8 and 9.

oped tension of the myofibril continued to increase (see the middle part of Fig. 6). And, when the tension reached the maximum, the first sarcomere started to lengthen again. Note that every sarcomere length oscillated with nearly the same saw-tooth wave form, irrespective of the developed tension (sustained load) of the myofibril.

It is empirically considered that the following factors are favorable to realize the organized state of SPOC: relatively thick myofibrils (the organized state is difficult to generate in a thin single myofibril, but easy in a thick bundle of myofibrils) with an appropriate total length and after staying in the SPOC state for a while. A small amount of stretch frequently triggers the organized state. Once the organized state was attained, it was stable against perturbation such as forced stretch or release and continued for more than 10 min without changing the essential features of its wave form. In the above example, the SPOC wave started from the side of the flexible needle, but this was not always the case; after the return to relaxation, the side from which the SPOC wave starts could not be controlled.

Analysis of tension oscillation of SPOC

After the organized state of SPOC was attained (cf Fig. 6), the stiffer micro-needle was moved slowly (~ 1 μm/s) so as to increase and reversibly decrease the load imposed on the myofibril. The tension response observed under a steady state for each load is shown in Fig. 7. Through this process, the pattern of propagation of the SPOC wave was unchanged. With increase of the load, both tension level and amplitude of oscillation increased, and average sarcomere length slightly increased. Also, Fig. 7 suggests that the period of oscillation increased and the wave form became nearly symmetrical with the increase of load.

Next, the wave form of oscillatory tension was analyzed by FFT. Fig. 8 shows the power spectra obtained from the data in Fig. 7. The spectra contained the main peak at 0.5–0.6 Hz and its higher harmonics. It became clear from the power spectra that with the increase of load, the main peak shifted to the lower frequency region, indicating that the fundamental period of SPOC increased, and besides, the amplitude of higher harmonics decreased, suggesting that the wave form of SPOC approached a sinusoidal form. The results of analysis are summarized in Fig. 9, showing that the period of SPOC (also the average sarcomere length) is nearly linear to the applied load and the change of the period is reversible.

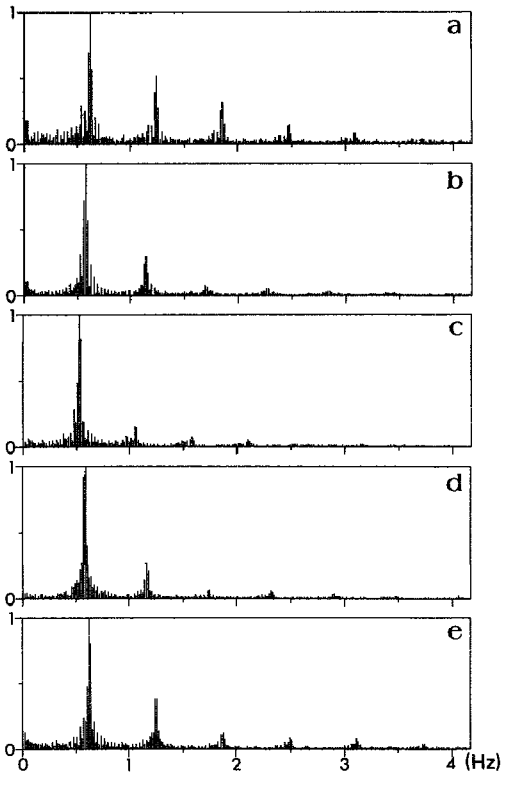

FIGURE 8 Power spectra of the wave form of tension oscillation of myofibrils. The power spectra, *a*, *b*, *c*, *d*, and *e*, (correponding to *a*–*e* in Fig. 7) were obtained by FFT of tension oscillation data for ~31 s (1,024 data points, with sampling every 30 ms). Abscissa, frequencies (Hz); ordinate, amplitude of each frequency component (arbitrary unit). For more details, see Materials and Methods.

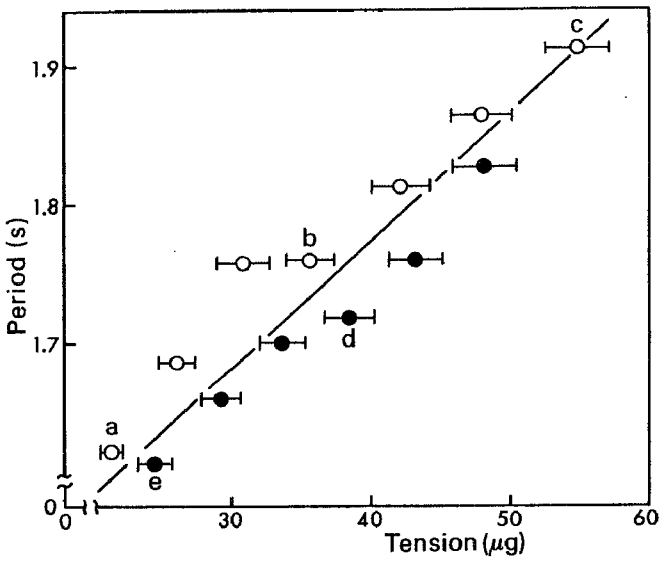

FIGURE 9 Dependence on load (average tension) of the fundamental period of tension oscillation. Abscissa, oscillated tension averaged (±SD, horizontal bars) with time; ordinate, a fundamental period obtained by FFT analysis of tension oscillation as shown in Fig. 8. Data were obtained in the order of *a*, *b*, *c*, *d*, and *e* by stepwise stretching (○) of the myofibril from the lower left to the upper right and then reversely shortening (●) it. Corresponding average sarcomere length (±SD; in μm unit) (oscillated total length of myofibril was averaged with time and divided by the number of sarcomeres) was 2.06 (0.02) for *a*, 2.22 (0.05) for *b*, 2.35 (0.07) for *c*, 2.19 (0.05 for *d*, and 1.97 (0.04) for *e*.

DISCUSSION

Advantages and disadvantages of our method

Up to the present, there have been only a few reports on the measurement of tension generated by a single skeletal myofibril, in spite of its importance (Borejdo and Schweitzer, 1977; Iwazumi, 1987 *a* and *b*; Bartoo et al., 1988; Pollack, 1990). The main reason is the difficulty of gently holding both ends of a myofibril while maintaining the internal structure.

The advantages of our method are that the means to hold myofibrils is simple, and the technique to measure the developed tension is also simple; besides, it is possible to observe the internal structure of myofibrils at the same time. The main disadvantage may be that the spatial (50 nm) and time (1/30 s) resolutions are limited by those intrinsic to the television camera-video system. Although the time resolution would be improved by using a high-speed camera, it will be more difficult to improve the spatial resolution as long as the system of image analysis with a television camera is used. If the movement of an object such as a glass micro-needle is suppressed to quite a small amount, an ultrasensitive detection system having a spatial resolution of the order of 0.1 nm can be used (Kamimura, 1987). Thus, this disadvantage of our system should be overcome in the future.

Our technique seems to be appropriate to examine the static properties of myofibrils such as resting tension rather than the dynamic properties, especially of fast phenomena; in fact, the present method has been successfully applied to investigate, for example, the contribution of the elasticity of connectin (titin) filaments (Wang, 1985; Maruyama, 1986) to the resting tension (concerning muscle fibers, see Funatsu et al., 1990). These results will be published elsewhere.

In the present work, we first applied our technique for measuring the oscillatory tension of myofibrils under a SPOC condition. Although the tension oscillation under SPOC conditions has been measured by using single fibers with a conventional method (Shimizu et al., 1992), it was impossible to detect the oscillation of sarcomere lengths at the same time. It has become possible, probably for the first time in the case of any auto-oscillation of skeletal muscle reported so far, to examine quantitatively the correlation between the oscillations of tension and sarcomere lengths by use of the method and system reported here to manipulate myofibrils and analyze the internal structure.

Phenomenological aspects of SPOC of myofibrils

We selected, as a typical example, an organized state of SPOC in which the SPOC wave steadily and repeatedly propagates from one end of myofibrils to the other. As reported previously (Okamura and Ishiwata, 1988), under SPOC conditions the length of each sarcomere (strictly speaking, half-sarcomere; cf Ishiwata et al., 1991) spontaneously oscillates with a saw-tooth wave form composed of a relatively rapid lengthening phase and a slow shortening phase. Here, the SPOC wave is defined as such a wave that propagates the lengthening phase of a (half)sarcomere to the adjacent one, the next one to that and so on. We found that in the organized state of SPOC, myofibrils generated oscillatory tension; the tension gradually decreased during the propagation of a SPOC wave and started to increase again after the SPOC wave had reached the end of myofibrils (cf Fig. 6). Thus, in the organized SPOC, the fundamental period of tension oscillation (Fig. 8) is equal to the average period of oscillation of sarcomere length, whereas this is not the case for the unorganized SPOC.

Because there is the restriction that the length of myofibrils plus the displacement of the flexible glass micro-needle, i.e., (the developed tension)/(the Hooke's elastic constant of the micro-needle), is maintained nearly constant in our experimental setup (auxotonic condition), the oscillations of tension and length of myofibrils are related as a mirror-image to each other. Thus, in the present experiments, we could not examine separately the oscillation of developed tension and the oscillation of total length of myofibrils. In future, we should examine them independently by keeping either the total length (isometric condition) or the developed tension (isotonic condition) constant, for example, by combining a piezo-electric element and a feed-back electronic system.

Effects of stretching of myofibrils on SPOC

What is the effect of stretching (imposing a load on) myofibrils on SPOC? Apparent features of the effects seem to be very similar to those in flight muscle (cf Pringle, 1967, 1978). In both cases, the activation of myofibrils is induced (stretch activation); one aspect of stretch activation in SPOC, the increase of the level of tension, is seen in Fig. 7. Concerning the mechanism of stretch activation, two types of mechanisms have been discussed in the preceding paper (Shimizu et al., 1992), where it is assumed that the enzymic activity is enhanced by the strain imposed on cross-bridges and/or thin filaments. We consider that such a large activation is possible because myofibrils are in the partially activated state, being intermediate between contraction and relaxation. Here, note that the stretch-induced increase of tension by partial Ca^{2+} activation (Endo, 1972, 1973) may belong to the same category.

The main reason why the period of SPOC was increased by the stretching of myofibrils (Figs. 8 and 9) is that the shortening phase was slightly prolonged. Whether or not the shortening velocity of each sarcomere obeys Hill's tension-velocity (P-V) relation is to be examined in future.

Relationship between oscillations of tension and sarcomere length

How is the oscillation of each sarcomere length related to the oscillation of tension of myofibrils? This is clearly seen in an "organized" state of SPOC. Fig. 6 suggests that the steady oscillation of each sarcomere length may not be directly related to the level of tension, and accordingly not related to the slow oscillation of tension generated by myofibrils, although the period of oscillation is affected by the level of tension. First, note that all (half)sarcomeres will bear nearly the same load at every moment, judging from the fact that the velocity of propagation of tension (mechanical impulse) along a myofibril is very fast, for example, 170 m/s under a contracting condition and only three to four times slower under a relaxing condition (Schoenberg et al., 1974), so that irrespective of conditions, the tension will be transmitted within a microsecond over the whole length of a myofibril. Thus, the oscillation of sarcomere length seems to be independent of the level of tension, because, as can be seen in Fig. 6, whereas the sarcomere at the right end starts to yield when the imposed load becomes maximum, the yielding of the sarcomere at the left end starts when the load becomes nearly minimum; this feature is not fixed but changeable, as is especially clear in an unorganized state of SPOC. Note that in spite of this fact, the wave forms of length oscillation of sarcomeres are similar to each other. From such considerations, we infer that the oscillation of sarcomeres may be controlled not by the level of tension but by the change of tension, i.e., mechanical impulse.

The integrated work performed by myofibrils during SPOC is effectively zero in an auxotonic condition, because the work performed during the contracting phase just cancels that performed during the lengthening phase. However, because of the feature described above, in the example shown in Fig. 6 the sarcomeres at the right-hand half received work from the outside but those at the left-hand half performed work to the outside. What is the difference among these sarcomeres? Here, the following questions arise: first, how is the timing of oscillation of each sarcomere controlled and second, how is the ATPase activity coupled to the oscillation of sarcomeres, which may be different in every sarcomere? In other words, is the feature of mechano-chemical coupling, i.e., the correspondence between chemical reaction (response) and mechanical response (event), different in every sarcomere? The answers to these questions may give us a key to resolve the mechanism of SPOC and, moreover, some insight into the mechanism of contraction and its regulation coupled to the mechanism of the ATPase reaction.

Molecular mechanism of SPOC

What is the mechanism of SPOC of each sarcomere and the propagation of the SPOC wave along a myofibril? Although we cannot present a definite answer, the key to resolve such questions may be present in the fact that, as pointed out above, each sarcomere bears the same load (produces the same tension) regardless of the difference of the internal state, that is, either lengthening or

shortening sarcomeres, and even stopped sarcomeres bear the same load.

Such a situation that half-sarcomeres in different states can maintain the same external force is probably possible because they are in an intermediate state between contraction and relaxation, in which they may self-control their state in response to the external force. The intermediate state can be induced not only by the SPOC condition as in the present work but also by low concentrations of Ca^{2+} (Fabiato and Fabiato, 1978; Iwazumi and Pollack, 1981; Stephenson and Williams, 1981) or high pH (Onodera and Umazume, 1984; Onodera, 1990).

Also note the inference that the oscillation of sarcomere length may be triggered by mechanical impulse but not by the level of tension. The mechanical impulse will be produced by quick yielding and reshortening of sarcomeres and propagate along a myofibril regardless of the level of tension. Based on these considerations, we present the following idea as a key to the mechanism of spontaneous oscillation of myofibrils. First, even if the internal states of sarcomeres happen to be different from each other, each sarcomere can bear the same load by self-control through changing the population of several chemical states of cross-bridges such as AM-ADP-Pi complex (AM, actomyosin), and AM-ADP complex. However, the response to the mechanical impulse may be different for each chemical state of cross-bridges (cf Huxley and Simmons, 1971; Goldman, 1987; Brenner, 1990); we assume that a particular chemical state which is weak against the mechanical impulse may be dominant in nearly stopped half-sarcomeres, so that they seem to yield easily. This yielding will produce a new mechanical impulse.

In summary, we suggest that the principal role of MgADP and Pi in SPOC is to maintain the intermediate state of (half)sarcomeres, that is, probably to make AM-ADP-Pi complex and AM-ADP complex dominant so that the state can be self-controlled in response to the mechanical impulse to keep the myofibril a dynamic state, SPOC.

This work was supported in part by Grants-in Aid for Scientific Research (No. 03680224) and for Scientific Research on Priority Areas from the Ministry of Education, Science and Culture of Japan.

Received for publication 23 August 1991 and in final form 16 December 1991.

REFERENCES

Anazawa, T., K. Yasuda, and S. Ishiwata. 1990. Measurement of tension of single myofibrils with micromanipulation. *Biophys. Suppl.* (*Jpn.*). 30:S75. (Abstr.)

Bartoo, M. L., T. Tameyasu, D. H. Burns, and G. H. Pollack. 1988. Stepwise shortening in single myofibrils. *Biophys. J.* 53:370*a*. (Abstr.)

Borejdo, J., and A. Schweitzer. 1977. Tension generation by isolated myofibrils. *J. Mechanochem. Cell Motil.* 4:189–204.

Brenner, B. 1990. Muscle mechanics and biochemical kinetics. *In* Molecular Mechanisms in Muscular Contraction. J. M. Squire, editor. The Macmillan Press Ltd. London. 77–149.

Chaen, S., K. Oiwa, T. Shimmen, H. Iwamoto, and H. Sugi. 1989. Simultaneous recordings of force and sliding movement between a myosin-coated glass microneedle and actin cables in vitro. *Proc. Natl. Acad. Sci. USA.* 86:1510–1514.

Cooke, R. 1986. The mechanism of muscle contraction. *CRC Rev. Biochem.* 21:53–118.

Endo, M. 1972. Stretch-induced increase in activation of skinned muscle fibres by calcium. *Nature* (*Lond.*) 237:211–213.

Endo, M. 1973. Length dependence of activation of skinned muscle fibers. *Cold Spring Harbor Symp. Quant. Biol.* 37:505–510.

Fabiato, A., and F. Fabiato. 1978. Myofilament-generated tension oscillations during partial calcium activation and activation dependence of the sarcomere length-tension relation of skinned cardiac cells. *J. Gen. Physiol.* 72:667–699.

Funatsu, T., H. Higuchi, and S. Ishiwata. 1990. Elastic filaments in skeletal muscle revealed by selective removal of thin filaments with plasma gelsolin. *J. Cell Biol.* 110:53–62.

Goldman, Y. E. 1987. Kinetics of the actomyosin ATPase in muscle fibers. *Annu. Rev. Physiol.* 49:637–654.

Goldman, Y. E., and B. Brenner. 1987. Special topic: molecular mechanism of muscle contraction. *Annu. Rev. Physiol.* 49:629–636.

Homsher, E., and N. C. Millar. 1990. Caged compounds and striated muscle contraction. *Annu. Rev. Physiol.* 52:875–896.

Huxley, A. F., and R. M. Simmons. 1971. Proposed mechanism of force generation in striated muscle. *Nature* (*Lond.*). 233:533–538.

Ishijima, A., T. Doi, K. Sakurada, and T. Yanagida. 1991. Subpiconewton force fluctuations of actomyosin in vitro. *Nature* (*Lond.*). 352:301–306.

Ishiwata, S., and T. Funatsu. 1985. Does actin bind to the ends of thin filaments in skeletal muscle? *J. Cell Biol.* 100:282–291.

Ishiwata, S., N. Okamura, H. Shimizu, T. Anazawa, and K. Yasuda. 1991. Spontaneous oscillatory contraction (SPOC) of sarcomeres in skeletal muscle. *Adv. Biophys.* 27:227–235.

Iwazumi, T., and G. H. Pollack. 1981. The effect of sarcomere nonuniformity on the sarcomere length-tension relationship of skinned fibers. *J. Cell Physiol.* 106:321–337.

Iwazumi, T. 1987*a*. High-speed ultrasensitive instrumentation for myofibril mechanics measurements. *Am. J. Physiol.* 252:C253–C262.

Iwazumi, T. 1987*b*. Mechanics of the myofibril. *In* Mechanics of the Circulation. H. E. D. J. ter Keurs, and J. V. Tyberg, editors. Martinus Nijhoff, Dordrecht. 37–49.

Kamimura, S. 1987. Direct measurement of nanometric displacement under an optical microscope. *Appl. Opt.* 26:3425–3427.

Kishino, A., and T. Yanagida. 1988. Force measurements by micromanipulation of a single actin filament by glass needles. *Nature* (*Lond.*). 334:74–76.

Maruyama, K. 1986. Connectin, an elastic filamentous protein of striated muscle. *Int. Rev. Cytol.* 104:81–114.

Okamura, N., and S. Ishiwata. 1988. Spontaneous oscillatory contraction of sarcomeres in skeletal myofibrils. *J. Muscle Res. Cell Motil.* 9:111–119.

Onodera, S., and Y. Umazume. 1984. Periodic contraction of skinned muscle fiber under high pH. *Biophys. Suppl.* (*Jpn.*). 24:S84. (Abstr.)

Onodera, S. 1990. Oscillatory contraction waves in skinned skeletal muscle at high pH without Ca^{2+}. *Jikeikai Med. J.* 37:447–455.

Pollack, G. H. 1990. Muscles and Molecules: Uncovering the Principles of Biological Motion. Ebner and Sons Publishers, Seattle, Washington. 300 pp.

Pringle, J. W. S. 1967. The contractile mechanism of insect fibrillar muscle. *Prog. Biophys. Mol. Biol.* 17:1–60.

Pringle, J. W. S. 1978. Stretch activation of muscle: function and mechanism. *Proc. R. Soc. Lond. B.* 201:107–130.

Schoenberg, M., J. B. Wells, and R. J. Podolsky. 1974. Muscle compliance and the longitudinal transmission of mechanical impulses. *J. Gen. Physiol.* 64:623–642.

Shimizu, H., T. Fujita, and S. Ishiwata. 1992. Regulation of tension development by MgADP and Pi without Ca^{2+}. Role in spontaneous tension oscillation of skeletal muscle. *Biophys. J.* 61:1087–1098.

Stephenson, D. G., and D. A. Williams. 1981. Calcium-activated force response in fast- and slow-twitch skinned muscle fibers of the rat at different temperatures. *J. Physiol. (Lond.).* 317:281–317.

Wang, K. 1985. Sarcomere-associated cytoskeletal lattices in striated muscle: reviews and hypothesis. *In* Cell and Muscle Motility. Vol. 6. J. W. Shay, editor. Plenum Publishing Corp., New York. 315–369.

Warshaw, D. M., and F. S. Fay. 1983. Cross-bridge elasticity in single smooth muscle cells. *J. Gen. Physiol.* 82:157–199.

Biochimica et Biophysica Acta, 1159 (1992) 94–98

BBAPRO 34294

Super helix formation of actin filaments in an in vitro motile system

Yuichiro Tanaka [a], Akihiko Ishijima [a] and Shin'ichi Ishiwata [b]

[a] *Wako Research Center, Honda Research and Development, Saitama (Japan) and* [b] *Department of Physics, School of Science and Engineering, Waseda University, Tokyo (Japan)*

(Received 15 April 1992)

Key words: Actin filament; Super helix formation; Motile system; Muscle contraction

Muscle contraction results from relative sliding of actin and myosin filaments. However, the possibility that actin filaments twist or rotate during sliding has not yet been experimentally investigated. We found that a super helix of an actin filament is formed in an in vitro motile system. This fact suggests that an actin filament twists and rotates due to a torque component of a sliding force generated at cross-bridges.

Introduction

It is established that muscle contraction results from relative sliding of actin and myosin filaments [1,2]. This sliding mechanism has been studied for a long time, usually in an organized contractile system, such as muscle fibers. However, the physical properties of the sliding force are not yet clarified. For example, although actin and myosin filaments have a helical symmetry, the direction of the sliding force is thought to be, on the average, parallel to the long axis of the filaments. It is unknown whether the force generated at each cross-bridge is tilted against the long axis of the filaments, i.e., whether the sliding force has a torque component. If it has a torque component,the sliding actin filaments may be rotated and/or twisted. The in vitro motile system, which was recently developed for studying sliding motion of single actin filaments [3,4], is expected to be suited for examining this possibility.

In an in vitro motile system, actin filaments labeled with rhodamine-phalloidin [5] move on myosin molecules which are bound to a silicone-coated [4] or nitrocellulose-coated [6] surface. Usually, actin filaments slide smoothly. We found that long actin filaments ($\geqslant 10$ μm) sometimes formed a super helix and a loop and even a ring. This fact indicates that the sliding filaments are twisted and probably rotated; i.e., the sliding force may be tilted against the long axis of actin filament.

Correspondence to: Y. Tanaka, Wako Research Center, Honda R&D Co., Ltd., 1-4-1 Chuo, Wako-shi, Saitama 351-01, Japan.

Materials and Methods

In the present work, rabbit skeletal muscle actin was extracted from acetone powder in 10 mM Tris-HCl (pH 7.8), 0.2 mM ATP and purified according to the procedure of Spudich and Watt [7] with slight modifications. Rabbit skeletal muscle myosin was prepared according to Kielley and Harrington [8]. Purified actin (0.1 mg/ml) was polymerized in 0.1 M KCl, 0.2 mM $MgCl_2$, 10 mM Hepes (pH 8.0) and then stored on ice overnight and labeled with equimolar tetramethylrhodamine-phalloidin (Molecular Probes, Eugene, OR, USA) [5].

The motility assay in the in vitro motile system was done as follows [4,9]. First, 1 mg/ml of myosin in 0.6 M KCl, 10 mM Hepes (pH 7.0) was applied onto the cover slip (24 × 40 mm) which was coated with silicone (Sigmacote, Sigma, St. Louis, MO, USA) and covered with a small cover slip (22 × 22 mm) (perfusion chamber) and then unbound myosin was washed away with 0.6 M KCl, 10 mM Hepes (pH 7.0).

Fluorescent actin filaments (10 nM actin) were then introduced into the perfusion chamber. Sliding of actin filaments was started at room temperature (25–28°C) in the sliding buffer (25 mM KCl, 4 mM $MgCl_2$, 20 mM Hepes (pH 7.8), 4 mM ATP, 2 mM DTT, 2 mM EGTA). Dissolved oxygen in the sliding buffer was previously removed by the addition of 4.5 mg/ml glucose, 0.216 mg/ml glucose oxidase and 0.036 mg/ml catalase [10].

Fluorescent actin filaments were observed under an inverted microscope (IMT-2, Olympus, Tokyo, Japan) equipped with epifluorescence optics, a ×100 objective

(Olympus UVFL, oil immersion, NA = 1.3, Olympus) and a 100 W mercury arc lamp. Fluorescence images were recorded on video tapes through a high-sensitive television camera (SIT camera C-2741, Hamamatsu Photonics, Hamamatsu, Japan) and a video recorder. Fluorescence images were processed (averaging over 4 frames; negative contrast and linear enhancement) with a video-image processor (Argus-10, Hamamatsu Photonics). In order to determine the sense of helix, we kept in mind the fact that the image obtained under the inverted microscope was the mirror image of the real one [11].

Results

In the in vitro motile system, we have noticed that when the front part of actin filaments slowed down or stopped sliding, the filaments were suddenly buckled in the middle part (Fig. 1a, b). A buckling of actin filament was already reported that occurs during sliding over the central bare zone of a thick filament isolated from clam adductor muscle [12]; this is simply due to the fact that the filament slides slower toward the tip ends of a thick filament (wrong direction) than toward the central bare zone (right direction) [12,13]. The reason why the sliding velocity is lower in the wrong direction seems to be that the orientation of myosin molecules is inverted. Thus, the slowdown of the actin filament observed in the present work is not always ascribed to the attachment of damaged myosin heads.

The buckling will be simply ascribed to that myosin molecules attached to the actin filaments at the central part can not sustain the stress imposed by a compressive force due to the successive sliding of the filament. The buckling side must be determined by accidental factors such as the tilting of axes between front and rear parts of the filament. In fact, the ratio of the buckling side (right : left) against the sliding direction was nearly 1 : 1.

The fore or hind half of the buckled part occasionally came off from the glass surface and largely deformed into a helix (Fig. 1c, d; to be strict, this should be called a super helix because the actin filament itself has a helical symmetry, so that hereafter we call it a

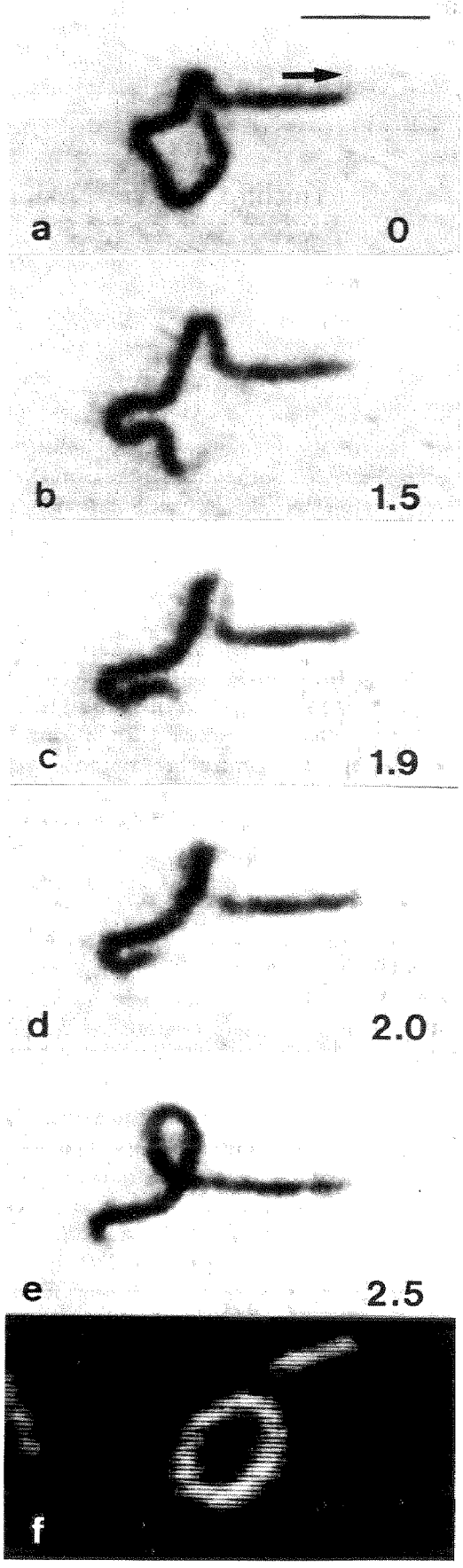

Fig. 1. Video-processed images showing the transformation from a flat buckle to a loop through a right-handed super helix in an actin filament sliding in an in vitro motile system. (a) and (b), The front part of filament nearly stopped but the rear part continued sliding. The buckling occurred at the left side of filament against the sliding direction shown by an arrow; (c) and (d), The fore half of the buckled part at the top was drawn apart from the surface and the buckled part was transformed into a single turn of super helix; (e), The super helix was then transformed into a loop. Numbers in each panel indicate time; (f), An example of an actin ring. Scale bar, 5 μm.

super helix); in this example (Fig. 1c, d), we could judge the helical sense was right-handed, because the fore half of the buckled part came off at the buckling side of left [11]; in this connection, if the buckling side is right, the helical sense is inverse. Then, the rear part of the filament kept on sliding and the super helix was further transformed into a loop (Fig. 1e). Finally, the loop was loosened.

Total number of super helixes of which sense could be identified was 64, within which 44 cases were right-handed and the remaining 20 cases were left-handed. As for the buckling side, 31 cases were right-hand side, while 33 cases were left-hand side against the sliding direction. Although the fore half of the buckled part had a tendency to get free easily of the glass surface (41 cases), the right-handed super helix was prevalent irrespective of the buckling side. The ratio of right- to left-handed super helixes was about 7 : 3, in an unequal probability.

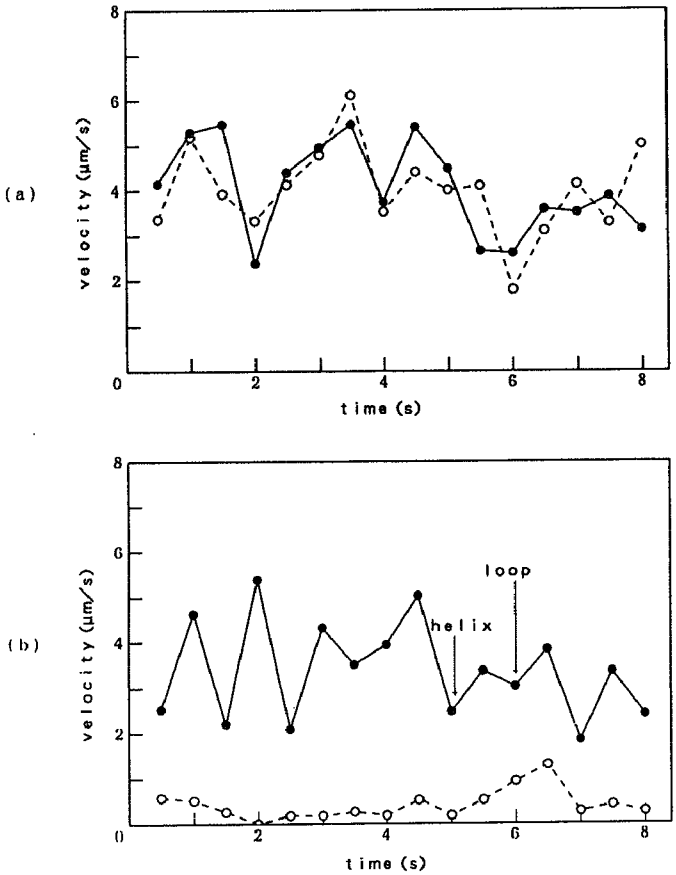

Fig. 2. Examples showing sliding velocities of front (○) and rear (●) ends of actin filaments. (a), A typical example showing the velocities of both ends of actin filament that smoothly slid during some interval arbitrarily chosen; (b), A typical example showing the velocities of both ends of actin filament in which super helix formation and helix-to-loop transformation occurred. Recorded images were replayed at intervals of 0.5 s on a video monitor and the positions of front and rear ends of filaments were measured with a cursor superimposed on a video monitor. The velocity was calculated by dividing the distance between the successive sampling points by 0.5 s. The separation between nearest dots on the video monitor was calibrated to be 0.091 μm with an objective micrometer.

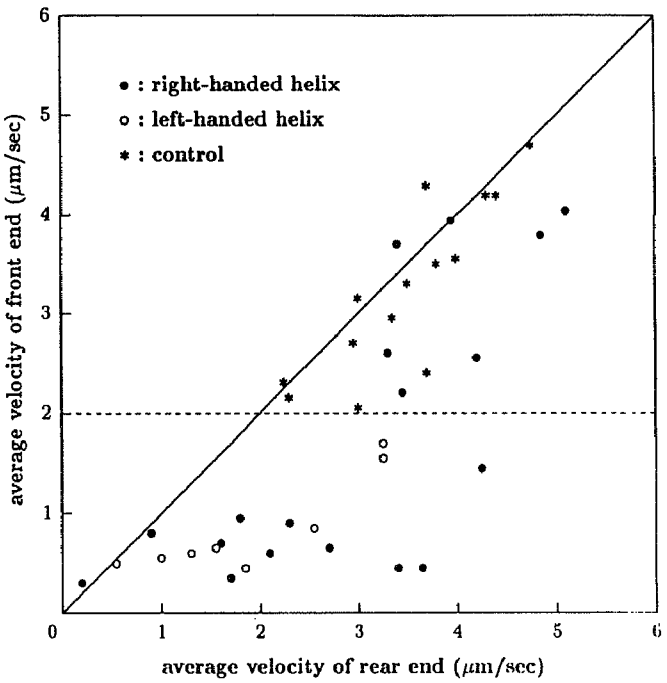

Fig. 3. Relationship between the average sliding velocities of front and rear ends of actin filaments. (*): The velocities of both ends of actin filaments that smoothly slid, averaged over 6 s during some intervals arbitrarily chosen. (●,○): The velocities of front and rear ends of actin filaments in which super helix (●: right-handed; ○: left-handed) was formed were averaged over 6 s just before and after the super helix formation (cf. Fig. 2). In cases when the slowdown of front ends was distinct, both right- and left-handed super helices were formed, whereas in rapidly sliding filaments of which average velocities of front ends were higher than about 2 μm/s (---), the sense of super helices was right-handed.

We found rings (a few μm in diameter) of actin filaments in which both ends were linked to each other (Fig. 1f). We could frequently observe the annealing of pointed and barbed ends of different filaments sliding to the same direction on the same track; in the ring formation also, the same event should have occurred within the same filament during sliding on a circular track. It appears that phalloidin functions as a strong glue for actin-actin bond.

In the filaments that moved smoothly without super helix formation, the rear part accurately traced a track of the front part and the average velocities of front and rear ends were nearly equal to each other (Fig. 2a and 3). On the other hand, in almost all the filaments that formed a super helix, the average velocities of front ends were lower than those of rear ends (Fig. 2b and 3). Even when there appeared to be little difference between the average velocities of both ends, momentary slowdown of the front ends occurred just prior to the super helix formation; after the super helix was formed, the front ends started to slide again.

It is to be noted that even when both front and rear parts of an actin filament appeared to stop sliding, the super helix formation could occur (nearly at the origin of Fig. 3; data not shown); in this case, winding and unwinding of the super helix occurred reversibly and repeatedly at the buckled part. This suggests that the continued sliding of the rear part of filament is not required for the super helix formation.

Discussion

The simplest and plausible explanation for these phenomena will be that a torsional stress is imposed on the buckled part of the filament and it is released by super helix formation and subsequent helix-to-loop transformation. The torsional stress will be ascribed to the assumption that the sliding force generated at the interface between actin and myosin by cross-bridges is tilted against the long axis of actin filament, so that it has a torque component. As a result, the sliding actin filament will rotate around its long axis. If the rotational angles of the front and rear parts of the filament are not matched to each other, the buckled part will be passively twisted and transformed into a super helix to release the accumulated strain.

The torque component may be produced by internal drag force which is passively generated by attached cross-bridges. This type of torque component probably exists only when the filament is sliding. The possibility that this mechanism predominates will be denied by the fact that nearly stopped filaments showed reversible winding and unwinding of super helix.

Another possible mechanism to induce a super helix will be the conformational changes in the actin filaments, making a twisted form more stable thermodynamically. At present, we can not deny this possibility; for this examination we may need a microspectroscopy [14]. Also, a super helix may be simply induced by compressive force given by the sliding of the rear part of filament; some proportion of super helixes may be ascribed to this mechanism, however, it is hard to explain all the features on super helix reported here according to these mechanisms, e.g., an unequal probability of right- and left-handed super helixes and reversible winding and unwinding of super helix of nearly stopped filaments.

The conclusion that the super helix is formed by the rotation of filament is compatible with the fact that both right- and left-handed super helixes appeared. If there happens to be the difference between rotational angles of front and rear parts of the filament, even if their directions of rotation are the same to each other, it is possible to explain the reason why two types of super helixes appeared; the sense of super helix depends on what is the direction of rotation and also depends on which part, front or rear, does exceed in rotation as schematically shown in Fig. 4. If the front part exceeds the rear part, the sense of helix accords with the direction of rotation. In contrast, in the opposite case, the sense of helix is opposite to the direction of rotation. It is also easy to understand reversible winding and unwinding of super helix according to the rotation. We frequently observed the fish-tailing motion of actin filaments, being consistent with the rotation of filaments, as previously suggested [15].

The overall structure of an actin ring (Fig. 1f) appears to be analogous to that of a circular DNA. If the twisted actin filament forms a ring, the strain of twist will be retained in the ring. So, in the course of release of strain, a typical supercoil must be formed as in the case of DNA (cf. Ref. 16); but this observation may be possible for an actin ring much larger than that we found.

In the above mechanism, no rigid requirements are assumed for the relation between the rotational angle and the sliding distance, in other words, for the relation between the angular velocity of rotation and the sliding velocity. It is rather implicitly assumed that the

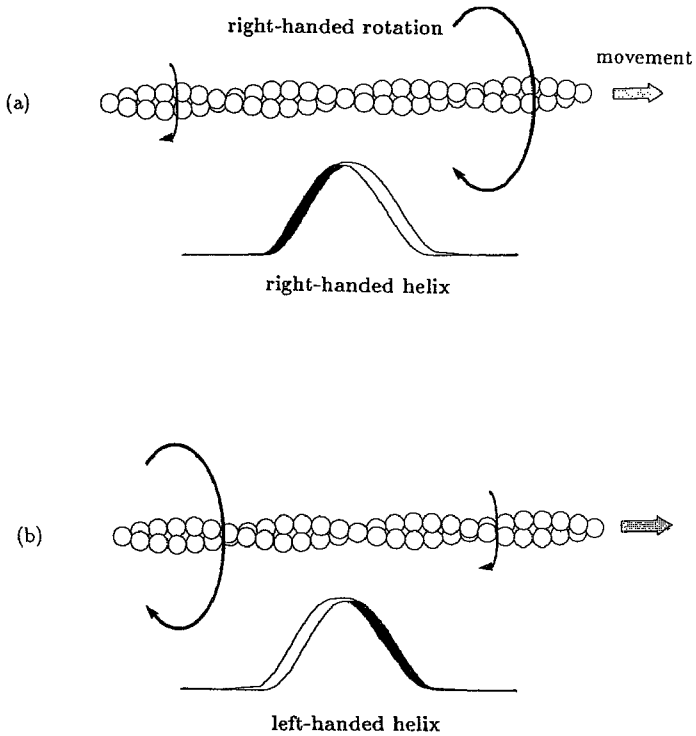

Fig. 4. The sense of super helix formed by the rotation of actin filament. Even if the direction of rotation is restricted to right or left, the sense of super helix is variable depending on which part, front or rear, of the filament exceeds in rotation. Here, only the case of right-handed rotation is shown. If the rotation of front part exceeds that of rear part, the sense of super helix accords with the direction of rotation (a). In the opposite case, the sense of super helix is opposite to the direction of rotation (b). The super helix to be formed is schematically illustrated by a ribbon of which white part is on this side and the black part is on the far side, respectively.

relation may be variable. As for the slowdown of the front part, we infer that there are at least two types: one is that the front part is tightly clung to myosin heads so that the sliding and rotation are both inhibited. Another is that only sliding of front part is momentarily slowed down by some obstacle or the attachment of myosin molecules with wrong direction; in this case, the number of interacting myosin heads may rather increase, so that the rotational speed may increase. Because there are no reasons for such two types to occur in an equal probability, an unequal probability of right- and left-handed super helixes is understandable.

It should be noted that the right-handed rotation of motile filaments was already demonstrated in the microtubule-dynein system [17]. Then, the next subject of interest is the direction of rotation. However, we can not determine it because, at present, we do not have any means to observe directly the rotation of actin filaments nor judge the rotation of which parts, front or rear, of filaments exceeds the other. However, if the above described second way for slowdown of the front part is the case in rapidly sliding filaments (faster than about 2 μm/s (Fig. 3)), the situation must be similar to that of Fig. 4a; i.e., the rotation is right-handed. Direct evidence for this suggestion is needed in future.

It is reasonable to assume that the torque component also exists in muscle contraction. However, it will be impossible for the actin filament to rotate freely in muscle fibers, because one end is anchored to the Z-line. We infer that local twist and untwist of actin filaments may occur; the strain will be stored transiently as a form of elastic energy of twisting. When the sliding is suppressed under an isometric condition, the strain may be so strong as to transform the lattice structure of Z-line as previously reported [18,19].

It is expected that further refinement of the in vitro motile system will give us new ideas and more detailed features on the molecular mechanism of sliding (motility) of myofilaments not only in muscle contraction but also in cell motility.

Acknowledgement

This work was supported in part by Grants-in-Aid for Scientific Research on Priority Areas from the Ministry of Education, Science and Culture of Japan.

References

1 Huxley, A.F. and Niedergerke, R. (1954) Nature 173, 971–973.
2 Huxley, H.E. and Hanson, J. (1954) Nature 173, 973–976.
3 Kron, S.J. and Spudich, J.A., (1986) Proc. Natl. Acad. Sci. USA 83, 6272–6276.
4 Harada, Y., Noguchi, A., Kishino, A. and Yanagida, T. (1987) Nature 326, 805–808.
5 Yanagida, T., Nakase, M., Nishiyama, K. and Oosawa, F. (1984) Nature 307, 58–60.
6 Toyoshima, Y.Y., Kron, S.J., McNally, E.M., Niebling, K.R., Toyoshima, C. and Spudich, J.A. (1987) Nature 328, 536–539.
7 Spudich, J.A. and Watt, S. (1971) J. Biol. Chem. 246, 4866–4871.
8 Kielley, W.W. and Harrington, W.F. (1960) Biochim. Biophys. Acta 41, 401–421.
9 Harada, Y., Sakurada, K., Aoki, T., Thomas, D.D. and Yanagida, T. (1990) J. Mol. Biol. 216, 49–68.
10 Kishino, A. and Yanagida, T. (1988) Nature 334, 74–76.
11 Shimada, K., Kamiya, R. and Asakura, S. (1975) Nature 254, 332–334.
12 Sellers, J.R. and Kachar, B. (1990) Science 249, 406–408.
13 Yamada, A., Ishii, N. and Takahashi, K. (1990) J. Biochem. 108, 341–343.
14 Kinosita, K., Jr., Itoh, H., Ishiwata, S., Hirano, K., Nishizaka, T. and Hayakawa, T. (1991) J. Cell Biol. 115, 67–73.
15 Jarosch, R. (1987) in Cytomechanics (Bereiter-Hahn, J. et al. eds.) pp. 54–75, Springer, Berlin.
16 Mathews, C.K. and Van Holde, K.E. (1990) Biochemistry, pp. 111–114, Benjamin/Cummings, Menlo Park, CA, USA.
17 Vale, R.D. and Toyoshima, Y.Y. (1988) Cell 52, 459–469.
18 Goldstein, M.A., Michael, L.H., Schroeter, J.P. and Sass, R.L. (1987) FASEB. J. 1, 133–142.
19 Yamaguchi, M., Izumimoto, M., Robson, R.M. and Stromer, M.H. (1985) J. Mol. Biol. 184, 621–644.

実験メモ

筋タンパク質繊維を用いたブラウン運動の観察

西坂崇之 〈早稲田大学理工学部物理学教室 169 東京都新宿区大久保 3-4-1〉
池田光洋 〈早稲田大学理工学部物理学教室 169 東京都新宿区大久保 3-4-1〉
中村 真 〈早稲田大学理工学部物理学教室 169 東京都新宿区大久保 3-4-1〉
石渡信一 〈早稲田大学理工学部物理学教室 169 東京都新宿区大久保 3-4-1〉

私達の学科では例年1年生を対象に，いくつかの課題（例えば，複素関数，中性子の発見，ブラウン運動など）についてグループごとに勉強して，その結果を発表するという授業を行ってきた．幾分理論に偏る傾向もあり，学生からの多様な希望に応える意味もあって，昨年度から，研究室に入って実験するグループを作ってはどうか，ということになった．その結果をまとめたのがこのメモである．学生（2名）は10日以上研究室に出入りしたので時間は十分にあったが，課題はなるべく単純にと考え，「繊維（棒）状高分子のブラウン運動における変位 (x) の自乗平均が時間 (t) に比例する（$\langle x^2\rangle = 2Dt$, D: 拡散係数）」ことを理解し，[1,2] それを実験的に確かめることとした．

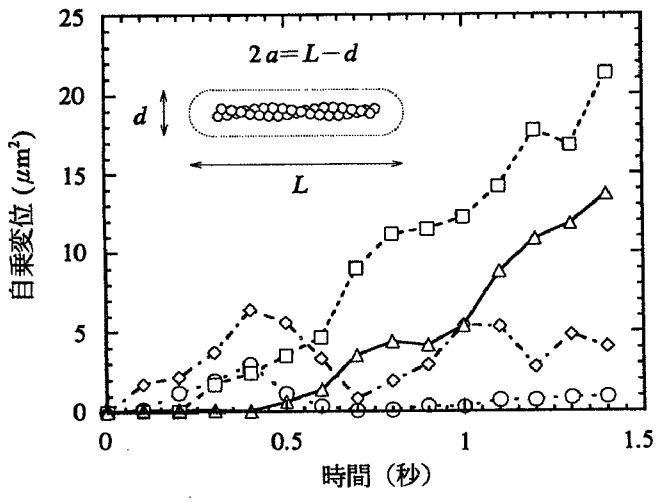

図1 アクチン溶液（標識FA, 0.5 μg/ml; 未標識FA, 0.1 mg/ml; 0.1 M KCl, 2 mM $MgCl_2$, 0.5 mM ATP, 1.5 mM NaN_3（防腐剤，0℃保存でFAは数カ月もつ），2 mM MOPS (pH 7.0), 0.22 mg/ml glucose oxidase, 0.036 mg/ml catalase, 4.5 mg/ml glucose, 10 mM dithiothreitol, 30℃）中の，FAの変位（2乗）の時間依存性（1.4 s間），4例．手荒く攪拌すると，FAは切断される．FAの長さは（ほぼ同じ長さの，短いFAを選んだ；2a，約1.6 μm），挿入図のようにFAの蛍光像から見積もった．最初は0.5 μg/mlに薄めたままのFAを観察していたが，1秒以上焦点が合い続けることは稀であったので，標識していないFAを大量（0.1 mg/ml）に加えて拡散をやや抑えて観察した．カバーガラスにはさまれた液厚は約50 μm．

用いた試料は筋肉を構成する主要なタンパク質“アクチン (actin)”である．1分子は直径5 nm程度の球状だが，適当な塩濃度の水溶液中で重合し，特にキノコ毒ファロイジン (phalloidin) 存在下では～20 μmにも達するフィラメント (FA) を作る．FAを蛍光ファロイジン（rhodamine phalloidin, Molecular Probe社製）で標識し，簡易防振台にのせた倒立型蛍光顕微鏡（TMD，対物×100 Fluor，ニコン）で観察すると，長いFAは「赤いうどん」が揺れているように見え，短いFAは棒のように見える．[3] 強い光にさらすため溶液は脱ガスしたのち脱酸素用の酵素系を加え，2時間以内に実験を終えた．画像は超高感度テレビカメラ（SIT C1000，浜松ホトニクス；低残像という点ではICCDの方が良い）を通してビデオ (SVHS) に記録し，1フレームごとの XY 座標をパソコンを通して読みとった．観測開始時刻 (t=0) から，フィラメントの位置を0.1秒おきに計測し，表計算ソフトを用いて処理した．

得られたデータを図1に示す．一見するとばらつきが大きいが，変位の2乗を10例平均しただけで図2に示すよう

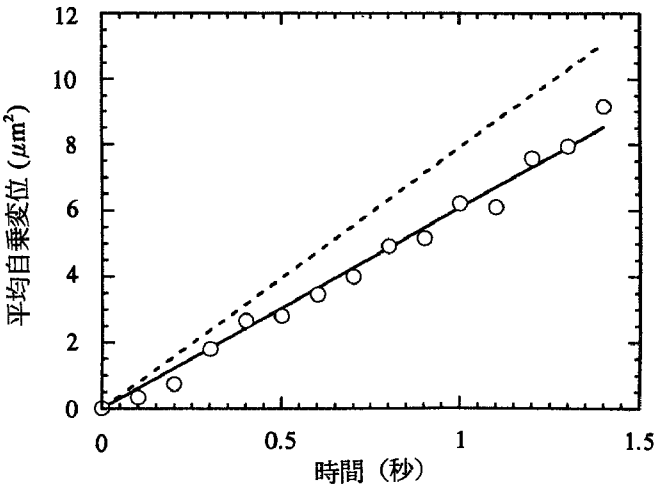

図2 図1のデータを10例，各時刻で平均したもの．直線は最小自乗法により求めた．破線はペランの式による計算値（$\langle x^2\rangle = 4Dt$）．

な直線性が得られた．この傾きが$2D$になるはずだと考え，計算値と比較した．そこで，$D=kT/f$（f: 摩擦係数）に細長い回転楕円体についてのペランの式 $f=6\pi\eta a/\ln(2a/b)$（η: 30℃での水の粘度，a: 長軸 0.8 μm，b: 短軸 5 nm）を代入したところ，実験値より幾分低い値が得られた．ところが我々が観察したのは2次元運動であり，図2の傾きは4Dであるべきなのであった．従ってDの理論値は2倍大きくなり，実験値 1.5×10^{-8}cm^2/s に対して 2.0×10^{-8}cm^2/s となった（光準弾性散乱法によるDの測定について，文献4参照）．実際には多量の FA を加えることによりηが見かけ上，若干上がることを考慮すると（事実，Dの FA 濃度依存性が見られた），良い一致といえるだろう．これには，当初4Dを2Dで計算していたこともあり，学生だけでなくみな大いに喜んだ（巧まざる教育効果？）．一方$\langle x\rangle$も求め$\langle x\rangle^2$を$\langle x^2\rangle$と比較したが，$\langle x\rangle^2/\langle x^2\rangle$は測定時間内で高々数%であった．溶液の巨視的流れがあったとしても，観測時間が短かったためにデータへの影響が少なかったのであろう．

ナノメートルオーダーのタンパク質相手にこれだけきれいな結果が得られたのは，予想外であった．今後 FA に別の筋タンパク質を結合させて比較するといった方向で，年々発展する学生実験が組めるかもしれない（ただし，次回からは故意に2Dと暗示することにしよう）．この実験には筋タンパク質を扱う研究室が近くにある方が良いが（アクチンは1 mg あれば十分なので購入も可 (Sigma Chem. Co.)），もちろん別の試料を選ぶのも良い．[5] このように高分子（超分子，微粒子）一個のブラウン運動を観察，記録して解析するという課題は，ミクロ領域での物理現象に対して想像力をかき立ててくれる点，平均操作の意味を考えさせてくれる点などで，学部学生向け実験として面白いと思う．

参考文献

1) 米沢富美子：ブラウン運動（共立出版，1986）．
2) H. C. Berg: 生物学におけるランダムウォーク（法政大学出版局，1989）．
3) T. Yanagida, *et al.*: Nature **307** (1984) 58.
4) S. Fujime: Adv. Biophys. **3** (1972) 1.
5) 慶大理工物理3年生の学生実験では，直径1 μm のポリスチレンビーズ（蛍光つき）を使用している．

非会員著者の紹介：西坂崇之氏は早大大学院理工学研究科物理学及応用物理学専攻修士課程2年在籍中，専門は生物物理学．池田光洋・中村真の両氏は早大理工学部物理学科2年生で，この実験を実際におこなった．

Right-handed rotation of an actin filament in an *in vitro* motile system

Takayuki Nishizaka*, Toshiki Yagi*, Yuichiro Tanaka† & Shin'ichi Ishiwata*‡

* Department of Physics, School of Science and Engineering, Waseda University, 3-4-1 Okubo, Shinjuku-ku, Tokyo 169, Japan
† Wako Research Center, HONDA R&D Co. Ltd, Saitama 351-01, Japan

‡ To whom correspondence should be addressed.

MUSCLE contraction occurs by mutual sliding between thick (myosin) and thin (actin) filaments[1,2]. But the physical and chemical properties of the sliding force are not clear; even the precise direction of sliding force generated at each cross-bridge is not known. We report here the use of a recently developed *in vitro* motile assay system[3–5] to show supercoiling of an actin filament in which the front part of the filament was fixed to a glass surface through cross-linked heavy-meromyosin and the rear part was able to slide on a track of heavy-meromyosin. A left-handed single turn of superhelix formed just before supercoiling, suggesting that the sliding force has a right-handed torque component that induces the right-handed rotation of an actin filament around its long axis. The presence of the torque component in the sliding force will explain several properties of the contractile system of muscle.

When the sliding velocity of the front part of an actin filament is lower than that of the rear part, the central part can become buckled[6,7]. The buckled part is then transformed into a single turn of superhelix and then into a loop[7] (we call this a superhelix, because the actin filament itself has a helical symmetry). When the front part stops sliding, the rear part wiggles like a fishtail, as previously predicted[8]. Such phenomena were interpreted as being due to the presence of a torque component in the sliding force which rotates the filament around its long axis. But the handedness of the torque could not be determined, mainly because both right- and left-handed superhelices appeared[7].

To determine the handedness of the torque component, we designed a new artificial *in vitro* motile system (Fig. 1), in which the front part of the actin filament was attached to a glass surface through undissociable heavy meromyosin (HMM) track[9]. We first prepared the acto-HMM complexes either covalently cross-linked or chemically modified to make the HMM undissociable in the presence of ATP. After fragmentation of these complexes, actin was polymerized preferentially onto the barbed end of the fragments. Then this growing type of block copolymers[10] was covered with HMM so they could be used as the HMM track[9]. We expected that the handedness of torque component, which induces the rotation of the filament, must be determined by the helical sense of the superhelix to be formed at the central part of the filament (Fig. 1*e*).

A typical result is shown in Fig. 2. Owing to the continued sliding of the rear part of the filament, the central part was buckled (Fig. 2*b*) and then transformed into a left-handed superhelix (Fig. 2*c*), as schematically illustrated in Fig. 3*a*. After the superhelix was transformed into a loop (Fig. 2*d*), the loop was unexpectedly transformed further into a multifold superhelix (Fig. 2*e*; we call this a supercoil). The supercoiled part sticking out sideways was composed of a small circle at the tip and a rod part. The length of the rod part increased with time (Fig. 2*e–g*) and the increase in length was nearly half the distance that the rear part slid. In addition, the fluorescence intensity of the rod part was much higher than that of the other parts, consistent with the rod part being composed of doubled filaments, as schematically illustrated in Fig. 3*b*. Finally, the

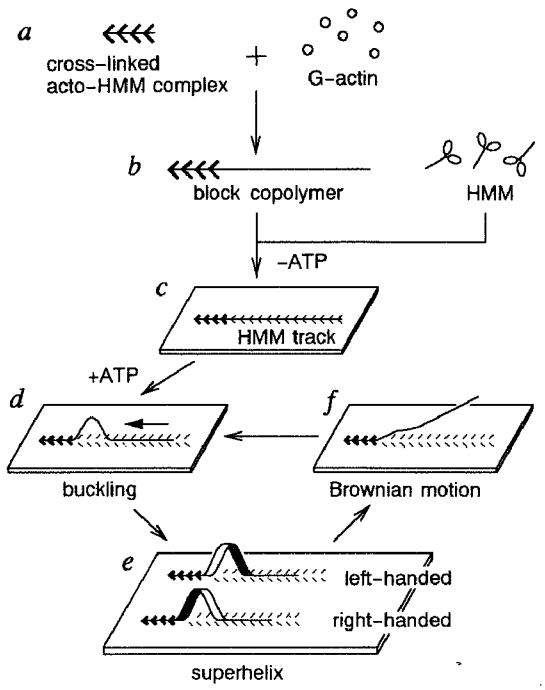

FIG. 1 A flow chart illustrating the arrangements of the artificial *in vitro* motile system which was designed to determine the handedness of torque component of the sliding force (for details on *a–f*, see below and text). Actin and myosin were prepared from the back and leg white skeletal muscle of a rabbit according to a standard procedure[10] HMM was prepared by chymotryptic digestion of myosin[15] without ammonium sulphate fractionation, stored in liquid N_2 and used within a few days after quick thawing. Acto-HMM complexes covalently cross-linked were prepared by treating the F-actin-HMM (1:4 weight ratio) complexes with 3 mM 1-ethyl-3-(3-dimethylaminopropyl)-carbodiimide (EDC; Nakarai Tesque Co. Ltd., Kyoto) under a rigor condition following the techniques of Ando[16] with slight modifications. Acto-HMM complexes chemically modified were prepared by mixing F-actin and *N*-ethylmaleimide (NEM)-treated HMM in a 1:4 weight ratio. The results were indistinguishable between the two types of acto-HMM complexes. The growing type of block copolymers were prepared as follows (*b*): either one of the acto-HMM complexes prepared as described above was first diluted to 0.6 mg ml^{-1} in solution A composed of 25 mM KCl, 2 mM MOPS (pH 7.0), 0.5 mM $MgCl_2$ and 1.5 mM NaN_3; the complexes were fragmented by sonication for 30 s at 0 °C in an insonator at 9 kHz and 100 W (Model 200M, Kubota Co., Tokyo). G-actin diluted in solution A to a final concentration of 0.12 mg ml^{-1} was added to the solution of acto-HMM fragments immediately after the dilution and preferentially polymerized onto the barbed end of the fragments at room temperature[10] (*a, b*). Fifteen minutes later, the solution was diluted to 0.1 M KCl, 2 mM $MgCl_2$ (finally, 0.1 mg ml^{-1} actin) and 45 min later, 3.6 μM rhodamine phalloidin (Rh-Ph, Molecular Probes, Eugene, OR) was added and stored on ice. An *in vitro* motility assay was done according to Toyoshima *et al.*[5] with slight modifications as follows: the nitrocellulose-coated glass cover was prepared by drying it after dipping it in 0.1% collodion. The Rh-Ph labelled block copolymers (0.05 mg ml^{-1} actin; *b*) were mixed with HMM (0.38 mg ml^{-1}) in 0.1 M KCl and 2 mM $MgCl_2$ and stored for 20 min at room temperature; this solution was then diluted 100 times with solution B composed of 25 mM KCl, 25 mM imidazole-HCl (pH 7.4), 4 mM $MgCl_2$ and 1 mM EGTA and put in a flow cell made of a pair of cover slips with a spacer 75 μm thick and sealed with white petrolatum (*c*). After 30–60 s, the flow cell was rinsed with solution B with the addition of 0.5 mg ml^{-1} BSA (Sigma) and free proteins were washed out with solution B with the addition of 10 mM DTT and the oxygen-depleting enzyme system (0.22 mg ml^{-1} glucose oxidase (Sigma), 0.036 mg ml^{-1} catalase (Sigma) and 4.5 mg ml^{-1} glucose)[17]. The sliding was initiated by flowing solution B with the addition of 4 mM ATP, 10 mM DTT and the oxygen-depleting enzyme system (*d–f*; the sliding direction is shown by an arrow) and observed under an inverted fluorescence microscope (Diaphoto-TMD; NCF Fluor ×100 objective lens (numerical aperture (NA) = 1.3); Nikon, Tokyo) equipped with a highly sensitive TV camera (SIT camera (C1000-12) with a contrast enhancer (M1438), Hamamatsu Photonics, Hamamatsu, Japan). The fluorescent images were recorded on a video-tape recorder (SR5050, Victor, Tokyo). The sense of the superhelix was determined following the methods of Shimada *et al.*[18], remembering that the image obtained under the inverted microscope we used was the mirror image of the real one. That is, in the superhelical part of *e*, each white part on this side is out-of-focus, while each black part on the glass surface is focused.

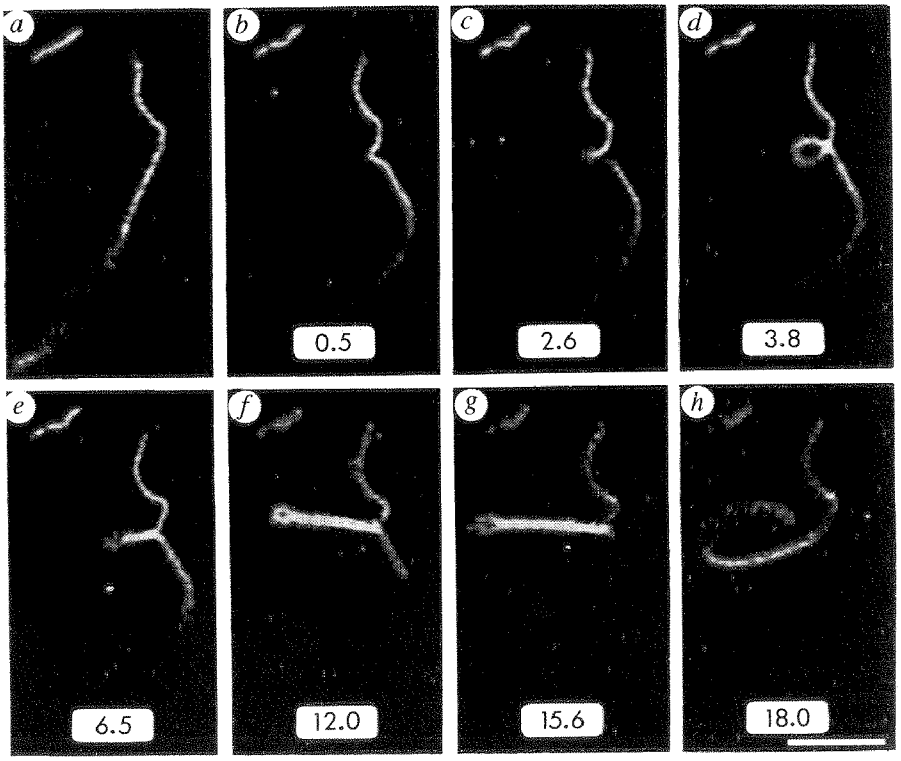

FIG. 2 An example showing supercoiling of an actin filament. A sequence (*a*–*h*) of fluorescent images of an actin filament, of which the front part, corresponding to the pointed end, is attached to a glass surface through cross-linked HMM molecules and the rear part slides on an HMM track. The figures on each panel indicate time (s) after the rear part attached itself to the HMM track. The small circle of supercoil rotated at least four times during the sliding of the rear part by about 5 μm, but it was difficult to determine the number of rotations precisely. Throughout the above process, the sliding velocity of the rear part was 1 μm s^{-1} on the average and changed within a factor of 2, irrespective of whether supercoiling occurred or not. Such a series of supercoiling repeated up to 7 times on the same HMM track and stopped for one of the following reasons: (1) the junction between the front part, covered with undissociable HMM, and the buckled part was broken; (2) the small circle of supercoil was broken, probably because of the accumulation of strain for both cases (1) and (2); or (3) the rear part stopped sliding on the HMM track. The buckled part was always transformed into a loop through a single turn of superhelix, but the supercoiling did not always occur. The occurrence frequency of supercoiling was about 20%, and in the remaining 80% only the radius of the loop increased, without supercoiling. We have 94 supercoils so far, among which 71 cases showed a left-handed superhelix, 2 cases a right-handed one and the remaining 21 cases were undetermined. In the superhelices which were not transformed into a supercoil (about 350 cases total), the number of superhelices for which handedness could be determined was 277, of which 251 cases (91%) were left-handed and 26 cases were right-handed (9%). About 80% of these data were obtained from cross-linked acto-HMM block copolymers. For more details, see text. Scale bar, 5 μm.

rear part of the filament was detached from the HMM track, and this was followed by an unwinding of the supercoil and then a brownian motion (Fig. 2*a*, *h*). When the rear part reattached to the HMM track, the same process started again (compare with Fig. 1*d*–*f*).

Judging from the fact that the superhelices formed just before supercoiling were left-handed in almost all cases (71 out of 73 cases), we conclude that the sliding force contains a right-handed torque component, which induces rotational sliding of an actin filament in the manner of a right-handed screw. (A microtubule also shows a right-handed screw movement on dynein attached to the glass surface[11].) In the exceptional right-handed superhelices (2 out of 73 cases), the rapid transformation from right- to left-handed may have occurred just before supercoiling; the reason we infer this is that, in the superhelices which were not transformed into a supercoil (about 350 cases), there were 4 cases in which a loop once formed through a right-handed superhelix was transformed into a left-handed one, but no reverse cases. In addition, there is a possibility that a certain proportion of superhelices are simply formed by the compressive force produced by the sliding of the rear part of the filament (compare with ref. 7), but the supercoil will not be.

Whether the supercoiling occurs or not is probably determined by the balance between the magnitude of the net torque and the rigidity of the actin filament. It seems that an essential factor

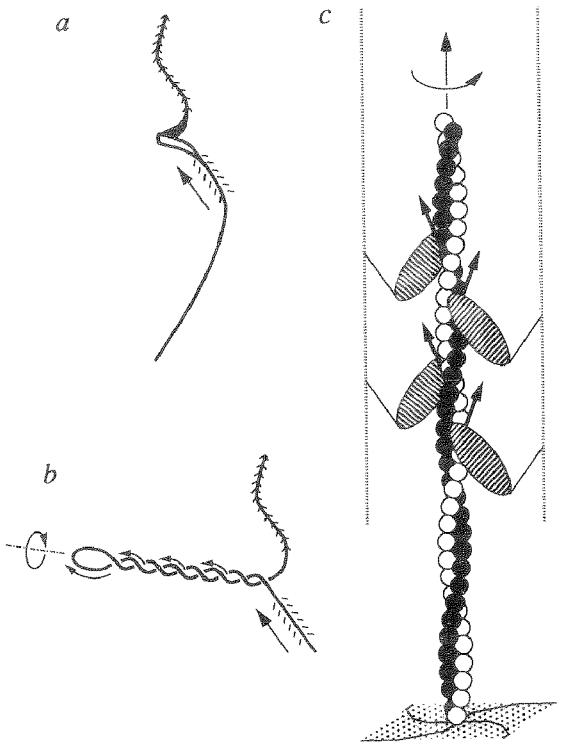

FIG. 3 Schematic illustration of a left-handed superhelix (*a*) and a supercoil (*b*) of actin filaments corresponding to Fig. 2*c* and *f*, respectively, and the situation expected in a sarcomere (*c*). Thin arrows indicate the direction of sliding and rotation. *c*, It is assumed that one end of the thin filament is fixed at the Z-line, whose lattice structure is schematically illustrated at the bottom, whereas the rest, including the end shown at the top, is free to rotate. For simplicity only a single head of myosin (the ellipsoids with hatching) is drawn. The direction of sliding force imposed on a thin filament through each cross-bridge is shown by a thick arrow. The reaction force having a direction opposite to the thick arrow will be imposed on each myosin head, which may induce the compression of the filament lattice. Although the direction of the sliding force may be nearly parallel to the long helical strand of the actin filament (the open or closed circles), as shown here, the direction of the resultant force will change depending on the external force (load) and its moment.

for supercoiling is to fix physically the front part while keeping the rear part sliding and to make the buckled part free to move without attaching extra HMM molecules. A particular arrangement of HMM molecules that may exist in the HMM track will not be indispensable for supercoiling. In fact, a 2-fold supercoil (the superhelix described above is a 1-fold supercoil) was also observed in the usual *in vitro* motile system, although only once. Thus, we conclude that the motive force for supercoiling is intrinsic to the sliding force generated at each cross-bridge.

In a muscle fibre, where an actin filament cannot rotate freely, a twist of thin filaments will accumulate, so that the elastic energy of the twist will be stored in the filament lattice, including the Z-line under an isometric condition (compare with Fig. 3*c*). Under an isotonic condition, both twisting and untwisting of a thin filament may occur along the filament here and there owing to its flexibility. In any case, the right-handed torque component tends to make the pitch of a right-handed long helix of thin filaments smaller. Such a strain may be strong enough to transform the lattice structure of the Z-line under certain conditions[8,12,13]. Also, the radial compression of a fibre observed with accompanying tension development[14] may be partly attributable to the radial component of the sliding force (compare with Fig. 3*c*). Thus, several properties of the contractile system of muscle (and also non-muscle cells) will be explained by the presence of a right-handed torque component in the sliding force (and the resultant supercoil). □

Received 11 August; accepted 12 November 1992.

1. Huxley, A. F. & Niedergerke, R. *Nature* **173**, 971–973 (1954).
2. Huxley, H. E. & Hanson, J. *Nature* **173**, 973–976 (1954).
3. Kron, S. J. & Spudich, J. A. *Proc. natn. Acad. Sci. U.S.A.* **83**, 6272–6276 (1986).
4. Harada, Y., Noguchi, A., Kishino, A. & Yanagida, T. *Nature* **326**, 805–808 (1987).
5. Toyoshima, Y. Y. *et al. Nature* **328**, 536–539 (1987).
6. Sellers, J. R. & Kachar, B. *Science* **249**, 406–408 (1990).
7. Tanaka, Y., Ishijima, A. & Ishiwata, S. *Biochim. biophys. Acta* **1159**, 94–98 (1992).
8. Jarosch, R. in *Nature and Function of Cytoskeletal Proteins in Motility and Transport* (ed. Wohlfarth-Bottermann, K. E.) 231–249 (Gustav Fischer, Stuttgart, 1987).
9. Toyoshima, Y. Y., Toyoshima, C. & Spudich, J. A. *Nature* **341**, 154–156 (1989).
10. Kondo, H. & Ishiwata, S. *J. Biochem.* **79**, 159–171 (1976).
11. Vale, R. D. & Toyoshima, Y. Y. *Cell* **52**, 459–469 (1988).
12. Goldstein, M. A., Michael, L. H., Schroeter, J. P. & Sass, R. L. *FASEB. J.* **1**, 133–142 (1987).
13. Yamaguchi, M., Izumimoto, M., Robson, R. M. & Stromer, M. H. *J. molec. Biol.* **184**, 621–644 (1985).
14. Cecchi, G., Bagni, M. A., Griffiths, P. J., Ashley, C. C. & Maeda, Y. *Science* **250**, 1409–1411 (1990).
15. Weeds, A. G. & Pope, B. *J. molec. Biol.* **111**, 129–157 (1977).
16. Ando, T. *J. Biochem.* **105**, 818–822 (1989).
17. Harada, Y., Sakurada, K., Aoki, T., Thomas, D. D. & Yanagida, T. *J. molec. Biol.* **216**, 49–68 (1990).
18. Shimada, K., Kamiya, R. & Asakura, S. *Nature* **254**, 332–334 (1975).

ACKNOWLEDGEMENTS. We thank K. Kinosita Jr for use of an image processor, K. Kinosita Jr and S. Fujime for reading of the manuscript and discussion and I. Sase for technical assistance. The research was partly supported by Grants-in-Aid from the Ministry of Education, Science and Culture of Japan.

Elastic Filaments in Situ in Cardiac Muscle: Deep-Etch Replica Analysis in Combination with Selective Removal of Actin and Myosin Filaments

Takashi Funatsu,* Eiji Kono,*‡ Hideo Higuchi,§ Sumiko Kimura,‖ Shin'ichi Ishiwata,¶ Toshitada Yoshioka,** Koscak Maruyama,‖ and Shoichiro Tsukita*

*Department of Information Physiology, National Institute for Physiological Sciences, Okazaki, Aichi 444; ‡Molecular Electric Laboratory, Tsukuba Research Center, SANYO Electric Co. Ltd., Koyadai, Ibaraki 305; §Department of Physiology, The Jikei University School of Medicine, Tokyo 105; ‖Department of Biology, Faculty of Science, Chiba University, Chiba 263; ¶Department of Physics, School of Science and Engineering, Waseda University, Tokyo 169; **Department of Physiology, St. Marianna University of Medicine, Kawasaki 213, Japan

Abstract. To clarify the full picture of the connectin (titin) filament network in situ, we selectively removed actin and myosin filaments from cardiac muscle fibers by gelsolin and potassium acetate treatment, respectively, and observed the residual elastic filament network by deep-etch replica electron microscopy. In the A bands, elastic filaments of uniform diameter (6–7 nm) projecting from the M line ran parallel, and extended into the I bands. At the junction line in the I bands, which may correspond to the N2 line in skeletal muscle, individual elastic filaments branched into two or more thinner strands, which repeatedly joined and branched to reach the Z line. Considering that cardiac muscle lacks nebulin, it is very likely that these elastic filaments were composed predominantly of connectin molecules; indeed, anti-connectin monoclonal antibody specifically stained these elastic filaments. Further, striations of ~4 nm, characteristic of isolated connectin molecules, were also observed in the elastic filaments. Taking recent analyses of the structure of isolated connectin molecules into consideration, we concluded that individual connectin molecules stretched between the M and Z lines and that each elastic filament consisted of laterally-associated connectin molecules. Close comparison of these images with the replica images of intact and S1-decorated sarcomeres led us to conclude that, in intact sarcomeres, the elastic filaments were laterally associated with myosin and actin filaments in the A and I bands, respectively. Interestingly, it was shown that the elastic property of connectin filaments was not restricted by their lateral association with actin filaments in intact sarcomeres. Finally, we have proposed a new structural model of the cardiac muscle sarcomere that includes connectin filaments.

It is widely accepted that the myofibrils in striated muscle consist predominantly of two types of filaments, thick (myosin) and thin (actin). In addition, intensive physiological analyses of muscular contraction have strongly suggested the presence of a third type of filament, tentatively named "elastic filaments," inside myofibrils. These elastic filaments are assumed to be responsible for the so-called "resting tension" of relaxed skeletal muscles (Funatsu et al., 1990), for keeping thick filaments at the center of the sarcomere on relaxation, for maintaining the tension output of the sarcomere despite thick-filament movement on contraction (Horowits and Podolsky, 1988; Horowits et al., 1989), and for recovering sarcomeres to the initial state after extreme stretching and release (Maruyama et al., 1989). Actually, possible morphological counterparts of these elastic filaments at the electron microscopic level have been described as "gap filaments" found between I and A bands in extremely stretched muscle fibers (Sjöstrand, 1962; Locker and Leet, 1976; Maruyama et al., 1985; Trombitás et al., 1991), as "third filaments," found in myofibrils after the removal of myosin and actin filaments with potassium iodide (dos Remedios and Gilmour, 1978), and as "end filaments," found at the tips of isolated myosin filaments (Trinick, 1981). However, mainly due to the failure to directly visualize these elastic filaments in situ, their actual existence in myofibrils is still a matter of debate.

The connectin (also called titin) molecule has recently been identified and characterized as a possible constituent of the elastic filaments (for reviews see Wang, 1985; Maruyama

T. Funatsu and H. Higuchi's present address is Yanagida Biomotron Project, Exploratory Research for Advanced Technology, Research Development Corporation of Japan, 2-4-14 Senba-higashi, Mino, Osaka 562, Japan.

et al., 1986; Trinick, 1991). The mother molecule, α-connectin, a huge molecule of ~3,000 kD, has recently been isolated from rabbit skeletal muscle (Kimura and Maruyama, 1989). By low-angle rotary shadowing EM, its proteolytic fragment, β-connectin (~2,000 kD), was reported to look like a very thin rod, ~0.9 μm long, with a single globular head, consisting of M-line constituents, at one end (Nave et al., 1989). Immunoelectron microscopic studies, using antibodies specific for various portions of the rod-like connectin (or titin) molecules, have suggested that a single connectin molecule extends from the Z line to the M line in a half-sarcomere (Fürst et al., 1988; Itoh et al., 1988a; Whiting et al., 1989; Nave et al., 1989). These biochemical and immunohistochemical data strongly favor the view of the existence of elastic filaments throughout myofibrils in situ.

This being the background situation, we believed that for further evidence it would be necessary, again, to directly visualize the elastic filaments which could consist predominantly of connectin. In a previous study, we developed a technique for the selective removal of actin filaments with plasma gelsolin, and by applying this technique to skeletal muscle we succeeded in clearly visualizing the elastic filaments in the actin filament-free I band by thin-section EM (Funatsu et al., 1990). However, as stated above, this type of elastic filament has not been identified in thin-section electron microscopic images of intact striated muscle sarcomeres. How can we explain this discrepancy? In the present study, we attempted to address this question, using cardiac muscle fibers, which lack nebulin (Locker and Wild, 1986; Hu et al., 1986; Itoh et al., 1988b; Wang and Wright, 1988; Kruger et al., 1991). To avoid the possible induction of artifacts by chemical fixation, which could occur in the case of delicate structures such as elastic filaments, we used a rapid freezing method with liquid helium. To obtain three-dimensional information on elastic filaments at high resolution, we used a deep-etch replica technique. Further, to clarify whether elastic filaments were present at the A bands, we used a technique for the selective removal of myosin filaments. Combining these methods, we carefully compared the replica images of intact and S1-decorated sarcomeres with those of actin filament-free I bands and/or thick filament-free A bands. Finally, these observations allowed us to propose a model for the arrangement of connectin filaments in myofibrils in situ.

Materials and Methods

Muscle Fibers

Rabbit papillary muscle (2 × 5 mm), carefully dissected out of the heart, was tied to a glass rod and incubated in 50% (vol/vol) glycerol containing 0.5 mM $NaHCO_3$, 5 mM EGTA, and 1 mM leupeptin at 0°C overnight. Fibers were then stored in the fresh solution at −20°C for >1 wk.

Proteins

Plasma gelsolin was purified as described previously (Funatsu et al., 1990). Myosin subfragment 1 (S1)[1] was prepared from rabbit leg and back white muscle according to the method of Weeds and Taylor (1975).

1. *Abbreviation used in this paper*: S1, myosin subfragment 1.

Antibodies

SM1, a monoclonal antibody against connectin, was kindly donated by Dr. Teruo Shimizu (Teikyo University). It was obtained from a BALB/c mouse immunized with a crude human myosin preparation (Shimizu et al., 1988). Anti-nebulin antiserum was prepared as described previously (Maruyama et al., 1989). Secondary antibodies (goat anti-mouse IgG and goat anti-rabbit IgG; Cappel, West Chester, PA) were purchased.

Selective Removal of Actin and Myosin Filaments

A bundle of glycerinated muscle fibers (~150 μm diam and ~3 mm long) was tied at both ends to a platinum wire (0.3 mm φ). Actin filaments were removed with gelsolin, as described previously (Funatsu et al., 1990). Briefly, muscle fibers were chemically skinned with 1% Triton X-100 in EGTA rigor solution (0.17 M KCl, 1 mM $MgCl_2$, 10 mM 3-[*N*-morpholino] propanesulfonic acid [MOPS; pH 7.0], 1 mM EGTA, 2 mM diisopropyl fluorophosphate [DFP], and 2 mM leupeptin) for 30 min. Samples were treated with 0.5 mg/ml of gelsolin in Ca rigor solution (0.1 mM $CaCl_2$ was substituted for 1 mM EGTA in EGTA rigor solution) and then in contracting solution (0.15 M KCl, 5 mM $MgCl_2$, 4 mM ATP, 10 mM MOPS, pH 7.0, 0.1 mM $CaCl_2$, 2 mM DFP, and 2 mM leupeptin) for 1 h each. They were finally washed for 1 h with relaxing solution (1 mM EGTA was substituted for 0.1 mM $CaCl_2$ in contracting solution).

To remove myosin filaments, the actin filament-free muscle fibers were further treated with a high salt solution containing 1 M potassium acetate, 5 mM $MgSO_4$, 4 mM ATP, 4 mM EGTA, 20 mM MOPS, pH 7.0, 2 mM DFP, and 2 mM leupeptin for 30 min, and then washed for 30 min with relaxing solution. To leave the elastic filaments intact, 2 mM DFP and 2 mM leupeptin must be added to all the solutions used and all the procedures must be carried out at 2°C.

S1-Decoration

Cardiac muscle was chemically skinned with 1% Triton X-100 in EGTA rigor solution for 30 min. The samples were incubated with 2 mg/ml of S1 in EGTA rigor solution, and then washed for 1 h with EGTA rigor solution.

SDS-Gel Electrophoresis and Immunoblotting

Muscle fibers were dissolved in 25 μl of SDS solution (7.5% SDS, 10% glycerol, 1 mM DTT, and 10 mM Tris-HCl, pH 6.8) and heated for 3 min at 90°C. SDS gel electrophoresis was carried out according to the method of Laemmli (1970), using a 3–13% polyacrylamide gradient gel; protein bands were visualized with Coomassie brilliant blue R. For immunoblotting, freshly excised rabbit papillary muscle fibers were gently homogenized in 2 vols of solution containing 10% SDS, 40 mM DTT, 10 mM EDTA, and 100 mM Tris-HCl, pH 8.0. The sample was boiled for 3 min and clarified by centrifugation at 15,000 *g* for 20 min. The supernatant was electrophoresed, using a 2–8% gradient of polyacrylamide gels, according to the method of Laemmli (1970). The separated proteins were electrophoretically transferred onto a nitrocellulose sheet (Towbin et al., 1979) and then incubated with anti-connectin mAb (SM1) or anti-nebulin antiserum. Bound antibodies were detected after treatment with HRP-conjugated anti-mouse or anti-rabbit IgG (Cappel, West Chester, PA).

Rapid Freezing

A bundle of muscle fibers mounted on a holder was rapidly frozen by being placed against a pure copper block that was cooled to 4°K with liquid helium by using a freezing apparatus, RF-23 (Eiko Engineering, Ibaraki, Japan; Tsukita and Yano, 1985; Usukura, J., E. Yamada, H. Akahori, and H. Takahashi. 1981. *J. Electron Microsc.* 30:214 [Abstr.]). Specimens thus frozen were stored in liquid nitrogen until use.

Freeze Substitution

The frozen samples were freeze substituted for 2 d with acetone containing 4% OsO_4 at −80°C (Tsukita and Yano, 1985; Tsukita et al., 1988). They were transferred to a freezer maintained at −20°C, kept there for 1 h, and were then stored at 4°C for 2 h. After being washed with acetone, the samples were stained en bloc for 2 h at room temperature in ethanol containing 5% uranyl acetate. They were washed in ethanol, then in propylene oxide, and embedded in POLY/BED 812 (Polyscience, Warrington, PA). Thin sections were stained sequentially with 4% uranyl acetate and 0.4% lead citrate for 3 min each at 25°C.

Deep-Etch, Rotary-Shadow Replica EM

The deep-etch replica method used in this study has been previously described in detail (Tsukita et al., 1986, 1988). Rapidly frozen samples were mounted on an ultramicrotome (ULTRACUT, Reichert-Jung Optische Werke AG, Wien, Austria) equipped with a low temperature sectioning system (FC4E), and they were then fractured with a glass knife at −150°C. The samples were placed in a holder, and covered with a cooled cap; they were then transferred to a freeze-etch device (BAF 400D; Balzers Union Aktiengesellschaft, Liechtenstein) in a nitrogen atmosphere. When a vacuum of 2×10^{-6} torr was achieved at −150°C, the sample was warmed to −100°C and the cooled cap covering the sample was removed. The sample was etched for 7 min at −100°C, followed by rotary shadowing with platinum-carbon and carbon at angles of 25° and 65°, respectively. The sample was then removed from the freeze-etch device, immersed in methanol at −20°C overnight, and then dissolved in household bleach. Replicas floating off the sample were washed three times with distilled water and collected on formvar-filmed grids. Stereo pair electron micrographs were taken on a JEM-1200EX electron microscope (JEOL, Tokyo, Japan), operated at 100 kV, by tilting the specimen stage at ±10°. Electron microscopic negatives (Fuji Electron Microscopic Film FG; Fuji Photo Film, Japan) were reversed onto Kodak fine grain positive films (Eastman Kodak Co., Rochester, NY), and were then printed as negative images. A 1.6-μm-wide A band (Huxley, 1963) was used as an internal standard of length.

Immunoelectron Microscopy

Muscle fibers were fixed in a fixative containing 3.8% formaldehyde, 80 mM KCl, 5 mM $MgSO_4$, 4 mM ATP, 4 mM EGTA, 2 mM DFP, and 10 mM piperazine-N,N'-bis(2-ethane) sulfonic Acid (Pipes; pH 7.0) for 6 h. All the procedures were carried out at 2°C unless otherwise stated. After the samples were washed in PBS (0.1 M NaCl, 1 mM DFP, 1 mM leupeptin, and 10 mM sodium phosphate, pH 7.0) for 15 min, reactive aldehyde groups were blocked by incubating the samples sequentially in PBS containing 20 mM glycine for 30 min and in PBS containing 1% egg albumin for 30 min. The samples were washed with PBS for 15 min and then exposed to anti-connectin mAb (SM1) in PBS for 24 h. As a control experiment, some fibers were incubated in PBS without primary antibody. After being washed with PBS for 12 h, the samples were reacted with anti-mouse IgG in PBS for 12 h. They were then washed with PBS for 12 h and with 0.1 M sodium cacodylate buffer, pH 7.2, for 10 min, and fixed with 2.5% glutaraldehyde in 0.1 M sodium cacodylate buffer, pH 7.2, for 2 h at 25°C and then overnight at 4°C. Samples were postfixed with 1% OsO_4 in the same buffer for 2 h at 2°C, washed with distilled water, stained with 0.5% uranyl acetate for 2 h at 25°C, dehydrated, and stained sequentially with 4% uranyl acetate and 0.4% lead citrate for 3 min each at 25°C.

Results

Elastic Filaments in Actin Filament-free I Bands of Cardiac Muscle

The selective removal of actin filaments from skeletal muscle was applied to rabbit cardiac muscle. As shown in Fig. 1, cardiac muscle fibers lack nebulin. When cardiac muscle cells were treated with plasma gelsolin, actin and tropomyosin were selectively and largely removed, indicating that this technique for the selective removal of actin filaments with gelsolin works also well in cardiac muscle fibers (Fig. 1 *A*).

First, the actin filament-free cardiac muscle fibers were rapidly frozen with liquid helium, freeze substituted, and observed by thin-section EM (Fig. 2). Actin filaments were completely removed, leaving myosin filaments, M lines, and Z lines intact, and residual elastic filaments were clearly visualized in the actin filament-free I bands. The actin filament-free I band appeared to be divided into two zones by the residual elastic filament network: A band–side and Z line–side zones (Fig. 2, *C* and *D*). The A band–side zone was characterized by straightly stretched elastic filaments with a uniform diameter, while the elastic filaments in the Z line–side zone appeared to be variable in their diameter and direction. The boundary line of these two zones is tentatively called "a junction line" here. This junction line was not so clear in intact I band, but was sometimes detectable (Fig. 2 *B*).

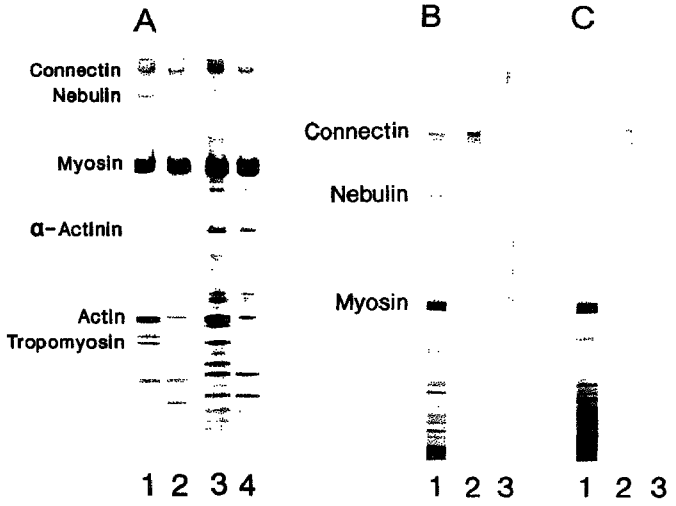

Figure 1. SDS-PAGE patterns and immunoblot test of skeletal and cardiac muscle fibers. (*A*), 3–13% polyacrylamide gradient gels stained with Coomassie brilliant blue. (Lane *1*) Intact rabbit skeletal muscle; (lane *2*) skeletal muscle treated with 0.5 mg/ml of gelsolin in Ca rigor solution and then in contracting solution at 2°C for 1 h each; (lane *3*) intact rabbit cardiac muscle; and (lane *4*) cardiac muscle treated with gelsolin. (*B* and *C*) Immunoblot tests of the reaction of anti-connectin and anti-nebulin antibodies with rabbit psoas (*B*) and papillary muscle (*C*) proteins. (Lane *1*) Coomassie brilliant blue–stained gel pattern of whole muscle proteins (2–8% polyacrylamide gradient gels); (lane *2*) treated with anti-connectin monoclonal antibody (SM1) and (lane *3*) treated with anti-nebulin polyclonal antibodies.

Next, to obtain three-dimensional images of these elastic filaments at high resolution, the I bands of actin filament-free cardiac muscle fibers were analyzed by the deep-etch replica method (Figs. 3 and 4). The junction line and A band–side/Z line–side zones were also clearly observed in the actin filament-free I bands in the deep-etch replica images. Close stereoscopic inspection allowed us to pursue individual elastic filaments. In the A band–side zone, a single elastic filament of uniform diameter was shown to project from the tip of each thick filament and to extend in a straight line toward the junction line. The diameter of the elastic filament was ~6–7 nm, assuming that the width of the backbone of the thick filament was 17.6 nm (Knight and Trinick, 1984) and that the thickness of the platinum replica was ~1 nm. At the level of the junction line, two or three adjoining elastic filaments were laterally associated with each other and each filament appeared to branch off into two (or more) thinner strands. In the Z line–side zone, these thinner strands repeatedly joined and branched toward the Z line, finally being integrated into the meshwork of the Z line. Occasionally, a striation of ~4 nm was observed on the surface of the elastic filaments. When the actin filament-free cardiac muscle fibers were stretched, the Z line–side zone, rather than the A band–side zone, appeared to be preferentially extended (Figs. 3 and 4).

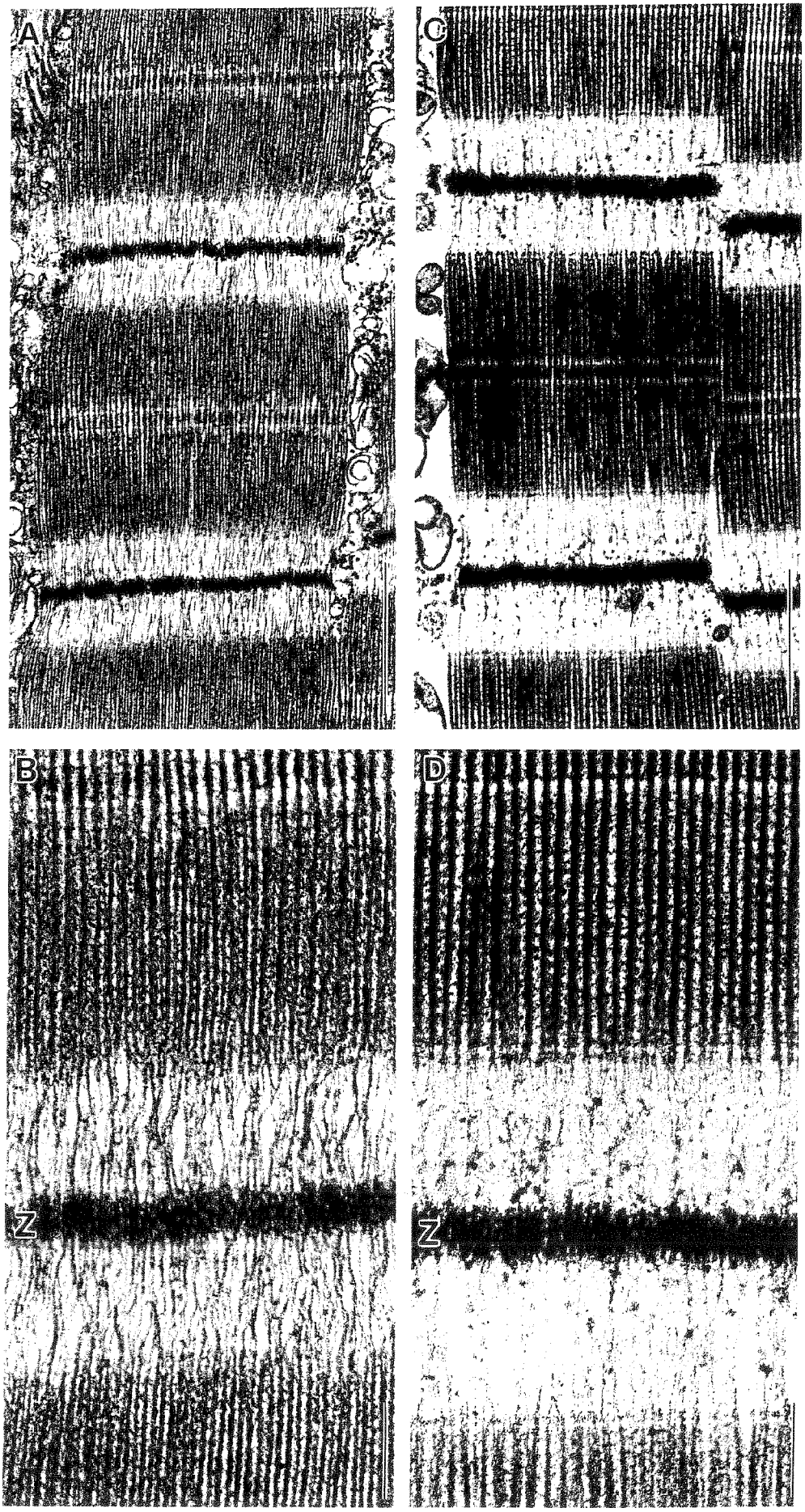

Figure 2. Thin sections of freeze-substituted cardiac muscle cells. (*A* and *B*) Intact muscle; and (*C* and *D*) muscle treated with 0.5 mg/ml of gelsolin in Ca rigor solution and then in contracting solution at 2°C for 1 h each. *Z*, Z line. (*A* and *C*) Lower magnifications; (*B* and *D*) higher magnifications. Bars: (*A* and *C*) 1 μm; (*B* and *D*) 0.2 μm.

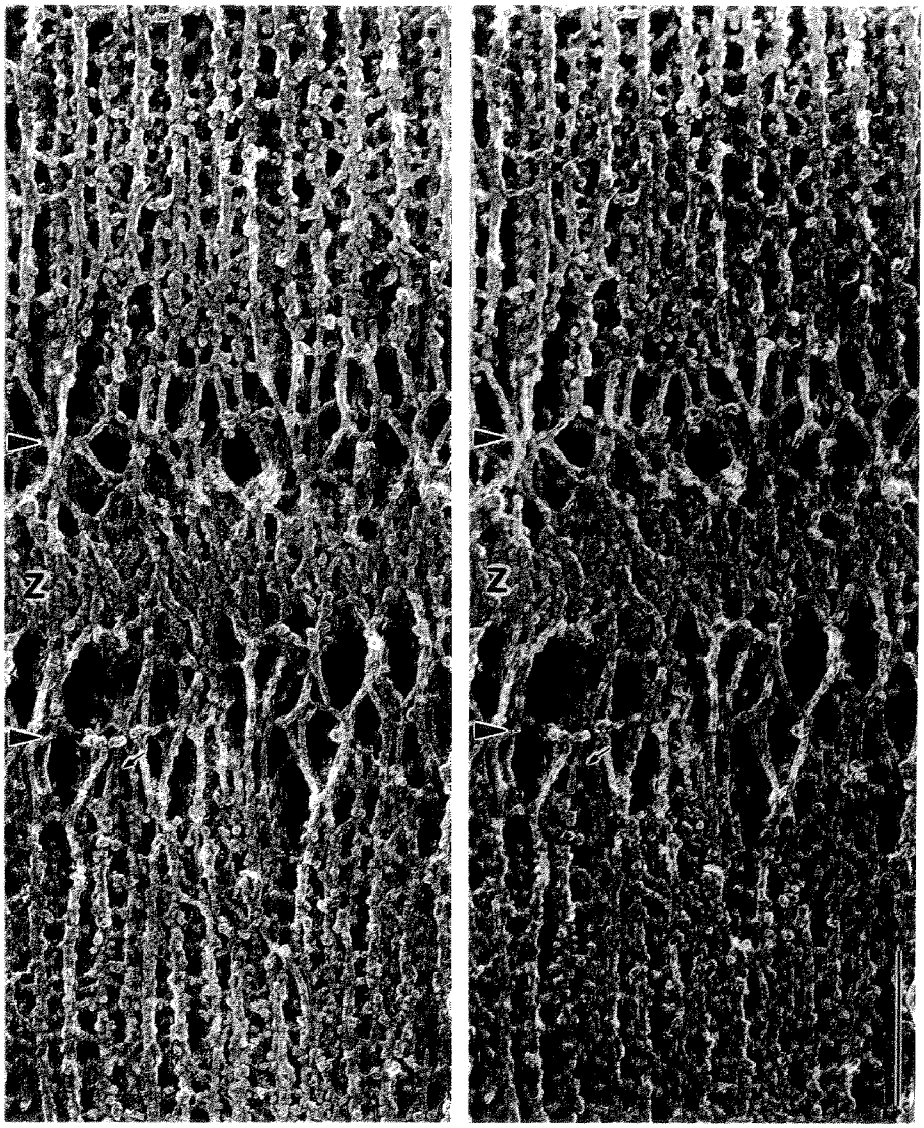

Figure 3. Stereo pair micrographs of freeze-etch replica of gelsolin-treated cardiac muscle at a sarcomere length of 2.1 μm. Arrowheads indicate the junction line of connectin filaments. An arrow indicates ~4-nm connectin filament striation. *Z*, Z line. Bar, 0.2 μm.

Elastic Filaments in Intact and S1-decorated I Bands of Cardiac Muscle

We attempted to identify the elastic filaments in intact I bands. For this purpose, we first carefully observed an intact I band by deep-etch replica EM (Fig. 5). We were then led to the following conclusions: (*a*) judging from the striations of ~5.5 nm on their surface (Heuser and Kirschner, 1980; Heuser and Cooke, 1983) and their diameter of ~10 nm, almost all of the longitudinally oriented filaments in intact I bands can be identified as so-called thin filaments consisting predominantly of actin; (*b*) the tips of the thick filaments could not be identified, probably due to the elastic filaments projecting from each tip. When individual thick filaments were traced toward the Z line, they appeared to continue and merge into thin filaments; and (*c*) very thin strands cross-linking neighboring thin filaments, which may correspond to the "lateral struts" described previously (Trombitás et al., 1988), were clearly observed, frequently around the junction line and the Z line.

Next, the S1-decorated I bands in the deep-etch replica images were analyzed (Fig. 6). All the longitudinally oriented filaments in the I bands were fully decorated with S1 and showed a rope-like double helix appearance (35-nm half pitch) with striations of ~5.5 nm on their surface. This indicates that all the longitudinally oriented filaments visualized in the intact I bands were so-called thin filaments consisting predominantly of actin. Lateral struts were also clearly observed in S1-decorated I bands (*small arrows* in Fig. 6). Close inspection revealed that the thick filaments appeared to merge into rope-like S1-decorated thin filaments, probably through elastic filaments projecting from their tips (*large arrow* in Fig. 6). On the other hand, when actin filament-free I bands were treated with S1 under the same conditions, the elastic fibers showed no change in morphology (data not shown). Taking these results together, we were led to the conclusion that, in intact I bands, the so-called thin filament was a complex of the elastic filament and the actin filament with tropomyosin and troponin, and that, in S1-treated I bands, the elastic filaments were associated with S1, together with actin filaments. This interpretation was conclusively confirmed by the images shown in Fig. 7. In this experiment, the S1-decorated cardiac muscle fibers were mechanically stretched under the condition of rigor. As a result, in the I band, rope-like S1-actin filament complexes were broken off, leaving thin strands stretching between breaking ends. Judging from their diameter and the ~4-nm striations on their surface, these thin strands seemed to be identical to the elas-

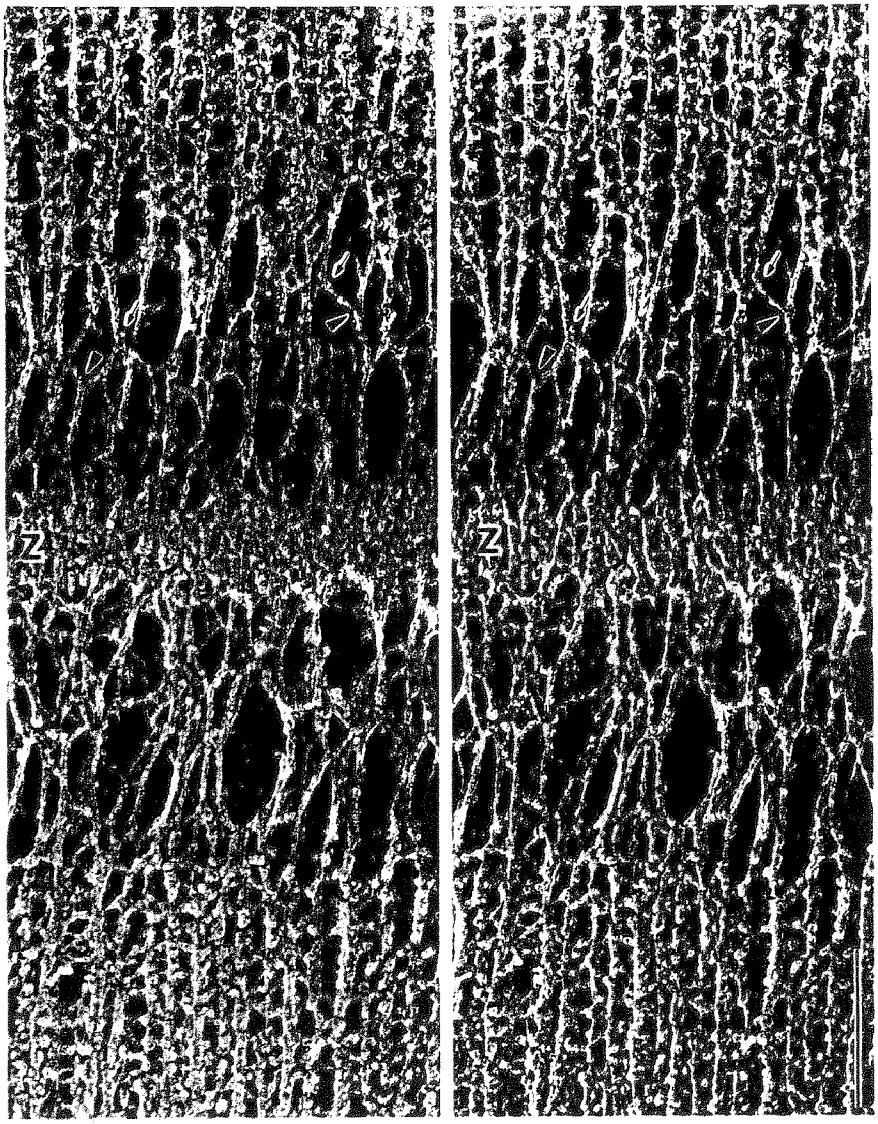

Figure 4. Stereo pair micrographs of freeze-etch replica of gelsolin-treated cardiac muscle at a sarcomere length of 2.5 μm. *Z*, Z line. Bar, 0.2 μm.

tic filaments visualized in the actin filament-free I bands. This image, then, not only favored the above interpretation, but also suggested the elastic properties of the elastic filaments laterally associated with actin filaments (so called thin filaments).

Elastic Properties of Elastic Filaments

It is reasonable to regard the elastic filaments visualized in this study as connectin (titin) filaments. Therefore, we attempted to mark the elastic filaments with anti-connectin mAb (SM1). Treatment of intact cardiac muscle with SM1 resulted in the formation of a single electron-dense stripe in each I band (Fig. 8 *A*). These stripes were also formed in gelsolin-treated cardiac muscle fibers at positions similar to those in the I band, indicating that the SM1 epitope was located on the elastic filaments around the level of the junction line and that dislocation of this epitope in the longitudinal direction was not induced by gelsolin treatment (Fig. 8 *B*).

To study the elastic properties of elastic filaments, we analyzed the position of the SM1 epitope under various sarcomere lengths, both in intact and in actin filament-free I bands (Fig. 9). The distances between the Z line and the epitope (ZE distance) and between the edge of the A band and the epitope (AE distance) were measured. When these distances were plotted as a function of the distance between the Z line and the edge of the A band (ZA distance) (see Horowits et al., 1989), both ZE and AE distances increased linearly with the ZA distance (Fig. 9 *B*). As shown in Table I, comparison of the slope and intercept in intact and actin filament-free I bands clearly indicated that actin filaments with tropomyosin and troponin had no influence on the elastic properties of elastic filaments. In both intact and actin filament-free I bands, the ZE part of the elastic filaments appeared to be 2.1–2.4 times as extensible as the AE part, which was consistent with the deep-etch replica observation (Figs. 3 and 4).

This type of elastic property should be accompanied by some structural changes in elastic filaments. As shown in Figs. 3 and 4, elastic filaments showed ~4-nm striations on their surface. Therefore, we measured the spacing of this striation in actin filament-free I bands under various sarcomere lengths (Fig 10). The striation spacing varied from ~4 to ~5 nm in proportion to the ZA distance. The reason is not clear why the striation spacing increases by ~20% while the ZA distance increases 100%, but it may be partly due to the fact that elastic filaments are slack in short sarcomeres. There was no significant difference in this change of spacing between the A band–side and Z line–side zones.

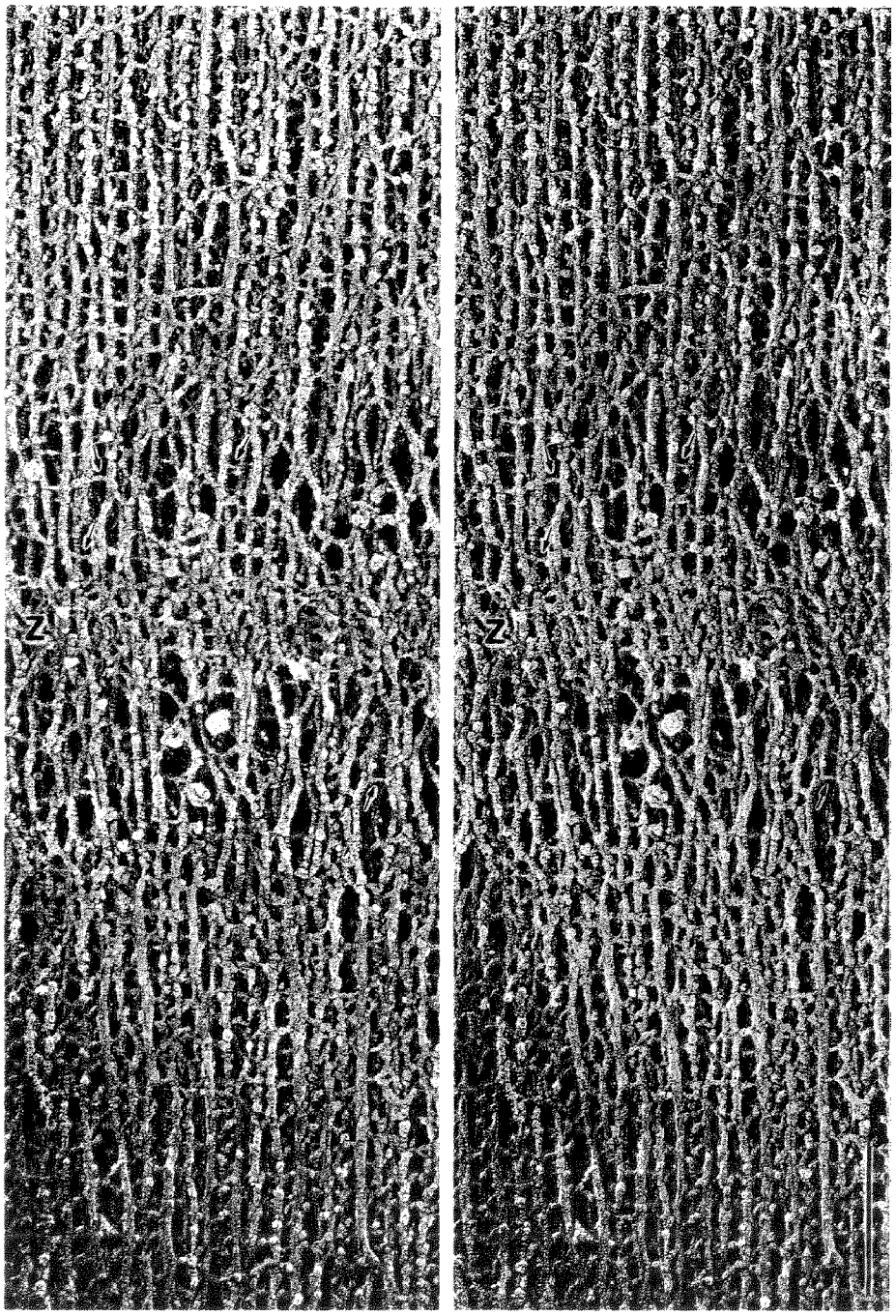

Figure 5. Stereo pair micrographs of freeze-etch replica of cardiac muscle sarcomere without gelsolin treatment at a sarcomere length of 2.2 μm. Arrows indicate lateral bridges connecting thin filaments. *Z*, Z line. Bar, 0.2 μm.

Elastic Filaments in Myosin and Actin Filament-free Cardiac Muscle

As shown in deep-etch replica images of actin filament-free I bands (Figs. 3 and 4), it is clear that single elastic filaments projected directly from the tips of individual thick filaments. In the A band of these gelsolin-treated cardiac muscle fibers, there were no longitudinally oriented filaments other than the so-called thick filaments. However, it has already been shown that the elastic filament binds onto the thick filament up to the edge of the M line (Fürst et al., 1988). To visualize

Table I. Linear Regression Parameters of the Position of the SM1 Epitope as a Function of the Distance from the Z line to the A–I Junction

	Control		Gelsolin-treated	
	Slope	Intercept	Slope	Intercept
		nm		*nm*
Epitope to Z line	0.67 ± 0.02	−34 ± 1	0.70 ± 0.02	−32 ± 1
Epitope to A band	0.32 ± 0.02	35 ± 1	0.30 ± 0.02	32 ± 1

Dependence of the position of the SM1 epitope on the distance from the Z line to the A–I junction (Fig. 9) was analyzed by linear regression. Data are the fitted values ± expected standard errors (n = 55).

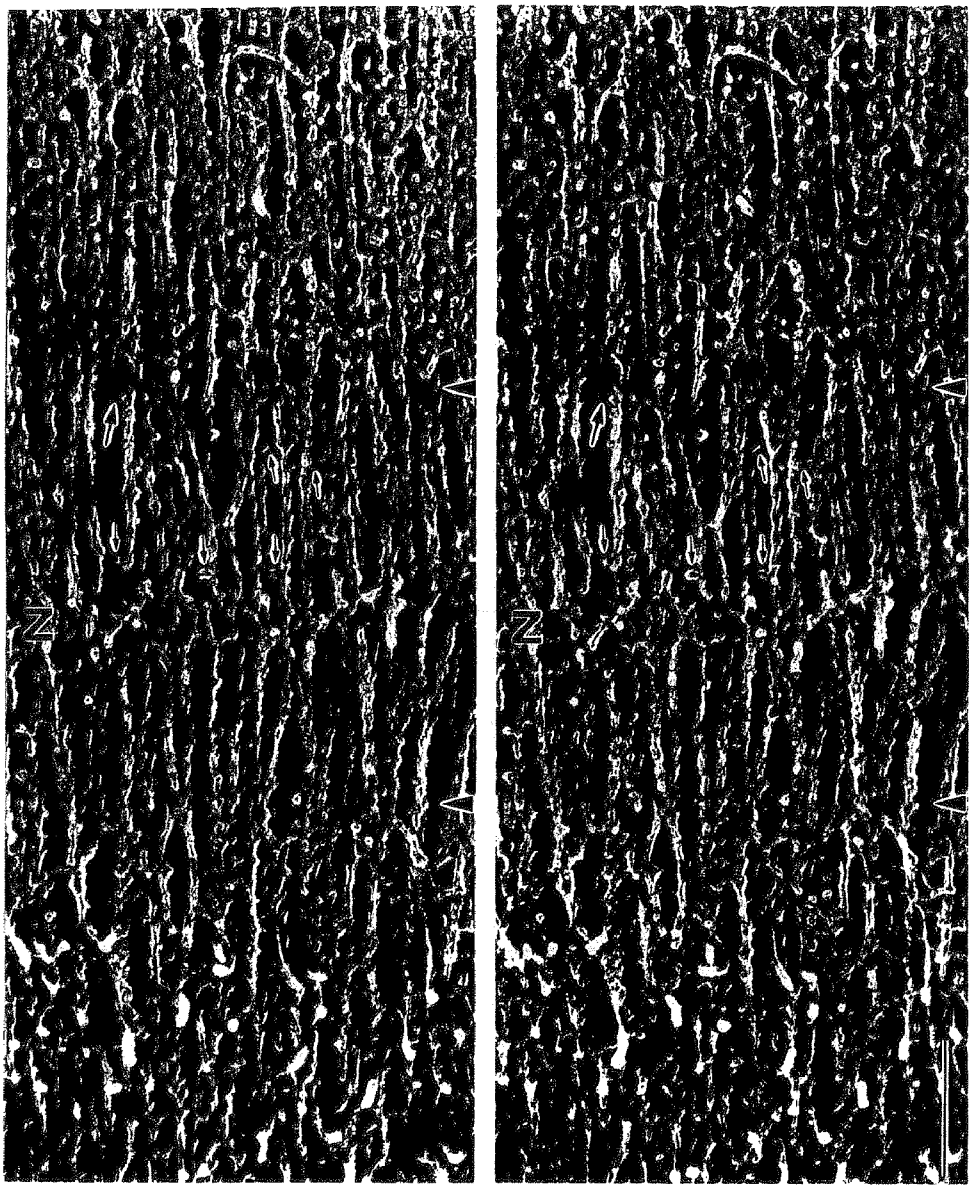

Figure 6. Stereo pair micrographs of freeze-etch replica of cardiac muscle sarcomere decorated with S1. Arrowheads indicate positions of ends of thick filaments; small arrows indicate lateral bridges connecting thin filaments; and large arrow indicates elastic filament projecting from the end of a thick filament. Z, Z line. Bar, 0.2 μm.

elastic filaments in the A band, we attempted to selectively remove myosin filaments from the actin filament-free cardiac muscle fibers. When a high concentration of potassium chloride was used to completely remove myosin filaments, all the elastic filaments appeared to be collapsed onto the Z line (Higuchi et al., 1992). Although intermediate potassium chloride concentrations can control A band length from 1.6 to 0.3 μm (Ishiwata et al., 1985; Higuchi and Ishiwata, 1985; Higuchi et al., 1992), this extraction leaves some myosin molecules on elastic filaments to make the ultrastructural observation difficult. Instead of potassium chloride, we used a high concentration of potassium acetate, since we found that this induced the depolymerization of myosin filaments from both tips, leaving the central part of the myosin filament (0.4 μm long) intact. When gelsolin-treated cardiac muscle fibers were further treated with a high concentration of potassium acetate, SDS-PAGE analyses revealed that myosin was largely removed, leaving the connectin unextracted (Fig. 11).

The potassium acetate-treated actin filament-free cardiac muscle fibers were rapidly frozen and observed by freeze substitution EM (Fig. 12 *A*). Interestingly, elastic filaments were also observed in A band and appeared to stretch from the Z line toward the M line. In deep-etch replica images, these elastic filaments in the A bands were stereoscopically visualized at high resolution (Fig. 12 *B*). The elastic filaments in the A band–side zone of the I bands, which were characterized by a straight appearance and uniform diameter, continued deeply into the A band in a straight line with rare branching, and reached the M line. Lateral struts were observed between these A band elastic filaments. ~4-nm striations were detected on the surface of these elastic filaments in the A bands similarly to those detected in the I bands.

Discussion

In the present study, we succeeded in selectively removing both actin and myosin filaments from cardiac muscle fibers and in directly visualizing the residual elastic filaments stretching between the M and Z lines by deep-etch replica EM (Fig. 12). To evaluate potential artifacts carried by the freeze-fracture/deep-etch method, ultrastructure was also

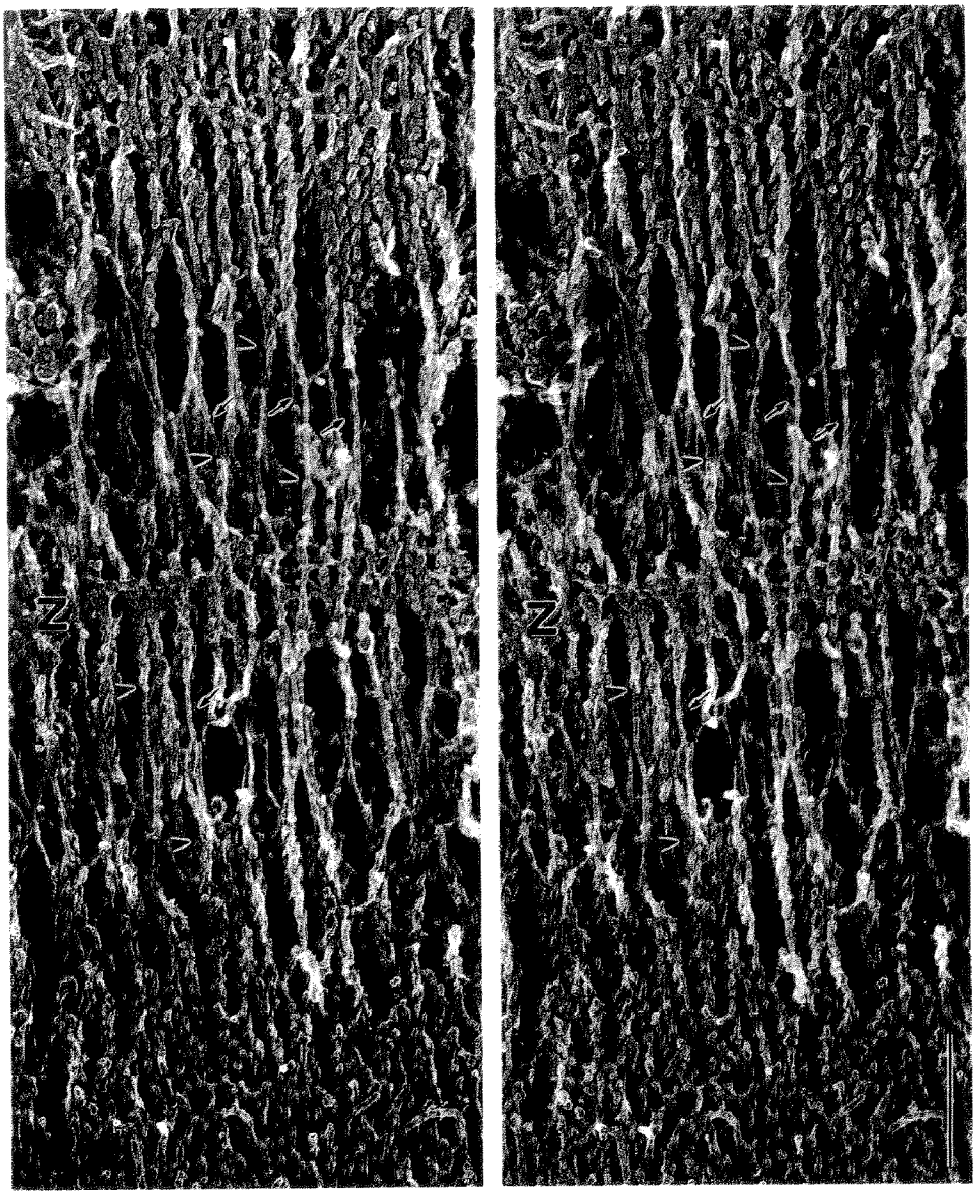

Figure 7. Stereo pair micrographs of freeze-etch replica of cardiac muscle sarcomere in which thin filaments decorated with S1 were torn off by stretching. Arrowheads indicate the ends of thin filaments cut by stretching; arrows indicate elastic filaments. *Z*, Z line. Bar, 0.2 μm.

examined with thin sections of freeze substituted or conventionally chemically fixed specimens. All these methods consistently showed images of the elastic filaments in situ. In the A band, the elastic filaments projecting from the M line which had a uniform diameter, run parallel, with rare branching, and extended as such to the junction line in the I band. At this line, individual elastic filaments branched off into two (or more) thinner strands, which repeatedly joined and branched to ultimately reach the Z line.

Recently, Nave et al. (1989) clearly visualized the molecular structure of the extractable form of titin (TII_A and TII_B; β-connectin) by low-angle rotary-shadowing EM with novel specimen orientation methods. They found that the monomeric molecules had a single globular head at one end of a long and very thin rod (~900 nm long) of uniform diameter; these molecules were shown to be laterally associated with each other in a parallel manner to form dimers, tetramers, or higher oligomers. Nave et al. (1989) concluded that the globular head was composed of M band constituents and that the two distinct ends of the titin (connectin) molecule attached to Z and M band material, respectively. Their images and their conclusion led us to the following interpretation regarding the molecular organization of the elastic filaments we visualized in the myosin and actin filament-free sarcomeres. Taking into consideration our finding of the epitope of anti-connectin mAb (SM1) on the elastic filaments in actin filament-free I bands (see Fig. 8) and our knowledge that cardiac muscle lacks nebulin, we believed it was evident that the elastic filaments we observed in this study were composed predominantly of connectin molecules. Connectin molecules stretched from the M to Z line, and, at the region between the M line and the junction, two (or more) connectin molecules appeared to be bundled in a parallel manner to form individual elastic filaments of uniform diameter, while at the level of the junction line this bundle appeared to break up into thinner strands consisting of one (or more) connectin molecule. This interpretation is highly consistent with the results obtained previously from immunoelectron microscopic studies that used antibodies specific for various portions of connectin (titin) molecules (Fürst et al., 1988; Itoh

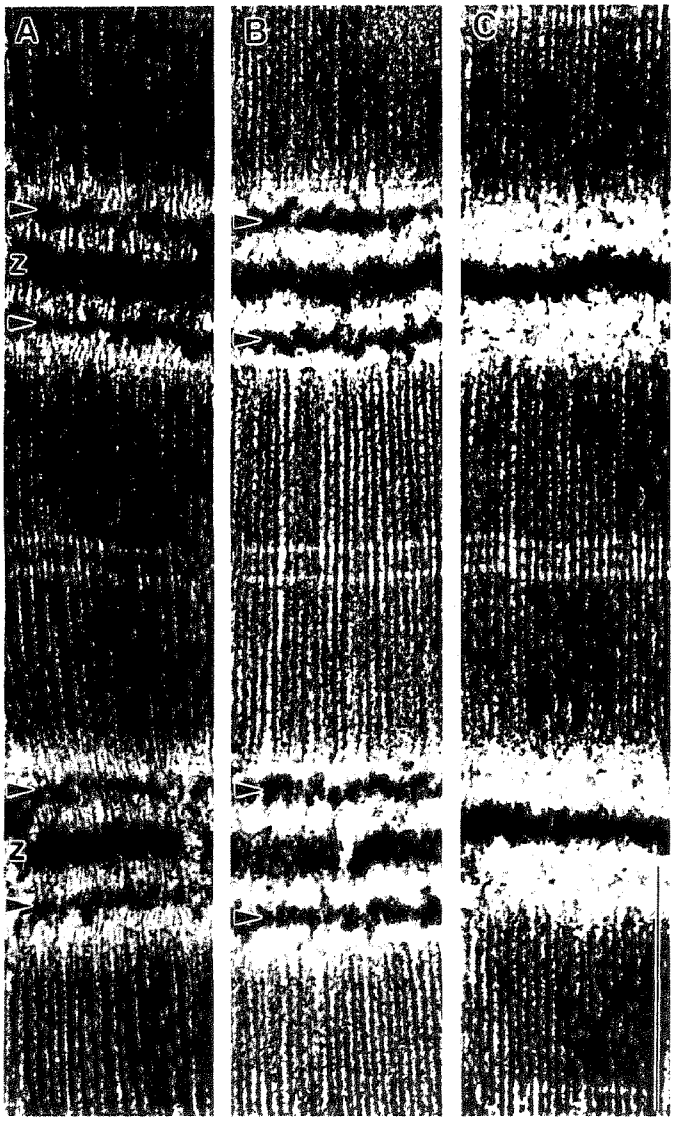

Figure 8. Immunoelectron micrographs of cardiac muscle sarcomeres. Papillary muscle fibers without or with gelsolin treatment were reacted with antibodies, as described in Materials and Methods. (*A*) Sarcomeres reacted with anti-connectin mAb (SM1) without gelsolin treatment; (*B*) gelsolin-treated sarcomeres reacted with SM1; and (*C*) gelsolin-treated sarcomeres reacted with second antibody only. Arrowheads indicated stripes due to antibody binding. Bar, 1 μm.

et al., 1988a; Whiting et al., 1989). Interestingly, the ~4-nm striations on the surface of elastic filaments in the actin and myosin filament-free sarcomeres were also detected in negative staining and low-angle rotary-shadowing images of purified titin (connectin) molecules (Trinick et al., 1984; Wang et al., 1984). In light of this evidence, we hereafter refer to the elastic filaments as "connectin filaments."

Of course, in the myosin and actin filament-free sarcomeres, some structures are likely to have formed by collapse of connectin molecules that were more widely separated before myosin and actin extraction. Questions have then naturally arisen as to why such well-defined connectin filaments have so far not been visualized in intact striated muscles in situ and how connectin filaments are arranged in intact sarcomeres. In some earlier studies, a small part of the filament was thought to have been observed in situ in extremely stretched muscle fibers as "gap filaments" (Sjöstrand, 1962; Locker and Leet, 1976; Maruyama et al., 1985; Trombitás et al., 1991). Also in the deep-etch replica images of intact sarcomeres, connectin filaments were hardly detected. It is now known that some flexible structures are apt to be collapsed artifactually during the process of deep etching. Therefore, it appears to be reasonable to speculate that in intact sarcomere the deep etching causes the artifactual collapse of all flexible connectin filaments onto actin and myosin filaments. However, careful comparison of the deep-etch replica images of gelsolin- and potassium acetate-treated sarcomeres with those of intact sarcomeres and/or S1-decorated intact sarcomeres did not favor this speculation, and led us to propose a model for the arrangement of connectin filaments (molecules) in an intact sarcomere (Fig. 13 *A*).

In the A bands, connectin filaments were barely visualized in actin filament-free muscle sarcomeres, and they could not be detected unless myosin filaments were removed by potassium acetate treatment. Lateral struts observed in the A band of gelsolin and potassium acetate-treated muscle might be morphological counterparts for unraveled connectin molecules or unidentified proteins. Further, connectin filaments were clearly observed to directly project from the tips of individual thick filaments. It is thus reasonable to conclude that, in the A bands, connectin filaments show an intimate spatial relationship with myosin filaments. Are the connectin filaments integrated inside the myosin filaments or not? Immunoelectron microscopic observations with anti-connectin (titin) antibodies have revealed that epitopes located in the A band were easily recognized in intact sarcomeres, favoring the view that the connectin filaments are not integrated inside the myosin filaments (Maruyama et al., 1985; Fürst et al., 1988; Whiting et al., 1989).

No connectin filaments were detected in the S1-decorated I bands. This observation compels us to speculate that connectin filaments are associated with actin filaments so intimately that they are cocovered by S1, together with actin filaments. This interpretation was conclusively confirmed by the deep-etch replica images of the mechanically torn S1-decorated I band (see Fig. 7). It should be noted that connectin filaments (β-connectin) bind to actin filaments in vitro (Maruyama et al., 1987). Taking all these lines of evidence together, we can conclude that the so-called thin filaments in the I band and the thick filaments in the A band, that have been visualized to date by electron microscopy in intact muscle, include connectin filaments as a major constituent.

As shown in Fig. 9 *B*, *a*, in intact cardiac muscle, the portion of connectin filaments between the Z line and SM1 epitope was 2.1–2.4 times as extensible as that between the SM1 epitope and the edge of the A band. Similar results were previously obtained in intact skeletal muscle (Horowits et al., 1989), indicating that cardiac and skeletal connectin filaments and their networks show similar elastic properties. Interestingly, these elastic properties were not affected by the removal of actin filaments by gelsolin treatment (see Fig. 9 *B*, *b*). We have previously shown that the resting tension of skeletal muscle does not change by the gelsolin treatment (Funatsu et al., 1990). These results suggest that, at the I bands, connectin filaments are laterally associated with actin

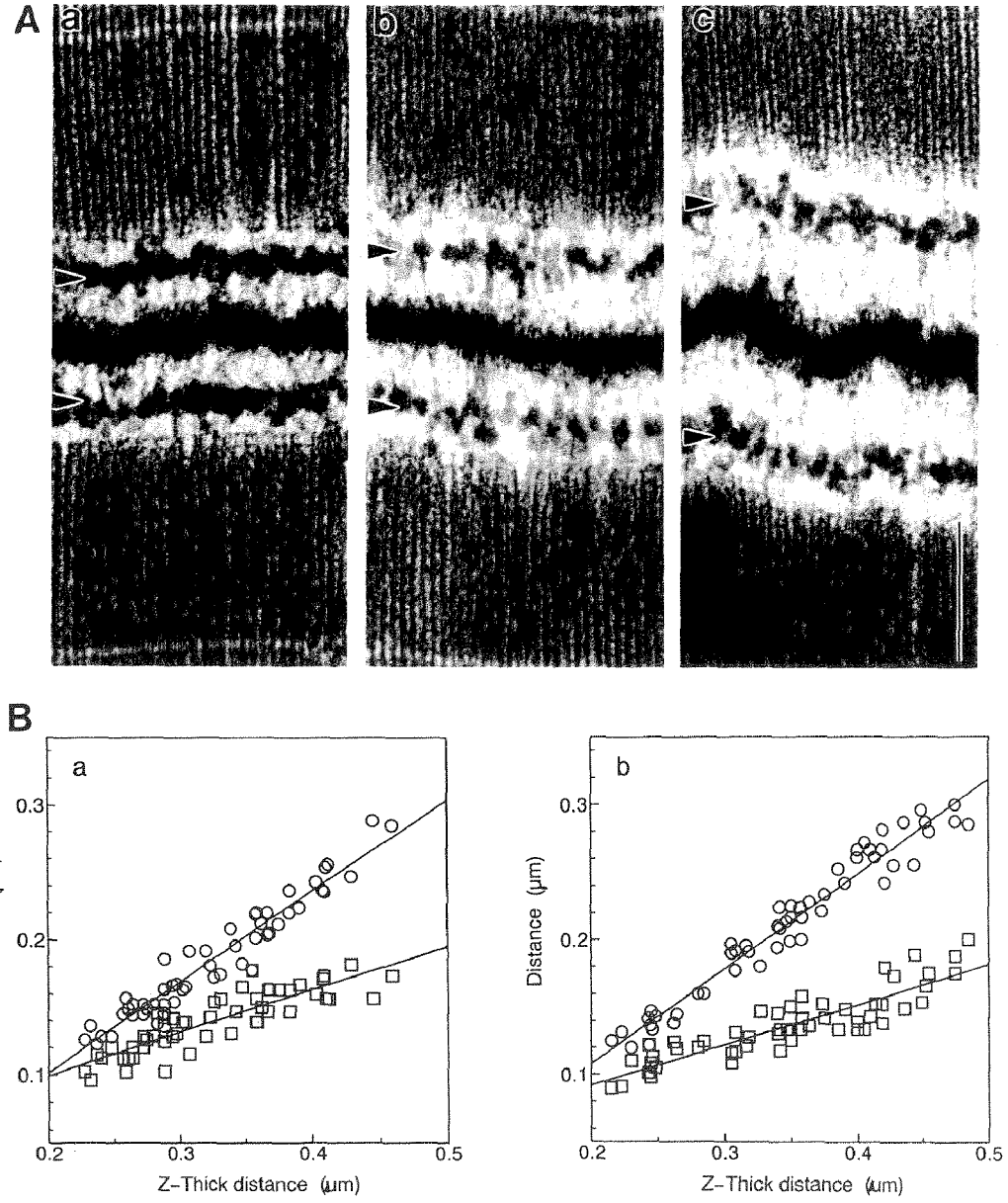

Figure 9. Changes in position of the epitopes of anti-connectin mAb (SM1) in cardiac muscle sarcomeres upon stretching. (*A*) Immunoelectron micrographs of gelsolin-treated and SM1-labeled muscle. Arrows indicate stripes due to antibody binding. Sarcomere length: (*a*) 2.3, (*b*) 2.5, and (*c*) 2.8 μm. (*B*) Position of SM1 epitopes without (*a*) or with (*b*) gelsolin treatment. Distances from the Z line to the epitopes (○) and from the epitopes to the edge of the A band (□) were plotted against the distance from the center of the Z line to the end of a thick filament. The lines were fitted to the data by linear regression.

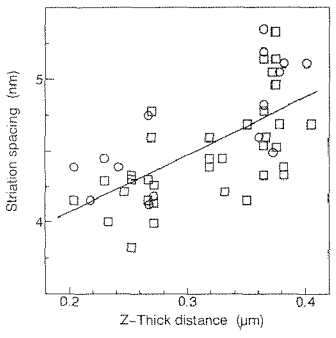

Figure 10. Changes in striation spacing of a connectin filament upon stretching of the sarcomere. Spacing periodicity on the surface of the connectin filament was plotted as a function of the distance from the center of the Z line to the end of the thick filaments. (○) Striation of connectin filament from the Z line to the junction line; (□) striation of connectin filament from the junction line to the thick filaments. The lines were fitted to the data by linear regression.

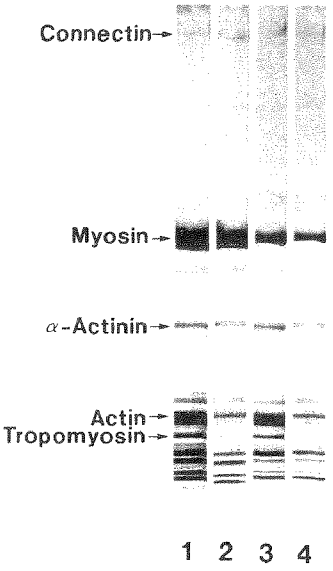

Figure 11. SDS-PAGE patterns of cardiac muscle fibers from which thin and thick filaments were removed; 3–13% polyacrylamide gels. (Lane *1*) Intact muscle; (lane *2*) gelsolin-treated muscle; (lane *3*) muscle treated with a high salt solution containing potassium acetate; and (lane *4*) muscle treated with gelsolin and then with potassium acetate.

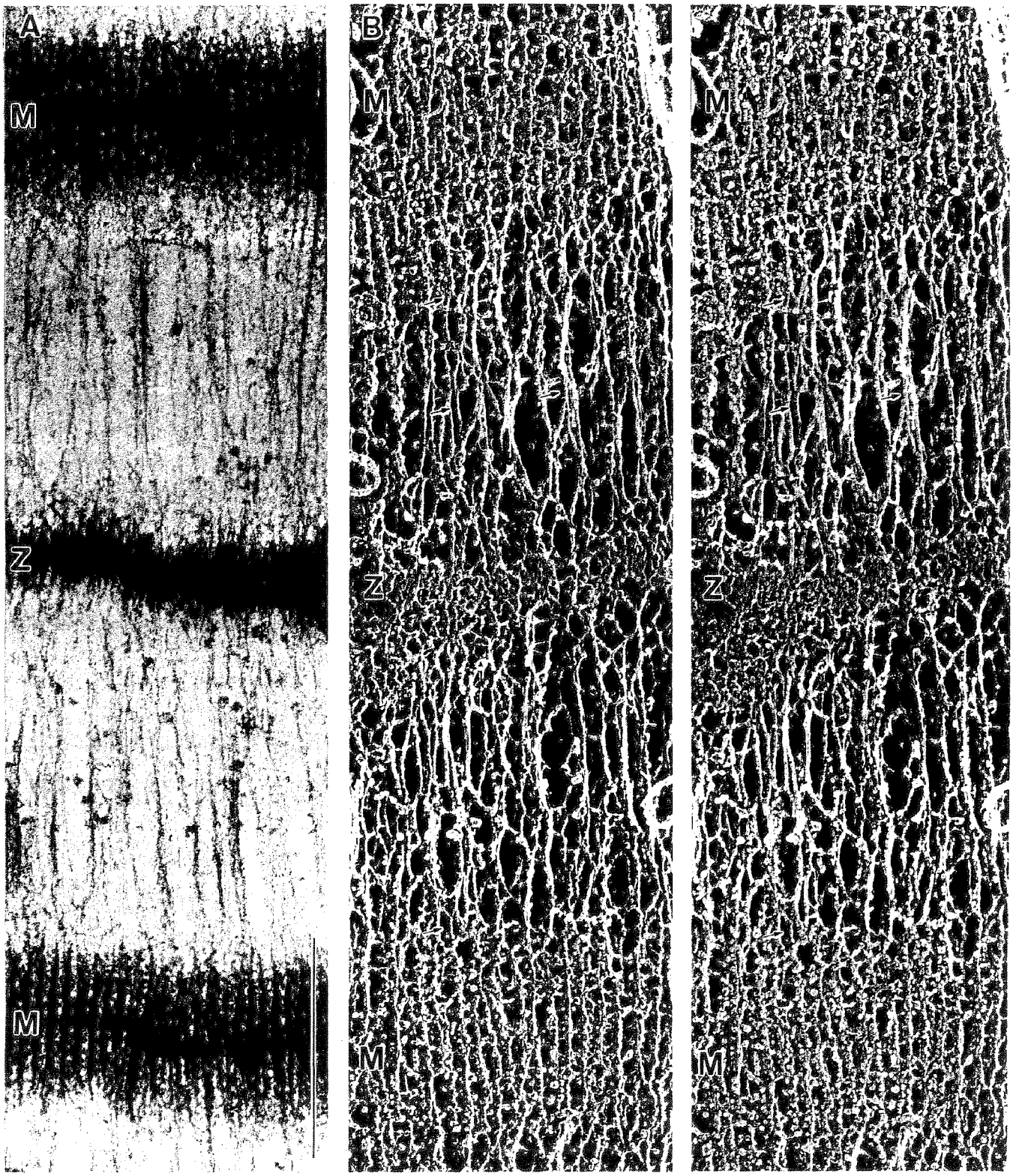

Figure 12. Cardiac muscle sarcomeres from which thin and thick filaments were removed. Muscles were treated with gelsolin and then with a high salt solution containing potassium acetate. (*A*) Thin section of freeze-substituted muscle. *Z*, Z line; *M*, M line. (*B*) Stereo pairs of deep-etch replica. Arrows indicate ~4-nm striation on the surface of connectin filaments. Bar, 0.5 μm.

filaments weakly or transiently in such a manner that actin filaments by no means interfere with the elasticity of connectin filaments. In sharp contrast, it is likely that in A bands, the elasticity of connectin filaments is highly restricted by laterally associated myosin filaments (Itoh et al., 1988a). Most recently, Higuchi et al. (1992) have shown that the connectin filaments freed from myosin filaments by KCl treatment, as well as those in the I band, were elastic.

The repeated β-sheet structures inside the connectin molecule are thought to account for its elastic properties (Maruyama et al., 1986). In our deep-etch replica images, connectin filaments showed ~4-nm striations on their surface. This

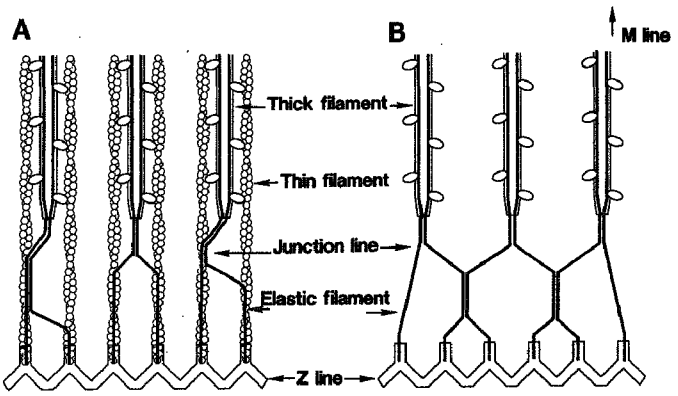

Figure 13. A model of the three-dimensional network of connectin filaments in the I band. (*A*) Possible model of the connection of thick filaments and the Z line by connectin filaments in situ. The connectin filament is divided into two thinner strands at the junction line and the strands are connected to the Z line. In intact muscle, connectin filaments may be weakly and randomly associated with thin filaments, so that only some portions of connectin bridging the thin filaments laterally are distinguishable from thin filaments. (*B*) After extraction of thin filaments, most of the connectin filaments between the junction line and the Z line would be associated with one another.

striation may correspond to the repeated β-sheet structures and/or to a repeated 100-residue motif previously identified in the connectin sequence (Benian et al., 1989; Labeit et al., 1990). Interestingly, in the I band, this striation was found to change in spacing, depending on the degree of stretching (see Fig. 10). In the A band, this ~4-nm striation was observed on the surface of connectin filaments after potassium acetate treatment (see Fig. 12). The rod of the myosin filament has been reported to have a 4.2-nm striation, with 28-amino acid residues (Parry, 1981; McLachlan et al., 1982). Considering that connectin filaments are laterally associated with the rods of myosin filaments, this accordance of their striation periodicity might be important for this association. Furthermore, it is tempting to speculate that connectin filaments might determine the length of thick filaments as a "molecular template" (Whiting et al., 1989).

Finally, we should discuss the junction line identified in the gelsolin-treated cardiac muscle fibers. We observed the junction line where connectin filaments projecting from the tips of thick filaments were branched into two or more thinner strands. The location of this junction line corresponds to the N2 line which was first identified and thought to represent the location of radial structures in skeletal muscle (Locker and Wild, 1984). Wang and Wright (1988) endorsed their idea and concluded that the N2 line may also be a site of accumulation of damaged nebulin. In a previous study of gelsolin-treated skeletal muscle, we confirmed that enhancement of the density of the N2 line depended on nebulin proteolysis (see Fig. 10 *B* of Funatsu et al., 1990). In cardiac muscle cells, however, nebulin is not expressed. Thus, the N2 line in skeletal muscle fibers might be defined as the line where connectin filaments branch off, as in cardiac muscle fibers. Branching of connectin filaments at the N2 line could be responsible for the lateral compression of the thick filament lattice that occurs when myofibrils are stretched (Higuchi, 1987). At the junction line, we found that two or three adjoining connectin filaments projecting from the tips of thick filaments were laterally bundled. This junction line may correspond to the ends of the end-filaments seen by negative staining in separated filaments (Trinick, 1981).

Our study is the first to visualize the connectin filament network inside the sarcomere while maintaining its morphological integrity. Based on comparison of this image with that of the intact and S1-decorated sarcomere, we proposed a model of the arrangement of connectin filaments in situ; this requires extensive alternations of the conventional model of sarcomere structure, which has been regarded as consisting predominantly of actin and myosin filaments. However, several important problems remain to be clarified. How many connectin molecules are laterally associated to form individual elastic filaments in the A and the I bands? How are the three different types of filaments, actin, myosin, and connectin, integrated into sarcomere structure during development? Further analyses of these problems will lead us to a better understanding of the physiological functions of connectin molecules.

We would like to thank Mr. Akio Ohba and Mr. Hiroshi Maebashi (National Institute for Physiological Sciences) for their assistance in EM.

This work was partly supported by Grants-in-Aids for the encouragement of young scientists (to T. Funatsu) and for scientific research (to S. Tsukita) from the Ministry of Education, Science and Culture of Japan. T. Funatsu was a recipient of a Fellowship of the Japan Society of the Promotion of Science for Japanese Junior Scientists.

Received for publication 17 June 1992 and in revised form 12 October 1992.

References

Benian, G. M., J. E. Kiff, N. Neckelmann, D. G. Moerman, and R. H. Waterston. 1989. Sequence of an unusually large protein implicated in regulation of myosin activity in *C. elegance. Nature (Lond.)*. 342:45–50.

dos Remedios, C. G., and D. Gilmour. 1978. Is there a third type of filament in striated muscle? *J. Biochem. (Tokyo)*. 84:235–238.

Funatsu, T., H. Higuchi, and S. Ishiwata. 1990. Elastic filaments in skeletal muscle revealed by selective removal of thin filaments with plasma gelsolin. *J. Cell Biol.* 110:53–62.

Fürst, D. O., M. Osborn, R. Nave, and K. Weber. 1988. The organization of titin filaments in the half-sarcomere revealed by monoclonal antibodies in immunoelectron microscopy: a map of ten nonrepetitive epitopes starting at the Z line extends close to the M line. *J. Cell Biol.* 106:1563–1572.

Heuser, J. E., and M. W. Kirschner. 1980. Filament organization revealed in platinum replicas of freeze-dried cytoskeletons. *J. Cell Biol.* 86:212–234.

Heuser, J. E., and R. Cooke. 1983. Actin-myosin interactions visualized by the quick-freeze, deep-etch replica technique. *J. Mol. Biol.* 169:97–122.

Higuchi, H. 1987. Lattice swelling with the selective digestion of elastic components in single-skinned fibers of frog muscle. *Biophys. J.* 52:29–32.

Higuchi, H., and S. Ishiwata. 1985. Disassembly kinetics of thick filaments in rabbit skeletal muscle fibers. Effects of ionic strength, Ca^{2+} concentration, pH, temperature, and cross-bridges on the stability of thick filament structure. *Biophys. J.* 47:267–275.

Higuchi H., T. Suzuki, S. Kimura, T. Yoshioka, K. Maruyama, and Y. Umazume. 1992. Localization and elasticity of connectin (titin) filaments in frog skinned muscle fibers studied by partial depolymerization of thick filaments. *J. Muscle Res. Cell Motil.* 13:285–294.

Horowits, R., and R. J. Podolsky. 1988. Thick filament movement and isometric tension in activated skeletal muscle. *Biophys. J.* 54:165–171.

Horowits, R., K. Maruyama, and R. J. Podolsky. 1989. Elastic behavior of connectin filaments during thick filament movement in activated skeletal muscle. *J. Cell Biol.* 109:2169–2176.

Hu, D. H., S. Kimura, and K. Maruyama. 1986. Sodium dodecyl sulfate gel electrophoretic studies of connectin-like high molecular weight proteins of various types of vertebrate and invertebrate muscles. *J. Biochem. (Tokyo).* 99:1485–1492.

Huxley, H. E. 1963. Electron microscope studies on the structure of natural and synthetic protein filaments from striated muscle. *J. Mol. Biol.* 7:281–308.

Ishiwata, S., K. Muramatsu, and H. Higuchi. 1985. Disassembly from both ends of thick filaments in rabbit skeletal muscle fibers. An optical diffraction study. *Biophys. J.* 47:257–266.

Itoh, Y., T. Suzuki, S. Kimura, K. Ohashi, H. Higuchi, H. Sawada, T.

Shimizu, M. Shibata, and K. Maruyama. 1988*a*. Extensible and less-extensible domains of connectin filaments in stretched vertebrate skeletal muscle sarcomeres as detected by immunofluorescence and immunoelectron microscopy using monoclonal antibodies. *J. Biochem. (Tokyo)*. 104:504–508.

Itoh, Y., T. Matsuura, S. Kimura, and K. Maruyama. 1988*b*. Absence of nebulin in cardiac muscles of the chicken embryo. *Biomed. Res.* 9:331-333.

Kimura, S., and K. Maruyama. 1989. Isolation of α-connectin, an elastic protein, from rabbit skeletal muscle. *J. Biochem. (Tokyo)*. 106:952–964.

Knight, P., and J. Trinick. 1984. Structure of the myosin projections on native thick filaments from vertebrate skeletal muscle. *J. Mol. Biol.* 177:461–482.

Kruger, M., J. Wright, and K. Wang. 1991. Nebulin as a length regulator of thin filaments of vertebrate skeletal muscles: Correlation of thin filament length, nebulin size, and epitope profile. *J. Cell Biol.* 115:97–107.

Labeit, S., D. P. Barlow, M. Gautel, T. Gibson, J. Holt, C.-L. Hsieh, U. Francke, K. Leonard, J. Wardale, A. Whiting, and J. Trinick. 1990. A regular pattern of two types of 100-residue motif in the sequence of titin. *Nature (Lond.)*. 345:273-276.

Laemmli, U. K. 1970. Cleavage of structural proteins during the assembly of the head of bacteriophage T4. *Nature (Lond.)*. 227:680–685.

Locker, R. H., and N. G. Leet. 1976. Histology of highly stretched beef muscle. IV. Evidence for movement of gap filaments through the Z-line, using the N2-line and M-line as markers. *J. Ultrastruct. Res.* 56:31-38.

Locker, R. H., and D. J. C. Wild. 1984. The N-lines of skeletal muscle. *J. Ultrastruct. Res.* 88:207-222.

Locker, R. H., and D. J. C. Wild. 1986. A comparative study of high molecular weight proteins in various types of muscle across the animal kingdom. *J. Biochem. (Tokyo)*. 99:1473–1484.

Maruyama, K. 1986. Connectin, an elastic filamentous protein of striated muscle. *Int. Rev. Cytol.* 104:81–114.

Maruyama,K., T. Yoshioka, H. Higuchi, K. Ohashi, S. Kimura, and R. Natori. 1985. Connectin filaments link thick filaments and Z lines in frog skeletal muscle as revealed by immunoelectron microscopy. *J. Cell Biol.* 101:2167–2172.

Maruyama, K., Y. Itoh, and F. Arisaka. 1986. Circular dicroism spectra show abundance of β sheet structure in connectin, a muscle elastic protein. *FEBS (Fed. Eur. Biochem. Soc.) Lett.* 202:353–355.

Maruyama, K., D. H. Hu, T. Suzukl, and S. Kimura. 1987. Binding of actin filaments to connectin filaments. *J. Biochem. (Tokyo)*. 101:1339–1346.

Maruyama, K., A. Matsuno, H. Higuchi, S. Shimaoka, S. Kimura, and T. Shimizu. 1989. Behaviour of connectin (titin) and nebulin in skinned muscle fibers after extreme stretch as revealed by immunoelectron microscopy. *J. Muscle Res. Cell Motil.* 10:350–359.

McLachlan, A. D., and J. Karn. 1982. Periodic charge distributions in the myosin rod amino acid sequence match cross-bridge spacings in muscle. *Nature (Lond.)*. 299:226–231.

Nave, R., D. O. Fürst, and K. Weber. 1989. Visualization of the polarity of isolated titin molecules: A single globular head on a long thin rod as the M band anchoring domain? *J. Cell Biol.* 109:2177–2187.

Parry, D. A. D. 1981. Structure of rabbit skeletal myosin. Analysis of the amino acid sequences of two fragments from the rod region. *J. Mol. Biol.* 153: 459–464.

Shimizu,T., K. Matsumura, Y. Itoh, T. Mannen, and K. Maruyama. 1988. An immunological homology between neurofilament and muscle elastic filament: a monoclonal antibody cross-reacts with neurofilament subunits and connectin. *Biomed. Res.* 9:227–233.

Sjöstrand, F. S. 1962. The connection between A- and I-band filaments in striated frog muscle. *J. Ultrastruct. Res.* 7:225–246.

Towbin, H., T. Staehelin, and J. Gordon. 1979. Electrophoretic transfer of proteins from polyacrylamide gels to nitrocellulose sheets: procedure and some applications. *Proc. Natl. Acad. Sci. USA*. 76:4350–4354.

Trinick, J. A. 1981. End-filaments: A new structural element of vertebrate skeletal muscle thick filaments. *J. Mol. Biol.* 151:309–314.

Trinick, J. 1991. Elastic filaments and giant proteins in muscle. *Curr. Opin. Cell Biol.* 3:112–119.

Trinick, J., P. Knight, and A. Whiting. 1984. Purification and properties of native titin. *J. Mol. Biol.* 180:331–356.

Trombitás, K., P. H. W. W. Baatsen, and G. H. Pollack. 1988. I-bands of striated muscle contain lateral struts. *J. Ultrastruct. Mol. Struct. Res.* 100: 13–30.

Trombitás, K., P. H. W. W. Baatsen, M. S. Z. Kellermayer, and G. H. Pollack. 1991. Nature and origin of gap filaments in striated muscle. *J. Cell Sci.* 100: 809–814.

Tsukita, S., and M. Yano. 1985. Actomyosin structure in contracting muscle detected by rapid freezing. *Nature (Lond.)*. 317:182–184.

Tsukita, Sh., Sa. Tsukita, T. Kobayashi, and G. Matsumoto. 1986. Subaxolemmal cytoskeleton in squid giant axon. II. Morphological identification of microtubule- and microfilament-associated domains of axolemma. *J. Cell Biol.* 102:1710–1725.

Tsukita, Sa., Sh. Tsukita, and G. Matsumoto. 1988. Light-induced structural changes of cytoskeleton in squid photoreceptor microvilli detected by rapid-freeze method. *J. Cell Biol.* 106:1151–1160.

Wang, K. 1985. Sarcomere-associated cytoskeletal lattices in striated muscle: reviews and hypothesis. *In* Cell and Muscle Motility. Vol. 6. J. W. Shay, editor. Plenum Publishing Corp., New York. 315–369.

Wang, K., and J. Wright. 1988. Architecture of the sarcomere matrix of skeletal muscle: immunoelectron microscopic evidence that suggests a set of parallel inextensible nebulin filaments anchored at the Z line. *J. Cell Biol.* 107: 2199–2212.

Wang, K., R. Ramirez-Mitchell, and D. Palter. 1984. Titin is an extraordinarily long, flexible, and slender myofibrillar protein. *Proc. Natl. Acad. Sci. USA*. 81:3685–3689.

Weeds, A. G., and R. S. Taylor. 1975. Separation of subfragment-1 isoenzymes from rabbit skeletal muscle myosin. *Nature (Lond.)*. 257:54–56.

Whiting, A., J. Wardale, and J. Trinick. 1989. Does titin regulate the length of muscle thick filaments? *J. Mol. Biol.* 205:263–268.

Changes in mobility of chromaffin granules in actin network with its assembly and Ca^{2+}-dependent disassemby by gelsolin

S. Miyamoto,* T. Funatsu,‡ S. Ishiwata,‡ and S. Fujime§

*Department of Biochemical Engineering, Faculty of Computer and Systems Engineering, Kyushu Institute of Technology, 680-4 Kawatsu, Iizuka, Fukuoka 820; ‡Department of Physics, School of Science and Engineering, Waseda University, 3-4-1 Okubo, Shinjuku, Tokyo 169; and §Graduate School of Integrated Science, Yokohama City University, 22-2 Seto, Kanazawa, Yokohama 236, Japan.

ABSTRACT As a final stage of cell signal transduction, secretory cells release hormones by exocytosis. Before secretory granules contact with the cell membrane for fusion, an actin-network barrier must dissociate as a prelude. To elucidate dynamical behaviors of secretory granules in actin networks, in vitro assembly and disassembly processes of actin networks were examined by means of dynamic light-scattering spectroscopy. We studied actin polymerization in the presence of chromaffin granules isolated from bovine adrenal medullas and found that the entanglement of actin filaments rapidly formed cages that confined granules in them. We also studied the effect of gelsolin, one of actin-severing proteins, on the network of actin filaments preformed in the presence of chromaffin granules. It turned out that the cages that confined granules rapidly disappeared when gelsolin was added in the presence of free Ca^{2+} ions. A semiquantitative analysis of dynamic light-scattering spectra permitted us to estimate the changes in the mobility (or the translational diffusion coefficient) of chromaffin granules in the actin network with its assembly and Ca^{2+}-dependent disassembly by gelsolin. Based on the present results and some pieces of evidence in the literature, a model is proposed for biophysical situations before, during, and after an exocytotic event.

INTRODUCTION

Many morphological investigations have shown that the cytoplasm of mammalian cells is highly organized and compartmentalized by the cytoskeleton. This organization and compartmentalization takes an important part in many processes of signal transduction, such as release of neuronal transmitters and secretion of hormones and enzymes. A cell receives external chemical signals by receptor molecules or electrical stimuli by channels in the membrane. Various molecular processes for transducing signals are activated by second messengers in the cytoplasm. As a final step, the cell releases the hormones or neurotransmitters by an exocytotic event. In secretory cells and neuronal synapses, hormones and neurotransmitters are stored, respectively, in secretory granules and synaptic vesicles. These granules and vesicles must contact with the cell membrane and fuse with it before release of their contents.

At a resting state, these granules are tightly or loosely held in dense cytoskeleton networks. Morphological and immunological investigations have shown that the dense network is made up of actin filaments, e.g., in the peripheral region of chromaffin cells and in the presynaptic nerve terminals (1–5). The actin network is considered to hold chromaffin granules in at least three ways, (Fig. 1): (*a*) actin filaments extending directly from α-actinin molecules on the granule membrane can form actin networks (6), (*b*) actin filaments connect granules to networks with a linkage molecule such as fodrin-like molecules (7–9), and (*c*) the network confines granules in a restricted space (a cage model). In a cytosolic situation, chromaffin granules would be trapped in combination of these possibilities and of equivalent ones. Our point is that only the liberation of cross-linker molecules from the network is not enough to mobilize the granules, because the movements of granules are still restricted in the dense network of actin filaments. In any case, the actin network must disassemble for granules to access the cell membrane as a prelude of exocytosis (2). Many actin-severing proteins have been identified in the cytoplasm of chromaffin cells (10–13). Severing functions of these proteins are activated by free Ca^{2+} ions in a micromolar level (14–18). In secretory and neuronal cells, the concentration of free Ca^{2+} ions in the cytosol, after receiving an external stimulus, increases to a micromolar level by releasing them from a carciosome and an influx through Ca^{2+} channels in the cell membrane (19, 20). In chromaffin cell cytosol and neuronal synaptic terminal, morphological and immunological investigations have confirmed, in the cortical region of the cell membrane, the existence of gelsolin (21, 22) and scinderin (18).

At present, it is technically difficult to observe the assembly and disassembly processes of the actin network in intact cell cytosol. In this study, therefore, we used an in vitro cell-free system to analyze dynamical processes of the network formation holding secretory granules and of the network dissociation by an actin-severing protein, gelsolin, in the presence of free Ca^{2+} ions. We used a dynamic light-scattering method (DLS) that is one of the most appropriate techniques to analyze a dynamical behavior of particles with submicrometer sizes in solution (23–25). So far, a falling ball method for viscosity measurements has been used to observe the formation and dissociation of actin filaments (7). This method,

This article is dedicated to Professor Sho Asakura, who is one of the pioneers of the study on actin polymerization, on the occasion of his retirement from Nagoya University (1991).

Please address all correspondence to S. Fujime.

Biophys. J. © Biophysical Society
Volume 64 April 1993 1139-1149

0006-3495/93/04/1139/11 $2.00

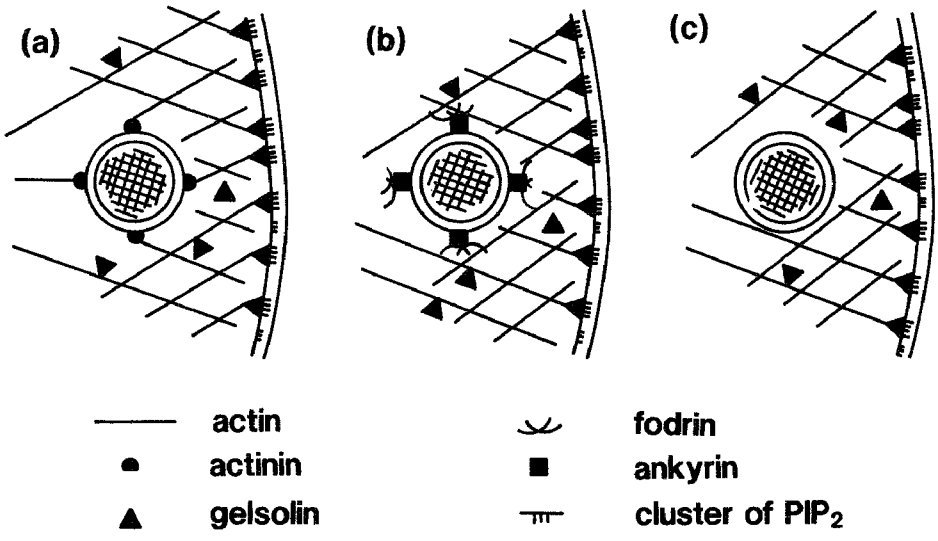

FIGURE 1 Schematic illustration of three model situations holding granules in the network of actin filaments in a resting cell (for details, see text).

however, may have a defect to cause a mechanical damage to the network/granules system. The DLS method makes it possible to detect the dynamical behavior of the granules and filaments without applying any mechanical perturbation. As a quick and intuitive method, however, viscometry was also used for some additional measurements.

Works related to the present study have been reported by Newman et al. (26, 27). They used polystylene latex spheres (PLS) instead of chromaffin granules in this study. They observed the change in mobility of PLS with formation of actin network (26). They also studied the mobility of PLS in solutions of F-actin, whose average length was varied by polymerization of actin in the presence of various amounts of gelsolin (27). In their studies, they set a condition that the scattering intensity from PLS was much higher than that from F-actin, so that they "saw" only the motion of PLS. In our system, which mimicked the cytosolic situation more closely than their system, the scattering intensity from granules was only several times higher than that from F-actin, so that we had to develop methods (given in the Appendixes) for estimation of mobility of chramaffin granules in F-actin network.

MATERIALS AND METHODS

Preparation of chromaffin granules

Bovine adrenal glands were obtained from a local slaughter house. After removing adipose tissue, the adrenal glands were extensively perfused to remove blood vessels perfectly at 37°C for 30 min with Ca^{2+}-free Krebs ringer solution (153 mM NaCl, 5.6 mM KCl, 3.6 mM $NaHCO_3$, 5 mM glucose, and 5 mM *N*-2-hydroxyethylpiperazine-*N'*-2-ethane sulfonic acid [Hepes] pH 7.0). The adrenal medullas were dissected to be free of cortical material and placed in 10 vol of an isotonic solution (300 mM sucrose, 10 mM Hepes, pH 7.0, 1 mM phenylmethylsulfonyl fluoride [PMSF], 1 mM dithiothreitol, 0.5 mM NaN_3, and 1 μg/ml leupeptin). The tissue was blended for 5 s in a blender (Waring Products Div., Dynamics Corp. of America, New Hartfort, CT), homogenized in a cylindrical glass homogenizer with a loose-fitting motor-driven Teflon pestle (Ikemoto Rika Co. Ltd., Tokyo, Japan), and filtered through four layers of gauze. The homogenate was centrifuged at 500 *g* for 5 min to remove unbroken cells and nuclei. The supernatant was centrifuged at 20,000 *g* for 30 min to pellet chromaffin granules. After discarding the supernatant, the isotonic solution was gently overlayed along the tube wall. The tube was carefully swirled to remove the upper fluffy layer of mitochondria on the pellet. The supernatant was carefully discarded without disturbing the pellet. The remainder of the pellet was gently resuspended in the same isotonic solution by hand homogenization in a glass/glass Ten Broek homogenizer (Wheaton Scientific Co. Ltd., Millville, NJ). The suspension was centrifuged at 10,000 *g* for 30 min. After the supernatant was discarded, the brown fluffy layer was dislodged by a gentle swirling as above. After the pellet was gently resuspended by hand homogenization, the suspension was centrifuged at 7,000 *g* for 30 min. After removing the fluffy layer, the pellet was resuspended in the isotonic solution. The discontinuous gradient was made by overlaying 3 ml of this suspension on 7 ml of 1.6 M sucrose solution in the centrifugation tube and centrifuged at 80,000 *g* for 60 min. The whitish-pink pellet (chromaffin granules) was resuspended in the isotonic solution and stored at 4°C. In this study, we used chromaffin granules within 48 h after their preparation.

Preparation of G-actin

G-actin from rabbit back and leg white muscle was prepared and purified by standard methods (28–30) with slight modifications. No column chromatography step was made. In the final step of purification, F-actin was dialyzed for 72 h against 0.1 mM Mg adenosine triphosphate (ATP) and 2 mM tris(hydroxymethyl)-aminomethane-HCl at pH 8.0.

Preparation of gelsolin

Gelsolin from calf plasma was prepared and purified by the method described elsewhere and stored in liquid nitrogen. In this light-scattering study, the gelsolin preparation used was from the same lot as in Funatsu et al. (31), where it was shown that the axial rigor stiffness of a chemically skinned muscle fiber, for example, decreased by 50% of the original size within 10 min after the fiber was bathed in Ca rigor solution containing 0.5 mg/ml gelsolin. The molecular weight of gelsolin was assumed to be 93 kD (32).

Polymerization of actin

Unless otherwise stated, solutions of 1 mg/ml G-actin (±0.5 mg/ml chromaffin granules) in 300 mM sucrose, 10 mM 3-(*N*-morpholino)propanesulfonic acid (MOPS), pH 7.0, 0.1 mM MgATP, 0.1 mM PMSF, and no (pCa > 7) or 10 μM free Ca^{2+} ions (pCa = 5) were prepared in light-scattering cells. The pCa values were determined by a multiequilibrium formulation, where the ethyleneglycol-bis(β-aminoethyl ether)-*N,N'*-tetraacetic acid-calcium binding constant in our condition was assumed to be $10^{5.5}$. Polymerization was initiated at 10°C by adding 2 mM $MgSO_4$ (final), where a small magnetic bar in the cell was used for quick mixing. Dilution by 2% of actin and chromaffin granules on addition of $MgSO_4$ was ignored.

DLS measurements

General background information about the DLS method is found in standard textbooks (33, 34). An (8 by N)-bit digital correlator (K7032CE; Malvern Instruments, Malvern, UK) was used to measure the intensity autocorrelation function of the scattered light. A 488-nm beam from an Ar^+ ion laser (model 95; Lexel Corp., Palo Alto, CA) was used as a light source. Details of our spectrometer were described elsewhere (35). The temperature of the scattering cell was controlled at 10 ± 0.05°C. The intensity autocorrelation function $G^2(t)$ is related to the normalized field correlation function $g^1(t)$ of the scattered light by

$$G^2(t) = B\{\beta[g^1(t)]^2 + 1\}, \qquad (1)$$

where $t = mT$ (m = 1, 2, . . . , 128; T, the sampling time), B is the baseline level ($B^{1/2}$ is proportional to the static scattering intensity $\langle I \rangle$), and β is a constant (see Appendix A). For a monodisperse suspension of small particles, we have a simple form of $g^1(t) = \exp(-DK^2t)$, where D is the translational diffusion coefficient of the particle and K is the length of the scattering vector, which equals $(4\pi/\lambda)\sin(\theta/2)$ (λ, the wavelength of light in the medium; θ, the scattering angle). The actual form of $g^1(t)$ of our system is a sum of exponential decays because of a length-distribution of F-actin and presence of granules. Then, the following expansion method is used to obtain a measure of the average decay rate;

$$g^1(t) = [1 + (\mu_2/2)t^2 - (\mu_3/6)t^3]\exp(-\bar{\Gamma}t), \qquad (2)$$

where $\bar{\Gamma}$ is the average value and μ_i is the ith moment around $\bar{\Gamma}$ of the decay rate distribution of $g^1(t)$. The size of B in Eq. 1 is known from data in the monitor channels of the correlator, and four unknowns in Eqs. 1 and 2, i.e., β, $\bar{\Gamma}$, μ_2, and μ_3, can be determined by a least-squares fit. The quantity $\bar{\Gamma}/K^2$ has the same dimension as that of D (cm²/s) and is called an apparent diffusion coefficient, D_{app}. If a simple model is assumed, then D_{app} for a mixture of granules and filaments is given by the weighted average of $D_{app}(*)$'s with respect to the static scattering intensities $I(*)$'s;

$$D_{app} = [D_{app}(f)I(f) + D_{app}(g)I(g)]/\langle I \rangle, \qquad (3)$$

where $\langle I \rangle = I(f) + I(g)$ and $* = f$ and g stand for filament and granule, respectively. For granules in a cage model, $D_{app}(g)$ will be substantially smaller than that for free granules. For more details, see Appendix B.

Throughout this article, we express D_{app} in units of 10^{-9} cm²/s and K^2 in units of 10^{10} cm^{-2}; i.e., $D_{app} = 3$ and $K^2 = 6$, e.g., mean 3×10^{-9} cm²/s and 6×10^{10} cm^{-2}, respectively. We also express $\langle I \rangle$ in an arbitrary but same scale throughout.

Viscosity measurements

The specific viscosity η_{sp} was measured by use of a falling ball viscometer with falling time of 2.2$_7$ s (an average of 10 measurements) for buffer.

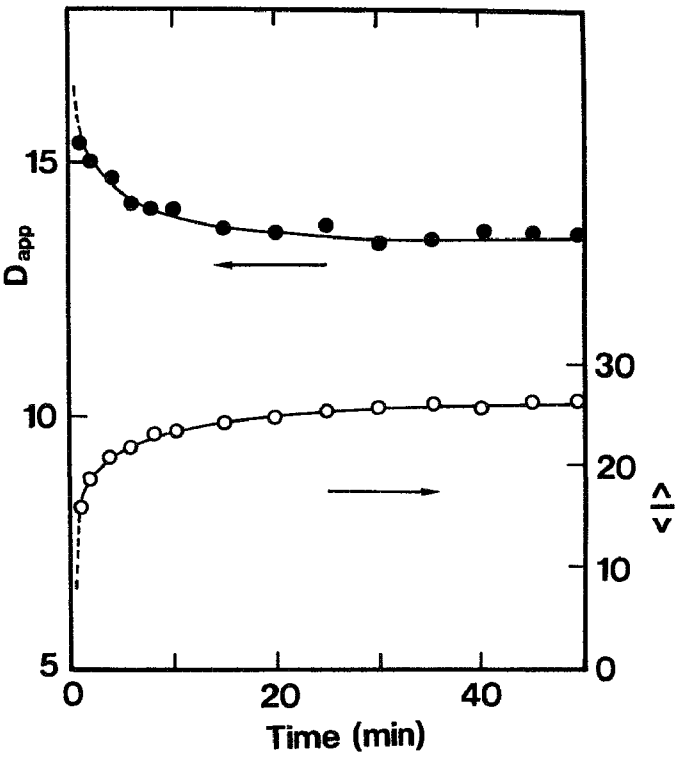

FIGURE 2 Changes in D_{app} and $\langle I \rangle$ after initiation of polymerization of G-actin alone. Data were collected at the scattering angle of 90°.

RESULTS

Actin polymerization

Polymerization of actin alone was first studied. Fig. 2 shows the time courses of the changes in D_{app} and $\langle I \rangle$ at the scattering angle of 90° or $K^2 = 5.86$. In the intensity scale in Fig. 2, $\langle I \rangle = \langle I \rangle_G$ for suspension of G-actin at the present concentration was less than unity. Also D_{app} of G-actin at this condition was ~600. Since polymerization was induced with Mg^{2+} ions, the nucleation process was so fast that we could not observe the very initial stage (i.e., nucleation and early elongation stages) of actin polymerization. Namely, $\langle I \rangle$ was so high and D_{app} was so low compared with those of G-actin even at the first observed point. Then, it is suggested that (*a*) the nucleation and elongation processes finished within the first few minutes and (*b*) the gradual increase in $\langle I \rangle$ and decrease in D_{app} with time in Fig. 2 were mainly due to size redistribution and partly due to further elongation of filaments.

The above suspension was left standing for >10 h at 4°C, and then the D_{app} vs. K^2 relationship was measured (Fig. 3). This D_{app} vs. K^2 relationship is quite compatible with the previous results on F-actin with the number-average length of 600–800 nm for actin preparation without a column chromatography step (36). The D_{app} vs. K^2 relationship for granules alone is also shown in Fig. 3 for a comparison. The slight wiggling behavior of

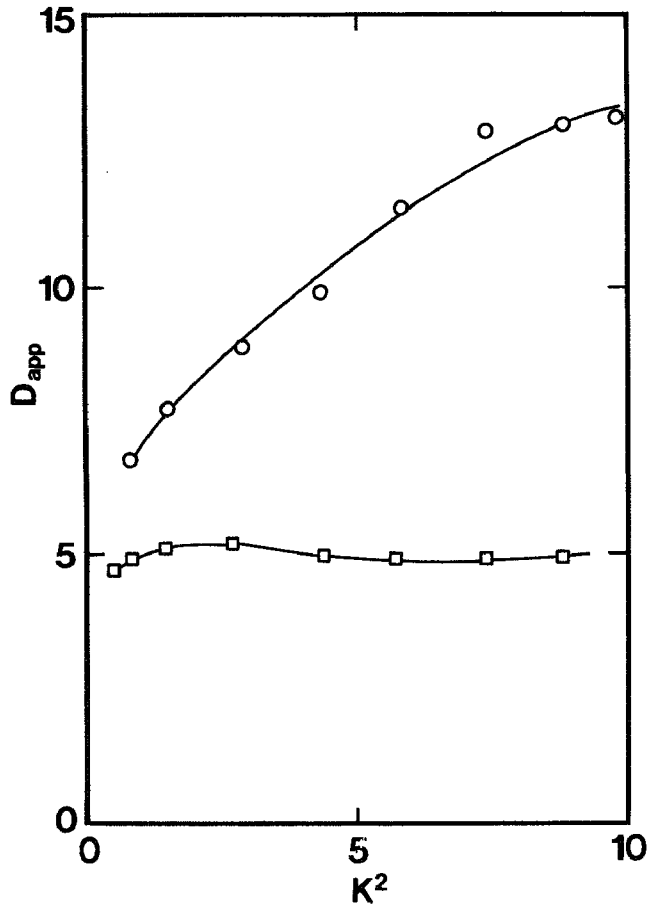

FIGURE 3 The D_{app} vs. K^2 relationships. (○) F-actin alone; the sample in Fig. 2 was left standing at 4°C for >10 h and then examined at 10°C. (□) Chromaffin granules alone (for comparison).

D_{app} against K^2 for granules has been analyzed quantitatively elsewhere (37).

Actin polymerization in the presence of chromaffin granules

Polymerization of actin in the presence of chromaffin granules was studied. Fig. 4 shows the first 20-min portions of the time courses of changes in D_{app} and $\langle I \rangle$ at the scattering angle of 90°. (Although not measured in this study, D_{app} might start from 5, the value for granules alone in Fig. 3, and $\langle I \rangle$ from $I(g)$ because of a very weak contribution to $\langle I \rangle$ from G-actin at time 0.) As is expected, no appreciable effect of free Ca^{2+} ions was observed on these time courses. As for a very slight increase in $\langle I \rangle$ with time, there are at least two possibilities: one is that a large and steady contribution to $\langle I \rangle$ ($=I(f) + I(g)$) from $I(g)$ of granules smeared a change in $I(f)$ due to elongation of filaments with time and another may be that the granules (α-actinin molecules on the surface of a granule) facilitated nucleation for polymerization of actin as observed by electron microscopy (6), so that the elongation finished very soon after initiation of polymerization. For the present system of a mixture of actin filaments and chromaffin granules, the D_{app} value will be given by Eq. 3. Then, from Figs. 2 and 4, it is observed that (*a*) the size redistribution with time of filaments more drastically decreased the D_{app} value in Fig. 4 than in Fig. 2, leading to a prediction that chromaffin granules were confined in cages formed by actin filaments, and (*b*) the D_{app} value in Fig. 4 rapidly became smaller than 5 for granules alone, leading to another prediction that the motion of granules in cages was strongly restricted. By the method described in Appendix B, the size of $D_{app}(g)$ can be estimated as shown by squares in Fig. 4. (The change in $D_{app}(g)$ with time is virtually the same as that in D of PLS previously observed (26).)

The above suspensions were left standing for 24 h at 4°C, and then the D_{app} vs. K^2 relationships were mea-

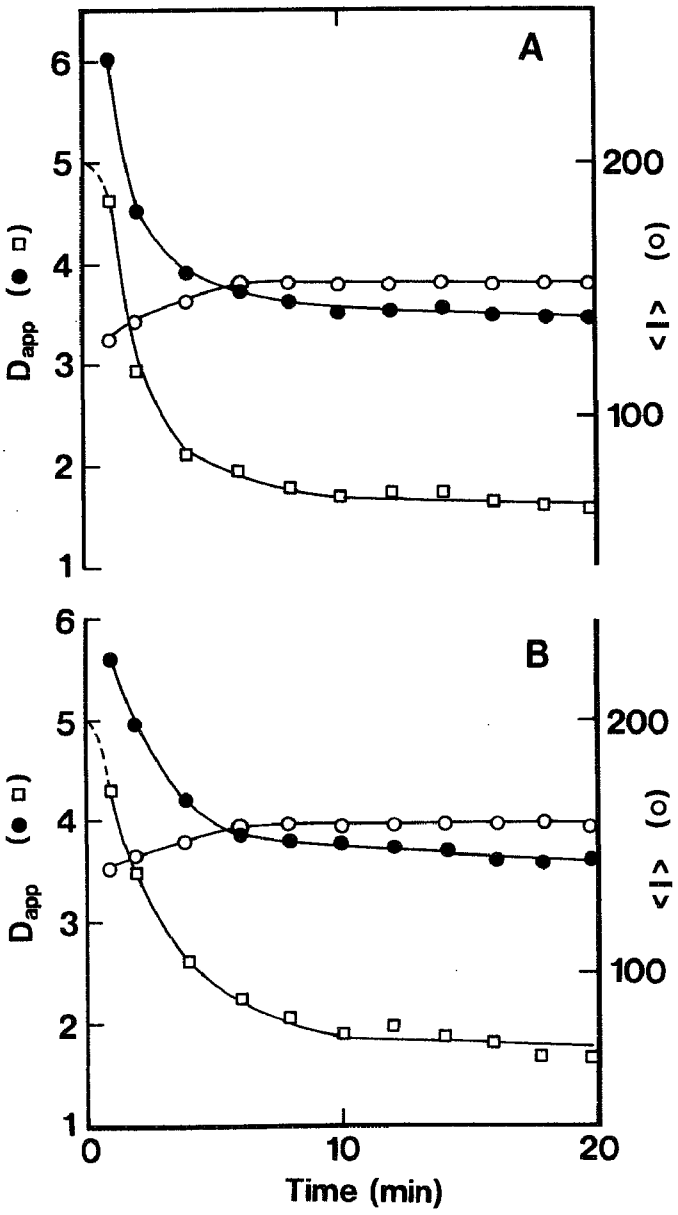

FIGURE 4 Changes in D_{app} (●) and $\langle I \rangle$ (○) after initiation of polymerization of G-actin in the presence of chromaffin granules. (*A*) pCa > 7 and (*B*) pCa = 5. Data were collected at the scattering angle of 90°. (□) The estimated size of $D_{app}(g)$ at 90° (see Appendix B).

sured (Fig. 5). The absolute size and K^2 dependence of D_{app} were essentially the same, both in the presence and absence of 10 μM free Ca^{2+} ions. Since $D_{app}(g)$ would behave virtually flat against K^2 also for granules confined in cages, the K^2 dependence of D_{app} in Fig. 5 came solely from the K^2-dependence of $I(f)/I(g)$ in Eq. 3 and K^2 dependence of $D_{app}(f)$ (something like D_{app} for F-actin alone in Fig. 3). Smaller values of D_{app} than 5 suggest that in the equilibrium state after size redistribution, a network was formed by entanglement of actin filaments, and chromaffin granules were confined in the cages. By the method described in Appendix B, the $D_{app}(g)$ vs. K^2 relationship also can be obtained as shown by squares in Fig. 5.

Effect of gelsolin on actin network preformed in the presence of chromaffin granules

Polymerization of actin in the presence of granules was first carried out, and the F-actin/granule suspensions were incubated for 24 h at 4°C. Then, 0.19 mg/ml gelsolin (final) was added to the above suspensions under a mild stirring in the light-scattering cell (the molar ratio of actin monomers to gelsolin of 10). The consecutive measurement of the DLS spectrum at the scattering angle of 90° was made immediately after mild stirring for 30 s. At pCa > 7 (Fig. 6 *A*), no appreciable change in D_{app} took place. In the $\langle I \rangle$ versus time relationship, a small increase followed by a small decrease was observed. This change in $\langle I \rangle$ may or may not be important, but we ignore it in what follows. (The initial large drop in $\langle I \rangle$ was due to dilution of actin filaments and chromaffin granules on addition of gelsolin; see Fig. 6.) At pCa = 5 (Fig. 6 *B*), on the other hand, a rapid and large increase in D_{app} took place in a first few minutes, which was then followed by a gradual increase. At this pCa, however, $\langle I \rangle$ slightly decreased with time. The severing function of gelsolin in the presence of 10 μM free Ca^{2+} ions is responsible for the large increase in D_{app}, because for this mixture, a value of D_{app} larger than 5 (the size for granules alone) could result only when a substantial number of granules became free due to disappearance of cages formed by actin filaments. Severing of long filaments results in larger $D_{app}(f)$ and $D_{app}(g)$ in

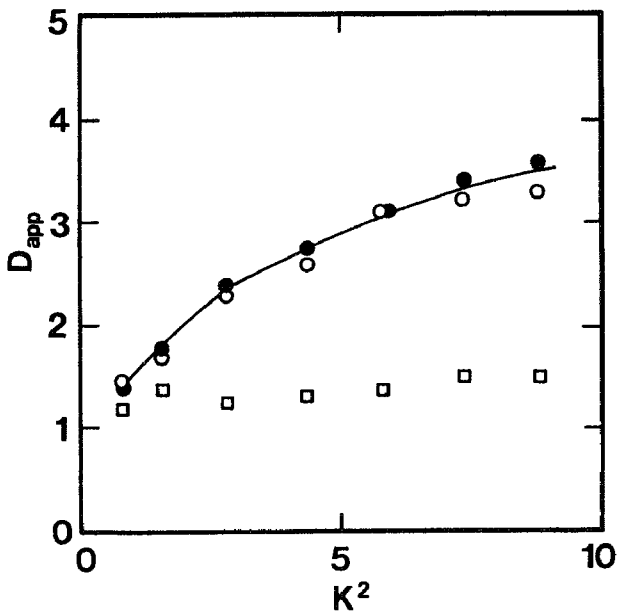

FIGURE 5 The D_{app} vs. K^2 relationships. (○) pCa > 7; (●) pCa = 5. The samples in Fig. 4 were left standing at 4°C for 24 h and then examined at 10°C. (□) The estimated size of $D_{app}(g)$ (see Appendix B).

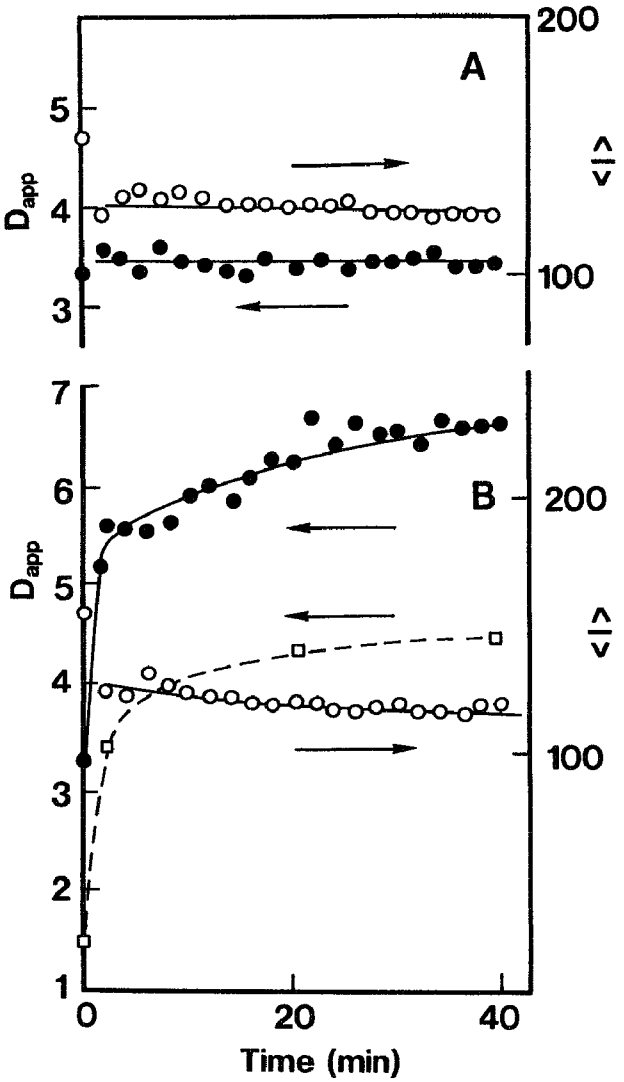

FIGURE 6 Changes in D_{app} (●) and $\langle I \rangle$ (○) after addition of gelsolin to a mixture of F-actin and chromaffin granules. (*A*) pCa > 7 and (*B*) pCa = 5. After the addition of 0.19 mg/ml gelsolin (final) to samples similar to those in Fig. 5, data were collected at the scattering angle of 90° (but, those at time 0 were taken from Fig. 5). Large drops in $\langle I \rangle$'s in *A* and *B* just after the addition of gelsolin were due to dilution of F-actin and chromaffin granules; the final concentration of chromaffin granules was 0.40_s mg/ml and that of F-actin was 0.81 mg/ml (the molar ratio of actin monomers to gelsolin of 10). (□) The estimated size of $D_{app}(g)$ at 90° (see Appendix C).

Eq. 3. By the method described in Appendix C, the sizes of $D_{app}(f)$ and $D_{app}(g)$ can be estimated, and $D_{app}(g)$ is shown by squares in Fig. 6 *B*.

It is well known that the length distribution of in vitro reconstituted F-actin is of an exponential type at the equilibrium state (38). It is not clear whether or not the length distribution is also exponential for F-actin polymerized in the presence of granules. In any case, at a time when each of longer filaments in the distribution is severed into two (to three) pieces, the cages formed by entanglement of long filaments virtually disappear. However, in the time range in Fig. 6, filaments are, on the average, still long enough for them to contribute to D_{app} of the mixture, because D_{app} is larger than 5 (the size of granules alone). As time goes on, free gelsolin molecules, if they still exist, further sever filaments into short pieces and remain bound to the barbed ends of these fragments. It is then expected that (*a*) actin monomers dissociate from the pointed ends of these fragments; (*b*) actin monomers thus produced can bind to the barbed ends of uncapped fragments and/or form nuclei for polymerization; and (*c*) as a result of these processes, the size redistribution will proceed to some extent with a very low rate.

The above suspensions were left standing for 24 h at 4°C, and then the D_{app} vs. K^2 relationships were measured (Fig. 7). At pCa > 7, the absolute values and K^2 dependence of D_{app} are quite the same as those in Fig. 5, suggesting no effect of gelsolin on actin filaments at all. At pCa = 5, on the other hand, the D_{app} vs. K^2 relationship at the equilibrium state is distinctly different from that at pCa > 7 and those in Fig. 5. The fact that D_{app} values at low K^2's are smaller than 5 suggests either most granules undergo a little restricted Brownian motion or some fractions of them are still confined in cages. In any case, motional freedom of granules is concluded to substantially increase as a result of severing action of gelsolin in the presence of free Ca^{2+} ions.

Additional measurements

After the analysis described in Appendixes B and C had been completed, we were aware of the following points. At the molar ratio of actin monomers to gelsolin of 10, G-actin is expected to polymerize into short F-actin with a length of, say, 50 nm on the average. If the preformed F-actin were severed into fragments with this length, then $I(f)$ would be so small that $\langle I \rangle$ would be close to $I(g)$. But this was not the case, because $I(f):I(g)$ decreased from 1:5 to 1:7 (Fig. 6 *B*) and D_{app}'s at $K^2 > 2.5$ were larger than 5 (Fig. 6 *B* and filled circles in Fig. 7). Although the analysis in Appendix C may not be very accurate, it indeed suggested that the preformed F-actin was severed into two to three pieces on the average. Then, we examined this difference by measuring the specific viscosity, η_{sp}, as a quick and intuitive reference. In this viscometry was used a gelsolin preparation different from that used in the above DLS, because almost 3 yr had passed between these two measurements.

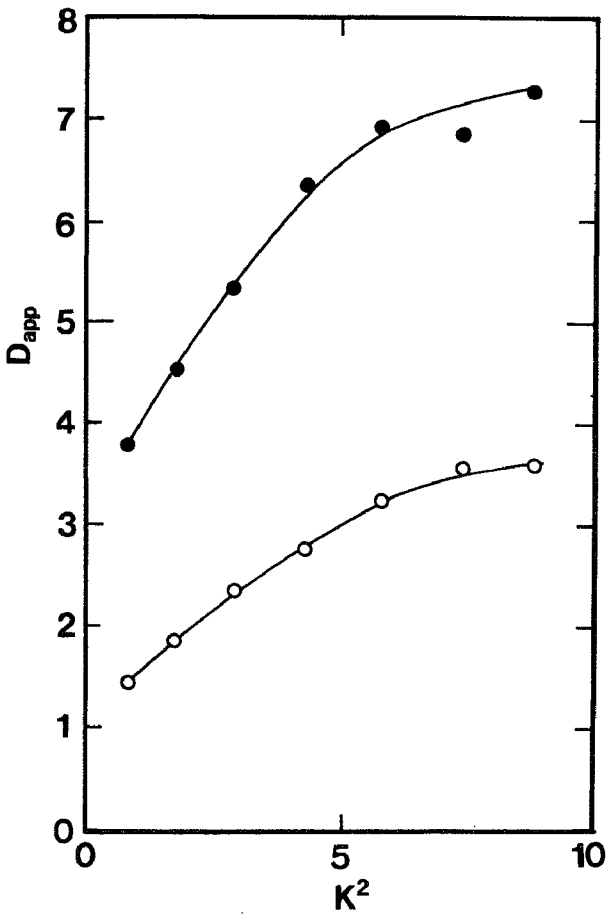

FIGURE 7 The D_{app} vs. K^2 relationships. (○) pCa > 7; (●) pCa = 5. The samples in Fig. 6 were left standing at 4°C for 24 h and then examined at 10°C.

Fig. 8 shows some of the η_{sp} versus time relationships. Irrespective of the presence (*filled symbols*) and absence (*open symbols*) of chromaffin granules, it is clearly seen that (*a*) a viscosity increase in the polymerization phase of G-actin was smaller in the presence of gelsolin (*triangles*) than in its absence (*circles*), (*b*) a large viscosity drop was observed just after the addition of gelsolin to the preformed network of F-actin (*circles* in the depolymerization phase), and (*c*) the falling-off level of viscosity at pCa = 5 in the depolymerization phase (*circles*) was twice or more larger than the final level of viscosity in the polymerization phase of G-actin in the presence of gelsolin (*triangles*). The observations very similar to the above ones (without chromaffin granules) have been reported for solvent components of 2 mM $MgCl_2$ and 100 mM KCl instead of 2 mM $MgSO_4$ in our case (39). The first two observations proved a high activity of gelsolin. The third observation suggested again that the average length of F-actin severed by gelsolin was substantially longer than the average length of F-actin polymerized in the presence of gelsolin.

Other observations to be noted in Fig. 8 are as follows. One is that the initial values of 0.60 (*top arrow*) and 0.43

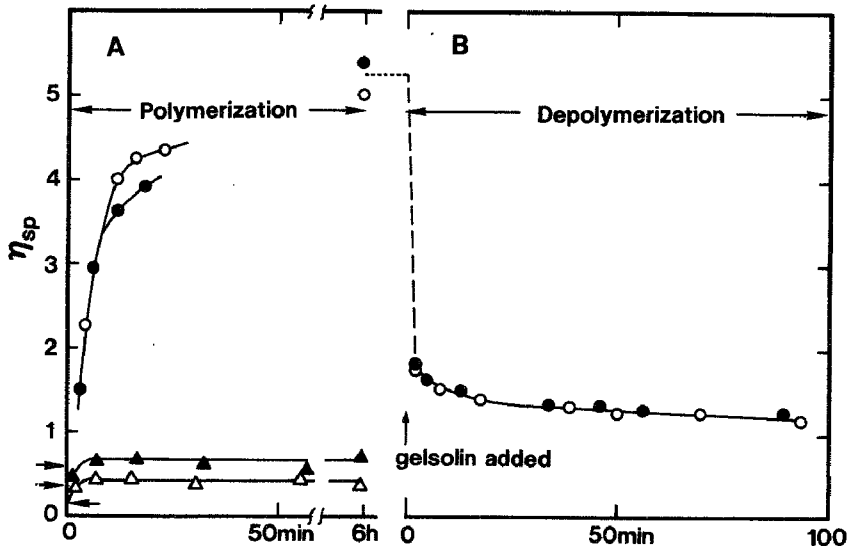

FIGURE 8 The η_{sp} versus time relationships. (*A*) Polymerization phase in the absence (*circles*) and presence (*triangles*) of gelsolin: (○) 0.5 mg/ml G-actin, (●) 0.5 mg/ml G-actin and 0.5 mg/ml chromaffin granules, (△) 0.5 mg/ml G-actin and 0.1 mg/ml gelsolin, and (▲) 0.5 mg/ml G-actin, 0.5 mg/ml, chromaffin granules, and 0.1 mg/ml gelsolin were polymerized at 20°C and pCa = 5 in 300 mM sucrose, 10 mM MOPS, pH 7.0, 0.2 mM MgATP, 0.1 mM PMSF, and 2 mM $MgSO_4$. The molar ratio of actin monomers to gelsolin was 11 in △, ▲. The initial η_{sp} values were measured in the absence of $MgSO_4$; the top arrow indicates the initial value for ●, the middle for ▲, and the bottom for ○, △. (*B*) Depolymerization phase in the absence (○) and presence (●) of chromaffin granules at pCa = 5. On addition of 0.09 mg/ml gelsolin (final) to the above solutions (○, ● in *A*), F-actin and chromaffin granules were diluted to 0.4 mg/ml, and the molar ratio of actin monomers to gelsolin was 10.

(*middle arrow*) were, respectively, three and two times larger than the sum of 0.13 (*bottom arrow*) and 0.08 for 0.5 mg/ml chromaffin granules alone. This observation probably suggests, even in the absence of 2 mM $MgSO_4$, formation of very short F-actin due to nucleation facilitated by α-actinin on the surface of granules. The other is that the final value of viscosity was larger in the presence of chromaffin granules (*filled triangle*) than in its absence (*open triangle*). These two observations may suggest that the situation in our model system was in part similar to that in Fig. 1 *a*. This possibility has to be taken into account in quantitative evaluation of the present results, because we derived Eq. 4, and hence Eqs. 3 and 5, by assuming no direct binding between chromaffin granules and F-actin as in Fig. 1 *c*. (The absolute size of viscosity, especially at high viscosity regions, was very sensitive to experimental conditions. This is a reason why the viscosity for F-actin alone at an intermediate time range was higher than that for F-actin/granules in this particular case.)

As to the third observation, we first considered it to be due to no addition of KCl to our preparation on actin polymerization. It was found, however, that irrespective of the presence and absence of Cl^-, K^+, and/or sucrose, the falling-off levels of viscosity strongly depended on the degree of mechanical perturbation (mixing) on addition of gelsolin to the preformed network of actin filaments. Under mild mixing of the suspension by sucking up and down two to three times with a pipette whose tip had been cut to widen it greatly, was obtained the η_{sp} versus time relationships as shown in Fig. 8. On the other hand, under vigorous mixing by sucking up and down more than five times with the pipette whose tip had not been cut, the falling-off levels of η_{sp} were almost close to the final values (*triangles*) in the polymerization phase. The falling-off levels of η_{sp} at the molar ratio of actin monomers to gelsolin of 10 under mild mixing (as in DLS measurements) were equal to the final values in the polymerization phase at the molar ratio around 100. This result was consistent with the DLS result analyzed in Appendix C. These findings strongly suggested a difference in capping and severing activities of gelsolin. We inferred that gelsolin molecules reduced the actin–actin bond strength at their attached points on F-actin to a great extent. The actin filaments with such weakened bonds would be fragmented by thermal agitation if they were long (fluctuation-induced severing) and also by mechanical perturbation even if they were short (applied force-induced severing). In any case, the barbed ends of fragments were immediately capped by gelsolin, resulting in a drop in η_{sp} depending on mixing conditions. It should be noted that the gelsolin we used indeed severed F-actin without any mechanical perturbation; I-bands disappeared when myofibrils were bathed in Ca-rigor solution containing gelsolin (31).

DISCUSSION

The secretory cell accepts an external chemical signal by receptor molecules on the cell surface. Through intervention of various molecular processes by second messengers, the free Ca^{2+} ion concentration in the cytosol finally increases from a submicromolar resting level to a micromolar activated one (19). The molecular mecha-

nism of signal transduction in the first stage has been studied extensively in the past several years (40, 41). However, few studies have been made for the final stage to exocytosis (42). Based on the present results and several pieces of evidence in the literature, we propose a molecular model of this final step.

Electron microscopic observations for macrophages and platelets showed that a large amount of gelsolin molecules resides in 80–100-nm cortical zones and on the cell membrane (21, 22). A large amount of gelsolin molecules must also exist in diffusible and/or bound states everywhere in cytoplasm of many mammalian cells. Electron microscopic observations by use of a quick-freeze method showed that highly dense actin filaments extend from protein molecules on the inner surface of the plasma membrane. By means of immunoelectron microscopy, these proteins are identified as gelsolin, each of which binds to a cluster of phosphatidylinositol 4,5-bisphosphate (PIP_2) (22).

In a static state, secretory granules are held in the actin network at least in three ways (Fig. 1). In the 80–100-nm peripheral region, which is a three times thinner layer than the diameter of granules, highly dense actin network prevents secretory granules from directly touching the cell membrane (6). As a prelude of exocytosis, this actin network must dissociate or loosen for granules to contact freely with fusion sites on the membrane (2). As has been generally assumed and partly confirmed experimentally (e.g., review references 9 and 17), we also assume a series of the following steps: (*a*) activation of actin-severing proteins, e.g., gelsolin, by free Ca^{2+} ions (at a micromolar level) for disassembly of actin network; (*b*) free, or slightly restricted, diffusion of a granule to a fusion site on the membrane; (*c*) fusion with cell membrane and release of the content of the granule; and (*d*) revesiculation from the fused membrane and reformation of actin network. We introduce a biophysical model for rearrangement of the actin network before and after exocytosis. In our simple model, the movement of granules at the resting state ($pCa > 7$) is restricted in cages formed by actin filaments (situation 1). Before exocytosis, these actin filaments are disassembled by gelsolin at $pCa \leq 6$ (situation 2). After an exocytotic event, the free Ca^{2+} ion concentration returns to the resting one ($pCa > 7$). Then, actin filaments are reformed in the peripheral region (situation 3). Subsequent size redistribution of filaments results in formation of cages that confine granules in them (going back to situation 1). This study concerned only situations 1 and 2.

The present results (Figs. 4 and 5) suggested a very restricted motion of granules in cages formed by actin filaments. In the present in vitro system, the cages are temporary, because they are ceaselessly created and annihilated as a result of almost free translation of filaments along their long axis. Thus, granules can travel over any distance with a very low mobility. As shown in Fig. 1, however, many filaments in an intact cell are anchored on the cell membrane (22), so that the cages formed by these filaments are permanent in the resting state. Thus, granules are confined literally in these permanent cages. This supports situation 1. As suggested (Fig. 6 *B*), gelsolin molecules ($+Ca^{2+}$) immediately fragmented actin filaments into short pieces and remained bound to the barbed ends of these actin fragments. The present results (Figs. 6 *B* and 7) suggested a substantial increase in motional freedom of granules. This supports situation 2. Simultaneously, actin filaments may disappear from the special area of a fusion site. In an intact cell, various actin-severing proteins may coexist with gelsolin, one of which is scinderin (13), and they will work to speed up the disassembly process of actin filaments in vivo. We did not study, by the DLS method, the polymerization process of G-actin in the presence of gelsolin. However, there are several studies that suggest formation of short pieces of actin filaments even in the presence of gelsolin and Ca^{2+} ions (15, 39, 43) (see also triangles in Fig. 8). These support situation 3. A gelsolin molecule bound to the barbed end of an actin fragment does not dissociate spontaneously even at $pCa > 7$ (44). In an intact cell, the cell membrane contains many PIP_2 molecules that may liberate gelsolin molecules from fragments of actin filaments (44–46), resulting in a rapid elongation and size redistribution of actin filaments by "annealing" (36) or a rapid reformation of cages that confine granules (going back to situation 1). In addition to PIP_2, various molecules not considered here (and not identified yet) would work to speed up the reassembly process of actin filaments in vivo.

In addition, in situation 2, some fusion proteins and phospholipases might be activated by free Ca^{2+} ions, and they might be involved in the process of membrane fusion. But, so far there is no evidence that the aid of these proteins is indispensable for membrane fusion. Rather, a change in the physical state of a granule membrane seems to be important for initiation of membrane fusion. The elasticity of the granule membrane has been found to decrease sharply and greatly at around $pCa = 6$ (23, 24). The flexibility of the granule membrane is necessary for the granule to touch the cell membrane with some size of area (and not a point contact).

To mimic a cytosolic situation as closely as possible, high concentrations of actin and granules were adopted at the expense of quality of DLS measurements to some extent. Although multiple scattering may be serious at low angles, we did not examine it quantitatively and assumed it to be negligible at the angle of 90° (Figs. 2, 4, and 6). Although $G^2(t)$ decayed smoothly, the third-order expansion, Eq. 2, gave very large Q values (see Fig. 10). In addition to these, the length distribution of in vitro reconstituted F-actin is very broad. Due to these facts, quite a quantitative analysis of DLS results is not possible. In the Appendixes below, some semiquantita-

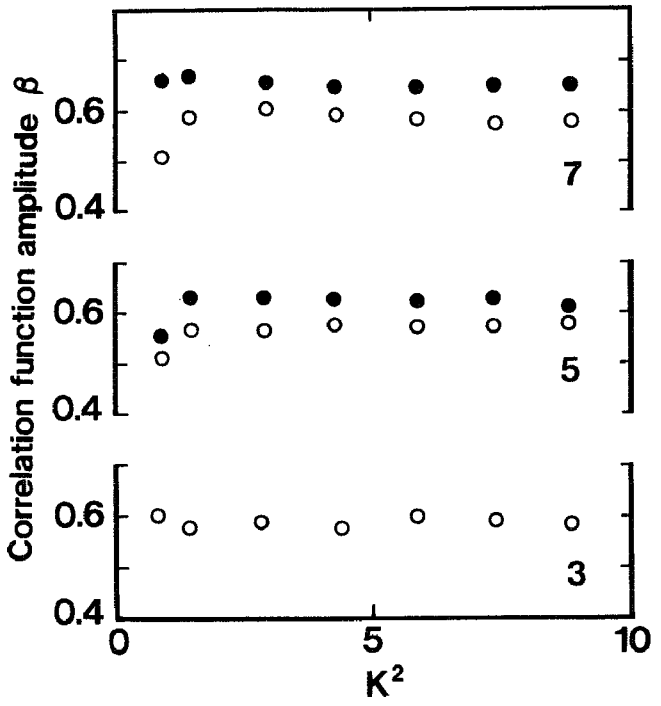

FIGURE 9 The β vs. K^2 relationships. The labels (*3*, *5*, and *7*) correspond to the figure numbers and the symbols to those therein.

tive analyses are made to complement the statements in the text.

APPENDIX A

Correlation function amplitude

The correlation function amplitude, β in Eq. 1, is a measure of how freely the particle diffuses over a probing distance $1/K$. In other words, if the β value becomes small at a given K^2, the particle is trapped on the distance scale of $1/K$. In our optical setup, a dilute suspension of freely diffusing particles gave the β value of ~0.65. The β vs. K^2 relationships (labels *5* and *7* in Fig. 9) suggest that chromaffin granules in the actin network diffuse almost freely over $1/K = 110$ nm even at the lowest K^2 (at the scattering angle of 30°) or a cage diameter is larger than 500 nm (the sum of $1/K$ and the diameter of the granule). Since, however, the β value at the lowest K^2 shows a tendency to become small, the average cage diameter may not be so much larger than 500 nm.

APPENDIX B

Apparent diffusion coefficient

The apparent diffusion coefficient, $D_{app} = \bar{\Gamma}/K^2$, is a measure of how quickly a particle undergoes the Brownian motion. Qualitatively speaking, the larger the D_{app} value is, the larger the mobility is. The decrease in D_{app} with time for actin alone (Fig. 2) is due to elongation/size redistribution of F-actin (36). For long and semiflexible filaments such as F-actin, however, D_{app} increases with K^2 (Fig. 3). This is due to the increasing contribution from rotational and segmental (bending) motions of filaments (47). A little wiggling behavior of the D_{app} vs. K^2 relationship for chromaffin granules alone (Fig. 3) is due to another reason detailed elsewhere (37) and can be ignored in the present examination. Then, the interpretation of a large K^2 dependence of D_{app} in Figs. 5 and 7 is a little complicated.

Although the specific viscosity (see arrows and triangles in Fig. 8) was indeed affected by the presence of granules, DLS results studied so far did not give clear evidence of direct binding between filaments and granules: if there were many filaments extending from α-actinin molecules on the granule membrane as in Fig. 1 *a*, then the scattering intensity $\langle I \rangle$ of the mixture of granules and filaments would be substantially higher than the simple sum of the intensities for filaments alone, $I(f)$, and granules alone, $I(g)$, at the same concentrations as components of the mixture. However, a relation $\langle I \rangle = I(f) + I(g)$ was valid within experimental errors. Furthermore, if the direct binding were appreciable, the β values would be substantially smaller than that for freely diffusing particles. This was not the case (see Appendix A). These lead to a conclusion of no appreciable direct binding between filaments and granules. (A possible effect of granules on the specific viscosity was observed only before the addition of 2 mM $MgSO_4$ and/or during the polymerization phase in the presence of gelsolin, i.e., when viscosity was low. If measurements were made for such situations, then presence of granules might also affect the DLS spectra. In the present experimental conditions, a contribution to DLS spectra from minor filaments extending from granules would be masked by a contribution from major filaments free from binding.) If we assume no direct-binding, then we have (cf. Eq. 2)

$$\langle I \rangle g^1(t) = \sum I(*)[1 + (\mu_2(*)/2)t^2 - (\mu_3(*)/6)t^3] \times \exp[-D_{app}(*)K^2 t], \quad (4)$$

where Σ stands for the sum over $* = f$ and g and notations are the same as those in the text. The first time derivative of Eq. 4 at $t = 0$ gives the average decay rate $\bar{\Gamma}$ of $g^1(t)$ for the mixture, which can be written as in Eq. 3 in the text.

For $D_{app}(f) = D_{app}$ and $I(f) = \langle I \rangle$ in Fig. 2 and D_{app} and $I(g) + I(f) = \langle I \rangle$ in Fig. 4, Eq. 3 gives the $D_{app}(g)$ versus time relationships at 90° as shown by squares in Fig. 4. A rapid decrease of $D_{app}(g)$ suggests a rapid formation of cages by entanglement of long filaments. The same analysis is possible for data in Fig. 5. At the scattering angle of 90°, $I(f) = 26$ is obtained from $\langle I \rangle$ in Fig. 2 and $I(f) + I(g) = 155$ from $\langle I \rangle$ in Fig. 4 (or $I(g) = 129$). These observed values give $I(f)/I(g) = 0.20$, which may be slightly smaller than that at the equilibrium state. At the same angle, we have $D_{app}(f) = 11.4$ from Fig. 3 and $D_{app} = 3.1$ from Fig. 5. Then, Eq. 3 gives $D_{app}(g) = 1.4$ at 90°, which is a little smaller than 1.6–1.7 at time 20 min in Fig. 4. For $D_{app}(f)$ from Fig. 3, D_{app} from Fig. 5, $I(g)$ from Fig. 6 in reference 37, and $I(f)$ from a separate measurement (and scaled as $I(f)/I(g) = 0.20$ at 90°), Eq. 3 gives the $D_{app}(g)$ vs. K^2 relationship as shown by squares in Fig. 5. (This analysis is valid also for open circles in Fig. 7.) The sizes of $D_{app}(g) = 1.2$–1.5 over the present range of K^2 support our interpretation in the text that the granules are confined in cages formed by filaments.

As for $D_{app}(f)$ in a mixture of granules and filaments, D_{app} of F-actin alone with empty cages was assumed. This assumption may or may not be true. Since, however, occupation of cages by granules may reduce only the $D_{app}(f)$ value to some extent, leaving $I(f)$ almost unchanged, the above analysis is still valid semiquantitatively in such a situation. Under such conditions as that, the scattering intensity from PLS was very much higher than that from F-actin; DLS measurements for PLS with diameters 350–400 nm in F-actin solutions gave $D/D_0 = 0.2$–0.3 at 1 mg/ml actin, where D_0 denotes the D value at 0 actin (26). Then, we have $D = 1.0$–1.5 for $D_0 = 5$ (the free value for chromaffin granules). An agreement of this D with the above estimated $D_{app}(g)$ supports the present analysis by use of Eq. 3. Unfortunately, the same analysis as above cannot be applied to the results in Fig. 6 *B*, because we did not study, by the DLS method, the effect of gelsolin on F-actin network preformed in the absence of chromaffin granules. Therefore, an alternative analysis is given below.

APPENDIX C

Polydispersity parameter

From the quantities $\bar{\Gamma}$ and μ_2 in Eq. 2, the so-called polydispersity parameter is defined as $Q = (\mu_2/\bar{\Gamma}^2)$. This Q is a measure of the width

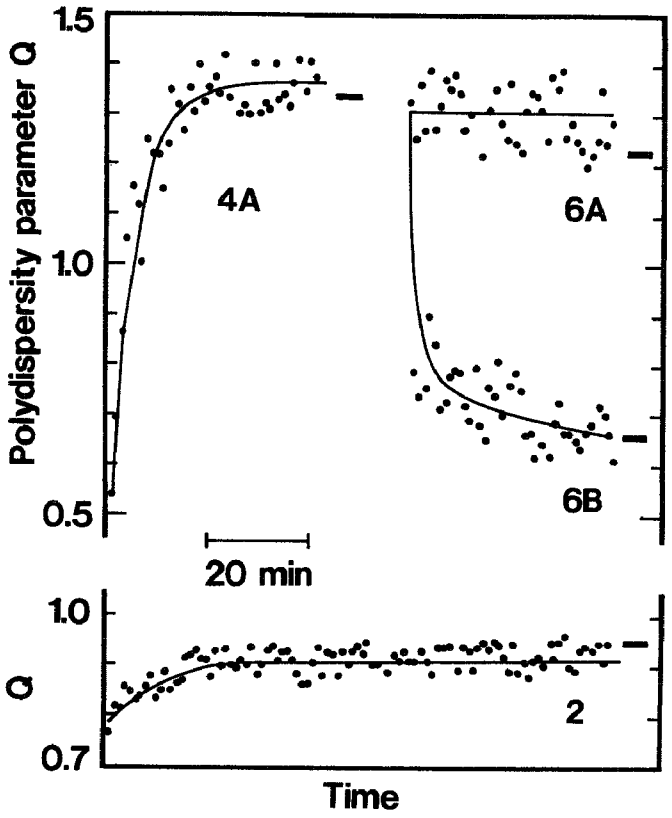

FIGURE 10 The Q versus time relationships. The labels (*2, 4A, 6A,* and *6B*) correspond to the figure numbers, and the thick line segment at the end of each set of data shows the equilibrium Q value.

in the decay rate distribution of $g^1(t)$ around $\bar{\Gamma}$. Fig. 10 depicts Q versus time relationships. The Q value for actin alone (label *2*) was ~0.9 at the plateau. This large Q value is due to very slowly decaying components coming from slow movements of entangled actin filaments. The Q versus time relationship for the mixture of actin and granules at pCa = 5 (data not shown) was almost the same as that with label *4A* at pCa > 7. The Q value (label *4A*) reached 1.3–1.4; this very large Q value is due to a large separation between $D_{app}(f)$ and $D_{app}(g)$ as well as the large Q value of F-actin alone. On addition of gelsolin, this very large Q value quickly decreased to 0.6–0.7 at pCa = 5 (label *6B*), whereas it stayed constant at pCa > 7 (label *6A*); the small Q value at pCa = 5 is mostly due to disappearance of slow movements of entangled filaments as a result of the severing effect of gelsolin.

The second time derivative of Eq. 4 at $t = 0$ gives

$$Q = [D_{app}(f) - D_{app}(g)]^2 I(f)I(g)/[\langle I\rangle D_{app}]^2 + C, \quad (5)$$

where $C = [Q(f)I(f)D_{app}(f)^2 + Q(g)I(g)D_{app}(g)^2]/[\langle I\rangle D_{app}^2]$ and use was made of Eq. 3. The first term on the righthand side of Eq. 5 gives the contribution to Q of the mixture from the separation between $D_{app}(f)$ and $D_{app}(g)$ and the second term, C, from $Q(f)$ and $Q(g)$ of the constituent components. There are four unknowns in Eq. 5, i.e., $D_{app}(*)$ and $Q(*)$ for $* = f$ and g in the mixture. Because we like to know approximate sizes of $D_{app}(f)$ and $D_{app}(g)$, we tentatively put $Q(f) = Q(g) = 0$ or $C = 0$. Then, for given values of Q, D_{app}, and $I(f):I(g) = (\langle I\rangle - I(g)):I(g)$, Eqs. 3 and 5 (with $C = 0$) can give estimates of $D_{app}(f)$ and $D_{app}(g)$.

For $I(f) = 26$ and $I(g) = 129$ (or $I(f):I(g) = 1:5$) at 90° and time 20 min (see Appendix B) and $D_{app} = 3.5$ at time 20 min in Fig. 4 and $Q = 1.4$ in Fig. 10 (label *4A*), Eqs. 3 and 5 give $D_{app}(f) = 12._8$ and $D_{app}(g) = 1.6_5$, which should be compared with the observed value of $D_{app}(f) = 13.5$ in Fig. 2 and the estimated value of $D_{app}(g) = 1.6$–1.7 in Fig. 4. This nice agreement, if not accidental, suggested applicability of Eq. 5 with $C = 0$ to other cases. Then, $g^1(t)$'s were numerically generated for various combinations of $I(*)$, $D_{app}(*)$, $\mu_2(*)$, and $\mu_3(*)$ for $* = f$ and g in Eq. 4, and they were analyzed by the same program as that in the analysis of experimental $G^2(t)$'s. From this simulation, it turned out that the analysis by use of Eqs. 3 and 5 (with $C = 0$) recovered $D_{app}(f)$ and $D_{app}(g)$ with 80% or better accuracy.

In the analysis of data in Fig. 6 *B* by this method, we must assume $I(g) = 129 \times (4/5) = 103$ due to dilution of chromaffin granules. Then, $\langle I\rangle = 118$ at time 40 min gives $I(f) = 15$ or $I(f):I(g) = 1:7$. Then, for $D_{app} = 6.5$ at time 40 min in Fig. 6 *B* and $Q = 0.7$ in Fig. 10 (label *6B*), Eqs. 3 and 5 give $D_{app}(f) = 20._8$ and $D_{app}(g) = 4.4$. Some of estimated $D_{app}(g)$ values are shown by squares in Fig. 6 *B*. Although this analysis may not be very accurate as compared with that in Appendix B, these estimated values for $D_{app}(f)$ and $D_{app}(g)$ are very suggestive. Namely, the estimated value of $D_{app}(f) = 21$ at time 40 min in Fig. 6 *B* is only two times larger than $D_{app}(f) = 11.4$ at 90° (or $K^2 = 5.86$) in Fig. 3. This suggests that longer filaments in the exponential length distribution were severed into two (to three) pieces on the average.

S. Miyamoto and S. Fujime appreciate the support from Mitsubishi Kasei Institute of Life Sciences (Tokyo, Japan), where all the DLS measurements in this study were carried out just before they moved to their present institutions (1989).

Received for publication 11 June 1992 and in final form 16 November 1992.

REFERENCES

1. Cheek, T. R., and R. D. Burgoyne. 1986. Nicotin-evoked disassembly of cortical actin filaments in adrenal chromaffin cells. *FEBS (Fed. Eur. Biochem. Soc.) Lett.* 207:110–114.
2. Burgoyne, R. D., and T. R. Cheek. 1987. Reorganization of peripheral actin filaments as a prelude to exocytosis. *Biosci. Rep.* 7:281–288.
3. Aunis, D., and M.-F. Bader. 1988. The cytoskeleton as a barrier to exocytosis in secretory cells. *J. Exp. Biol.* 139:253–266.
4. Sontag, J. M., D. Aunis, and M. F. Bader. 1988. Peripheral actin filaments control calcium-mediated catecholamine release from streptolysin-O-permeabilized chromaffin cells. *Eur. J. Cell Biol.* 46:316–326.
5. Hirokawa, N., K. Sobue, K. Kanda, A. Harada, and H. Yorifuji. 1989. The cytoskeletal architecture of the presynaptic terminal and molecular structure of synapsin 1. *J. Cell Biol.* 108:111–126.
6. Burgoyne, R. D. 1984. Mechanisms of secretion from adrenal chromaffin cells. *Biochim. Biophys. Acta.* 779:201–216.
7. Pollard, H. B., C. E. Creutz, V. Fowler, J. Scott, and C. J. Pazoles. 1982. Calcium dependent regulation of chromaffin granule movement, membrane contact, and fusion during exocytosis. *Cold Spring Harbor Symp. Quant. Biol.* 46:819–834.
8. Aunis, D., and D. Perrin. 1984. Chromaffin granule membrane-F actin interactions and spectrin-like protein of subcellular organelles: a possible relationship. *J. Neurochem.* 42:1558–1569.
9. Trifaro, J.-M., M.-F. Bader, and J.-P. Doucet. 1985. Chromaffin cell cytoskeleton: its possible role in secretion. *Can. J. Biochem. Cell Biol.* 63:661–679.
10. Bader, M.-F., J.-M. Trifaro, O. K. Langley, D. Thierse, and D. Aunis. 1986. Secretory cell actin-binding proteins: identification of a gelsolin-like protein in chromaffin cells. *J. Cell Biol.* 102:636–646.
11. Maekawa, S., M. Toriyama, S. Hisanaga, N. Yonezawa, E. Endo,

N. Hirokawa, and H. Sakai. 1989. Purification and characterization of a Ca^{2+}-dependent actin filament severing protein from bovine adrenal medullae. *J. Biol. Chem.* 264:7458–7465.

12. Maekawa, S., and H. Sakai. 1990. Inhibition of actin regulatory activity of the 74-kDa protein from bovine adrenal medullae (adseverin) by some phospholipids. *J. Biol. Chem.* 265:10940–10942.
13. Rodriguez Del Castillo, A., S. Lemaire, L. Tchakarov, M. Jeyapragasan, J.-P. Doucet, M. L. Vitale, and J.-M. Trifaro. 1990. Chromaffin cell scinderin, a novel calcium-dependent actin filament-severing protein. *EMBO (Eur. Mol. Biol. Organ.) J.* 9:43–52.
14. Yin, H. L., and T. P. Stossel. 1979. Control of cytoplasmic actin gelsol transformation by gelsolin, a calcium dependent regulatory protein. *Nature (Lond.)* 281:583–586.
15. Yin, H. L., J. H. Hartwig, K. Maruyama, and T. P. Stossel. 1981. Ca^{2+} control of actin filament length. Effect of macrophage gelsolin on actin polymerization. *J. Biol. Chem.* 256:9693–9697.
16. Matsudaira, P., and P. Janmey. 1988. Pieces in the actin severing protein puzzle. *Cell.* 54:139–140.
17. Stossel, T. P. 1989. From signal to pseudopod: how cells control cytoplasmic actin assembly. *J. Biol. Chem.* 264:18261–18264.
18. Vitale, M. L., A. Rodriguez Del Castillo, L. Tchakarov, and J.-M. Trifaro. 1991. Cortical filamentous actin disassembly and scinderin redistribution during chromaffin cell stimulation precede exocytosis, a phenomenon not exhibited by gelsolin. *J. Cell Biol.* 113:1057–1067.
19. Cheek, T. R., T. R. Jackson, A. J. O'Sullivan, R. B. Moreton, M. J. Berridge, and R. D. Burgoyne. 1989. Simultaneous measurements of cytosolic calcium and secretion in single bovine adrenal chromaffin cells by fluorescence imaging of fura-2 in cultured cells. *J. Cell Biol.* 109:1219–1227.
20. O'Sullivan, A. J., T. R. Cheek, R. B. Moreton, M. J. Berridge, and R. D. Burgoyne. 1989. Localization and heterogeneity of agonist-induced changes in cytosolic calcium concentration in single bovine adrenal chromaffin cells from video imaging of fura-2. *EMBO (Eur. Mol. Biol. Organ.) J.* 8:401–411.
21. Cooper, J. A., D. J. Loftus, C. Frieden, J. Bryan, and E. L. Elson. 1988. Localization and mobility of gelsolin in cells. *J. Cell Biol.* 106:1229–1240.
22. Hartwig, J. H., K. A. Chambers, and T. P. Stossel. 1989. Association of gelsolin with actin filaments and cell membranes of macrophages and platelets. *J. Cell Biol.* 108:467–479.
23. Miyamoto, S., and S. Fujime. 1988. Regulation by Ca^{2+} of membrane elasticity of bovine chromaffin granules. *FEBS (Fed. Eur. Biochem. Soc.) Lett.* 238:67–70.
24. Miyamoto, S., and S. Fujime. 1990. Elastic behavior of zymogen granule membranes in response to changes in pH and pCa. *Biophys. J.* 57:615–619.
25. Miyamoto, S., T. Maeda, and S. Fujime. 1988. Change in membrane elastic modulus on activation of glucose transport system of brush border membrane vesicles studied by osmotic swelling and dynamic light scattering. *Biophys. J.* 53:505–512.
26. Newman, J., N. Mroczka, and K. L. Schick. 1989. Dynamic light scattering measurements of the diffusion of probes in filamentous actin solutions. *Biopolymers.* 28:655–666.
27. Newman, J., G. Gukelberger, K. L. Schick, and K. S. Zener. 1991. Probe diffusion in solutions of filamentous actin formed in the presence of gelsolin. *Biopolymers.* 31:1265–1271.
28. Straub, F. B. 1943. Actin. *Studies Inst. Med. Chem. Univ. Szeged.* 2:3–15.
29. Ebashi, S., and K. Maruyama. 1965. Preparation and some properties of α-actinin-free actin. *J. Biochem. (Tokyo).* 58:20–26.
30. Spudich, J. A., and S. J. Watt. 1971. The regulation of rabbit skeletal muscle contraction. 1. Biochemical studies of the interaction of the tropomyosin-troponin complex with actin and the proteolytic fragments of myosin. *J. Biol. Chem.* 246:4866–4871.
31. Funatsu, T., H. Higuchi, and S. Ishiwata. 1990. Elastic filaments in skeletal muscle revealed by selective removal of thin filaments with plasma gelsolin. *J. Cell. Biol.* 110:53–62.
32. Kwiatkowski, D. J., T. P. Stossel, S. H. Orkin, J. E. Mole, H. R. Colten, and H. L. Yin. 1986. Plasma and cytoplasmic gelsolins are encoded by a single gene and contain a duplicated actin-binding domain. *Nature (Lond.).* 323:455–458.
33. Chu, B. 1974. Laser Light Scattering. Academic Press Inc., New York. 317 pp.
34. Berne, B., and R. Pecora. 1975. Dynamic Light Scattering. Interscience, New York. 376 pp.
35. Fujime, S., S. Ishiwata, and T. Maeda. 1984. Dynamic light scattering study of muscle F-actin. *Biophys. Chem.* 20:1–20.
36. Masai, J., S. Ishiwata, and S. Fujime. 1986. Dynamic light scattering study on polymerization process of muscle actin. *Biophys. Chem.* 25:253–269.
37. Fujime, S., M. Takasaki-Ohsita, and S. Miyamoto. 1988. Dynamic light scattering from polydisperse suspensions of large spheres. Characterization of isolated secretory granules. *Biophys. J.* 54:1179–1184.
38. Oosawa, F., and S. Asakura. 1975. Thermodynamics of the Polymerization of Proteins. Academic Press Inc., London/New York/San Francisco. 204 pp.
39. Porte, F., and M.-C. Harricane. 1986. Interaction of plasma gelsolin with actin. Isolation and characterization of binary and ternary plasma-gelsolin-actin complexes. *Eur. J. Biochem.* 154:87–93.
40. Gilman, A. G. 1987. G-proteins: transducers of recepter-generated signals. *Annu. Rev. Biochem.* 56:615–649.
41. Berridge, M. J., and R. F. Irvine. 1989. Inositol phosphates and cell signaling. *Nature (Lond.).* 341:197–205.
42. De Camilli, P., and R. Jahn. 1990. Pathways to regulated exocytosis in neurons. *Annu. Rev. Physiol.* 52:625–645.
43. Janmey, P. A., J. Peetermans, K. S. Zaner, T. P. Stossel, and T. Tanaka. 1986. Structure and mobility of actin filaments as measured by quasielastic light scattering, viscometry and electron microscopy. *J. Biol. Chem.* 261:8357–8362.
44. Janmey, P. A., and T. P. Stossel. 1987. Modulation of gelsolin function by phosphatidylinositol 4,5-bisphosphate. *Nature (Lond.)* 325:362–364.
45. Janmey, P. A., and P. T. Matsudaira. 1988. Functional composition of villin and gelsolin. (Effects of Ca^{2+}, KCl and polyphosphoinositides). *J. Biol. Chem.* 236:16738–16743.
46. Yin, H. L., K. Iida, and P. A. Janmey. 1988. Identification of a polyphosphoinositide-modulated domain in gelsolin which binds to the sides of actin filaments. *J. Cell Biol.* 106:805–812.
47. Fujime, S., M. Takasaki-Ohsita, and S. Ishiwata. 1987. Dynamic light scattering study of muscle F-actin II. *Biophys. Chem.* 27:211–224.

ORIENTATION OF ACTIN MONOMERS IN MOVING ACTIN FILAMENTS

Kazuhiko Kinosita, Jr., Naoya Suzuki, Shin'ichi Ishiwata*, Takayuki Nishizaka*, Hiroyasu Itoh, Hiroyuki Hakozaki, Gerard Marriott and Hidetake Miyata**

Department of Physics
Faculty of Science and Technology
Keio University
Hiyoshi 3-14-1, Kohoku-ku
Yokohama 223, Japan
**Department of Physics*
School of Science and Engineering
Waseda University
Okubo 3-4-1, Shinjuku-ku
Tokyo 169, Japan
***Tsukuba Research Laboratory*
Hamamatsu Photonics K. K.
Tokodai 5-9-2
Tsukuba-shi, Ibaraki 300-26, Japan

ABSTRACT

We have visualized, under an optical microscope, the orientations of actin monomers in individual actin filaments undergoing Brownian motion in solution, actively sliding past myosin molecules, or immobile on a surface. For the visualization, two strategies have been adopted. One is to exploit the fluorescence polarization of a fluorescent probe firmly attached to actin. Using the probe phalloidin-tetramethylrhodamine, the fluorescence was clearly polarized along the filament axis, showing alignment of the probe molecules along the filament axis. Within our temporal resolution of 33 ms and spatial resolution of better than 1 μm (average over ~ 10^2 actin monomers), the orientation of the probe (hence of actin monomers) did not change upon interaction of the filament with heavy meromyosin; myosin-induced reorientation was estimated to be a few degrees at most. This first method, while highly sensitive to small reorientations of monomers off or toward the filament axis, does not report on reorientations around the axis. To detect rotation around the filament axis, we adopted the second strategy in which we attached small plastic beads to the actin filaments. Axial turns would be immediately apparent from

Mechanism of Myofilament Sliding in Muscle Contraction, Edited by H. Sugi and G.H Pollack, Plenum Press, New York, 1993

the movement of the beads. Preliminary observations indicate that actin filaments can slide over a heavy meromyosin-coated surface without axial rotations. Since rotations have been implicated in different experiments, we are currently investigating the source of the apparent discrepancy. The attached bead also serves as a handle through which we can apply force, via optical tweezers, on the filament. By letting the sliding actin filament pull the bead against the optical force, we were able to estimate the sliding force and its fluctuation.

INTRODUCTION

The establishment of the sliding theory[1)2)] was a break-through in the study of muscle contraction. However, unraveling the molecular mechanism of sliding, or the molecular events at the myosin-actin interface, is yet a challenging task. A recent progress toward this goal has been the introduction of the *in vitro* motility assay systems[3-5)], which allow direct and continuous observation of molecular events under an optical microscope. Here we use this system in an attempt at elucidating several aspects of molecular motions at the myosin-actin interface during sliding.

ORIENTATION OF ACTIN PROTOMERS IN SLIDING ACTIN FILAMENTS[6)]

Orientation Measurement by Dual-Polarization Microscopy

To reveal the orientation of actin protomers, we used the technique of fluorescence polarization: when a fluorophore emits fluorescence, the emitted light is fully polarized along the emission transition moment of the fluorophore. By measuring the polarization of the fluorescence, therefore, one can determine the orientation of the fluorophore at the moment of emission. If the fluorophore is firmly attached to a protein molecule, the fluorescence polarization serves as a marker of the protein orientation. In our case, we labeled actin filaments with the fluorescent probe phalloidin-tetramethylrhodamine at the ratio of one fluorophore per one actin protomer. The binding appeared to be rigid.

To quantify the polarization of fluorescence under a microscope, we invented what we call "W(double view video) microscopy", in which two different images of an object are projected side by side on a video camera. The two images in the present case were two mutually orthogonal components of the polarized fluorescence, as shown in Figs. 1A and 1B. The figures clearly indicate that the fluorescence, excited with unpolarized light, was polarized along the axis of actin filaments. The transition moment of the rhodamine dye was aligned nearly parallel to the filament axis.

The polarization of fluorescence, calculated from Figs. 1A and 1B, is shown in Fig. 1C. Positive polarization shown in white color indicates that the dye molecules lay along the vertical axis in the figure, and negative polarization in black along the horizontal axis. The parallelism between the dye axis and filament axis is immediately clear in this representation. Quantitative analysis of the polarization

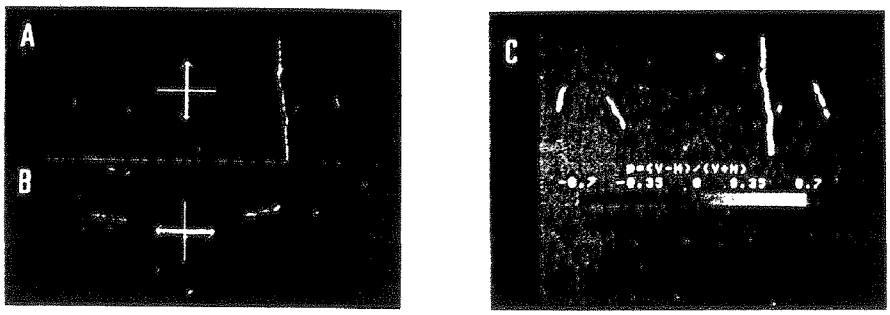

Fig. 1. (A and B), a pair of polarized fluorescence images of actin filaments stained with phalloidin-tetramethylrhodamine. Thick arrows indicate the direction of polarization. The filaments were bound, in the absence of ATP, by heavy meromyosin lying on a nitrocellulose-coated coverglass. (C), polarization, p, of fluorescence calculated from A and B. V, vertically polarized fluorescence; H, horizontal. For details, see ref. 6.

values suggests that the angle between the emission transition moment of the dye and the filament axis was about 30°.

DOES ACTIN PROTOMER ROTATE IN THE FILAMENT?

Our interest is whether actin protomers rotate in the actin filament when the filament interacts with myosin. If the sliding motion is caused by the rotation of bound myosin heads relative to the filament axis, we expect some rotation also in the actin part, which would be detected in the fluorescence polarization of the bound rhodamine. The rotation of rhodamine toward the filament axis would result in an increase in the absolute value of the polarization (in the polarization image as in Fig. 1C, vertical parts of the filaments would become more white and horizontal parts more black), and the rotation off the filament axis would reduce the polarization.

The actin filaments shown in Fig. 1 lay on a layer of heavy meromyosin which was adsorbed on a glass surface coated with a nitrocellulose film[7]. In the absence of ATP, the filaments rested still forming the rigor complex. When ATP was added, the filaments started to slide as shown in Fig. 2A. The fluorescence polarization of the sliding filaments, however, was not significantly different from that of the rigor complex in Fig. 1C. Actin filaments alone, undergoing Brownian motion in solution, also showed the same polarization (Fig. 2B). Apparently, interaction with myosin did not induce detectable reorientation of actin protomers either off or toward the filament axis.

On the nitrocellulose film, as discussed below, the number of myosin molecules actively interacting with an actin filament might be quite small. The fluorescence polarization shown in Figs. 1 and 2, on the other hand, is the average over ~10^2 actin protomers, since 1 μm of the filament contains 363 protomers and the resolution in the images is of the order of the wavelength of light. Reorientation of a small

number of actin protomers may thus have taken place without affecting the polarization. To test this possibility, we made a preparation in which excess heavy meromyosin was added to actin filaments in the absence of ATP. In this fully decorated rigor complex, too, the fluorescence polarization was indistinguishable from that in other samples (Fig. 2C). Myosin-induced reorientation of actin protomers appears to be at most a few degrees. A study on muscle fibers has indicated a reorientation by a few degrees[8], which is not inconsistent with our present results.

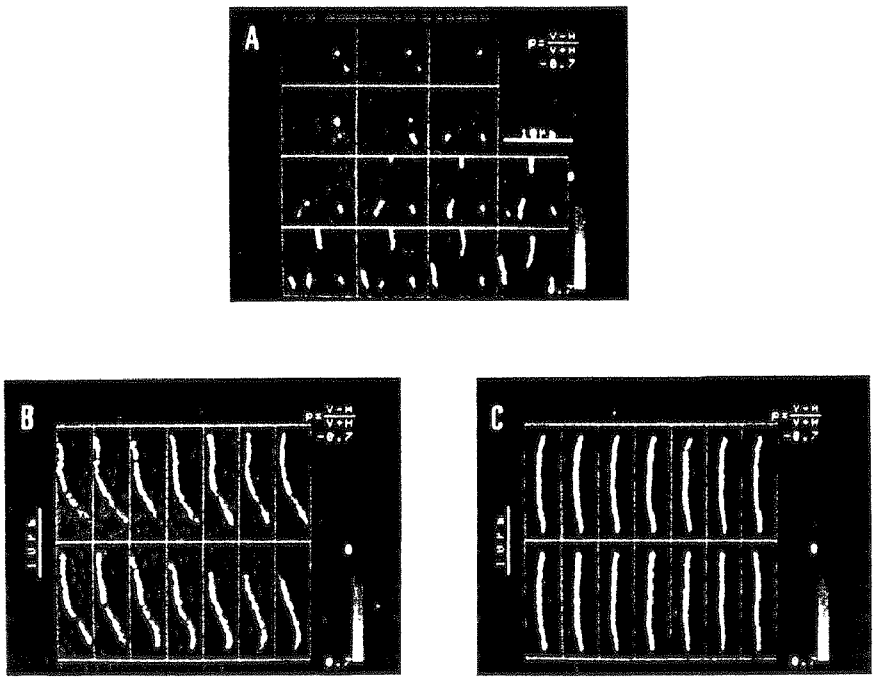

Fig. 2. (A), fluorescence polarization of actin filaments sliding over heavy meromyosin. ATP was added to the sample in Fig. 1C. Snap shots at intervals of 0.2 s, from left to right and then from top to bottom. (B), an actin filament undergoing Brownian motion in solution. Part of the filament went out of focus in some images. 33 ms intervals. (C), an actin filament undergoing Brownian motion in the presence of excess heavy meromyosin and in the absence of ATP. 33 ms intervals.

Among several models of the sliding mechanism proposed by Huxley and Simmons[9], one postulates that the force arises from the rotation of actin protomers in the filament. Now this particular model seems rather unlikely. If, on the other hand, it is part of myosin that rotates and produces force, associated reorientation of actin protomers may be quite small. This possibility cannot be excluded at the current precision.

DOES SLIDING ACTIN FILAMENT ROTATE AXIALLY?

The fluorescence polarization measurements above are not sensitive to rotations of actin protomers (or of the whole filament) around the filament axis. Since an actin filament has a helical structure, one may expect that the filament rotates axially when it slides past myosin. The axial rotation has in fact been indicated by Tanaka et al.[10] for filaments in which the sliding motion of the front part was slower than that of the rear part. To see the axial rotation in a smoothly sliding actin filament, we attached a visible marker on the filament.

The marker we chose was a polystyrene bead with a diameter of 1 μm. By coating the bead surface with gelsolin, we were able to attach the bead selectively at the barbed end of actin filaments. Since the barbed end is the rear end when the filament slides over myosin, we call this preparation "bead-tailed F-actin". The bead was visualized by lightly staining it with tetramethylrhodamine, while the actin filament was labeled with the phalloidin-tetramethylrhodamine. On a layer of heavy meromyosin on a nitrocellulose-coated glass surface, the bead-tailed F-actin was seen to slide smoothly, trailing the bead at its end. The sliding velocity was indistinguishable from that of the unbeaded filaments.

The single bead at the tail end did not serve as the marker for axial rotation, but occasionally we found another bead or two firmly attached to the tail bead (Fig. 3). Then the orientation of the bead aggregate could be followed continuously on a video monitor while the filament was sliding over heavy meromyosin. So far, we have not seen any evidence for axial rotation apart from random fluctuation: actin filaments slid over distances of many tens of micrometers without showing a complete turn of the bead aggregate.

A possible reason for the failure in observing a turn of the bead aggregate is the

Fig. 3. An actin filament with two polystyrene beads attached to its tail. All filaments are sliding over heavy meromyosin.

hydrodynamic friction. To rotate double beads in water at one turn per second around the center of one of the double beads, one needs a torque of 100 pN•nm. At the surface of an actin filament with a radius about 5 nm, the required force is 20 pN. This force, which should be produced by the actin-myosin interaction and should operate in a direction perpendicular to the filament axis, is higher than the sliding force along the filament axis which, as shown below, is about 1 pN per μm of actin filament. Thus the bead aggregate appears to be too heavy a load for the force generators. (Note that the double beads produce a friction against the translational motion of only 0.1 pN at the sliding velocity of 5 μm/s. This friction is negligible compared to the sliding force. The friction against rotation is significant because the torque has to be generated at the surface of the thin actin filament.)

The friction against rotation is proportional to the cube of the bead radius. We therefore tested beads with a diameter of 0.5 μm, half the previous size. The small beads, too, did not show any sign of unidirectional rotation.

Thus the actin-myosin interaction does not produce a large torque, at least in the present system of heavy meromyosin lying on a nitrocellulose film. Or, the torque produced by individual power strokes does not accumulate to a level sufficient to rotate the beads, presumably because of some kind of slipping at the actin-myosin interface.

MEASUREMENT OF SLIDING FORCE

The bead at the tail served as a handle, with which we were able to manipulate a single actin filament. We used the technique of optical tweezers[11], in which a tightly focused laser beam produces an attractive force toward the light spot. The bead could be trapped in the light spot, and by moving the spot we were able to pull the bead-tailed F-actin in a desired direction, either along the myosin-coated surface or off the surface. That is, the trapping force was stronger than the sliding force.

When we turned on the laser while bead-tailed actin filaments were freely sliding over heavy meromyosin, a bead which happened to come close to the light spot was drawn to the spot and trapped. If the laser beam was sufficiently weak, a long actin filament could pull its bead out of the trap once the filament became straight (Fig. 4). From the result of this tug of war, we estimated that the sliding force was about 1 pN per μm of actin filament.

A bead attached to a short actin filament (or to a long filament but in a stronger laser beam) remained trapped in the light spot even after the actin filament became straight. In this case, the bead exhibited noticeable fluctuation in the direction of the filament. Precise analysis of the bead location, from the phase-contrast image of the bead, indicated that the amplitude of the fluctuation was several tens of nm. The average bead position was ~100 nm away from the center of the light trap and toward the actin filament, implying that the filament was always pulling the bead but the pulling force fluctuated. The average pulling force was again estimated to be about 1 pN per μm of actin filament. The pattern of the fluctuation was similar to those reported by Ishijima et al[12] in their isometric conditions.

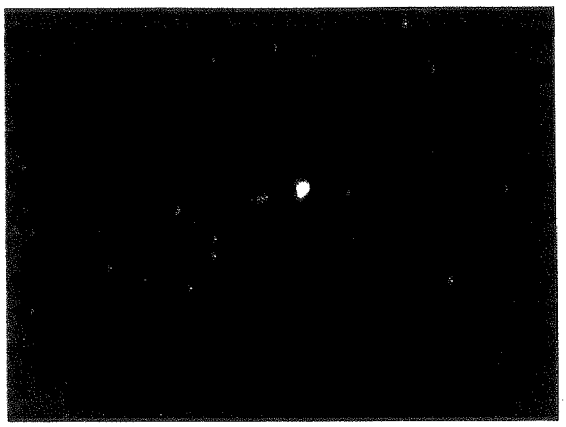

Fig. 4. A bead-tailed F-actin trapped by optical tweezers. Other actin filaments are sliding over heavy meromyosin.

In muscles, one myosin head is considered to produce an average force of the order of 1 pN[13]. The above results may then imply that, in our system, only several myosin heads were actively interacting with the actin filament which was, on the average, several μm long. With such a small number of heads, the fluctuation in generated force is an expected consequence.

Measurement of the EDTA-ATPase of the heavy meromyosin, however, suggested that the myosin density was of the order of 10^3 molecules/μm^2, as has already been reported[14]. This number suggests that tens of myosin heads must be available for 1 μm of actin filament. To reconcile this with the force data above, two extreme views are to be considered. One is that the EDTA-ATPase correctly estimated the number of active myosin heads and therefore the observed force was produced by tens of heads per μm of actin, all working more or less uniformly but probably in a more or less sequential manner. In this view, the average force produced by a single head on the nitrocellulose film is far less than the value in native muscles. The other extreme view is to suppose that, somehow, the number of really active heads was far fewer than the number suggested by the EDTA-ATPase assay. Misoriented heads, for example, should be discounted. If the active heads were as small as one or a few per μm of actin filament, the force per head was normal. In this case, each head should have spent a considerable portion of time pulling actin, since otherwise the bead would have been drawn to the trap center. The length of the stroke by each head should also have been large to account for the observed fluctuation over tens of nm.

The first of the two views above is obviously based on the view of Spudich group[14]. The second view is on the side of Yanagida group[15]. These two groups debate on the "step size", the length of the force generating movement of actin past myosin upon the hydrolysis of one ATP molecule. Spudich group maintains, on the basis of experiments using the nitrocellulose system, that the step size is well within 40 nm, whereas Yanagida group, using a glass surface covered with Sigma coat,

claims that the step size exceeds 100 nm under unloaded conditions. Our present result might shed some light on this discrepancy. If myosin heads on the nitrocellulose film cannot produce the normal force, as in the first view above, it may imply that the head motion on this substrate is severely limited (e.g., by tight binding at the neck part) because, at least in the Huxley model[13], the magnitude of generated force is proportional to the size of the head motion. Or, if the number of active heads on the nitrocellulose film is much less than the estimation from the ATPase assay, as in the second view, the conclusion of Spudich group needs be revised (toward a larger step size), because their estimate critically depends on the myosin density.

At present, we cannot draw any definite conclusion. Our present experimental system, however, should prove useful in the analysis of molecular details, since it allows simultaneous measurements of displacement at nm resolution and force at subpiconewton resolution, together with real-time imaging of the filament motion.

ACKNOWLEDGEMENTS

This work was supported in part by Grants-in-Aid from the Ministry of Education, Science and Culture of Japan, and in part by Special Coordination Funds for Promoting Science and Technology given by the Agency of Science and Technology of Japan.

REFERENCES

1. Huxley, A.F. & Niedergerke, R. *Nature* **173**, 971-973 (1954).
2. Huxley, H.E. & Hanson, J. *Nature* **173**, 973-976 (1954).
3. Kron, S.J. & Spudich, J.A. *Proc. Natl. Acad. Sci. USA* **83**, 6272-6276 (1986).
4. Honda, H., Nagashima, H. & Asakura, S. *J. Mol. Biol.* **191**, 131-133 (1986).
5. Harada, Y. Noguchi, A., Kishino, A. & Yanagida, T. *Nature* **326**, 605-608 (1987).
6. Kinosita, K., Jr., Itoh, H., Ishiwata, S., Hirano, K., Nishizaka, T. & Hayakawa, T. *J. Cell Biol.* **115**, 67-73 (1991).
7. Kron, S.J., Toyoshima, Y.Y., Uyeda, T.Q.P. & Spudich, J.A. *Methods Enzymol.* **196**, 399-416 (1991).
8. Prochniewicz-Nakayama, E., Yanagida, T. & Oosawa, F. *J. Cell Biol.* **97**, 1663-1667 (1983).
9. Huxley, A.F. & Simmons, R.M. *Cold Spring Harbor Symp. Quant. Biol.* **37**, 669-680 (1972).
10. Tanaka, Y., Ishijima, A. & Ishiwata, S. *Biochim. Biophys. Acta* **115**, 94-98 (1992).
11. Ashkin, A., Dziedzic, J.M., Bjorkholm, J.E. & Chu, S. *Optics Lett.* **11**, 288-290 (1986).
12. Ishijima, A., Doi, T., Sakurada, K. & Yanagida, T. *Nature* **352**, 301-306 (1991).
13. Huxley, A.F. *Prog. Biophys. Biophys. Chem.* **7**, 255-318 (1957).
14. Uyeda, T.Q.P., Kron, S.J. & Spudich, J.A. *J. Mol. Biol.* **214**, 699-710 (1990).
15. Harada, Y., Sakurada, K., Aoki, T., Thomas, D.D. & Yanagida, T. *J. Mol. Biol.* **216**, 49-68 (1990).

Discussion

Edman: Do you think that the rotation you observed would take place *in situ* in a muscle fiber? Wouldn't it be difficult, since one end is fixed?

Kinosita: Yes, but in theory, the other can rotate.

Edman: Wouldn't it put a constraint on the sliding movement of actin?

Kinosita: The actin filament has a helical structure, so to me it's natural that the actin rotate to some extent when the myosin pulls the actin or the actin goes over the myosin.

Tregear: What is the limit of resolution of that rhodamine-polarization measurement? Supposing they were all turning around, how small an angle could you detect?

Kinosita: I would say one or two degrees. The current uncertainty is several degrees. The reason for this is that we do not know whether the filament is really straight or not. So, now we pull the filament with optical tweezers and repeat the measurement, making the precision at least two degrees.

Tregear: So, then even with the very low duty cycle that Spudich suggested in his recent paper, you would still be able to see it?

Kinosita: Yes, if the rotation is very large, something like 40° or 50°.

Homsher: Dr. Kinosita, did you say that the step size at 3 pN was 30 nm distance per ATP?

Kinosita: I used wrong words. In a sense it is a step size, but it is not a step size per one ATP hydrolysis.

Gillis: When you show that the filament with the bead is in a laser trap, it fluctuates in some cases. Does the frequency of fluctuation depend on the density of the myosin molecules?

Kinosita: That is the kind of experiment we are now in the process of conducting, so I cannot give you the answer yet. I can tell you one difference, however: when the trap force is strong, the speed of forward motion slows down, and the amplitude of the motion decreases. But we haven't changed the myosin density yet.

SPONTANEOUS TENSION OSCILLATION (SPOC) OF MUSCLE FIBERS AND MYOFIBRILS MINIMUM REQUIREMENTS FOR SPOC

Shin'ichi Ishiwata, Takashi Anazawa, Takashi Fujita, Norio Fukuda, Hideharu Shimizu and Kenji Yasuda

Department of Physics
School of Science and Engineering
Waseda University
3-4-1 Okubo, Shinjuku-ku, Tokyo 169, Japan

ABSTRACT

Several years ago, we found a new chemical condition for the spontaneous oscillatory contraction of glycerinated skeletal muscle and named it "SPOC". The condition was such that MgATP coexists with its hydrolytic products, MgADP and inorganic phosphate (Pi). Micromolar concentrations of free Ca^{2+} were not necessarily required for this oscillation. Here, we summarize our recent work on the mechano-chemical properties of SPOC not only in glycerinated single fibers and myofibrils of skeletal muscle (fast type) but also in glycerinated small bundles of cardiac muscle; the isometric tension and its oscillation were examined at various concentrations of MgATP, MgADP and Pi while controlling the concentration of free Ca^{2+}; we constructed a three-dimensional "state diagram" taken against the concentrations of MgADP, Pi and free Ca^{2+}. The 3-D state diagram clearly showed the existence of three regions corresponding to three muscular states; the SPOC region was located in between the regions for contraction (without oscillation) and relaxation. Based on these results, we discuss the mechanism of SPOC, especially the minimum requirements for its occurrence. Finally, we suggest that slow shortening and quick lengthening repeatedly occur every half-sarcomere through the transition between the two states, where weak-force-generating complexes or strong-force-generating complexes are dominant; the transition may be induced by a coupling with the mechanical states of cross-bridges and/or thin filaments.

INTRODUCTION

The contractile system of muscle usually takes two states, i.e., contraction and

Mechanism of Myofilament Sliding in Muscle Contraction, Edited by H. Sugi and G.H. Pollack, Plenum Press, New York, 1993

relaxation. It has been reported, however, that auto-oscillation of tension and sarcomere lengths of muscle fibers occurs with either intermediate pCa values[1-5], high pH in the absence of Ca^{2+},[6] or the coexistence of MgATP, MgADP and Pi[7-11]. We named the oscillation induced by the last condition "SPOC"[7][8]. The common characteristics to these oscillations are that the oscillatory state is intermediate between contraction and relaxation. The developed tension is not full but medium, irrespective of whether the oscillation is induced by partial Ca^{2+} activation or the coexistence of MgADP and Pi with MgATP; to distinguish these two conditions for oscillation, we here call the former "Ca-SPOC" and the latter "ADP-SPOC", respectively. To induce SPOC, it seems to be essential to realize a stable intermediate state. In the present work, we made an effort to find out the minimum requirements for SPOC, which may be common to all kinds of SPOCs, and to get deep insights into the molecular mechanism of SPOC.

MATERIALS AND METHODS

Preparation of Glycerinated Muscle and Myofibrils

Skeletal Muscle[12]: a bundle of muscle fibers (3-5 mm thick, 5-7 cm long) dissected from rabbit psoas muscle was tied to a thin glass rod (3-4 mm diam.) with a cotton thread which was boiled in distilled water and dried beforehand. It was then immediately immersed in cold glycerol solution (pH, about 7.5) containing 50 % (v/v) glycerol, 0.5 mM $NaHCO_3$ and 5 mM EGTA (usually, 1 mM leupeptin was also added to protect the proteolysis of elastic filaments[12]) and stored over night (longer than 12 hrs) at 0°C. The next day, the glycerol solution was exchanged for a fresh one and about 6 hrs later stored in a deep freeze (-20°C). Three weeks later we started to use it. To prepare myofibrils, several pieces of a small bundle of glycerinated fibers (about 1 mm thick, 5 mm long) were immersed in a few ml of solution A containing 60 mM KCl, 5 mM $MgCl_2$, 10 mM Tris-maleate buffer (pH 6.8) and 1 mM EGTA at 0°C. Then the solution was gently homogenized at a low speed for about 10 s with a homogenizer (Ultra turrax; IKA-WERK STAUFEN, Staufen, FRG; 8N type of edge) on ice. To remove glycerol and other materials released from fibers, the solution was centrifuged at 2000 rpm for 10 min and the pellet was dispersed in solution A. This procedure was repeated two to three times to prepare a homogeneous suspension of myofibrils. This washing procedure could be replaced by washing under an optical microscope. The Triton treatment was done by washing with solution A containing 1 % (v/v) Triton X-100 either under a microscope or with centrifugation.

Cardiac Muscle: A small segment of muscle bundle was dissected from a papillary muscle of a bovine heart and treated with a glycerol solution through the same procedure as described above. More details will be described elsewhere[14][15].

Tension Measurement

The isometric tension of fibers (single fibers for skeletal muscle and small bundles for cardiac muscle; both, 40-120 μm thick and a few mm long) was measured with a tension transducer using a standard method[10)15)]. To measure the tension of myofibrils, we devised a simple method: both ends of isolated myofibrils were held by a pair of glass micro-needles under an inverted phase-contrast microscope and the deflection of the flexible needle was measured with the accuracy of 50 nm by using a computer(image processor)-aided system of optical microscopy. Thus developed tension of an order of 10-100 μg (1 μg = 10 nN) could be measured with an accuracy of 50 ng (1 ng = 10 pN). The average sarcomere length of myofibrils was estimated from the total length divided by the number of sarcomeres. Details will be published elsewhere[11)].

RESULTS AND DISCUSSION

Figure 1 shows an example of a time course of length oscillation of sarcomeres in a myofibril obtained under a standard SPOC condition. The oscillation of sarcomeres consisted of a slow shortening phase and a quick lengthening phase with a period of 2 to 3 s. The sliding of thick and thin filaments could be recognized from the change in the width of the overlapping region and the accompanying change in the width of the H-zone[8)9)]. This occurred reversibly and repeatedly. Sometimes this oscillation propagated from one end to the other of the myofibril (we call such a state of SPOC an "organized" SPOC[9)11)]; cf. Fig. 5). Figure 1 shows an example of an "unorganized" SPOC, where there is no organization of oscillations among adjacent sarcomeres, although the oscillation of each sarcomere appears to be regular with time.

Next, we examined the effects of MgADP and Pi on the isometric tension of rabbit psoas glycerinated single muscle fibers and compared the results with those of cardiac muscle. The results are summarized schematically in Fig. 2. Figure 2a shows that in the presence of Ca^{2+}, the tension increased slightly with the addition of MgADP and then decreased. On the other hand, in the absence of Ca^{2+} (Fig. 2b), muscle, which is relaxed without MgADP, developed tension along a sigmoidal curve with the addition of MgADP (ADP-induced tension generation), reaching 80 to 90 % of the tension in the presence of Ca^{2+}. Although the final level of tension was high, the shortening velocity was slow, about one tenth of that at a normal contraction condition. The concentration of MgADP at which the increase of tension shows a half-maximum (critical MgADP concentration) increased in proportion to the concentration of MgATP, suggesting the competitive binding of MgADP and MgATP to the binding sites on the actomyosin complexes. Such features were common to both types of muscle. The only difference was that the critical MgADP concentration was lower in cardiac muscle irrespective of the presence or the

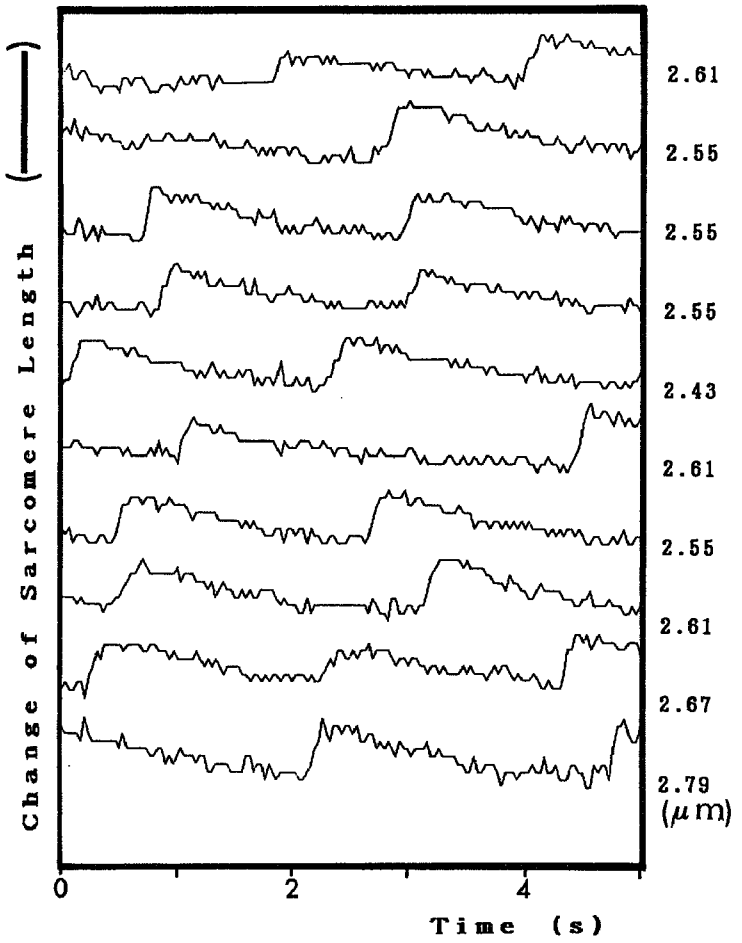

Fig. 1. Time course of length change during SPOC of 10 adjacent sarcomeres in a central part of a myofibril (rabbit psoas) of which both ends were attached to a glass surface; here, the myofibril is placed vertically. The myofibril was labeled with rhodamine-phalloidin to clearly identify the position of Z-lines under a fluorescence microscope 13). The distances between the Z-lines of the sarcomeres (sarcomere lengths) were measured from a single frame of video tape by using an image processor every 1/30 s, and only the portion of the change is shown on the ordinate. The average length of each sarcomere is shown on the right (S.D. = 0.12 μm); the average position of each sarcomere is arbitrary. Conditions (a standard SPOC condition): 0.12 M KCl, 0.2 mM ATP, 4 mM ADP, 4 mM $MgCl_2$, 4 mM Pi, 4 mM EGTA, and 10 mM MOPS (pH 7.0) at room temperature. Vertical scale bar, 0.5 μm.

absence of Ca^{2+}. This suggests that the actomyosin system of cardiac muscle has relatively higher binding affinity for MgADP.

In living muscle, it has been established that contraction and relaxation are regulated by micromolar concentrations of free Ca^{2+},16)17), where it is essential to regulate the state of thin filaments, either on-state or off-state. The ADP-induced activation suggests that the state of thin filaments can be regulated through not only regulatory proteins but also cross-bridges.

Next, we examined the effect of Pi on ADP-induced tension. In the presence of Ca^{2+}, Pi decreased tension monotonically irrespective of the presence or absence of MgADP (Fig. 2a), although MgADP reduced the effect of Pi. In any case, in the

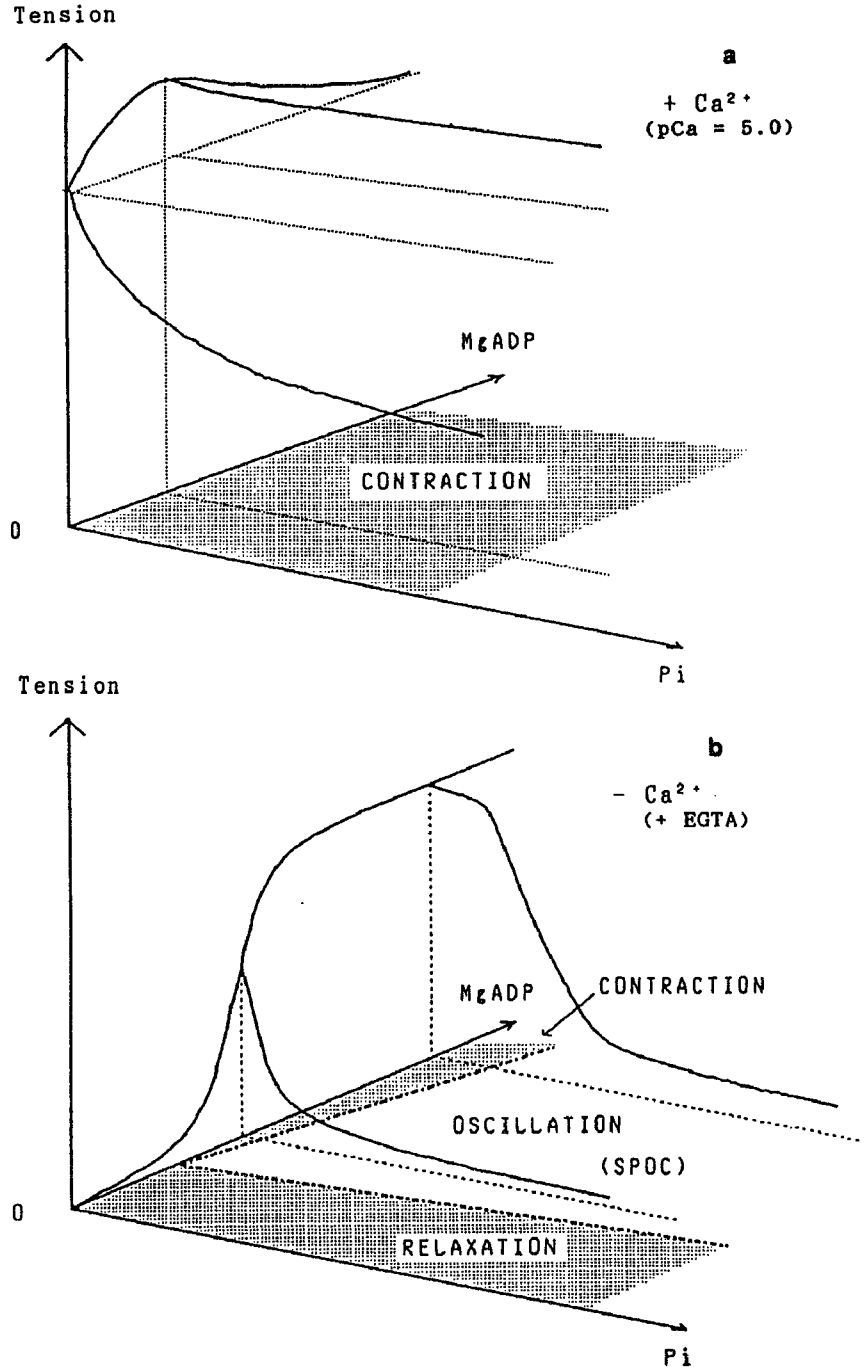

Fig. 2. Schematic diagram showing the isometric tension of fibers developed under various concentrations of MgADP and Pi in the presence of MgATP and the presence (a) or absence (b) of Ca^{2+}. The state of muscle is indicated on the MgADP-Pi plane. This diagram was constructed from data taken under the following conditions by using fibers: 1-3 mM MgATP, 0-20 mM MgADP, 2 mM Mg^{2+}, 0-20 mM Pi, 10 mM MOPS (pH 7.0), 0.1 mM AP_5A and (a) pCa = 5.0 or (b) pCa = 8 (+ 2 mM EGTA), and the ionic strength was maintained at 0.15 M with KCl at 25°C.

presence of Ca^{2+}, the muscle developed tension and contracted. In the absence of Ca^{2+}, on the other hand, the tension decreased sigmoidally and reached a very low level through the addition of Pi (Fig. 2b). Accompanying the decrease of tension, the spontaneous length oscillation of sarcomeres and also the tension oscillation of muscle fibers and myofibrils appeared. So, near the MgADP axis, contraction occurred without oscillation, but with the addition of Pi, the SPOC state appeared. Thus, in the absence of Ca^{2+}, the muscle took three states; the SPOC state was located in between contraction and relaxation.

The state of muscle under the above conditions is summarized schematically in the two-dimensional state diagram on the MgADP-Pi plane (Fig. 2). In the presence of Ca^{2+}, the state of the muscle was always contraction. In the absence of Ca^{2+}, the SPOC region occupied a large region between contraction and relaxation regions. The fact that the SPOC is not a transient state but a stable one suggests that it is a third state for the contractile system of muscle.

In summary, *MgADP* and *Pi* function respectively as an *activator* and an *inhibitor* of tension development. In the ADP-induced activation, *actomyosin(AM)-ADP complex* probably functions as an allosteric desuppressor for the regulatory system, similar to the so-called rigor complex[17].

Next, we examined the effect of Ca^{2+} concentration, in addition to MgADP and Pi, on the isometric tension. Through increasing the concentration of free Ca^{2+}, the tension gradually increased from that without Ca^{2+} to that with Ca^{2+}, that is, the tension curve moved between the two extremes schematically shown in Figs. 2a and b.

To summarize the above results, a three-dimensional state diagram of muscle was constructed. In Fig. 3, three regions corresponding to three states of muscle are schematically illustrated against three axes, pCa and the concentrations of Pi and MgADP. In the case of a fast type of skeletal muscle (Fig. 3a), the SPOC region was difficult to identify on the pCa axis, whereas in cardiac muscle (Fig. 3b) the SPOC region was present (judging from the tension oscillation of muscle fibers)[1)2)5)15)]. In cardiac muscle, the ADP-SPOC region on the MgADP-Pi plane and the Ca-SPOC region on the pCa axis were continuously connected by a thin SPOC region, which was sandwiched in between the contraction and relaxation regions; this suggests that the molecular mechanism of oscillation is common to both types of SPOC, although the apparent chemical conditions are quite different from each other.

According to this diagram and the properties of SPOC described above, we present the following hypothesis concerning the minimum requirements for SPOC; these seem to be common to all types of SPOC reported so far. Because the SPOC state is located between contraction and relaxation, i.e., in an intermediate state, the state of cross-bridges will be, on the average, in between a non(or weak)-force-generating state and a (strong)-force-generating state. With the increase of either the concentration of free Ca^{2+} or the MgADP concentration, the proportion of such non(or weak)-force-generating species as AM•ADP•Pi (and/or AM•ATP) complex, which is dominant under relaxation, will decrease as shown in Fig. 4, whereas that of such (strong)-force-generating species as AM•ADP complex, which is dominant

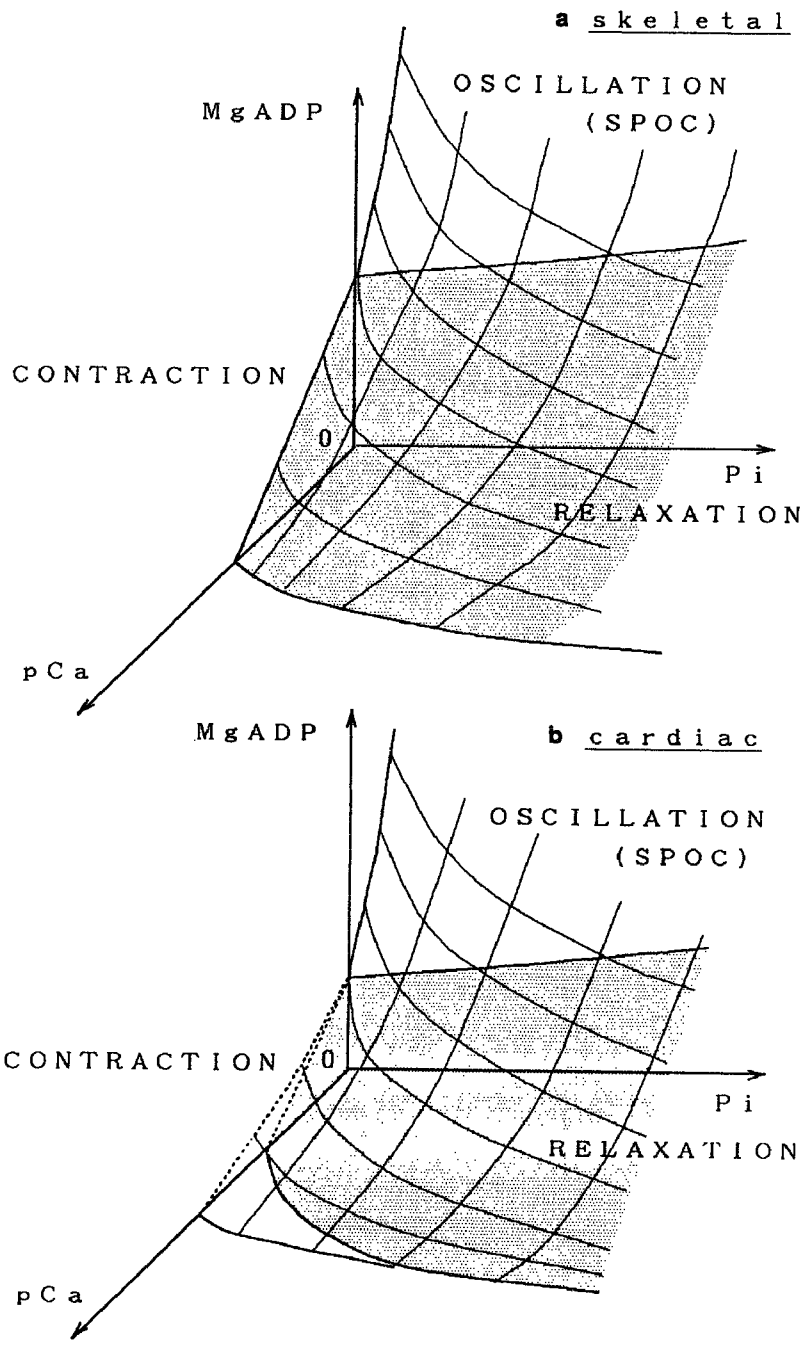

Fig. 3. Three-dimensional state diagram schematically showing the regions of three states of muscle, i.e., spontaneous oscillation (SPOC), contraction (without oscillation) and relaxation in the presence of MgATP. Three axes are taken for pCa (8-5) and the concentrations of Pi (0-20 mM) and MgADP (0-20 mM). Other conditions for the construction of this diagram were the same as those in Fig. 2. The contraction region is located in front of the meshed surface, the relaxation region is behind the dotted surface and the SPOC region is sandwiched between the meshed and dotted surfaces. Diagrams (a) and (b) are for skeletal and cardiac muscle, respectively. The dotted lines in (b) are drawn without experimental data.

under contraction, will increase. Under SPOC conditions, both kinds of complexes will coexist in some proportion (for details about the chemical species of actomyosin complex during ATPase cycle, see refs. 18 & 19).

Now, we infer that for SPOC to occur there is a minimum requirement for the proportions of such complexes: that is, we postulate that the SPOC state appears only when the proportions of both of the types of complexes indicated above are *beyond*

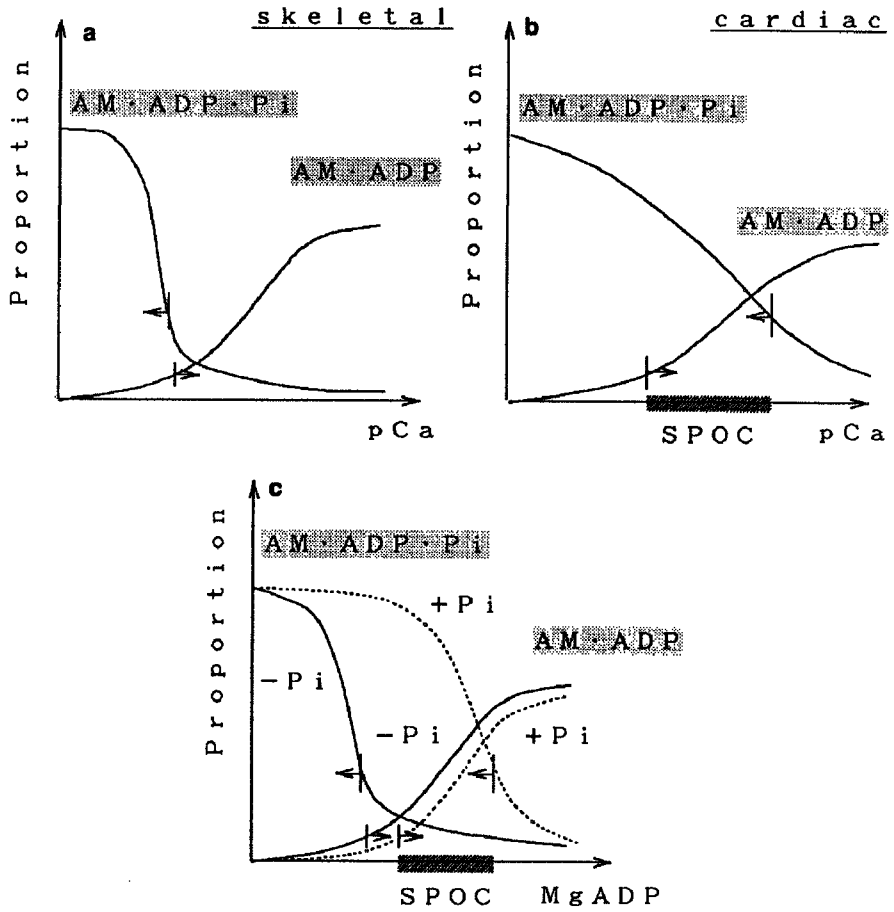

Fig. 4. Hypothesis about the minimum requirements for SPOC on the molecular level. We assume that a stable SPOC state appears only when the proportions of particular chemical species of cross-bridges, such as AM-ADP-Pi (and/or AM-ATP) and AM-ADP complexes, are beyond certain threshold values (indicated by arrows). For more details, see the text.

certain threshold values. This requirement may be fulfilled at submicromolar concentrations of free Ca^{2+} in cardiac muscle (Fig. 4b) because of low cooperativity for tension development, whereas in skeletal muscle the requirement may be difficult to be fulfilled because of high cooperativity (Fig. 4a). When Pi coexists with MgADP, however, the requirement can be fulfilled even in skeletal muscle, so that the SPOC region appears (dotted curves in Fig. 4c).

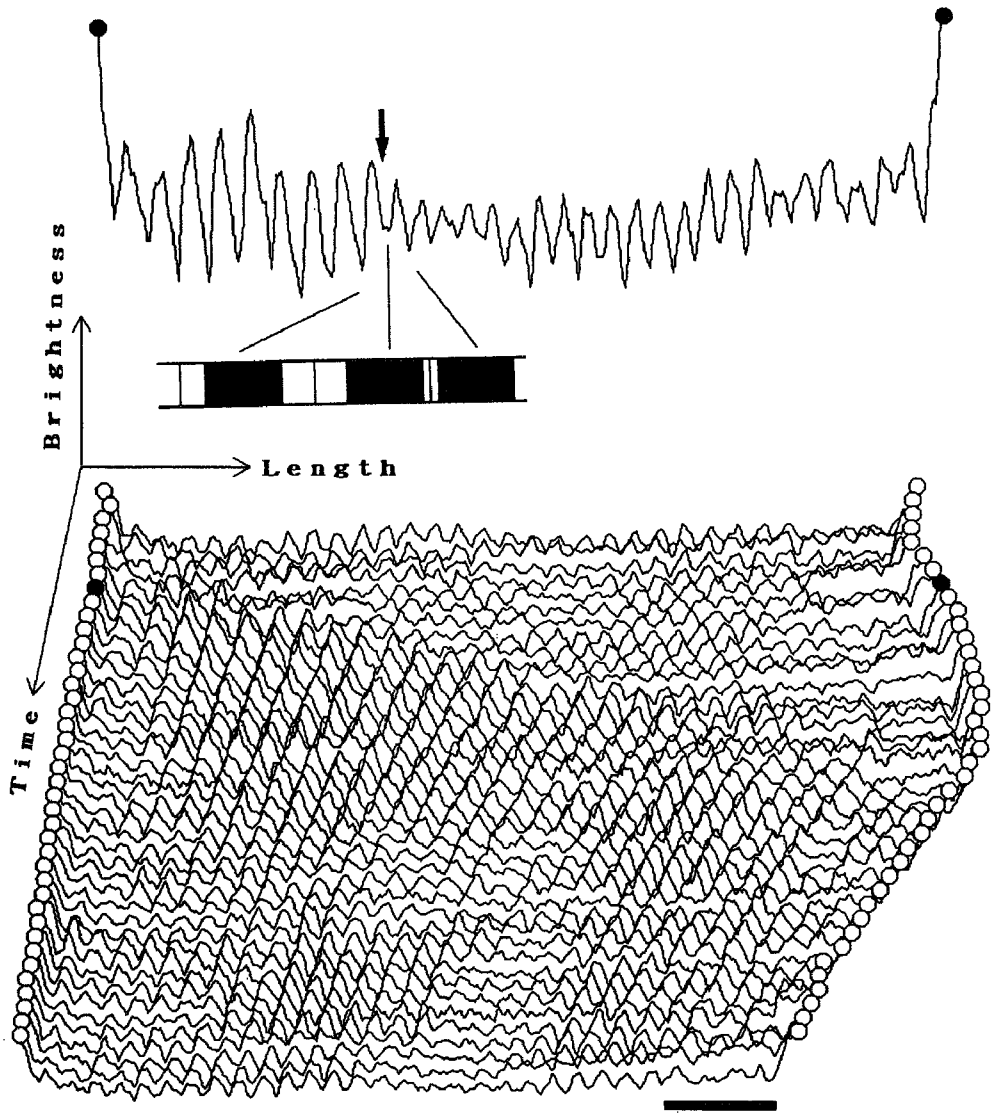

Fig. 5. Time course of the phase-contrast image profile of myofibrils showing the propagation of an "organized" SPOC wave along a myofibril of which both ends were attached to a pair of glass micro-needles. Serial images were taken every 1/15 s from top to bottom. The lengthening phase of sarcomeres propagated from the edge of a stiff micro-needle (the circle on the left end) to the edge of a flexible micro-needle (the circle on the right end). Some parts, such as the upper right and the lower middle, were out of focus, so that the image is not clear. A typical example of an image profile of the myofibril is shown at the top, where the lengthening phase (a few sarcomeres to the left part from the arrow) and the shortening phase (sarcomeres in the right half and the left end) of sarcomeres coexist; the arrow indicates the boundary between the two phases as schematically illustrated below. The developed tension can be estimated from the deflection of the flexible needle. In this example, a small bundle of myofibrils (about 6 μm thick, 32 sarcomeres long) composed of several single myofibrils was used in order to obtain an "organized" SPOC. The other conditions are the same as in Fig. 1. Scale bar, 10 μm.

Finally, we briefly describe the results of a microscopic analysis of "organized" SPOC obtained under an inverted phase-contrast microscope with image processing (Fig. 5). Under standard SPOC condition, a small bundle of myofibrils developed oscillatory tension steadily; correspondingly, a lengthening phase of sarcomeres (to be exact, a half-sarcomere is a unit of oscillation[9]), which appeared from the left end of a myofibril, propagated to the right end along the myofibril (SPOC wave).

Although it is difficult to determine the molecular mechanism of SPOC from such simple experimental analyses, and even though there are still many unresolved problems, we point out one thing deduced from the present study. First, we infer that every sarcomere bears the same load during the SPOC, because the velocity of a mechanical impulse traveling along a myofibril should be very fast. This means that every sarcomere develops the same tension at the same time, irrespective of whether it is in a stretching phase, shortening phase or nearly stopped phase (cf. Fig. 5). This would be possible only through the spontaneous arrangement of the proportions of different chemical states of cross-bridges, such as a non-force-generating state, a weak-force-generating state (e.g., AM•ADP•Pi and AM•ATP complexes) and a strong-force-generating state (e.g., AM•ADP complex), and also a state only sustaining a load (e.g., AM•ADP complex which may be formed by the exogenous ADP). Such an arrangement would be possible from the self-control mechanism through mechano-chemical coupling; that is, the chemical states of cross-bridges would be regulated by the mechanical states (strain) of cross-bridges and/or thin filaments, and *vice versa*.

REFERENCES

1. Fabiato, A. & Fabiato, F. *J. Gen. Physiol.* **72**, 667-699 (1978).
2. Brenner,B. *Basic Res. Cardiol.* **74**, 177-202 (1979).
3. Iwazumi, T. & Pollack, G.H. *J. Cell. Physiol.* **106**, 321-337 (1981).
4. Stephenson, D.G. & Williams, D.A. *J. Physiol. (Lond.)* **333**, 637-653 (1982).
5. Sweitzer, N.K. & Moss, R.L. *J. Gen. Physiol.* **96**, 1221-1245 (1990).
6. Onodera, S. *Jikeikai Med. J.* **37**, 447-455 (1990).
7. Ishiwata, S., Okamura, N. & Shimizu, H. *J.Muscle Res. Cell Motility* **8**, 275 (1987) (Abstr.).
8. Okamura, N. & Ishiwata, S. *J. Muscle Res. Cell Motility* **9**, 111-119 (1988) (Erratum, *ibid.*, **10**, 93 (1989)).
9. Ishiwata, S., Okamura, N., Shimizu, H., Anazawa, T.. & Yasuda, K. *Adv. Biophys.* **27**, 227-235 (1991).
10. Shimizu, H., Fujita, T. & Ishiwata, S. *Biophys. J.* **61**, 1087-1098 (1992).
11. Anazawa, T., Yasuda, K. & Ishiwata, S. *Biophys. J.* **61**, 1099-1108 (1992).
12. Ishiwata, S. & Funatsu, T. *J. Cell Biol.* **100**, 282-291 (1985).
13. Funatsu, T., Higuchi, H. & Ishiwata, S. *J. Cell Biol.* **110**, 53-62 (1990).
14. Fukuda, N., Fujita, T. & Ishiwata, S. *J. Muscle Res. Cell Motility* 12, **304** (1991) (Abstr.).
15. Fukuda, N., Fujita, T. & Ishiwata, S. (manuscript in preparation).
16. Ebashi, S. & Endo, M. *Prog. Biophys. Mol. Biol.* **18**, 123-183 (1968).
17. Weber, A. & Murray, J.M. *Physiol. Rev.* **53**, 612-673 (1973).
18. Goldman, Y. *Ann. Rev. Physiol.* **49**, 637-654 (1987).
19. Homsher, E. & Millar, N.C. *Ann. Rev. Physiol.* **52**, 875-895 (1990).

Discussion

Godt: Your work with SPOC is quite an enterprise. You can get these tension oscillations in skinned fibers, as shown by Richard Nichols at Emory University, in the absence of ATP, ADP, or P_i. By rapidly stretching slow muscle fibers, he produced an oscillation. It never happens in his hands in the fast fibers. I wonder if you think that is the same sort of situation you are looking at with SPOC.

Ishiwata: I don't know the work of Dr. Nichols, but the situation of oscillation seems to be similar to our SPOC. I would like to stress that under our SPOC condition you get a stable auto-oscillation even in fast muscle fibers. It is certain that the SPOC occurs more easily in slow muscle fibers. In other words, the SPOC region in the state diagram of muscle presented here is probably larger in the slow fibers than in the fast fibers.

Pollack: One of the intriguing features of your result is that the signal appears to be propagated very regularly along the myofibril, in spite of the fact that the force is apparently relatively constant. So, there seems to be some signal transmitted from one half-sarcomere or one sarcomere to the very next one, but not necessarily to ones far away. I wonder if you have some speculations. Do you think the work by Professor Ogata, in which he demonstrates that the structure of water is different in the activated versus the non-activated muscle is relevant? (*A collapse of the water structure during the muscle contraction*, poster, this symposium). I wonder if that is a possibility for signalling from one sarcomere to the very next, or if you have some other ideas.

Ishiwata: I think that is one possibility, but I don't have a definite idea about the molecular mechanism. I may have forgotten to point this out, but the propagation of the SPOC wave from one end to the other of the myofibril (organized SPOC) easily occurs when you apply a stretching force. If you release the muscle, tension develops slowly—probably because of the slow shortening velocity—and the organized SPOC occurs with difficulty. Only local propagation of oscillation occurs. Also, when the width of the myofibril bundle is larger, the organized SPOC occurs easily. This may be important information about the SPOC mechanism; it may suggest that mechanical properties such as tension and stiffness are important factors.

Morales: First, let me say I think you are studying a very clever and interesting system. I have one simple-minded idea that may fit very well, forgetting the calcium, in the simpler case of magnesium ADP. It seems to me that there are general rules stating that in a linear system whenever the thing can be approximated by a linear system, it has no periodic solution. But, when you put in ADP and orthophosphate at the same time, then you introduce a non-linearity that probably gives this non-linear auto-oscillation. That seems to fit very well with the way you are getting at this. I would think that to work out the differential equations for the calcium would be valuable. It might relate to pace-making.

Ishiwata: The non-linearity should exist in such an antooscillation mechanism, but I don't know how it plays a part. The oscillation of calcium concentration is not

coupled with our SPOC; however, a similar differential equation may be worth considering in our SPOC system.

Phase Transitions, 1993, Vol. 45, pp. 105–136
Reprints available directly from the publisher
Photocopying permitted by license only

MECHANO-CHEMICAL COUPLING IN SPONTANEOUS OSCILLATORY CONTRACTION OF MUSCLE

SHIN'ICHI ISHIWATA[1] and KENJI YASUDA[2]

Department of Physics, School of Science and Engineering, Waseda University, 3-4-1 Okubo, Shinjuku-ku, Tokyo 169[1] and Advanced Research Laboratory, Hitachi Ltd., Saitama[2], Japan

(Received 6 December 1992; in final form 24 December, 1992)

Muscle cells take either one of two states, namely contraction (*on-state*) and relaxation (*off-state*), under a particular physiological condition (physiological ionic strength, neutral pH and a few mM MgATP). The transition between these two states is regulated by micromolar concentrations of free Ca^{2+}. Here we review spontaneous oscillation phenomena named *SPOC*. The SPOC state is attained in a contractile system of muscle (muscle model without cell membrane) as a *third intermediate state*. It appears either at an intermediate concentration of free Ca^{2+} (*Ca-SPOC*) or under the coexistence of MgATP with its hydrolytic products, i.e., MgADP and inorganic phosphate (Pi), where Ca^{2+} is not required (*ADP-SPOC*). We have constructed a three-dimensional *phase diagram* showing three regions corresponding to three states of muscle realized under various concentrations of MgADP, Pi and free Ca^{2+} in the presence of MgATP; the SPOC region was sandwiched between contraction and relaxation regions. We tried to understand the *mechano-chemical coupling* in SPOC by explaining the mechanical properties of SPOC based on a standard kinetic scheme of actomyosin ATPase; the experimental results could be well simulated, except for the function of Pi, by assuming that a particular kinetic step regulated by Ca^{2+} is also regulated by the feed-back effect of the actomyosin-ADP complex. It is suggested that the SPOC state is attained by cyclic transition among the different chemical states of the actomyosin complex within each half-sarcomere, which occurs spontaneously through the mechanochemical coupling characteristic to the actomyosin complex, i.e., a *mechano-enzyme*.

KEY WORDS: Spontaneous oscillation of muscle; mechano-chemical coupling; mechano-enzyme; actomyosin ATPase; myofibril; muscle fiber; muscle contraction; regulatory mechanism of muscle contraction.

1 INTRODUCTION

1.1 Structure and function of muscle

Muscle contraction results from relative sliding of myosin (thick) and actin (thin) filaments (*sliding mechanism*, Huxley and Niedergerke, 1954; Huxley and Hanson, 1954). The sliding motion is induced by the hydrolysis of adenosine 5′-triphosphate (ATP) to adenosine 5′-diphosphate (ADP) and inorganic phosphate (Pi) through the interaction between myosin and actin (cf. Cooke, 1986; Hibberd and Trentham, 1986; Goldman, 1987; Goldman and Brenner, 1987; Brenner, 1990; Homsher and Miller, 1990; Geeves, 1991). A part of the chemical energy released accompanying the

hydrolysis of ATP is converted into mechanical work (chemo-mechanical energy transduction). The efficiency of this energy transduction reaches as much as 80% under a certain condition in a certain type of muscle.

Myosin is an enzyme that hydrolyzes ATP (a true substrate for this enzymatic reaction is not ATP but a complex of ATP and Mg^{2+}, i.e., MgATP). The active site for the ATP hydrolysis of myosin is located on a part called the myosin head, so that each moysin molecule has two ATPase sites. The myosin ATPase is activated very much (of an order of 100 times) by the interaction with an actin filament (F-actin); therefore, actin is considered to be an activator for the myosin ATPase. However, it may be possible to consider a complex of actin and myosin, i.e., an actomyosin complex, to be an ATPase having a mechanism qualitatively different from that of myosin alone. In this sense, not only myosin alone but also the actomyosin complex should be called a *mechano(chemical)-enzyme.*

In a muscle fiber, a myosin head bound to an actin filament is called a *cross-bridge*; each cross-bridge is a unit of a molecular machine (or molecular engine) responsible for tension development and sliding motion (Huxley, 1957; Huxley, 1969; Huxley and Simmons, 1971 and 1973).

Striated muscle, such as skeletal and cardiac muscle, has a hierarchic structure (Figure 1; cf. Squire, 1981). The muscle cell surrounded by the cell membrane is composed of a bundle of myofibrils; each myofibril, whose diameter is about 1 μm, is surrounded by an internal membrane system (not shown in Figure 1), a storage of Ca^{2+} (cf. Ebashi, 1991). A myofibril is composed of a series connection of many sarcomeres, whose length is about 2 μm; each sarcomere is made of a crystalline lattice of myofilaments, i.e., a *thick filament* that is composed of a helical polymer of myosin molecules (Huxley, 1963) decorated with several regulatory proteins (cf. Squire, 1981) and a *thin filament* that is composed of a helical polymer of actin molecules (Hanson and Lowy, 1963; Oosawa and Kasai, 1962) decorated with regulatory proteins, i.e., tropomyosin and troponin (Ebashi and Endo, 1968; Ebashi, Endo and Ohtsuki, 1969; Ohtsuki, Maruyama and Ebashi, 1986). It has recently been established that both ends of each thick filament are connected to the Z-line through an elastic gigantic protein called connectin (also named titin) (Wang, 1985; Maruyama, 1986; Funatsu, Higuchi and Ishiwata, 1990; Funatsu, Kono, Higuchi, Kimura, Ishiwata, Yoshioka, Maruyama and Tsukita, 1993). As can be observed in Figure 1, a half-sarcomere is a minimum structural and functional unit in an organized contractile system of striated muscle.

Muscle usually takes two states, i.e., either contraction or relaxation. Under a relaxing state, free Ca^{2+} inside a contractile system of muscle is maintained at much less than 1 μM (Ebashi and Endo, 1968; Weber and Murray, 1973). Although active tension is not generated under this condition, passive tension is gradually developed through lengthening a muscle fiber by stretching it forcibly. The passive tension vs. sarcomere length relation shows a convex curve downward. This passive tension is ascribed to the stretching of a part of the connectin (titin) molecule (cf. Funatsu *et al.*, 1990).

To maintain the muscle length constant under an activating condition (isometric condition), we need to apply an external force (load) equal to the summation of the

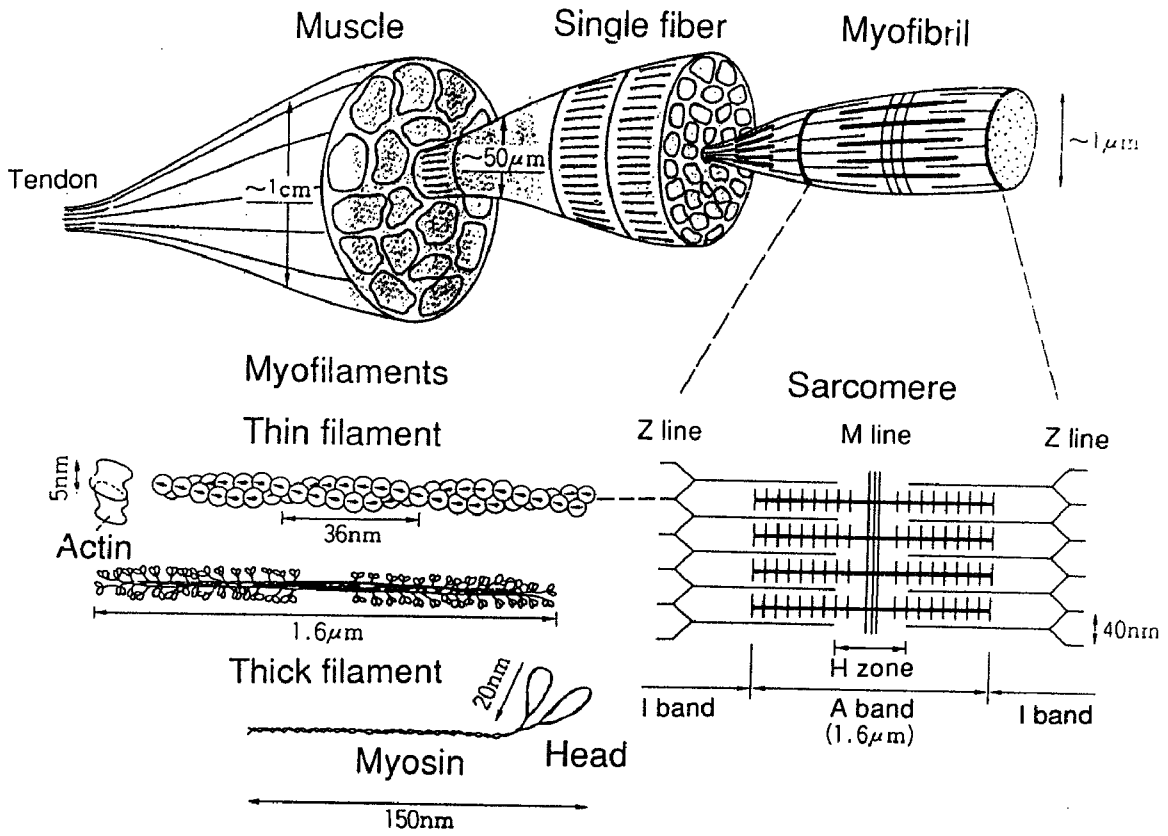

Figure 1 Schematic illustration showing the hierarchic structure of the contractile system of muscle. A skeletal muscle cell is called a single fiber, the diameter of which is about 50 μm and the total length reaches to 10 cm; rabbit muscle is routinely used for our experiments. A single cell of cardiac muscle, on the other hand, is comparatively small, so that we use a bundle of cells whose size is nearly the same as that of a single fiber of skeletal muscle. In both types of muscle the membrane system is removed (skinned) by treatment with 50% (v/v) glycerol and a certain detergent, so that the properties of the contractile system can be examined. In case of skeletal muscle, we manipulated under an optical microscope a single myofibril whose diameter was of an order of 1 μm (Anazawa *et al.*, 1992).

active tension and the passive tension. The active tension generated under an isometric condition is called isometric tension. The isometric tension is nearly proportional to the overlap between thick and thin filaments; this is one item of experimental evidence for the sliding mechanism (Huxley, 1957). When the applied external force is lower than the tension that muscle develops (isotonic condition), the muscle starts to shorten with nearly a constant velocity; in other words, the shortening velocity is determined by the external force. The maximum shortening velocity is attained when an external force is not applied (no-load shortening).

During contraction, the lengths of both thick and thin filaments are maintained nearly constant (Huxley and Niedergerke, 1954; Huxley and Hanson, 1954). It is highly probable, however, that the lengths change by an order of 1% judging from the elasticity of the filaments. As an exceptional case, in a certain type of striated muscles, e.g., crustacean skeletal muscle, shortening of the thick filament is observed accompanying the contraction of muscle (cf. Pollack, 1990).

1.2 Regulatory mechanism

In the contractile system of vertebrate striated muscle, the interaction between myosin and actin is inhibited by the regulatory proteins called tropomyosin and troponin bound to the actin filaments (Ebashi and Endo, 1968; Ohtsuki *et al.*, 1986). When Ca^{2+} ions released from the storage consisting of the internal membrane system are bound to troponin, the state of the actin is changed from an "off-state" to an "on-state"; this proceeds the ATP splitting reaction through the interaction with myosin, resulting in the sliding movement of thick and thin filaments. Conversely, when Ca^{2+} ions are pumped up by the membrane system using chemical energy supplied by ATP splitting, the concentration of free (unbound) Ca^{2+} becomes lower than the dissociation constant of Ca^{2+} with troponin, so that Ca^{2+} is released from troponin; as a result, the enzymatic function of the actomyosin complex is inhibited again and muscle is relaxed.

There are two theories on the molecular mechanism of inhibition in the absence of Ca^{2+}, i.e., one is a steric blocking mechanism in which the myosin binding site on actin is sterically blocked by tropomyosin and troponin (Huxley, 1973); the other is an allosteric mechanism in which the binding of myosin to actin is not blocked but the step of Pi release of actomyosin-ADP-Pi (AMADPPi) complex (Chalovich and Eisenberg, 1982) and/or some step of the isomerization of AMADPPi complexes is inhibited (Millar and Homsher, 1990; Danzig, Goldman, Millar, Lacktis and Homsher, 1992). In the present work, as described below, we analyze our experimental data based on the latter mechanism.

On the other hand, it is well known that at unphysiologically low concentrations of MgATP (pMgATP > 4), an actomyosin complex without bound nucleotides (AM called a rigor complex) functions as a desuppressor for the inhibition (Bremmel and Weber, 1972; Weber and Murray, 1973). It is also known that the addition of MgADP (5 mM) induces tension even at low concentration of Ca^{2+} (Hoar, Mahoney and Kerrick, 1987). In any case, however, the state of thin filaments *in vivo* is considered to be regulated through the association and dissociation of Ca^{2+} with troponin. Such a sequential control mechanism with Ca^{2+} is schematically shown in Figure 2.

In a muscle model prepared by removing the membrane system, the state of the contractile system can be controlled by changing several factors, such as the concentration of MgATP, the ionic strength (I.S.) and pH; these factors are usually maintained nearly constant *in vivo*. This situation is summarized in Figure 3.

1.3 State of the contractile system

The state of the contractile system is attained not at equilibrium but at a steady state, because the chemical energy is continuously supplied from the steady hydrolysis of ATP. If the supply of the chemical energy is stopped by the consumption of ATP (by the death of the body, for example), the muscle is thrown into an equilibrium dead state called a "rigor" state, where strong binding between myosin and actin occurs. Under the rigor state, association and dissociation equilibrium between myosin and actin is attained without mutual sliding of filaments. At very low

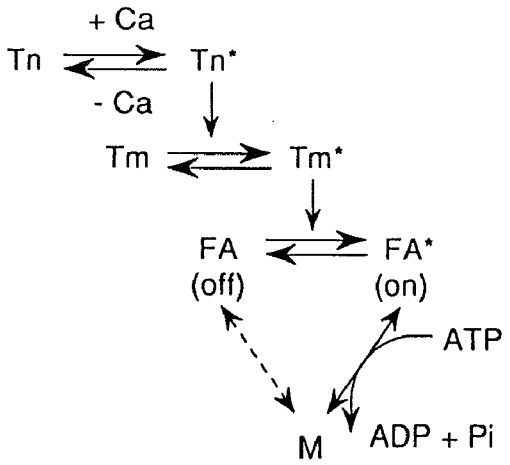

Figure 2 Sequential control of the interaction between actin and myosin (Scheme 1). Specific binding of Ca^{2+} to troponin (Tn) induces the transition of state of troponin from a relaxed form to an active form (with an asterisk). Following this event, the states of tropomyosin (Tm) and actin (FA) are sequentially activated. Finally, the interaction between actin and myosin (M) that proceeds to the hydrolysis of ATP to ADP and Pi becomes possible. When Ca^{2+} is released from troponin, a reverse process occurs and the system is relaxed.

concentrations of MgATP, a certain proportion of cross-bridges are in the rigor state, under which muscle fiber develops rigor tension (Figures 3a and b); Figure 3c is a phase diagram obtained on a pMgATP-pCa plane.

Striated muscle usually takes either one of two states *in vivo*. However, at least in a muscle model, there is a third state of muscle at certain conditions intermediate between contraction and relaxation. For example, in chemically skinned model of a cardiac muscle and a slow type of skeletal muscle, a steady oscillatory state appears when the concentration of free Ca^{2+} is maintained at around or less than 1 μM, just below that required for full tension development.

2 SPONTANEOUS OSCILLATORY CONTRACTION (SPOC)

2.1 Brief history of research on SPOC

In the autumn of 1984, we (Okamura and S.I.) happened to find under a phase-contrast microscope that a myofibril (glycerinated muscle model) prepared from a fast type of rabbit skeletal muscle spontaneously oscillated under a usual relaxing condition consisting of physiological ionic strength with a few mM MgATP without free Ca^{2+} (pCa > 8). Because this oscillation appeared after observation for more than 10 min at room temperature without exchanging the relaxing solution and it tended to appear near a large aggregate of myofibrils, we suspected that hydrolytic products of ATP, i.e., ADP and Pi, may be responsible for this oscillation. This happening triggered a series of our research. After many trials and errors over nearly two months we were able to reach a condition under which the steady oscillation of

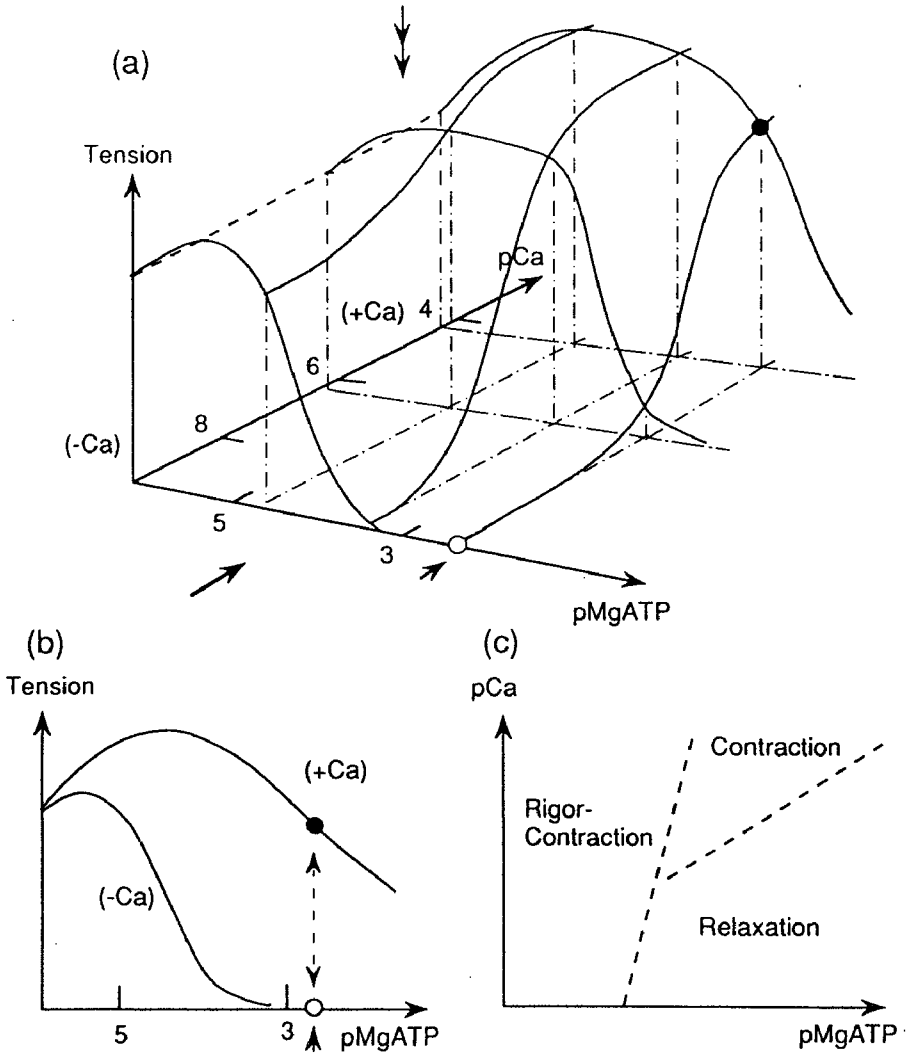

Figure 3 Schematic diagram showing states of muscle. (a), Isometric tension of the contractile system of muscle developed under various concentrations of MgATP (pMgATP = $-\log$[MgATP]) and free Ca^{2+} (pCa = $-\log$[free Ca^{2+}]). Under a physiological condition, pMgATP is maintained nearly constant around the value indicated by a small single arrow. (b), The isometric tension vs. pMgATP relation in the presence (+Ca) and absence (−Ca) of Ca^{2+} (side view of Figure (a), as marked by a large single arrow). The contractile system of muscle takes either a contracting or relaxing state depending on whether the concentration of free Ca^{2+} is higher (closed circle) or lower (open circle) than about 1 μM (pCa = 6.0). (c), Phase (state) diagram of the contractile system of muscle (top view of Figure (a), as marked by a double arrow) on a pCa-pMgATP plane. The state of muscle gradually changes at the boundaries shown by dashed lines. The boundaries shift depending on physical and chemical factors, such as temperature, I.S., pH and so on.

sarcomere lengths occurred reproducibly (Okamura and Ishiwata, 1988). The coexistence of MgADP and Pi was needed to realize the steady oscillatory state as expected, but the concentrations of MgADP and Pi required were unexpectedly much higher than that of MgATP, while Ca^{2+} was not required. We named this phenomenon *SPOC* (*sp*ontaneous *o*scillatory *c*ontraction: Ishiwata, Okamura and Shimizu, 1987; Okamura and Ishiwata, 1988). If a fresh SPOC solution is steadily flowed, the SPOC

continued for more than several tens of minutes. Thus, SPOC is not a transient phenomenon but exists as a thermodynamically stable third state of muscle.

A few years after we finished the initial stage of the experiments, one of the authors (S.I.) was informed that there were meeting reports on the oscillation of myofibrils that had been obtained under a condition similar to ours (Pratt, Mooseker, Kiehart and Stephens, 1986; Mooseker, Pratt, Kiehart and Stephens, 1977). Pratt, Mooseker and their coworkers reported that the spontaneous oscillation of sarcomere lengths was sometimes observed in glycerinated skeletal myofibrils under a relaxing condition, but they could not control the condition. Then, we (S.I. and Shimizu, 1988, unpublished) carefully reexamined their condition and reached a conclusion that they had probably observed the oscillation without a flow of fresh solution, so that the hydrolytic products of ATP would have accumulated. If this conclusion is correct, it turns out that the situation they experienced was exactly the same as we experienced.

In this paper, we would like to review the auto-oscillation phenomena (SPOC) found in the contractile system of muscle from a view point that this is a third state of muscle. The main interest is focused on the mechanism of SPOC realized under the coexistence of MgATP, MgADP and Pi. Our interests are also focused on the regulatory roles (feedback effects) of MgADP and Pi in the mechanism of muscle contraction together with the regulatory role of Ca^{2+} that is a primary regulator of contraction and relaxation *in vivo* (Ebashi and Endo, 1968; Weber and Murray, 1973; cf. Rüegg, 1988).

2.2 Classification of SPOC

Although vertebrate skeletal muscle takes either a contracting state or relaxing state, other types of muscle take an oscillating state. Cardiac muscle, for example, is always oscillating as long as it is alive (cf. Katz, 1977); invertebrate flight muscle takes either a steady oscillatory state or a relaxing state (Pringle, 1967 and 1978).

The oscillatory state has, at least, two types; one is that induced by the oscillation of external factors, such as the concentration of certain chemical substances, e.g., Ca^{2+}. An oscillating cardiac muscle cell belongs to this type. Another is the one that occurs without oscillation of external factors; that is, tension and sarcomere length spontaneously oscillate under a steady environment, so that this type of auto-oscillation is ascribed to the intrinsic properties of the contractile system itself. We define the latter state as "SPOC". It has been pointed out, however, that even when the latter is apparently the case, there is a possibility that the concentration of free Ca^{2+} oscillates if the internal membrane system is not completely destroyed (Brenner, 1979); thus, we have to make sure that the membrane system is removed before we conclude that the oscillation is of the latter type.

The oscillatory state has been extensively studied by using flight muscle (Jewell and Rüegg, 1966; Schadler, Steiger and Rüegg, 1971; Pringle, 1978; Abbott and Cage, 1984). To clarify the mechanism of oscillation on the molecular level, it is indispensable to examine oscillation under the control of various chemical conditions. For this purpose, several kinds of muscle models that are composed solely of the

contractile system without a membrane system have been developed. We usually use a single fiber prepared by treatment with 50% (v/v) glycerol (glycerinated fiber; Szent-Gyorgyi, 1951; cf. Shimizu, Fujita and Ishiwata, 1992) and an appropriate detergent, such as Triton X-100, or occasionally we use a single fiber prepared by mechanically removing the cell membrane (Natori, 1954). Recently we established a microscopic method to manipulate and analyze a single myofibril under an optical microscope (Anazawa, Yasuda and Ishiwata, 1992). Our method is simple compared with the previous ones (Borejdo and Schweitzer, 1977; Fabiato and Fabiato, 1978; Iwazumi, 1987a and b; Bartoo, Tameyasu, Burns and Pollack, 1988; Pollack, 1990). Table 1 summarizes examples of SPOC observed in vertebrate muscle models.

SPOC is classified into two types according to the condition as observed in Table 1: that is, *Ca-SPOC* and *ADP-SPOC*. The conditions reported in two papers of 1956 (Goodall, 1956; Lorand and Moos, 1956) are apparently complicated, so that it is difficult to get an idea about the mechanism of oscillation from the conditions. Other SPOCs are classified into either Ca-SPOC or ADP-SPOC; the SPOC reported by Onodera and Umazume (1984) can probably be classified into ADP-SPOC, because the hydrolytic products of ATP should tend to be accumulated in the fiber due to the high ATPase activity of an actomyosin complex under a high pH region (Onodera, 1990; for another interpretation, see below).

There is a common property for Ca-SPOC and ADP-SPOC: the condition for SPOC is intermediate between those for contraction and relaxation. As described below in detail, ADP is considered to be a regulatory (activating) factor for contraction, similar to Ca^{2+}.

Table 1 Brief history of studies on spontaneous steady oscillation of the contractile system in vertebrate striated muscle.

Year	*Researchers*	*Muscle type**	*Condition***
1956	Goodall	skeletal (f); g.f.	complex (+CP)
1956	Lorand and Moos	skeletal (f); g.f.	complex (+PEP)
1976	Pratt *et al.*	skeletal (f); g.mf.	pCa, 6
1977	Mooseker *et al.*	skeletal (f); g.mf.	pCa, 6
1978	Fabiato and Fabiato	cardiac; g.thin bundle	pCa, 6
1979	Brenner	cardiac; g. bundle	pCa, 6
1981	Iwazumi and Pollack	skeletal(s); mech. skinned	pCa, 6
1981	Stephenson and Williams	skeletal(s); g.f.	pCa, 6
1985	Onodera and Umazume	skeletal (f,s); g.f.	high pH(−Ca)
1988	Okamura and Ishiwata	skeletal (f); g.mf.	MgADP + Pi(−Ca)
1990	Sweitzer and Moss	cardiac; g.bundle	pCa, 6
1992	Shimizu *et al.*	skeletal (f); g.f.	MgADP + Pi(±Ca)
1992	Anazawa *et al.*	skeletal (f); g.mf.	MgADP + Pi(−Ca)
1992	Fukuda *et al.*	cardiac; g. bundle	MgADP + Pi(±Ca)

* Skeletal (f) and (s), fast and slow type of skeletal muscle; g.mf., g.f. and g.bundle, glycerinated myofibril, fiber and bundle.

** Complex, the solvent condition is not simple; +CP, 10 mM creatine phosphate was added; +PEP, 100 mM phosphoenol pyruvate was added. pCa, 6, the solvent condition is normal and the concentration of free Ca^{2+} was about 1 μM just below that required for full tension development. For more details, see text.

2.3 Phenomenological aspects of SPOC

Under the SPOC conditions, the lengths of all sarcomeres oscillate spontaneously. A typical pattern of the SPOC of a single myofibril observed under a phase-contrast microscope is shown in Figure 4 (cf. Okamura and Ishiwata, 1988; Ishiwata, Okamura, Shimizu, Anazawa and Yasuda, 1991). Narrowing and widening of the H-zone and the I-band (cf. Figure 1) are observed corresponding to the shortening and lengthening of the sarcomere; the sliding motion of myofilaments occurs maintaining the filament lengths as constant, at least within the resolution limit of a phase-contrast microscope. The oscillation of each sarcomere length was asymmetrical against time, consisting of a rapid lengthening phase and a slow shortening phase. The unit of oscillation is a half-sarcomere, although "half-" is usually omitted hereafter. The period of oscillation was 1 to 6 s depending on conditions (Ishiwata *et al.*, 1991). The ratio of the lengthening phase and the shortening phase was nearly 1:5–10. The peak-to-peak amplitude of the oscillation of sarcomere length reached as much as 30% of the average sarcomere length, e.g., 0.8 μm for the average sarcomere length of 2.5 μm.

The oscillation of sarcomere length usually propagated along a myofibril; we call such phenomenon a *SPOC wave*. Sometimes, the SPOC wave was not limited locally but propagated from one end to the other of a myofibril; we call such a state of SPOC an *organized SPOC* (Ishiwata *et al.*, 1991). A typical pattern of the organized SPOC is shown in Figure 5 (Anazawa *et al.*, 1992). The organized SPOC easily occurred in a bundle of myofibrils. In a case of a thin bundle of myofibrils or a single myofibril, the SPOC was usually unorganized, that is, the propagation of a SPOC wave was limited to within a group of several sarcomeres and there was no time correlation among the group of sarcomeres; the oscillation of each sarcomere length was, however, regular with time and similar to each other within the same myofibril. There was a tendency for the organized SPOC to be induced by stretching a myofibril (Anazawa *et al.*, 1992). Those observations suggest that mechanical stress is an important factor for the organization of SPOC.

2.4 Physical and chemical factors affecting SPOC

We have examined several physical and chemical factors that seem to affect the properties of SPOC, e.g., temperature, ionic strength and pH. Generally speaking, the factors that tend to induce contraction prolonged the period of oscillation and increased the amplitude of oscillation (cf. Ishiwata *et al.*, 1991); that is, the higher temperature, the lower the ionic strength and the higher the pH value were, the longer the oscillation period and the larger the oscillation amplitude were. It is widely known that Pi is a suppressor for active tension under normal contracting conditions (Rüegg, Schadler, Steiger and Muller, 1971b; Herzig, Peterson, Rüegg and Solaro, 1981; Altringham and Johnston, 1985; Cooke and Pate, 1985; Hibberd, Dantzig, Trentham and Goldman, 1985; Kawai, 1986; Dawson, Smith and Wilkie, 1986; Nosek, Fender and Godt, 1987; Cooke, Franks, Luciani and Pate, 1988; Chase and Kushmerick, 1988; Kawai and Halvorson, 1991); correspondingly, the higher the

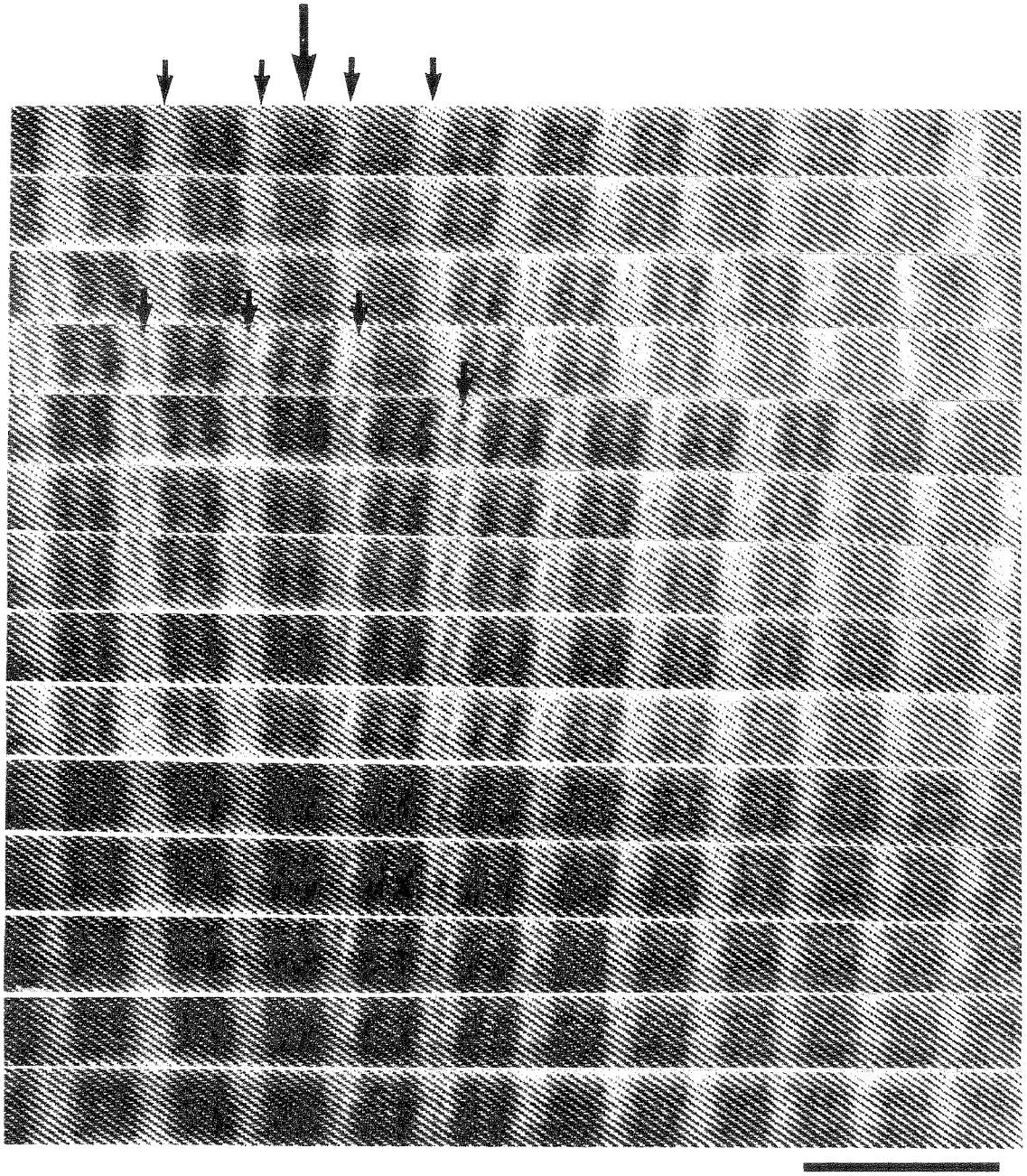

Figure 4 Time course (from top to bottom) of SPOC showing the oscillation of sarcomeres in a myofibril observed under a phase-contrast microscope. Condition (standard SPOC condition): 0.12 M KCl, 0.2 mM ATP, 4 mM ADP, 4 mM $MgCl_2$, 4 mM Pi, 4 mM EGTA, and 10 mM MOPS (pH 7.0) at room temperature. A single myofibril of which both ends were attached to a cover slip by chance was chosen for observation; only the central part of the myofibril floating in the solution is shown. A large arrow indicates a sarcomere whose center is fixed in order to show clearly how the length of each sarcomere oscillates. Small arrows indicate the Z-lines. The time interval between photographs is 2/15 s. The total length of the myofibril was maintained at approximately 60 μm. Horizontal bar, 5 μm. For more details, see Ishiwata *et al.* (1991).

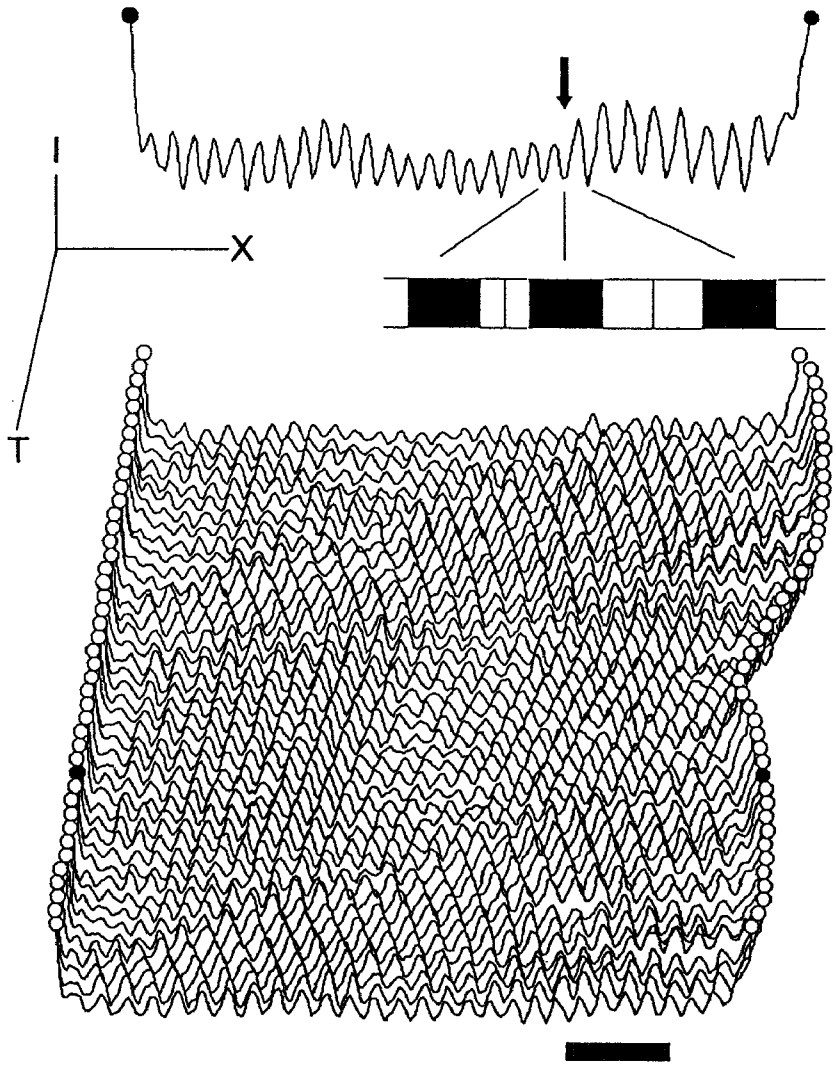

Figure 5 Time course of image profile of a myofibril showing the propagation of a SPOC wave from right to left. The T, X and I axes respectively represent the time course of the SPOC (every 1/5 s), the position along the myofibril and the brightness of the phase-contrast image. Two circles, one on each side, correspond to the edges of the micro-needles to which both ends of the myofibril is attached; the needle at the right-hand side is flexible, so that the developed tension is represented by its movement. Solvent conditions are the same as in Figure 4. Scale bar, 10 μm. For more details, see Anazawa *et al.* (1992), from which this figure was taken.

concentration of Pi, the shorter the period and the smaller the amplitude of SPOC. SPOC disappears and normal contraction occurs when the concentration of free Ca^{2+} is high enough to induce full activation; within the intermediate concentration range of free Ca^{2+}, the higher the concentration of free Ca^{2+}, the longer the period of SPOC and the larger its amplitude.

2.5 Roles of MgADP, Pi and Ca in SPOC

To examine the regulatory roles of MgADP and Pi in tension generation and also to compare them with the function of Ca^{2+}, the active isometric tension of single

glycerinated skeletal muscle fibers was examined under various concentrations of MgADP and Pi in the presence of 1–3 mM MgATP and in the presence or absence of Ca^{2+}. The experimental results are shown in Figures 6 and 7 (Shimizu *et al.*, 1992) and they are schematically summarized in Figure 8 (cf. Ishiwata, Anazawa, Fujita, Fukuda, Shimizu and Yasuda, 1993).

In the presence of Ca^{2+}, the tension increased by 10–20% with the addition of MgADP (cf. Cooke and Pate, 1985; Kawai and Halvorson, 1989) and then decreased with the further addition of MgADP (Figure 6a; Shimizu *et al.*, 1992). On the other

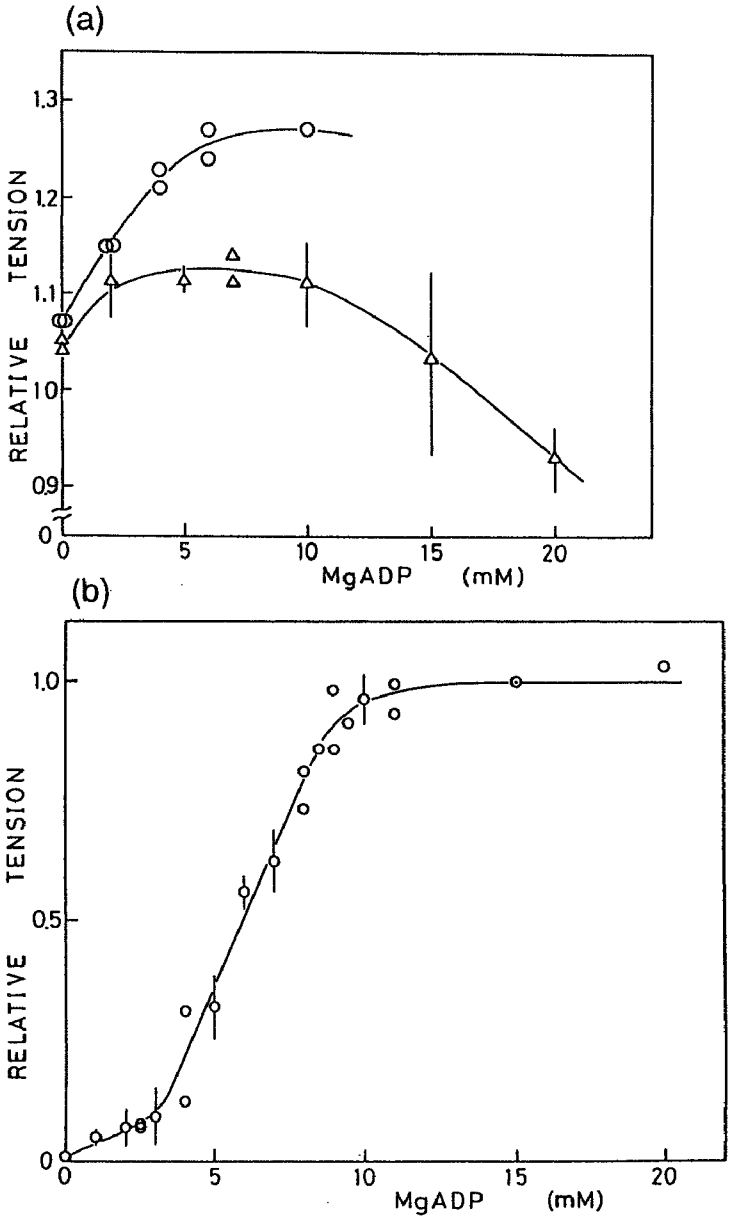

Figure 6 Effect of MgADP on the isometric tension of single fibers in the presence (a) and absence (b) of Ca^{2+}. MgATP, 1 mM (triangles in (a) and circles in (b)) and 2 mM (circles in (a)); for other conditions and more details, see Shimizu *et al.* (1992), from which these figures were taken.

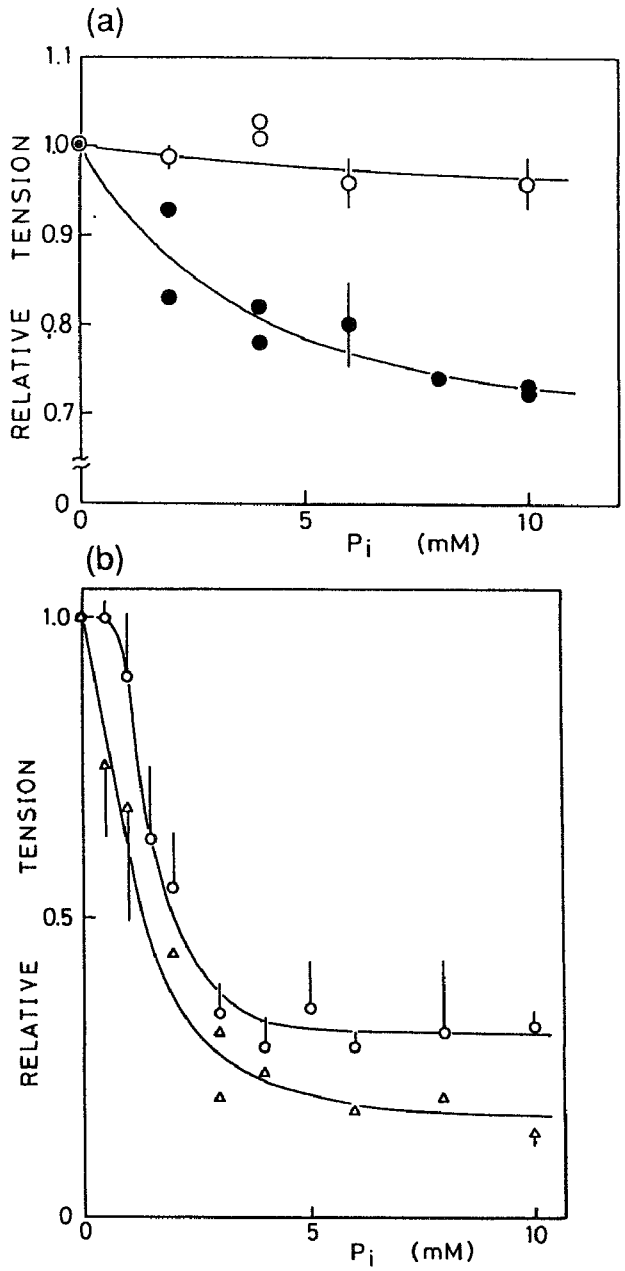

Figure 7 Effect of Pi on the isometric tension of single fibers in the presence (a) and absence (b) of Ca^{2+}. The filled circles in (a) represent the normal contracting condition (−MgADP); open circles in (a) and (b), + 15 mM MgADP; triangles in (b), + 8 mM MgADP. For more details, see Shimizu *et al.* (1992), from which these figures were taken.

hand, in the absence of Ca^{2+}, the fiber that was relaxed without MgADP gradually developed tension along a sigmoidal curve with the addition of MgADP (we call this *ADP-induced tension generation*; ADP-induced tension generation at 5 mM MgADP was reported by Hoar *et al.*, 1987). The ADP-induced tension reached about 80% of the full tension obtained in the presence of Ca^{2+} (Figure 6b). The shortening velocity under the ADP-induced contraction was slow, about one tenth of that under

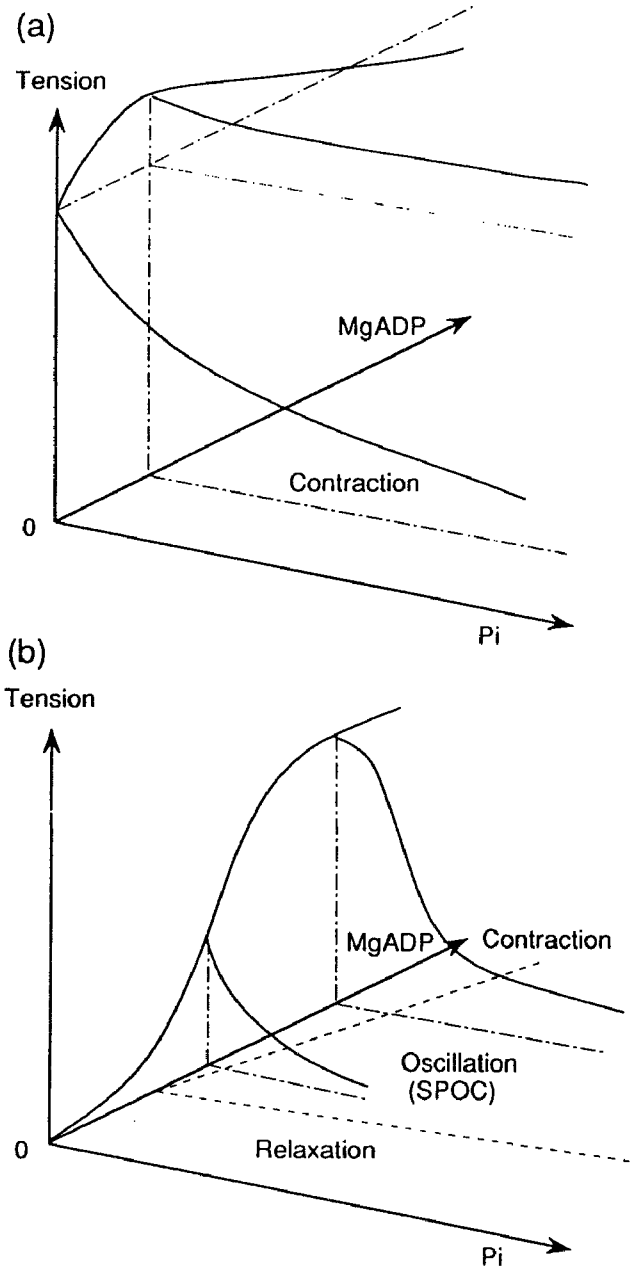

Figure 8 Schematic diagram showing the effects of MgADP, Pi and Ca^{2+} on the isometric tension (a summary of the results of Figures 6 and 7). From this figure we obtained a two-dimensional phase diagram on a MgADP-Pi plane showing the states of muscle, i.e., contraction (without oscillation), SPOC and relaxation under various concentrations of MgADP and Pi in the presence of 1–3 mM MgATP and the presence (a; pCa < 5) or the absence (b; pCa > 8) of Ca^{2+}. The state of muscle was determined by the extent of developed tension and its characteristics (see also Ishiwata *et al.*, 1993).

a normal activating condition. It was confirmed that the ATPase was activated in parallel with the increase in the ADP-induced tension (Shimizu *et al.*, 1992).

The ADP-induced tension decreased with the addition of Pi to a considerable extent, especially in the absence of Ca^{2+} (cf. Figures 6b and 7b). Accompanying the decrease in tension, the spontaneous oscillations of tension and sarcomere length appeared in muscle fibers (Shimizu *et al.*, 1992) and also myofibrils (Anazawa *et al.*,

1992). The results of such studies made it possible to construct a 2-D phase diagram on the MgADP-Pi plane (Figure 8). In the presence of Ca^{2+}, muscle always contracted without oscillation (Figure 8a). In the absence of Ca^{2+}, muscle was relaxed at the origin of the diagram and when the concentration of MgADP became more than a certain value along the MgADP axis the muscle contracted (Figure 8b); we call the concentration of MgADP at which the developed tension is half-maximum the *critical ADP concentration.*

Summarizing the above results, we conclude that MgADP functions as an activator and Pi as an inhibitor regardless of the presence and absence of Ca^{2+}.

2.6 Relation between ADP-SPOC and Ca-SPOC

Next we examined the relation between ADP-SPOC and Ca-SPOC; for this purpose, the effects of Ca^{2+} on the isometric tension of a thin bundle of cardiac muscle were also examined under the coexistence of MgADP and Pi (Fukuda, Fujita and Ishiwata, 1991 and 1992 and in preparation). Summarizing these results, a 3-D phase diagram of muscle was constructed (cf. Ishiwata *et al.*, 1993). In Figure 9, three regions corresponding to contraction, SPOC and relaxation are schematically illustrated against three axes, i.e., the concentrations of MgADP and Pi, and pCa. The ADP-SPOC region on the MgADP-Pi plane and the Ca-SPOC region on the pCa axis were continuously connected by a single SPOC region (data not shown here;

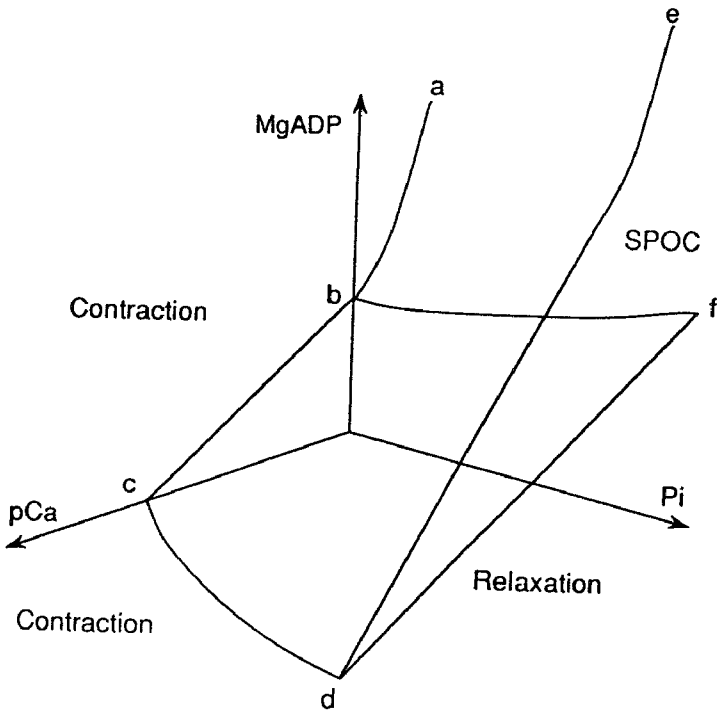

Figure 9 Three-dimensional phase diagram schematically showing the regions of the three states of muscle under various concentrations of MgADP, Pi and free Ca^{2+} (pCa) in the presence of 1–3 mM MgATP. The contraction region is located in this side of the *abcde*-plane, the relaxation region is behind the *bcdf*-plane and the SPOC region is sandwiched between these two planes (see Ishiwata *et al.*, 1993).

cf. Ishiwata *et al.*, 1993; Fukuda *et al.*, in preparation). The SPOC region was sandwiched in between the contraction and relaxation regions, indicating again that the SPOC is an intermediate state between contraction and relaxation. The fact that the two SPOC regions are connected suggests that both types of SPOCs have a common molecular mechanism; we infer that, although the apparent chemical conditions are quite different from each other, the functions of Ca^{2+} and MgADP may be similar in a sense that the populations of the chemical species of the actomyosin complex are similar in ADP-SPOC and Ca-SPOC (see the discussion below).

2.7 *Model calculation of tension generated under SPOC conditions based on the kinetic scheme of actomyosin ATPase*

We tried to understand the characteristics of isometric tension developed under the SPOC condition based on the kinetics and its regulation of an actomyosin ATPase. Here, we adopted the kinetic scheme shown in Figure 10a (cf. Goldman and Brenner, 1987; Goldman, 1987), in which the kinetic constants and equilibrium constants we finally used are consistent with the values experimentally obtained (cf. Inoue, Takenaka, Arata and Tonomura, 1979; Taylor, 1979; Kodama, 1985; Goldman, 1987; Goldman and Brenner, 1987; Homsher and Miller, 1990). We tried to simulate the

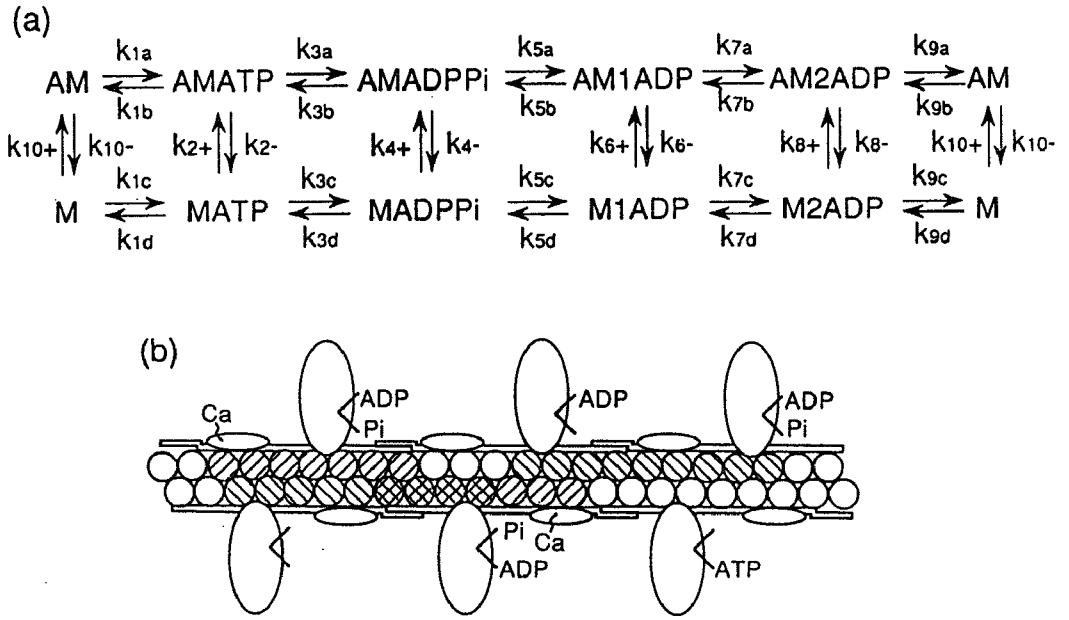

Figure 10 Kinetic scheme of ATPase activity of the actomyosin complex (cf. Goldman and Brenner, 1987; Goldman, 1987) that was used to simulate isometric tension under SPOC conditions (a); k_{5a} is assumed to be regulated by the fraction of turned-on actin ([Aon]), which depends on the concentration of free Ca^{2+} (pCa) and the population of AM2ADP and AM. (b), A schematic illustration showing the state of actin under various conditions. Actin shown by an open circle is in the off-state; that shown by a hatched circle is in an on-state induced either by the binding of Ca^{2+} to troponin or by the association of myosin heads with MgADP or without nucleotides. Here, we assumed that the state of the actin is turned-on cooperatively and myosin heads with MgADPPi do not proceed to release Pi till the actin is turned-on.

tension vs. MgADP curve at various pCa values and the effects of Pi on it (Figures 6, 7 and 8) by assuming that the isometric tension (F) is proportional to the population of the force generating (or sustaining) complex (f.g.c.), such as AM1ADP, AM2ADP and AM (Eq. 1).

$$F = [\text{AM1ADP}] + a \cdot \{[\text{AM2ADP}] + [\text{AM}]\} \tag{1}$$

where a is a constant that determines the ratio of the generated force of AM2ADP and AM to that of AM1ADP. The assumption that the developed tension is proportional to the population of certain species of the actomyosin complex (Eq. 1) is consistent with the current theory of muscle contraction, as far as it is applied to the isometric condition. Under the isotonic condition or SPOC condition, where sliding of myofilaments occurs, we will have to take into account the position dependence of cross-bridge kinetics (Huxley, 1957; Huxley and Simmons, 1971 and 1973; White and Thorson, 1973; Hill, 1974; Pate and Cooke, 1989) and the strain dependence of the regulation of the mechano-enzyme activity (cf. Goldman, 1987; Danzig, Hibberd, Trentham and Goldman, 1991; Danzig *et al.*, 1992).

Here we assumed that the state of thin filaments ([Aon], a population of on-state) is regulated not only by Ca^{2+} but also by the population of f.g.c. independently as follows (Eq. 2):

$$\text{Aon} = C \cdot [\text{Ca}]^l / \{[K_{\text{Ca}}]^l + [\text{Ca}]^l\} + (1 - C) \cdot [\text{f.g.c.}]^m / \{[K_f]^m + [\text{f.g.c.}]^m\} \tag{2}$$

where $[\text{f.g.c.}] = p \cdot [\text{AM1ADP}] + q \cdot [\text{AM2ADP}] + r \cdot [\text{AM}]$ (p, q and r are constants and $p + q + r = 1$), C is a constant ($0 < C < 1$), both l and m are Hill coefficients and both K_{Ca} and K_f are constants. Such a regulatory function of f.g.c. is considered to be similar to that of the rigor (AM) complex previously proposed by Weber and her colleagues (Bremmel and Weber, 1972; Weber and Murray, 1973).

The situation assumed in the above is explained by the diagram given in Figure 10b. The state of actin in a thin filament is cooperatively turned "on" either by the binding of Ca^{2+} to troponin or the formation of f.g.c., especially AM2ADP and AM, independently (see the hatched region on the thin filament).

Moreover, the kinetic step between AMADPPi and AM1ADP was assumed to be regulated by the state of the thin filaments, so that k_{5a} depends on [Aon] as follows:

$$k_{5a} = C_1 + C_2 \cdot [\text{Aon}]^n / \{[K_{\text{on}}]^n + [\text{Aon}]^n\} \tag{3}$$

where C_1, C_2 and K_{on} are constants and n is a Hill coefficient.

We calculated the isometric tension (F) based on the above kinetic scheme under a stationary condition, i.e., $d[*]/dt = 0$, where $(*)$ represents each species in the kinetic scheme. As for AM1ADP, for example,

$$\begin{aligned} d[\text{AM1ADP}]/dt = &-(k_{5b} \cdot [\text{P}_5] + k_{6-} + k_{7a}) \cdot [\text{AM1ADP}] + k_{5a} \cdot [\text{AMADPPi}] \\ &+ k_{6+} \cdot [\text{A}] \cdot [\text{M1ADP}] + k_{7b} \cdot [\text{AM2ADP}] = 0 \end{aligned} \tag{4}$$

where [A] was taken to be the concentration of actin that did not form a complex with a myosin head. The total concentrations of actin, $[\text{A}_0]$, and myosin heads, $[\text{M}_0]$,

were assumed to be 900 and 300 μM, respectively. Here,

$$[A_0] = [A] + [AM] + [AMATP] + [AMADPPi] + [AM1ADP] + [AM2ADP]$$

and

$$[M_0] = [M] + [AM] + [AMATP] + [AMADPPi] + [AM1ADP] + [AM2ADP] + [MATP] + [MADPPi] + [M1ADP] + [M2ADP].$$

The above molar concentrations correspond to those in the A-band in a sarcomere (cf. Figure 1). It should be noted that in the calculation of Eq. 4, we assumed a law of mass action. The law of mass action, however, may not strictly be realized in an organized structure, so that the above molar concentrations should be considered apparent ones.

For this computer simulation, we first adopted the kinetic constants reported in the literatures (cf. Goldman, 1987; Homsher and Miller, 1990). After many trial and errors we selected a set of kinetic constants by means of which F fitted to our experimental data (Shimizu *et al.*, 1992; Fukuda *et al.*, 1991, 1992 and a manuscript in preparation). The kinetic constants and other constants in the above equations that we finally used are listed in Table 2. Those kinetic constants coincided very well with those obtained in the *in vitro* experiments in spite of the fact that the law of mass action was applied to such an ordered system as a myofilament lattice.

2.8 *Application of our model calculation to SPOC*

The tension vs. pCa relations obtained by the above computer calculation are shown in Figure 11; here, larger values of the Hill coefficients, l and m, were chosen for skeletal than for cardiac muscles because of the higher cooperativity in skeletal muscle. Next, the results on the effects of MgADP at various pCa values are shown in Figure 12. The essential features of the experimental data could be simulated (cf. Figures 6 and 8): First, the critical concentration of MgADP for the ADP-activation

Table 2 Kinetic constants in the kinetic scheme of actomyosin ATPase (cf. Figure 10a) and the values of parameters used for the computer simulation (cf. Eqs. 1–3).

$k_{10+} = 1 \times E+5/M/s$	$k_{4+} = 1 \times E+5/M/s$	$k_{8+} = 1 \times E+5/M/s$
$k_{10-} = 1 \times E-3/s$	$k_{4-} = 1 \times E+1/s$	$k_{8-} = 1 \times E-1/s$
$k_{1a} = 2 \times E+6/M/s$	$k_{5a} = 0.1 - 30/s$	$k_{9a} = 9(5) \times E+2/s$
$k_{1b} = 1 \times E+1$	$k_{5b} = 1.5 \times E+3/M/s$	$k_{9b} = 1 \times E+7/M/s$
$k_{1c} = 2 \times E+9/M/s$	$k_{5c} = 5 \times E-2/s$	$k_{9c} = 4/s$
$k_{1d} = 1 \times E+1/s$	$k_{5d} = 5 \times E-1/M/s$	$k_{9d} = 4(8) \times E + 6/M/s$
$k_{2+} = 1 \times E+7/M/s$	$k_{6+} = 1 \times E+5/M/s$	
$k_{2-} = 1 \times E+3/s$	$k_{6-} = 1 \times E-1/s$	$[Actin]_0 = 9 \times E - 4(M)$
$k_{3a} = 1 \times E+1/s$	$k_{7a} = 3/s$	$[Myosin]_0 = 3 \times E-4(M)$
$k_{3b} = 3 \times E+1/s$	$k_{7b} = 3 \times E-1/s$	
$k_{3c} = 1.5 \times E+2/s$	$k_{7c} = 3 \times E-1/s$	
$k_{3d} = 1.5 \times E+1/s$	$k_{7d} = 3 \times E-2/s$	

Other parameters: $a = 0.15$; $C = 0.2$; $C_1 = 0.1$; $C_2 = 30$; $l = 3(1)$; $K_{Ca} = 1 \times E - 6(M)$; $m = 2(1)$; $K_f = 0.2$; $n = 5$; $K_{on} = 0.2$; $p = 0$; $q = r = 1$. All numbers are for skeletal muscle except those in parentheses for cardiac muscle.

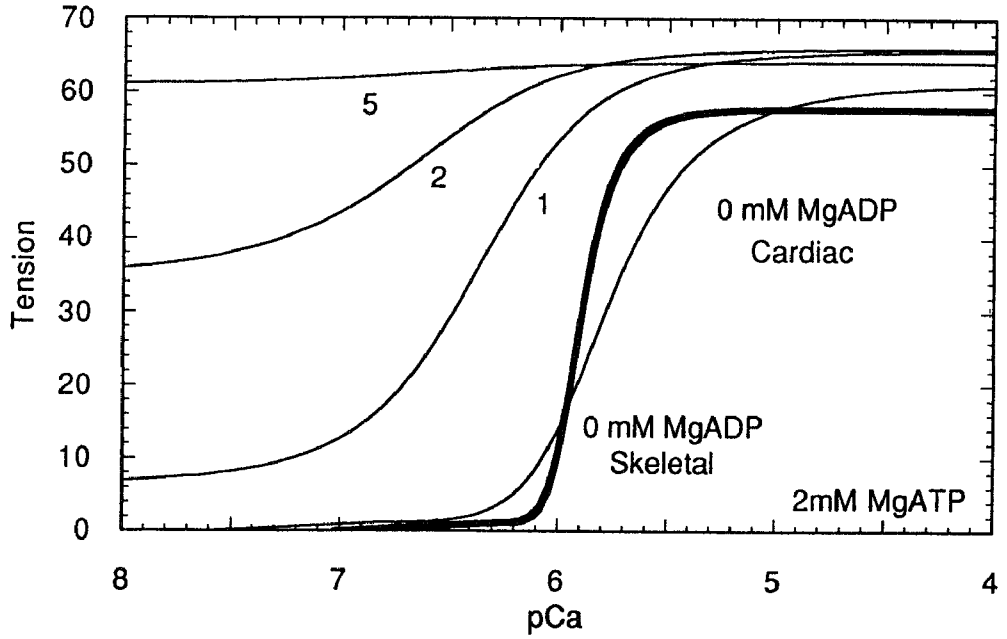

Figure 11 Computer simulation of isometric tension vs. pCa under various concentrations of MgADP. These were obtained according to the model described in Figure 10 and Table 2. Thick line, skeletal muscle without addition of MgADP; thin lines, cardiac muscle without MgADP or with 1, 2 or 5 mM MgADP.

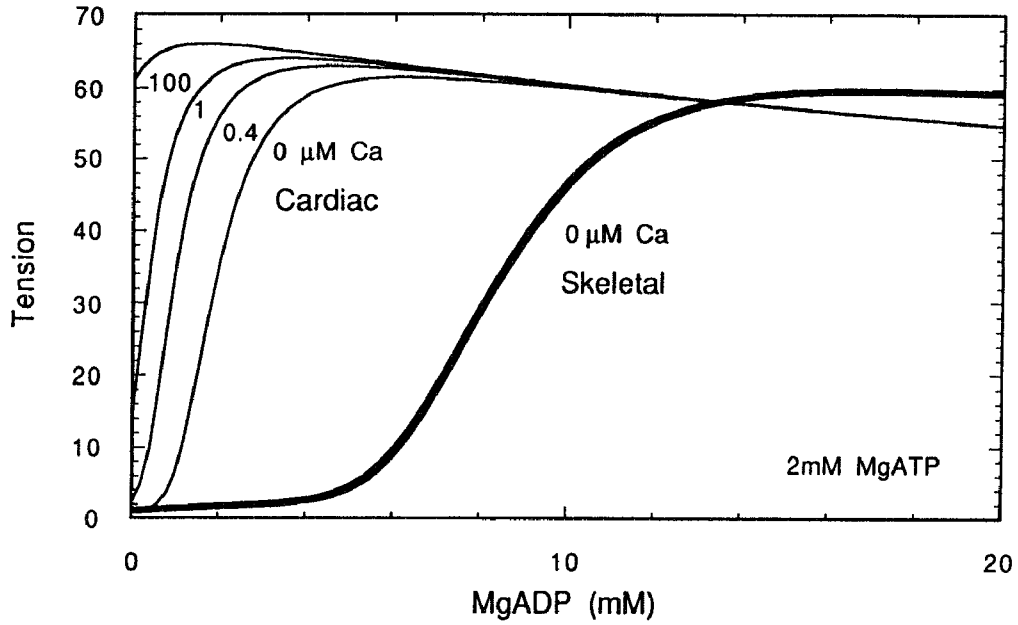

Figure 12 Computer simulation of isometric tension vs. MgADP concentration under various concentrations of Ca^{2+}. These were obtained according to the model described in Figure 10 and Table 2. Thick line, skeletal muscle without Ca^{2+}; thin lines, cardiac muscle without Ca^{2+} or with 0.4, 1 or 100 μM Ca^{2+}.

decreased accompanying the decrease in pCa value (experimental data, not shown; cf. Fukuda *et al.*, in preparation); this feature could be realized by assuming that both Ca^{2+} and the f.g.c. affect the same kinetic step independently, as in Eq. 2, and by making the Hill coefficient n in Eq. 3 larger than l and m in Eq. 2. Second, in the presence of Ca^{2+}, the tension once increased slightly decreased with the addition of MgADP; this feature was realized by assuming that the contribution of AM2ADP to F was lower than that of AM1ADP, i.e., $a = 0.15$.

Such a good coincidence between the computer simulation and the experimental results seems to be evidence for the assumption that the f.g.c. allosterically and cooperatively accelerates the release of Pi from AMADPPi by a positive feed-back reaction. However, before concluding this we will have to examine the possibility that the experimental results are similarly simulated by assuming that the f.g.c. accelerates the binding steps, for example, between A and MADPPi (for a theoretical treatment based on this idea, see Deshcherevsky, 1977).

The contribution of AM1ADP to [Aon] was determined to be negligibly low compared with those of AM2ADP and AM, i.e., $p = 0$ and $q = r = 1$; this means that although AM1ADP largely contributes to the tension generation, AM1ADP is a weak desuppressor for the regulatory proteins, while AM2ADP and AM do not contribute to the tension so much, but they are strong desuppressors and largely contribute to the cooperativity of the tension generation.

The effects of Pi on tension generation (Figure 7) could not be simulated adequately by the above simple scheme, especially in the absence of Ca^{2+}. As shown in Figure 13, the developed tension monotonously decreased with the addition of Pi irrespective of conditions, so that the reversed sigmoidal curve observed in the ADP-activated

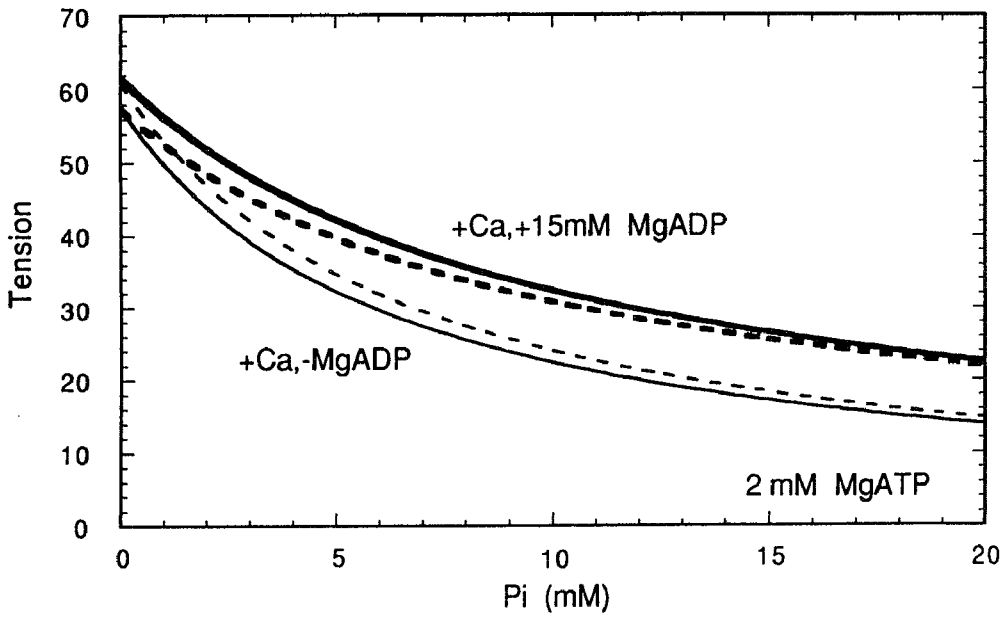

Figure 13 Computer simulation of isometric tension vs. Pi concentration in the presence of Ca^{2+}. These were obtained according to the model described in Figure 10 and Table 2. Thick and thin lines, skeletal muscle with and without MgADP, respectively; thick and thin dashed lines, cardiac muscle with and without MgADP, respectively.

tension in the absence of Ca^{2+} could not be simulated (data not shown, because they are quite similar to those in the presence of Ca^{2+} with MgADP). In addition, the extent of decrease of tension did not largely depend on the conditions, which was not consistent with the experimental results (cf. Figure 7). We infer that Pi also functions as a regulator of tension development. A possibility that Pi bound not only to myosin heads but also to actin filaments functions as a regulator is to be examined in future.

Recent experimental studies have suggested that the AMADPPi complex is composed of at least three distinct isomers as follows (Miller and Homsher, 1990; Dantzig *et al.*, 1992):

$$\cap \text{AMADPPi(1)} \cap \text{AMADPPi(2)} \cap \text{AMADPPi(3)} \cap$$

where the kinetic step between (1) and (2) is regulated by Ca^{2+} and the species (3) contributes to tension development, while the others do not. It seems to us that even if this new scheme is included in the above scheme (Figure 10a), it will not be able to explain the effects of Pi under the SPOC conditions.

Finally, we constructed a tension-MgATP curve by using the same parameters as obtained above. Figure 14 shows that the above model can simulate the essential features of tension generated under various concentrations of MgATP (cf. Cooke and Bialek, 1979); especially in the absence of Ca^{2+}, the tension that is not generated under a physiological concentration of MgATP (a few mM) sharply increased with the decrease of MgATP concentration and showed a peak at around 10 μM and then further decreased. Such a trend of tension generation in the absence of Ca^{2+} has been explained by the mechanism that a myosin head without bound nucleotides binds tightly to a thin filament, forming a rigor complex (AM) (cf. Figure 16b), and

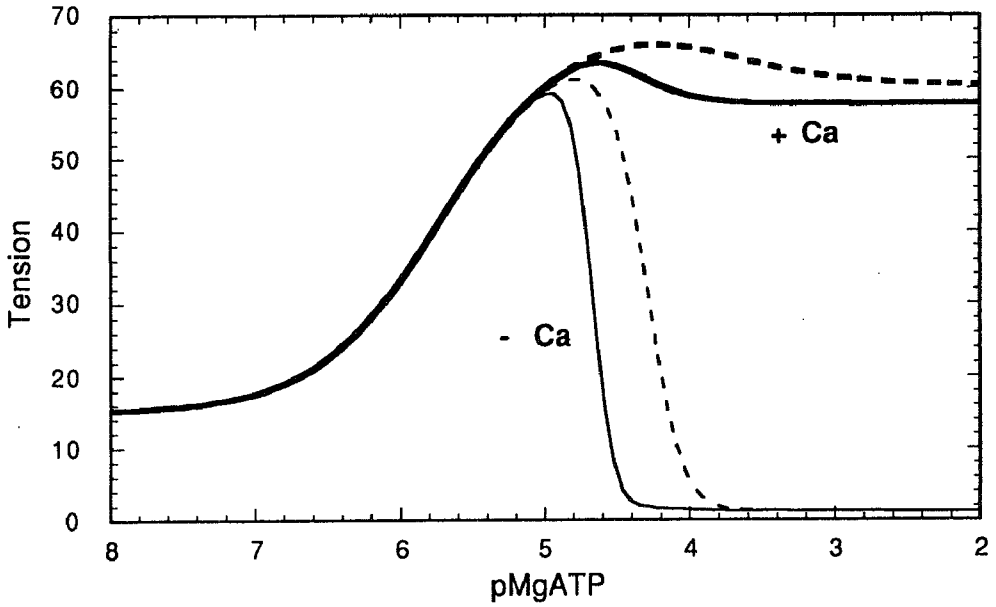

Figure 14 Computer simulation of isometric tension vs. MgATP concentration in the presence (thick lines) and absence (thin lines) of Ca^{2+}. These were obtained according to the model described in Figure 10 and Table 2. Solid lines, skeletal muscle; dashed lines, cardiac muscle.

allosterically desuppresses the inhibitory state of a thin filament (Bremmel and Weber, 1972; Weber and Murray, 1973). In this sense, the function of the rigor complex is the same as that of AM2ADP as assumed in the present work.

The tension-MgATP curves slightly shifted to the right-hand side in case of cardiac muscle (this must be examined experimentally). This is ascribed to the fact that cardiac muscle was assumed to have lower cooperativity ($m = 1$) so that [Aon] and k_{5a} decreased slowly with an increasing concentration of MgATP, but not to the fact that the association constant of MgADP to AM was chosen to be 1.8 times higher than that of skeletal muscle (for this difference of 1.8 times, see Siemankowski; Wiseman and White, 1985).

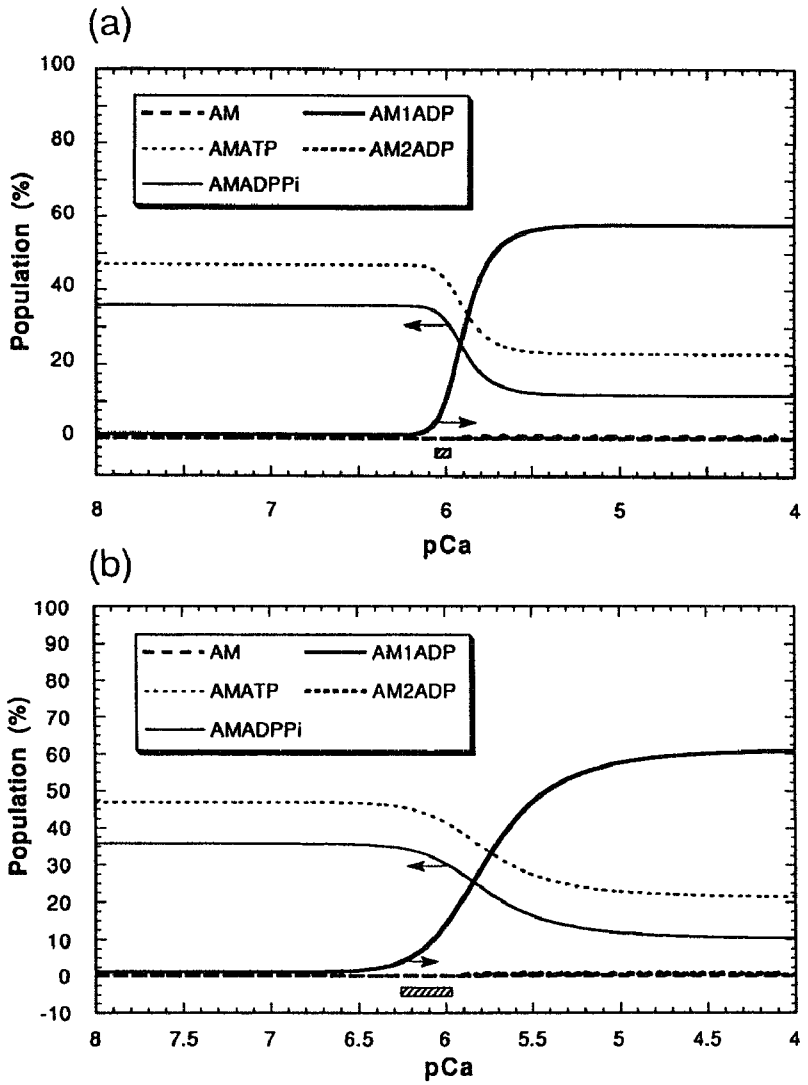

Figure 15 Populations of chemical species of the actomyosin complex under various concentrations of free Ca^{2+}. These curves correspond to the computer simulation of Figure 11 obtained for skeletal (a) and cardiac (b) muscle in the absence of MgADP. We propose that a stable SPOC state appears only when the populations of particular chemical species of cross-bridges, i.e., AMADPPi (AMATP) and AM1ADP, are beyond certain threshold values, as indicated by arrows. The SPOC region that fulfills this requirement is indicated by a hatched bar.

The ATPase activity (v) can be estimated according to the equation $v = k_{5a} \cdot [\text{AMADPPi}] + k_{5c} \cdot [\text{MADPPi}]$ in the absence of Pi, and, in the presence of Pi, v includes $-k_{5b} \cdot [\text{AM1ADP}] \cdot [\text{Pi}] - k_{5d} \cdot [\text{M1ADP}] \cdot [\text{Pi}]$. As inferred from Figures 15 and 16, v vs. pCa and v vs. MgATP curves nearly overlapped with the tension vs. pCa and the tension vs. MgATP curves respectively. In practice, however, the change in v is gradual, whereas the change in tension is very sharp. This discrepancy between the simulation and the experimental data may be overcome by assuming that the regulatory step is taken at an isomerization step(s) as mentioned above instead of the step of k_{5a} and/or by assuming that the binding step(s) is also regulated by f.g.s.

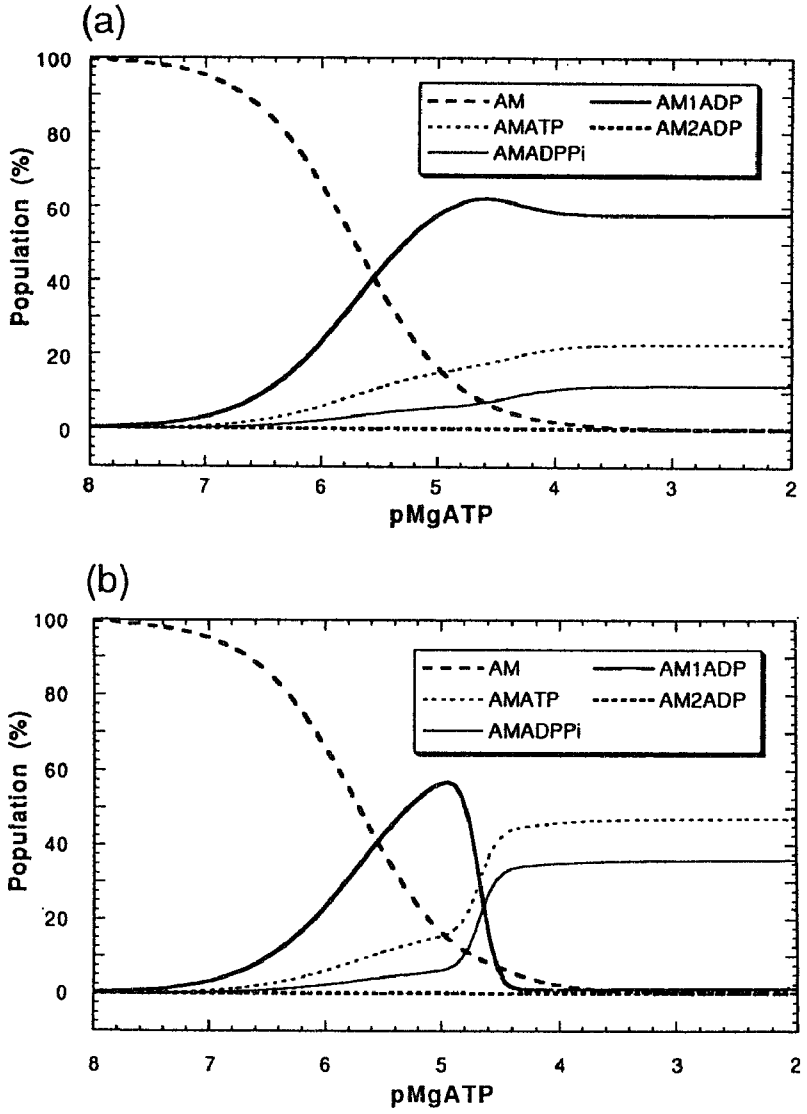

Figure 16 Populations of chemical species of the actomyosin complex under various concentrations of MgATP. These curves correspond to the computer simulation of Figure 14 obtained for skeletal muscle in the presence (a) and absence (b) of Ca^{2+}.

2.9 Minimum requirements for SPOC

The populations of chemical species of the actomyosin complex under various states of muscle could be obtained by the above computer simulation (cf. Figures 11–14). Accompanying the transition of state from relaxation to contraction, the populations of AMADPPi and AMATP reverse-sigmoidally decreased, whereas the population of AM1ADP sigmoidally increased (Figures 15 and 16). The population of these species under the SPOC conditions, either Ca-SPOC or ADP-SPOC, seems to be intermediate between those under contraction and relaxation.

First, the essential requirement for SPOC to occur seems to be that AMADPPi (and AMATP) should exist over a certain threshold population, much larger than that attained under normal contraction condition. Second, some (active) tension should be developed at the same time, although this condition is contrary to the first requirement; a certain population of AM1ADP will be required for this tension development. We would like to suggest that the populations of AMADPPi (probably also AMATP) and AM1ADP should be over than, say, 30% and 5% respectively (Figure 15) as a minimum requirement for SPOC (cf. Ishiwata *et al.*, 1993).

The above hypothesis can explain why Ca-SPOC is observed in cardiac muscle but not or only with difficulty in skeletal muscle, because in cardiac muscle this minimum requirement seems to be easily realized because of the low cooperativity (cf. Figure 15). We infer that the requirement may be fulfilled by the addition of Pi to the ADP-activated muscle, so a stable SPOC state appears even in skeletal muscle (Ishiwata *et al.*, 1993).

2.10 Mechano-chemical coupling and molecular mechanism of SPOC

There are several theoretical works to explain the auto-oscillation of contractile system of muscle (Akamatsu, Hannaford and Stark, 1986; Murase, Tanaka, Nishiyama and Shimizu, 1986; Sicilia and Smith, 1991; Smith 1991). However, it seems that there are no theories specifically applicable to SPOC, especially to organized SPOC.

Incidentally, more than ten years ago, using a newly devised flow system, Yano, Shimizu and their colleagues demonstrated that ATPase activity depends on the direction of flow of the medium applied to the motile system (Yano, Yamada and Shimizu, 1978; Yano and Shimizu, 1978; Shimizu, 1979). They proposed a theory explaining the mechano-chemical phenomenon: they ascribed the cooperativity (non-linearity) of the phenomenon to the cooperative increase in the enzymatic activity through hydrodynamic effect. Although such a mechanism may be operating in SPOC, at least in the present work we will only suggest that the cooperative properties of cross-bridges may be realized through the cooperativity of the structural change and distortion of actin molecules on each thin filament. This situation is qualitatively illustrated in Figure 17.

During SPOC, each sarcomere in a myofibril repeats slow shortening and quick stretching. As pointed out previously (Shimizu *et al.*, 1992), the active tension (F) developed by sarcomeres will be almost equal to each other along a myofibril regardless of whether a sarcomere is shortening or stretching, because the propaga-

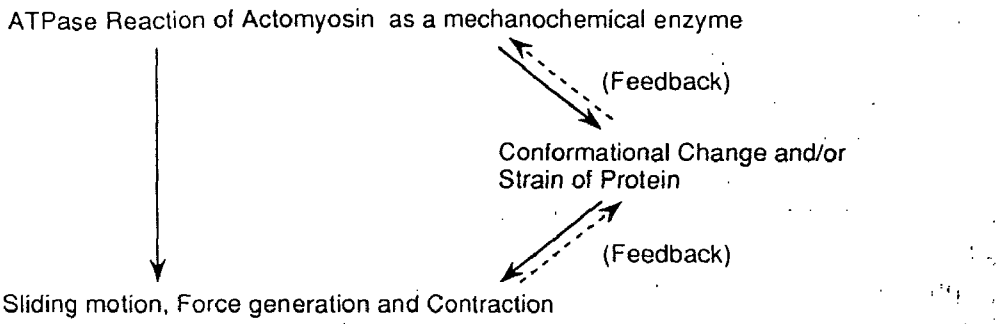

Figure 17 Mechano-chemical coupling in the contractile system as observed in SPOC phenomena. The actomyosin complex functions as a mechano-enzyme, which transduces chemical energy supplied from the hydrolysis of ATP to the mechanical work that is required for sliding movement and contraction with tension development. This chemo-mechanical energy transduction may occur through a conformational change of contractile proteins or directly without a conformational change, as shown by solid arrows. Conversely, irrespective of the molecular mechanism of tension development, strain will be induced on the contractile proteins by the developed tension, as shown by a dashed arrow. The enzymatic activity may be modified by this strain. We expect that such a mechano-chemical feedback effect is indispensable for SPOC.

tion velocity of a mechanical impulse along a myofibril must be very fast (Schoenberg, Wells and Podolsky, 1974). Here, the population of chemical species of cross-bridges in the above kinetic scheme may change for each sarcomere depending on the shortening and stretching, because the mechanical properties of each species will be different from each other. In summary, we infer that the tension represented by $F = [\mathrm{AM1ADP}] + a \cdot \{[\mathrm{AM2ADP}] + [\mathrm{AM}]\}$ is maintained as nearly constant during SPOC, but the populations of AMATP, AMADPPi, AM1ADP, AM2ADP and so on may change.

Moreover, we infer that a cycling among different populations of chemical states of cross-bridges occurs in an auto-catalytic manner through feedback from a distortion of cross-bridges to a chemical reaction, as summarized in Figure 17. Such a regulation occurs for each set of cross-bridges interacting with each thin filament.

To be more specific and concrete, we infer the following scheme as the mechanism of SPOC: First, just after the solvent condition is changed from relaxation to SPOC, every sarcomere starts to generate tension and contract slowly; second, when maximum tension is reached, an inhomogeneity of sarcomere lengths appears. Such an inhomogeneity of sarcomere lengths within a myofibril during tension development is experimentally confirmed even under normal contraction condition (Fujime, 1975; Umazume and Yoshioka, 1979; Horowits and Podolsky, 1987) and has also been theoretically examined (Jackson and Oplatka, 1974). However, it should be noted that the elasticity of a parallel elastic component such as connectin (titin) is not involved in the mechanism of SPOC, because the selective removal of connectin by mild tryptic digestion did not at all affect the properties of SPOC. It is thus safe to assume that the mechanism of SPOC is solely attributable to cross-bridges dynamics.

Among all sarcomeres in a myofibril, the tension of the shortest/longest sarcomere is sustained by the largest/smallest number of cross-bridges, so the average tension for each cross-bridge to bear is the smallest/largest and accordingly the distortion of

cross-bridges must be the smallest/largest. Here, we assume that the larger the distortion of AMADPPi cross-bridge is, the more the AMADPPi cross-bridge tends to dissociate Pi (this property has been reported; cf. Goldman, 1987; Danzig *et al.*, 1992), that is, the kinetic constant, k_{5a}, becomes larger; conversely, the smaller the distortion, the more k_{5a} becomes smaller. This means that the equilibrium of the actomyosin ATPase reaction shifts to the side of AMADPPi, i.e., a non-force-generating species, in shortening sarcomeres, while in stretched sarcomeres the population of chemical species of cross-bridges shifts to the side of AM1ADP, i.e., a force-generating species. We propose that this is the reason why shortening sarcomeres start to yield in spite of the fact that the overlap is large, while stretched sarcomeres start to shorten again inspite of the fact that the overlap between thick and thin filaments is small.

Under a steady state, the above properties that seem to be contradictory to the current theory of sliding mechanism will not appear under a full activation or a relaxation condition, but then appear under an intermediate condition for activation. In practice it is well known that the above property, that the isometric tension increases with increasing sarcomere length, appears at around or less than μM Ca^{2+} (Endo, 1972 and 1973; Fabiato and Fabiato, 1978; Iwazumi and Pollack, 1981; Stephenson and Wendt, 1984). Also, the above characteristics may be responsible for such transient properties as stretch activation (cf. Armstrong, Huxley and Julian, 1966; Rüegg, Steiger and Schadler, 1971; Sugi, 1971; Steiger, 1971 and 1977) and release relaxation (Edman, 1980; Ekelund and Edman, 1982).

In the yielded sarcomere, all cross-bridges must be dissociated in a moment; at that moment, the populations of MATP and MADPPi must be large, because just before the dissociation the populations of AMATP and AMADPPi are large (see the populations under the SPOC condition in Figure 15b). MATP is quickly transformed into MADPPi at a rate of 150/s, but the rate that Pi is released from MADPPi is quite slow (see Figure 10 and Table 2), so that MADPPi is accumulated; thus, AMADPPi will immediately become dominant. During stretching phase, instantaneous binding of MADPPi (and partly of M1ADP and M2ADP) to actin would occur; this probably becomes a drag viscous force (cf. Tawada and Sekimoto, 1991) that balances the load imposed on each sarcomere. This situation is just suitable for the mechanism (the distortion-dependent release of Pi from AMADPPi cross-bridges) suggested to occur above; that is, during the stretching phase the population of AMADPPi increases.

The thin filaments from which cross-bridges are dissociated may be still "on" during the stretching phase. Even if the thin filaments are turned-off, MADPPi, M1ADP and M2ADP will quickly bind to the thin filaments, if the binding steps hardly depend on the state of thin filaments. Because the number of cross-bridges thus formed (mainly AMADPPi) becomes smaller with stretching, the distortion of the AMADPPi cross-bridges should become larger so that the kinetic constant, k_{5a}, should become larger in a non-linear fashion; thus, the chemical reaction proceeds forward and stretching stops and shortening restarts. In such a way, slow shortening and quick stretching are repeated for each sarcomere.

We assumed that the distortion of cross-bridges is a key factor for the auto-regulation mechanism. However, there is also a possibility that the distortion (strain) of thin filaments is responsible for the regulation, judging from the fact that the flexibility of the thin filaments is regulated not only by the concentration of Ca^{2+} (Ishiwata and Fujime, 1971 and 1972) but also by the number of attached cross-bridges both in the absence of MgATP (Fujime and Ishiwata, 1971) and in the presence of MgATP (Oosawa, Fujime, Ishiwata and Mihashi, 1973). In a longer sarcomere, the width of the I-band (cf. Figure 1) is broader compared with the others, so that the length of exposed thin filaments is larger and accordingly this part of the thin filaments will be elongated. If the state of thin filaments shifts to the on-state by the elongation, and *vice versa*, such properties as stretch activation and release deactivation will be explained. Such an idea and some experimental evidence for it has already been presented (cf. Endo, 1972 and 1973; Edman, 1980; Ekelund and Edman, 1982; Gordon, Ridgway and Martyn, 1984; Fuchs and Wang, 1991).

We have recently found that an actin filament slides with a right-handed rotation in an *in vitro* motile system so that the sliding force contains a right-handed torque component (Nishizaka, Yagi, Tanaka and Ishiwata, 1993; Tanaka, Ishijima and Ishiwata, 1992). This means that the thin filament in a sarcomere is twisted during tension development. Therefore, we would like to point out that the twist of thin filaments may play a part not only in the sliding mechanism (cf. Schutt and Lindberg, 1992) but also in the strain-dependent regulation of thin filaments described above.

Thus, the next step for this line of study on SPOC is to confirm the above hypotheses either theoretically (by computer simulation) or experimentally. In experimental work, we have a plan to monitor the states of cross-bridges and thin filaments through labeled fluorescent dyes under a fluorescence microscope (cf. Ishiwata, Kinosita, Yoshimura and Ikegami, 1987; Kinosita, Itoh, Ishiwata, Hirano, Nishizaka and Hayakawa, 1991) equipped with a micromanipulator (cf. Anazawa *et al.*, 1992) and to demonstrate that they change in a cyclic manner for each sarcomere as inferred above.

3 SUMMARY

We first summarized the phenomenological aspects of the SPOC of muscle fibers and myofibrils and described how the state of contractile system of muscle is regulated. Then we tried to analyze the condition of SPOC based on the kinetic scheme of actomyosin ATPase and clarify the relationship between the mechanical properties and the chemical reaction of ATPase under the SPOC conditions. Finally, we suggested that a mechano-chemical coupling on the level of cross-bridges and thin filaments is involved in the mechanism of auto-oscillation; that is, not only chemical to mechanical energy transduction but also feedback from mechanical event to chemical reaction through allosteric and cooperative manner are important for the mechano-enzyme system to realize a steady and spontaneous oscillatory state.

Acknowledgements

The authors thank Mr. Nobuyuki Okamura (Bridgestone Corp.), Mr. Hideharu Shimizu (Central Research Lab., Denki Kagaku Kogyo K. K.), Mr. Takashi Anazawa (Central Research Lab., Hitachi Ltd.), Mr. Norio Fukuda (Research Center, Sankyo K. K.) and Mr. Takashi Fujita (Waseda Univ.) for their cooperation and Dr. Paul D. Black (Waseda Univ.) for reading of the manuscript. This work was supported in part by Grants-in-Aid from the Ministry of Education, Science and Culture of Japan. Waseda University fund is also acknowledged.

References

Abbott, R. H. and P. E. Cage (1984). A possible mechanism of length activation in insect fibrillar flight muscle. *J. Muscle Res. Cell Motil.* **5**, 387–397.

Akamatsu, N., B. Hannaford and L. Stark (1986). An intrinsic mechanism for the oscillatory contraction of muscle. *Biol. Cybern.* **53**, 219–227.

Altringham, J. D. and I. A. Johnston (1985). Effects of phosphate on the contractile properties of fast and slow muscle fibers from an antarctic fish. *J. Physiol. (Lond.)* **368**, 491–500.

Anazawa, T., K. Yasuda and S. Ishiwata (1992). Spontaneous oscillation of tension and sarcomere length in skeletal myofibrils. Microscopic measurement and analysis. *Biophys. J.* **61**, 1099–1108.

Armstrong, C. F., A. F. Huxley and F. J. Julian (1966). Oscillatory responses in frog skeletal muscle fibres. *J. Physiol. (Lond.)* **186**, 26–27.

Bartoo, M. L., T. Tameyasu, D. H. Burns and G. H. Pollack (1988). Stepwise shortening in single myofibrils. *Bioiphys. J.* **53**, 370a. (Abstr.)

Borejdo, J. and A. Schweitzer (1977). Tension generation by isolated myofibrils. *J. Mechanochem. Cell Motil.* **4**, 189–204.

Bremmel, R. D. and A. Weber (1972). Cooperative behavior within the functional unit of the actin filament in vertebrate skeletal muscle. *Nature (Lond.)*. **238**, 97–101.

Brenner, B. (1979). An indirect proof of stretch-induced Ca^{++} release from the sarcoplasmic reticulum in glycerinated skeletal and heart muscle preparations. *Basic Res. Cardiol.* **74**, 177–202.

Brenner, B. (1990). Muscle mechanics and biochemical kinetics. *In* Molecular mechanisms in muscular contraction. J. M. Squire, ed., The Macmillan Press Ltd., London pp. 77–149.

Chalovich, J. M. and E. Eisenberg (1982). Inhibition of actomyosin ATPase activity by troponin-tropomyosin without blocking the binding of myosin to actin. *J. Biol. Chem.* **257**, 2432–2437.

Chase, P. B. and J. J. Kushmerick (1988). Effects of pH on contraction of rabbit fast and slow skeletal muscle fibers. *Biophys. J.* **53**, 935–946.

Cooke, R. (1986). The mechanism of muscle contraction. *CRC Rev. Biochem.* **21**, 53–118.

Cooke, R. and W. Bialek (1979). Contraction of glycerinated muscle fibers as a function of the ATP concentration. *Biophys. J.* **28**, 241–258.

Cooke, R. and E. Pate (1985). The effects of ADP and phosphate on the contraction of muscle fibers. *Biophys. J.* **48**, 789–798.

Cooke, R., K. Franks, G. B. Luciani and E. Pate (1988). The inhibition of rabbit skeletal muscle contraction by hydrogen ions and phosphate. *J. Physiol. (Lond.)* **395**, 77–97.

Danzig, J. A., M. G. Hibberd, D. R. Trentham and Y. E. Goldman (1991). Cross-bridge kinetics in the presence of MgADP investigated by photolysis of caged ATP in rabbit psoas muscle fibres. *J. Physiol. (Lond.)* **432**, 639–680.

Danzig, J. A., Y. E. Goldman, N. C. Millar, J. Lacktis and E. Homsher (1992). Reversal of the cross-bridge force-generating transition by photogeneration of phosphate in rabbit psoas muscle fibres. *J. Physiol. (Lond.)* **451**, 247–278.

Dawson, M. J., S. Smith and D. R. Wilkie (1986). The $[H_2PO_4^{-1}]$ may determine cross-bridge cycling rate and force reduction in living fatiguing muscle. *Biophys. J.* **49**, 268a. (Abstr.)

Deshcherevsky, V. I. (1977). Kinetic model of regulation of muscle protein activity. *J. Theor. Biol.* **64**, 517–534.

Ebashi, S. (1991). Excitation-contraction coupling and the mechanism of muscle contraction. *Annu. Rev. Physiol.* **53**, 1–16.

Ebashi, S. and M. Endo (1968). Calcium ions and muscle contraction. *Prog. Biophys. Mol. Biol.* **18**, 123–183.

Ebashi, S., M. Endo and I. Ohtsuki (1969). Control of muscle contraction. *Quart. Rev. Biophys.* **2**, 351–384.

Edman, K. A. P. (1980). Depression of mechanical performance by active shortening during twitch and tetanus of vertebrate muscle fibres. *Acta Physiol. Scand.* **109**, 15–26.

Ekelund, M. C. and K. A. P. Edman (1982). Shortening induced deactivation of skinned fibres of frog and mouse striated muscle. *Acta Physiol. Scand.* **116**, 189–199.

Endo, M. (1972). Stretch-induced increase in activation of skinned muscle fibres by calcium. *Nature (Lond.).* **237**, 211–213.

Endo, M. (1973). Length dependence of activation of skinned muscle fibers. *Cold Spring Harbor Symp. Quant. Biol.* **37**, 505–510.

Fabiato, A. and F. Fabiato (1978). Myofilament-generated tension oscillation during partial calcium activation and activation dependence of the sarcomere length-tension relation of skeletal cardiac cells. *J. Gen. Physiol.* **72**, 667–699.

Fuchs, F. and Y. P. Wang (1991). Force, length and Ca^{2+}-troponin C affinity in skeletal muscle. *Am. J. Physiol.* **261**, C787–C792.

Fujime, S. (1975). Optical diffraction study of muscle fiber. *Biochim. Biophys. Acta* **379**, 227–238.

Fujime, S. and S. Ishiwata (1971). Dynamic study of F-actin by quasielastic scattering of laser light. *J. Mol. Biol.* **62**, 251–265.

Fukuda, N., T. Fujita and S. Ishiwata (1991). Effects of ADP, inorganic phosphate and calcium on spontaneous tension oscillation of glycerinated cardiac muscle. *J. Muscle Res. Cell Motil.* **12**, 304 (Abstr.)

Fukuda, N., T. Fujita and S. Ishiwata (1992). Spontaneous tension oscillation in glycerinated cardiac muscle induced by ADP, inorganic phosphate and calcium. *J. Muscle Res. Cell Motil.* **13**, 477 (Abstr.)

Funatsu, T., H. Higuchi and S. Ishiwata (1990). Elastic filaments in skeletal muscle revealed by selective removal of thin filaments with plasma gelsolin. *J. Cell Biol.* **110**, 53–62.

Funatsu, T., E. Kono, H. Higuchi, S. Kimura, S. Ishiwata, T. Yoshioka, K. Maruyama and S. Tsukita (1993). Elastic filaments *in situ* in cardiac muscle: Deep-etch replica analysis in combination with selective removal of actin and myosin filaments. *J. Cell Biol.* **120**, 711–724.

Geeves, M. A. (1991). The dynamics of actin and myosin association and the cross-bridge model of muscle contraction. *Biochem. J.* **274**, 1–14.

Goldman, Y. E. (1987). Kinetics of the actomyosin ATPase in muscle fibers. *Annu. Rev. Physiol.* **49**, 637–654.

Goldman, Y. E. and B. Brenner (1987). Special topic: molecular mechanism of muscle contraction. *Annu. Rev. Physiol.* **49**, 629–636.

Goodall, M. C. (1956). Auto-oscillations in extracted muscle fibre systems. *Nature (Lond.)* **177**, 1238–1239.

Gordon, A. M., E. B. Ridgway and D. A. Martyn (1984). Calcium sensitivity is modified by contraction. *In* Contractile mechanisms in muscle (ed. by G. H. Pollack and H. Sugi). pp. 553–563. Plenum Pub. Corp., New York.

Hanson, J. and J. Lowy (1963). The strucure of F-actin and of actin filaments isolated from muscle. *J. Mol. Biol.* **6**, 46–60.

Herzig, J. W., J. W. Peterson, J. C. Rüegg and R. J. Solaro (1981). Vanadate and phosphate ions reduce tension and increase cross-bridge kinetics in chemically skinned heart muscle. *Biochim. Biophys. Acta.* **672**, 191–196.

Hibberd, M. G., J. A. Dantzig, D. R. Trentham and Y. E. Goldman (1985). Phosphate release and force generation in skeletal muscle fibers. *Science (Wash. DC).* **228**, 1317–1319.

Hibberd, M. G. and D. R. Trentham (1986). Relationships between chemical and mechanical events during muscular contraction. *Annu. Rev. Biophys. Biophys. Chem.* **15**, 119–161.

Hill, T. L. (1974). Theoretical formalism for the sliding filament model of contraction of striated muscle. *Prog. Biophys. Mol. Biol.* **28**, 267–340.

Hoar, P. E., C. W. Mahoney and W. G. L. Kerrick (1987). MgADP-increases maximum tension and Ca^{2+} sensitivity in skinned rabbit soleus fibers. *Pfluegers Arch. Eur. J. Physiol.* **410**, 30–36.

Homsher, E. and N. C. Millar (1990). Caged compounds and striated muscle contraction. *Annu. Rev. Physiol.* **52**, 875–896.

Horowits, R. and R. J. Podolsky (1987). The positional stability of thick filaments in activated skeletal muscle depends on sarcomere length: evidence for the role of titin filaments. *J. Cell Biol.* **105**, 2217–2223.

Huxley, A. F. and R. Niedergerke (1954). Interference microscopy of living muscle fibres. *Nature (Lond.).* **173**, 971–973.

Huxley, A. F. (1957). Muscle structure and theories of contraction. *Prog. Biophys. Biophys. Chem.* **7**, 255–318.

Huxley, A. F. and R. M. Simmons (1971). Proposed mechanism of force generation in striated muscle. *Nature (Lond.).* **233**, 533–538.

Huxley, A. F. and R. M. Simmons (1973). Mechanical transients and the origin of muscular force. *Cold Spring Harbor Symp. Quant. Biol.* **37**, 669–680.

Huxley, H. E. (1963). Electron microscopic studies on the structure of natural and synthetic protein filaments from striated muscle. *J. Mol. Biol.* 7, 281–318.

Huxley, H. E. (1969). The mechanism of muscular contraction. *Science (Wash. DC).* **164**, 1356–1366.

Huxley, H. E. (1973). Structural changes in the actin- and myosin-containing filaments during contraction. *Cold Spring Harbor Symp. Quant. Biol.* **37**, 361–376.

Huxley, H. E. and J. Hanson (1954). Changes in the cross-striations of muscle during contraction and stretch and their structural interpretation. *Nature (Lond.).* **173**, 973–976.

Inoue, A., H. Takenaka, T. Arata and Y. Tonomura (1979). Functional implications of the two-headed structure of myosin. *Adv. Biophys.* **13**, 1–194.

Ishiwata, S. and S. Fujime (1971). Effect of Ca^{2+} on dynamic properties of muscle proteins studied by quasielastic light scattering. *J. Phys. Soc. Japan.* **31**, 1601.

Ishiwata, S. and S. Fujime (1972). Effect of calcium ions on the flexibility of reconstituted thin filament of muscle studied by quasielastic scattering of laser light. *J. Mol. Biol.* **68**, 511–522.

Ishiwata, S., K. Kinosita, Jr., H. Yoshimura and A. Ikegami (1987). Rotational motions of myosin heads in myofibril studied by phosphorescence anisotropy decay measurements. *J. Biol. Chem.* **262**, 8314–8317.

Ishiwata, S., N. Okamura and H. Shimizu (1987). Spontaneous oscillation of sarcomeres in skeletal myofibrils. Observation with a phase-contrast microscope. *J. Muscle Res. Cell Motil.* **8**, 275 (Abstr.)

Ishiwata, S., N. Okamura, H. Shimizu, T. Anazawa and K. Yasuda (1991). Spontaneous oscillatory contraction (SPOC) of sarcomeres in skeletal muscle. *Adv. Biophys.* **27**, 227–235.

Ishiwata, S., T. Anazawa, T. Fujita, N. Fukuda, H. Shimizu and K. Yasuda (1993). Spontaneous tension oscillation (SPOC) of muscle fibers and myofibrils. Minimum requirements for SPOC. *In* Mechanism of myofilament sliding in muscle contraction. ed. H. Sugi, and G. H. Pollack. Plenum Pub. Corp., in press.

Iwazumi, T. and G. H. Pollack (1981). The effect of sarcomere nonuniformity on the sarcomere length-tension relationship of skinned fibers. *J. Cell Physiol.* **106**, 321–337.

Iwazumi, T. (1987a). High-speed ultrasensitive instrumentation for myofibril mechanics measurements. *Am. J. Physiol.* **252**, C253–C262.

Iwazumi, T. (1987b). Mechanics of the myofibril. *In* Mechanics of the circulation. H. E. D. J. ter Keurs and J. V. Tyberg, eds. Martinus Nijhoff, Dordrecht. pp. 37–49.

Jackson, J. L. and A. Oplatka (1974). A mechanochemical theory of fluctuation in muscles. I. Introduction to the theory. *Biorheology* **11**, 315–322.

Jewell, B. R. and J. C. Rüegg (1966). Oscillatory contraction of insect fibrillar muscle after glycerol extraction. *Proc. Roy. Soc. B.* **164**, 428–459.

Katz, A. M. (1977). Physiology of the heart. Raven Press Books, Ltd., New York.

Kawai, M. (1986). The role of orthophosphate in cross-bridge kinetics in chemically skinned rabbit psoas fibres as detected with sinusoidal and step length alterations. *J. Muscle Res. Cell Motil.* **7**, 421–434.

Kawai, M. and H. R. Halvorson (1989). Role of MgATP and MgADP in the cross-bridge kinetics in chemically skinned rabbit psoas fibers. *Biophys. J.* **55**, 595–603.

Kawai, M. and H. R. Halvorson (1991). Two step mechanism of phosphate release and the mechanism of force generation in chemically skinned fibers of rabbit psoas muscle. *Biophys. J.* **59**, 329–342.

Kinosita, Jr., K., H. Itoh, S. Ishiwata, K. Hirano, T. Nishizaka and T. Hayakawa (1991). Dual-view microscopy with a single camera: Real-time imaging of molecular orientations and calcium. *J. Cell Biol.* **115**, 67–73.

Kodama, T. (1985). Thermodynamic analysis of muscle ATPase mechanisms. *Physiol. Rev.* **65**, 467–551.

Lorand, L. and C. Moos (1956), Auto-oscillations in extracted muscle fibre system. *Nature (Lond.).* **177**, 1239.

Maruyama, K. (1986). Connectin, and elastic filamentous protein of striated muscle. *Int. Rev. Cytol.* **104**, 81–114.

Millar, N. C. and E. Homsher (1990). The effect of phosphate and calcium on force generation in glycerinated rabbit skeletal muscle fibers. A steady-state and transient kinetic study. *J. Biol. Chem.* **265**, 20234–20240.

Mooseker, M. S., M. Pratt, D. P. Kiehart and R. E. Stephens (1977). Cyclic contraction and relaxation of sarcomeres in isolated myofibrils. *Biophys. J.* **17**, 173a (Abstr.)

Murase, M., H. Tanaka, K. Nishiyama and H. Shimizu (1986). A three-state model for oscillation in muscle: sinusoidal analysis. *J. Muscle Res. Cell Motil.* **7**, 2–10.

Natori, R. (1954). The property and contraction process of isolated myofibrils. *Jikeikai Med. J.* **1**, 119–126.

Nishizaka, T., T. Yagi, Y. Tanaka and S. Ishiwata (1993). Right-handed rotation of an actin filament in an *in vitro* motile system. *Nature (Lond.)* **361**, 269–271.

Nosek, T. M., K. Y. Fender and R. E. Godt (1987). It is diprotonated inorganic phosphate that depresses force in skinned skeletal muscle fibers. *Science (Wash. DC).* **236**, 191–193.

Ohtsuki, I., K. Maruyama and S. Ebashi (1986). Regulatory and cytoskeletal proteins of vertebrate skeletal muscle. *Adv. Prot. Chem.* **38**, 1–67.

Okamura, N. and S. Ishiwata (1988). Spontaneous oscillatory contraction of sarcomeres in skeletal myofibrils. *J. Muscle Res. Cell Motil.* **9**, 111–119.

Onodera, S. (1990). Oscillatory contraction waves in skinned skeletal muscle at high pH without Ca^{2+} *Jikeikai Med. J.* **37**, 447–455.

Onodera, S. and Y. Umazume (1984). Periodic contraction of skinned muscle fiber under high pH. *Biophys. (Jpn)* **24**, S84 (Abstr.)

Oosawa, F. and M. Kasai (1962). A theory of linear and helical aggregations of macromolecules. *J. Mol. Biol.* **4**, 10–21.

Oosawa, F., S. Fujime, S. Ishiwata and K. Mihashi (1973). Dynamic property of F-actin and thin filament. *Cold Spring Harbor Symp. Quant. Biol.* **37**, 277–286.

Pate, E. and R. Cooke (1989). A model of cross-bridge action: the effects of ATP, ADP and Pi. *J. Muscle Res. Cell Motil.* **10**, 181–196.

Pollack, G. H. (1990). Muscles and molecules: Uncovering the principles of biological motion. Ebner and Sons Publishers, Seattle.

Pratt, M. M., M. S. Mooseker, D. P. Kiehart and R. E. Stephens (1976). Cyclic contraction and relaxation of glycerinated myofibrils isolated from skeletal muscle. *Biol. Bull.* **151**, 426 (Abstr.)

Pringle, J. W. S. (1967). The contractile mechanism of insect fibrillar muscle. *Prog. Biophys. Mol. Biol.* **17**, 1–60.

Pringle, J. W. S. (1978). Stretch activation of muscle: function and mechanism. *Proc. R. Soc. Lond. B.* **201**, 107–130.

Rüegg, J. C. (1988). Calcium in muscle activation. Springer Verlag, Berlin.

Rüegg, J. C., G. J. Steiger and M. Schadler (1971a). Mechanical activation of the contractile system in skeletal muscle. *Pfluegers Arch. Eur. J. Physiol.* **319**, 139–145.

Rüegg, J. C., M. Schadler, G. J. Steiger and G. Muller (1971b). Effects of inorganic phosphate on the contractile mechanism. *Pfluegers Arch. Eur. J. Physiol.* **325**, 359–364.

Schadler, M., G. J. Steiger and J. C. Rüegg (1971). Mechanical activation and isometric oscillations in insect fibrillar muscle. *Pfluegers Arch. Eur. J. Physiol.* **330**, 217–229.

Schoenberg, M., J. B. Wells and R. J. Podolsky (1974). Muscle compliance and the longitudinal transmission of mechanical impulses. *J. Gen. Physiol.* **64**, 623–642.

Schutt, C. E. and U. Lindberg (1992). Actin as the generator of tension during muscle contraction. *Proc. Natl. Acad. Sci. U.S.A.* **89**, 319–323.

Shimizu, H. (1979). Dynamic cooperativity of molecular processes in active streaming, muscle contraction, and subcellular dynamics. The molecular mechanism of self-organization at the subcellular level. *Adv. Biophys.* **13**, 195–278.

Shimizu, H., T. Fujita and S. Ishiwata (1992). Regulation of tension development by MgADP and Pi without Ca^{2+}. Role in spontaneous tension oscillation of skeletal muscle. *Biophys. J.* **61**, 1087–1098.

Sicilia, S. and D. A. Smith (1991). Theory of asynchronous oscillations in loaded insect flight muscle. *Math. Biosci.* **106**, 159–201.

Siemankowski, R. F., M. O. Wiseman and H. D. White (1985). ADP dissociation from actomyosin subfragment 1 is sufficiently slow to limit the unloaded shortening velocity in vertebrate muscle. *Proc. Natl. Acad. Sci. U.S.A.* **82**, 658–662.

Smith, D. A. (1991). Quantitative model for Schadler's isometric oscillations in insect flight and cardiac muscle. *J. Muscle Res. Cell Motil.* **12**, 455–465.

Squire, J. (1981). The structural basis of muscular contraction. Plenum Press, New York & London.

Steiger,G. J. (1971). Stretch activation and myogenic oscillation of isolated contractile structure of heart muscle. *Pfluegers Arch. Eur. J. Physiol.* **330**, 347–361.

Steiger, G. J. (1977). Stretch activation and tension transients in cardiac, skeletal and insect flight muscle. *In* Insect flight muscle (ed. by R. T. Tregear). pp. 221–268. North-Holland, Amsterdam.

Stephenson, D. G. and D. A. Williams (1981). Calcium-activated force response in fast- and slow-twitch skinned muscle fibres of the rat at different temperature. *J. Physiol. (Lond.)* **317**, 281–317.

Stephenson, D. G. and I. R. Wendt (1984). Length dependence of changes in sarcoplasmic calcium concentration and myofibrillar calcium sensitivity in striated muscle fibres. *J. Muscle Res. Cell Motil.* **5**, 243–272.

Sugi, H. (1972). Tension changes during and after stretch in frog muscle fibres. *J. Physiol. (Lond.)* **225**, 237–253.

Sweitzer, N. K. and R. L. Moss (1990). The effect of altered temperature on Ca^{2+}-sensitive force in permeabilized myocardium and skeletal muscle. *J. Gen. Physiol.* **96**, 1221–1245.

Szent-Gyorgyi, A. (1951). Chemistry of muscular contraction. 2nd edn. Academic Press, London.

Tanaka, Y., A. Ishijima and S. Ishiwata (1992). Super helix formation of actin filaments in an in vitro motile system. *Biochim. Biophys. Acta* **1159**, 94–98.

Tawada, K. and K. Sekimoto (1991). A physical model of ATP-induced actin-myosin movement in vitro. *Biophys. J.* **59**, 343–356.

Taylor, E. W. (1979). Mechanism of actomyosin ATPase and the problem of muscle contraction. *CRC Crit. Rev. Biochem.* **6**, 103–164.

Umazume, Y. and T. Yoshioka (1980). Sarcomere disorder in skinned fibers during contraction. *In* Muscle contraction: Its regulatory muscle mechanisms (ed. by S. Ebashi *et al.*). pp. 475–481. Japan Sci. Soc. Press, Tokyo/Springer Verlag, Berlin.

Wang. K. (1985). Sarcomere-associated cytoskeletal lattices in striated muscle: reviews and hypothesis. *In* Cell and muscle motility. Vol. 6. J. W. Shay, ed. Plenum Publishing Corp., New York, pp. 315–369.

Weber, A. and J. M. Murray (1973). Molecular control mechanisms in muscle contraction. *Physiol. Rev.* **53**, 612–673.

White, D. C. S. and J. Thorson (1973). The kinetics of muscle contraction. *Prog. Biophys. Molec. Biol.* **27**, 173–255.

Yano, M., T. Yamada and H. Shimizu (1978). Studies of chemo-mechanical conversion in artificially produced streamings. 1. Reconstruction of a chemo-mechanical system from acto-HMM of rabbit skeletal-muscle. *J. Biochem.* **84**, 277–283.

Yano, M. and H. Shimizu (1978). Studies of chemo-mechanical conversion in artificially produced streamings. 2. Order-disorder phase-transition in chemo-mechanical conversion. *J. Biochem.* **84**, 1087–1092.

Corrections and Comments (Ishiwata & Yasuda, 1993)

p. 108, l. 25: Bremmel → Bremel (Sorry! Dr. Bremel)
p. 111, l. 6: 1986 → 1976
p. 112, Table1: 1985 Onodera and Umazume → 1984 Onodera and Umazume
p. 121, l. 5: It is better to replace a sign of equality "=" in Eq. (1) by a sign of proportionality "∝"; a unit of F (cf. Figs. 11-14) is taken to be arbitrary.
p. 121, l. 19: $\{K_f\}^m$ → $\{[K_f]^m$
p. 121, l. 20: [f. g. c.] should be divided by $[M_0]$, total concentration of myosin heads defined in p. 122.
p. 121, l. 21: delete "and p + q + r = 1"
p. 121, l. 37: $[P_b]$ → [Pi]
p. 122, Table2: k_{1b} = 1xE+1 → k_{1b} = 1xE+1/s
p. 125, l. 11: the scheme should be "→AMADPPi (1)→AMADPPi (2)→AMADPPi (3)→"
p. 126, l. 1: Bremmel → Bremel
p. 127, l. 10: f. g. s. → f. g. c.
p. 130, l. 3: The sentense in the parenthesis, "this property has been reported; cf. Goldman, 1987; Danzig et al., 1992", seems to be misleading. To be strict, the following is correct: "it has been reported that the Pi release step under full-activation conditions is regulated by the distortion of AMADPPi cross-bridges (cf. Goldman, 1987; Danzig et al., 1992), although the trend is reverse to our assumption".
p. 132, l. 20: Bioiphys. → Biophys.
p. 132, l. 23: Bremmel → Bremel
p. 133, l. 46: MgADP-increases → $MgADP^-$ increases

J. Biochem. **115**, 644-647 (1994)

Stepwise Motion of an Actin Filament over a Small Number of Heavy Meromyosin Molecules Is Revealed in an *In Vitro* Motility Assay[1]

Hidetake Miyata,* Hiroyuki Hakozaki,*,[2] Hiroshi Yoshikawa,* Naoya Suzuki,*,[3] Kazuhiko Kinosita Jr.,*,[4] Takayuki Nishizaka, and Shin'ichi Ishiwata****

**Department of Physics, Faculty of Science and Technology, Keio University, 3-14-1 Hiyoshi, Kohoku-ku, Yokohama, Kanagawa 223; and **Department of Physics, School of Science and Engineering, Waseda University, 3-4-1 Okubo, Shinjuku-ku, Tokyo 169*

Received for publication, January 31, 1994

In order to determine the relative motions of an actin filament and a myosin molecule upon hydrolysis of one ATP, an *in vitro* motility assay, in which individual actin filaments slide over heavy meromyosin molecules bound to a substrate, was combined with an optical trapping technique. An actin filament, attached to a gelsolin-coated bead, was captured with an optical trap. The surface-bound heavy meromyosin molecules pulled the filament against the trapping force, which resulted in back and forth motions of the actin-bound bead. The number of heavy meromyosin molecules interacting with an actin filament (at most 1/μm filament) and the ATP concentration ($\leq$0.5 μM) were chosen so as to facilitate detection of each "pull." Calculation of the centroid of the bead image revealed abrupt displacements of the actin filament. The frequency of such displacements was between 0.05 and 0.1 per 1 s per 1 μm actin filament, being consistent with calculated values based on the reported bimolecular binding constants of ATP and the actomyosin rigor complex. The distribution of the displacements peaked around 7 nm at a trapping force of 0.016 pN/nm, but it became broader, and some displacements were as large as 30 nm, when the trapping force was reduced to 0.0063 pN/nm, suggesting that the force generation due to the structural change of a myosin head may be insufficient to explain such displacements.

Key words: actomyosin force, motor protein, optical trapping.

In muscle contraction, relative sliding between actin and myosin occurs upon hydrolysis of ATP by myosin. The molecular event underlying this process is the displacement of an actin filament by one myosin molecule upon hydrolysis of an ATP molecule by the myosin head. In this report we term this process the elementary event. Many models have been proposed [for example, Refs. *1-4*] to explain the elementary event, but because they were derived through experiments involving muscle fibers and actomyosin solutions, both containing large numbers of actin and myosin molecules, these models should be tested at the level of a single molecule. The *in vitro* motility assay can fulfill such a requirement, because the number of HMM molecules supporting the sliding of individual actin filaments and the ATP concentration can be varied over wide ranges (*5, 6*). Thus, by lowering both the number density of HMM and the ATP concentration in this assay, one can expect to detect the occurrence of the elementary event. To measure the movement and the force, we prepared "bead-tailed" actin filaments (Suzuki *et al.*, manuscript in preparation) and manipulated the filament by trapping the actin-bound bead with an optical trap (*7*). The trapping of the bead reduced its random motion, thereby facilitating determination of its displacement from the trap center (*8*).

HMM was prepared from rabbit skeletal myosin by chymotryptic digestion (*9*). Actin filaments were prepared as described (*10*). All chemicals were of analytical grade.

The motility assay (*11*) combined with the optical trapping technique (*7*) was performed as follows. HMM was adsorbed to a nitrocellulose-coated coverslip (see below). Actin filaments were visualized with rhodamine-conjugated phalloidin (Molecular Probes, Eugene, OR), and then bound to gelsolin-coated polystyrene beads (0.88 μm diameter; Polyscience, Warrington, PA) by mixing the filaments and the beads at an appropriate ratio, followed by overnight incubation at 0°C. A bead carrying only one sufficiently long (between 3.5 and 4.6 μm) filament was selected under a fluorescence microscope (Nikon TMD; Nikon, Tokyo; equipped with an oil-immersion objective, 100×, NA 1.3, with a phase ring). The selected actin-bound bead was captured with a home-made optical trap apparatus (with a 350 mW Nd-YAG laser ALC1064; Amoco Laser, IL; as the light source), and was held at about 1 μm above the HMM surface during the measurements. Methylcellulose (0.2%)

[1] This work was supported by Grants-in-Aid from the Ministry of Education, Science and Culture of Japan, by Special Coordination Funds for Promoting Science and Technology from the Agency of Science and Technology of Japan, and by grants from Keio and Waseda Universities.

Present addresses: [2] Nikon Corporation, Yokohama Plant, 471 Nagaodai-machi, Sakae-ku, Yokohama, Kanagawa 244; [3] Department of Physics, Faculty of Science, Nagoya University, Chikusa-ku, Nagoya, Aichi 464-01.

[4] To whom correspondence should be addressed.

Abbreviations: CCD, charge coupled device; HMM, heavy meromyosin.

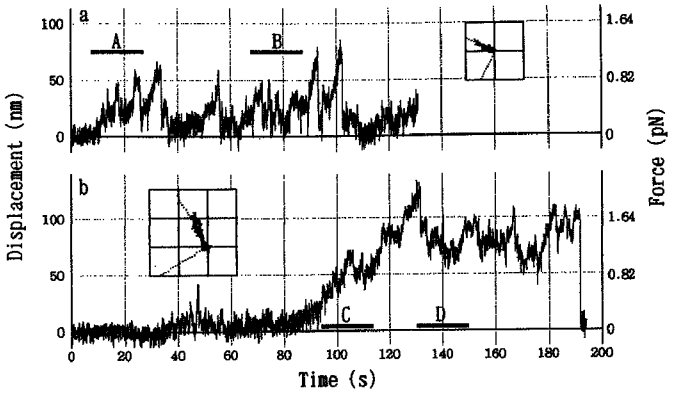

Fig. 1. **Two representative traces of the bead motion obtained at 0.25 μM (a) and 0.5 μM (b) ATP.** Horizontal bars indicate the range which is shown in Fig. 2 with an expanded time scale (A and B for Fig. 2, c and d; C and D for Fig. 2, g and h). Ordinates: left, the bead displacement; right, the trapping force. Insets: x-y traces of displacement of each bead. The major direction of the bead displacements is taken as the x direction. Grids, 100 nm.

was added to reduce dissociation of the actin filament from the HMM surface (*12*).

The fluorescence image of the bead-tailed filament and the phase-contrast image of the bead were simultaneously observed with a modified W-microscopy apparatus (*13*): the fluorescence images were taken with an image intensifier (KS1381; VIDEO SCOPE, Washington, DC) connected to a CCD camera (CCD-72; DAGE MTI, IN), and the phase-contrast images, used to calculate the bead position, with another CCD camera. The two images were combined electronically (MV24-C; For A, Tokyo) and then recorded on 8 mm video tape (EVO-9650; Sony, Tokyo) for further processing.

The bead position was determined at 33 ms intervals from the centroid of the bead image calculated with an image processor (DIPS-C2000; Hamamatsu Photonics, Shizuoka). The position of the trap center was determined from the video sequence in which the actin filament was not interacting with the HMM surface. The potential for the trapping force was estimated from the distribution of the positions of an actin-free bead in the trap at reduced laser intensities; for this measurement, we raised the viscosity of the medium to avoid image blurring due to fast Brownian motions. The potential was found to be approximated by that of a Hookean spring up to 200 nm from the trap center.

To determine the surface density of HMM on a substrate, HMM (1 μg/ml) was infused into a flow chamber (thickness $\sim$50 μm) constructed from one nitrocellulose-coated and one uncoated coverslip, and then allowed to adsorb for 1 min. The difference between the amount of infused HMM and that of unadsorbed HMM was determined from the NH_4-EDTA ATPase activity: about 80% of the infused HMM was adsorbed, giving a density of 150 HMM per μm^2.

The ATP concentration used in our experiment (<1 μM) is lower than the usual values (*5*), and hence the rate of ATP binding, which triggers the generation of force and motion, is expected to be at most 1 per 1 s per myosin head, given the bimolecular rate constant of ATP binding (*14*) of $0.2\text{-}1\times10^6\ M^{-1}\cdot s^{-1}$. Thus, individual events should be observable at a video rate of 30 Hz. The HMM density (about 150/μm^2) was also low so that the elementary

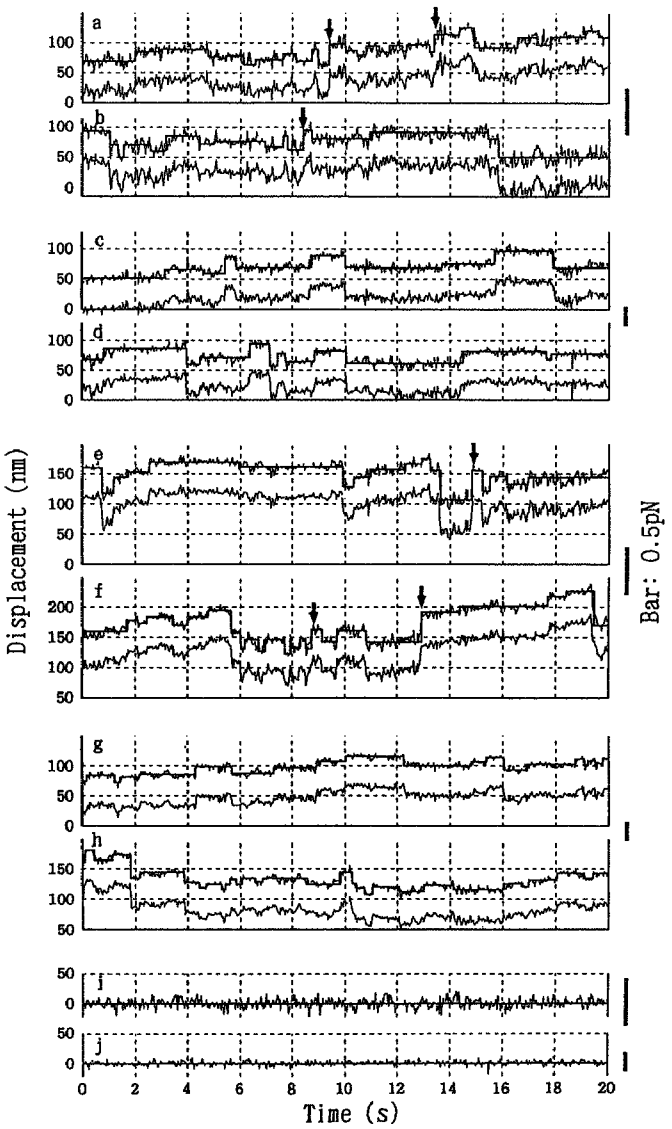

Fig. 2. **Examples of the stepwise motion of an actin-bound bead observed at 0.25 and 0.5 μM ATP.** The steps identified by eye are indicated with bold lines. Due to random noise it was not possible to count all stepwise displacements in the upper traces in each panel (a-h). a to d, the steps observed at 0.25 μM ATP; e to h, the steps at 0.5 μM ATP. a, b, e, and f, the steps at 0.0063 pN/nm; c, d, g, and h, at 0.016 pN/nm. i and j, traces obtained when the actin filament was not in contact with the HMM surface are shown for comparison. Arrows indicate where the displacements of $\gtrsim$30 nm occurred. Ordinates, bead displacement in nm. The vertical bars on the right indicate 0.5 pN.

events could be resolved, but still high enough to hold actin filaments on the HMM surface in the presence of ATP ($\leq$0.5 μM).

Bead motions in the presence of ATP consisted of forward (motion away from the trap center) and backward displacements (Fig. 1, a and b). That these motions were caused by a small number of HMM was confirmed in the absence of ATP (rigor conditions), where almost all HMM near an individual actin filament binds tightly to the filament. Fluorescence observation of the actin filaments on the HMM surface indicated that the individual filaments were bound to the surface through several points, in the order of 1 point per 1 μm filament. In another experiment,

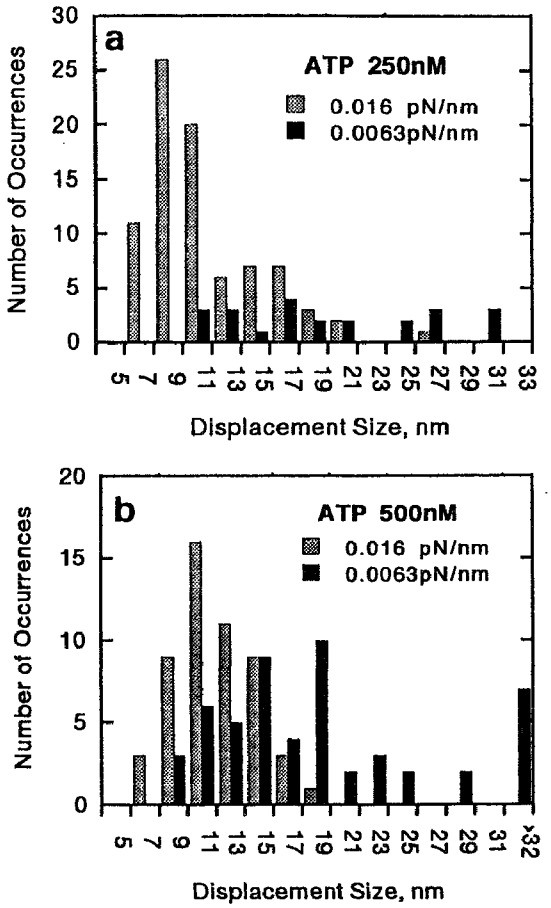

Fig. 3. **Distributions of sizes of steps determined for forward displacements.** a, at 0.25 μM ATP; b, at 0.5 μM ATP. Shaded bars, at 0.016 pN/nm; bold bars, at 0.0063 pN/nm.

a bead-tailed actin filament bound to the HMM surface was torn off by pulling the bead with the optical trap: the abrupt dissociations of the filaments from the individual HMM were counted. Hence, the number per 1 μm filament was also about 1 or less. ATP caused dissociation of some of these rigor heads, but most of the undissociated heads must have remained in the rigor state to hold the filament at the surface because of the low ATP.

Examination of the bead motion with an expanded time scale revealed abrupt displacements, which occurred within scores of milliseconds (Fig. 2, a to h). Because of the noise level (Fig. 2, i and j), we only took those displacements which had a magnitude of $\geq$5 nm as abrupt displacements. The frequency of the displacements was between 0.05 and 0.1 per 1 s per 1 μm actin filament.

Each of these displacements most likely resulted from the elementary event. The stationary bead position between the steps is expected to be determined by a balance among the three forces: (a) the force of the heads which pulls the bead away from the trap center (positive force), (b) the force of the other heads which pulls the bead backward (negative force), and (c) the trapping force. If a head exerting the negative force is dissociated by ATP binding, the force balance is disrupted and the bead advances, which is immediately followed by rebinding of the dissociated head to achieve a further advanced position. Two successive advancements will be recognized as a single displacement in most cases because of our low time resolution. If a head exerting the positive force is dissociated, on the other hand, a backward motion occurs, which is immediately followed by a forward motion as a result of reassociation and force generation. The final position in this case would be positive, negative or zero.

If the above interpretation is correct, the frequency of abrupt displacements should be equal to the rate of ATP binding; from the bimolecular rate constant (*14*) and the number of interacting HMM molecules per 1 μm actin filament, the values are calculated to be 0.05-0.5 at 0.25-0.5 μM ATP per 1 s per 1 μm filament, which are consistent with the experimental results, if one considers that we did not count the small displacements buried in the random noise.

The size distribution of the forward displacement peaked around 7 to 9 nm with a stronger trap at both ATP concentrations (Fig. 3, a and b). The rather wide distribution of the displacement size, as compared with in the case of kinesin (*8*), might be due to some difference in the mechanism of force generation between kinesin and myosin (*15*), or, perhaps because of the structural differences between microtubules and actin. Since a kinesin molecule makes 8 nm steps along a protofilament of a microtubule, this step size may reflect the size of the tubulin dimer, the structural unit of a protofilament (*8*). In the case of actin, each helical strand of an actin filament might impose a structural restriction on the binding of each myosin head to an actin monomer, so that the interval between the bound heads might not be so regular, except for the 37 nm interval arising from the periodicity of the two-start helix of an actin filament.

When the trapping force was weaker, the size distribution was broader with no clear peak, and the size of some displacements was $\gtrsim$30 nm. These displacement sizes are close to or within the recently suggested range of distances over which a head displaces an actin filament with one ATP (*12, 16*). If the displacement for this elementary event is as small as 15 nm, our displacement size of 30 nm is still explainable: two heads successively hydrolyze two ATP molecules to produce a displacement which will be twice the above distance. The probability of the occurrence of such a process must be low, but cannot be ignored in our experiments. However, a displacement of 6 nm, which has been derived from a proposed structural change of a myosin head (*17*), seems to be too small to account for our value. Thus, if structural changes in fact cause the displacements, changes in other portions of a myosin molecule might be involved. A mechanism in which a head hydrolyzes one ATP and generates the force for a longer distance at a lower load than conventionally assumed (*6*) might be another possible way to explain our value.

The authors wish to thank Dr. Y.Y. Toyoshima (Tokyo University) for the valuable comments, Drs. G. Marriott and G.W. Feigenson for their reading the manuscript, and Professor A. Ikegami (Keio University) and Dr. Y. Inoue (Riken) for their support, and Mr. M. Hosoda (Hamamatsu Photonics, Inc.) for development of the image analysis system. The authors also thank Mr. I. Sase (Keio University) for preparing Fig. 3.

REFERENCES

1. Huxley, A.F. (1957) *Progr. Biophys. Biophys. Chem.* **7**, 255-318

2. Huxley, H.E. (1969) *Science* **164**, 1356-1366
3. Eisenberg, E., Hill, T.L., & Chen, Y. (1980) *Biophys. J.* **29**, 195-227
4. Vale, R.D. & Oosawa, F. (1990) *Adv. Biophys.* **26**, 97-134
5. Kron, S.J. & Spudich, J.A. (1986) *Proc. Natl. Acad. Sci. USA* **83**, 6272-6276
6. Harada, Y., Sakurada, K., Aoki, T., Thomas, D.D., & Yanagida, T. (1990) *J. Mol. Biol.* **216**, 49-68
7. Ashkin, A., Dziedzic, J.M., Bjorkholm, J.E., & Chu, S. (1986) *Optics Lett.* **11**, 288-290
8. Svoboda, K., Schmidt, C.F., Schnapp, B.J., & Block, S.M. (1993) *Nature* **365**, 721-727
9. Weeds, A.G. & Pope, B. (1977) *J. Mol. Biol.* **111**, 129-157
10. Spudich, J.A. & Watt, S. (1971) *J. Biol. Chem.* **246**, 4866-4871
11. Kron, S.J., Toyoshima, Y.Y., Uyeda, T.Q.P., & Spudich, J.A. (1991) *Methods Enzymol.* **196**, 399-416
12. Uyeda, T.Q.P., Kron, S.J., & Spudich, J.A. (1990) *J. Mol. Biol.* **214**, 699-710
13. Kinosita, K., Jr., Itoh, H., Ishiwata, S., Hirano, K., Nishizaka, T., & Hayakawa, T. (1991) *J. Cell Biol.* **115**, 67-73
14. Goldman, Y.E. (1987) *Annu. Rev. Physiol.* **49**, 637-654
15. Howard, J., Hudspeth, A.J., & Vale, R.D. (1989) *Nature* **342**, 154-158
16. Higuchi, H. & Goldman, Y.E. (1991) *Nature* **352**, 352-354
17. Rayment, I., Rypniewski, W.R., Schmidt-Base, K., Smith, R., Tomchick, D.R., Benning, M.M., Winlkelmann, D.A., Wesenberg, G., & Holden, H.M. (1993) *Science* **261**, 50-58

Journal of Muscle Research and Cell Motility **15**, 158–171 (1994)

Structural and functional reconstitution of thin filaments in skeletal muscle

TAKASHI FUNATSU[1*], TAKASHI ANAZAWA[2] and SHIN'ICHI ISHIWATA[2]

[1]*Yanagida Biomotron Project, ERATO, JRDC, 2-4-14 Senba-Higashi, Mino, Osaka 562, Japan, and* [2]*Department of Physics, School of Science and Engineering, Waseda University, 3-4-1, Okubo, Shinjuku-ku, Tokyo 169, Japan*

Received 14 July 1993; revised 22 November 1993; accepted 23 November 1993

Summary

Thin filaments were reconstituted by incorporating exogenous actin, tropomyosin and troponin into glycerinated skeletal muscle fibres or myofibrils. Firstly, thin filaments except short fragments at the Z line were selectively removed by treatment with plasma gelsolin, an actin severing protein. As a result, the fibres (or fibrils) lost the ability to generate active tension. Next, actin filaments were reconstituted by adding purified G-actin which polymerizes onto the actin fragments which remained at the Z line. Rhodamine phalloidin staining of myofibrils showed that exogenous actin was incorporated into the position where the intrinsic thin filaments located. Thin section electron micrographs of fibres showed that reconstituted actin filaments ran from the Z line to the inside of the A band, with some reaching the H zone. The number density of reconstituted actin filaments in the A band was about 20% of that found in intact fibres. The actin filament-reconstituted fibres (or fibrils) generated active tension in a Ca^{2+}-insensitive manner and the tension was reversibly suppressed by 2,3-butanedione 2-monoxime. The recovered active tension was about 20% of tension developed by intact fibres. These results indicate that reconstituted actin filaments bear active tension similar to that borne by intact thin filaments. Thin filament-reconstituted fibres, which were prepared by adding purified tropomyosin-troponin complexes into actin filament-reconstituted fibres, showed Ca^{2+}-sensitive tension generation. The maximum tension generated was not affected by the presence of tropomyosin and troponin. SDS-PAGE analysis showed that more than 25% of actin and 20% of tropomyosin and troponin was incorporated into the reconstituted fibres. These results indicate that the structure and function of thin filaments are substantially reconstituted by self-assembly of actin, tropomyosin and troponin. The reconstituted fibres and fibrils will be useful for studying the molecular mechanism of muscle contraction and its regulation.

Introduction

A structural and functional unit of skeletal muscle is a sarcomere that is composed of liquid-crystalline arrays of thick and thin filaments. In a sarcomere the lengths of the thick and thin filaments are strictly determined. How is such an organized structure of the sarcomere formed, how is its stability maintained and what is the functional significance of the organized structure?

Structural and functional reconstitution of thin filaments *in vitro* is possible by mixing pure actin molecules with tropomyosin and troponin under the appropriate conditions. The length distribution of reconstituted filaments *in vitro* is, however, broad and of an exponential type in equilibrium (Kawamura & Maruyama, 1970). On the other hand, myosin filaments have a length distribution and average length similar to the thick filament *in vivo* and are spontaneously formed under the appropriate conditions *in vitro* (see review by Katsura & Noda, 1973). Formation of these myofilaments *in vitro* can be explained by self-assembly of the constituent proteins. The question arises then as to whether the formation of sarcomeres *in vivo* can be explained by the self-assembly of the constituent proteins. One way to answer this question is to examine how the sarcomere structure is reconstituted by using exogenous proteins after selective removal of the thick or thin filaments.

Thick filaments can be selectively removed with a high salt solution from muscle fibres and myofibrils (Huxley & Hanson, 1954). There have been several attempts to reconstitute thick filaments starting with these 'ghost' fibres and fibrils (Tawada *et al.*, 1976; Taniguchi & Ishikawa, 1982; Maw & Rowe, 1986). In contrast, it is difficult to remove thin filaments only by changing composition of the solutions. Recently we have succeeded in selectively removing thin filaments by using calf plasma gelsolin, an actin severing protein (Funatsu *et al.*, 1990). In the present work, using the thin filament-free

*To whom correspondence should be addressed.

fibres and fibrils as starting materials, we attempted to reconstitute thin filaments by adding exogenous actin, tropomyosin and troponin. Reconstitution of thin filaments in single fibres and fibrils was examined structurally by observing rhodamine phalloidin-labelled myofibrils under a fluorescence microscope and reconstituted filaments by thin section electron microscopy. The function of these fibre preparations was determined by measuring the recovered active tension and Ca^{2+} sensitivity.

As an application of this newly developed experimental system, we examined the effect of 2,3-butanedione 2-monoxime (BDM) on the tension generation of the actin filament-reconstituted fibres without tropomyosin and troponin. 2,3-butanedione 2-monoxime is a nucleophilic agent which reversibly inhibits contraction of muscle (Li *et al.*, 1985; Horiuti *et al.*, 1988; Higuchi & Takemori, 1989). We also examined whether tropomyosin and troponin potentiated the active tension. With the use of fluorescence- or spin-labelled actin, the technique described here would be a powerful and unique tool for studying the structural change of actin molecules associated with muscle contraction and its regulation. Some of the results in this paper have been reported in preliminary form (Funatsu & Ishiwata, 1989).

Materials and methods

Muscle fibres, myofibrils, and proteins

Rabbit psoas muscle fibres (diameter of 3 mm) were tied to a glass rod and incubated in 50% (v/v) glycerol, 0.5 mM $NaHCO_3$, 5 mM EGTA and 1 mM leupeptin at 0°C overnight. Fibres were then stored in the fresh glycerol solution at −20°C. Myofibrils were prepared by homogenizing the glycerinated fibres in a solution containing 0.17 M KCl, 1 mM $MgCl_2$, 1 mM EGTA, 10 mM 3-(N-morpholino) propane sulfonic acid (MOPS; pH 7.0) (Ishiwata & Funatsu, 1985). Calf plasma gelsolin was prepared as described previously (Funatsu *et al.*, 1990). Muscle proteins were prepared from rabbit back and leg white muscle. Actin was extracted from acetone powder and purified according to the method of Spudich and Watt (1971). The tropomyosin-troponin complex was prepared according to the method of Ebashi and colleagues (1968).

Selective removal and reconstitution of thin filaments in myofibrils

Removal and reconstitution of thin filaments were usually performed on myofibrils which were attached to a coverslip under an optical microscope. Myofibrils were first treated with 0.25 mg ml^{-1} of gelsolin in Ca rigor solution (0.17 M KCl, 1 mM $MgCl_2$, 0.1 mM $CaCl_2$, 2 mM diisopropyl fluorophosphate (DFP), 2 mM leupeptin, and 10 mM MOPS (pH 7.0)) and then in contracting solution (0.12 M KCl, 5 mM $MgCl_2$, 4 mM ATP, 0.1 mM $CaCl_2$, 2 mM DFP, 2 mM leupeptin, and 10 mM MOPS (pH 7.0)) for 15 min each. For each treatment 50 µl of gelsolin solution was used. After gelsolin was washed out with relaxing solution (0.12 M KCl, 5 mM, $MgCl_2$, 4 mM ATP, 1 mM EGTA, 2 mM DFP, 2 mM leupeptin, and 10 mM MOPS (pH 7.0)), the solution was exchanged with the contracting solution to confirm that shortening of the myofibrils did not occur upon the removal of thin filaments. The solution was then immediately exchanged with BDM-relaxing solution (relaxing solution containing 20 mM BDM). To reconstitute actin filaments, purified G-actin (0.5 mg ml^{-1}), which was mixed into BDM-relaxing solution just prior to use, was added to the gelsolin-treated myofibrils. The myofibrils were then incubated for 10 min (Ishiwata & Funatsu, 1985). Unbound actin molecules were washed out with BDM-relaxing solution. To determine the location of the reconstituted F-actin, myofibrils were stained with 0.3 µM of rhodamine phalloidin (Molecular Probes Inc., Eugene, OR, USA.) for 10 min. Unbound dye was removed by washing with BDM-relaxing solution. Shortenings and active tension generation of myofibrils were induced by replacing the bathing solution with the relaxing solution without BDM. Phase-contrast and fluorescence micrographs were taken with an optical microscope (Fluophoto VFD-R; CF Plan oil DM 100× objective lens (1.25 NA); Nikon Inc., Tokyo, Japan). Only when the tension generation was examined, both ends of myofibrils were held by a pair of glass micro-needles in a perfusion chamber on an inverted phase-contrast microscope (Diaphoto TMD; Plan Apo oil DM 60× objective lens (1.40 NA); Nikon Inc.) as described previously (Anazawa *et al.*, 1992). As one of the micro-needles was two orders of magnitude more flexible than the other, the tension produced by the myofibrils was determined by measuring the displacement of the flexible one (Anazawa *et al.*, 1992). The accuracy of tension measurement was ~0.5 µg. All the procedures were performed at room temperature (~25°C).

Selective removal and reconstitution of thin filaments in single muscle fibres

One end of single glycerinated muscle fibres (~60 µm in diameter and 6–7 mm in length) was tied to a thin tungsten wire attached to a tension transducer (UL-2GR, Nippon Denki Co. Ltd., Tokyo, Japan) and the other end to a wire attached to a micro-manipulator. Fibres were chemically skinned with solution containing 0.17 M KCl, 1 mM $MgCl_2$, 1 mM EGTA, 2 mM DFP, 2 mM leupeptin, 10 mM MOPS (pH 7.0) and 1% Triton X-100 for 30 min. After washing for 10 min in Ca rigor solution, the fibres were treated for 2 h each with 0.5 mg ml^{-1} of gelsolin in Ca rigor solution and then in contracting solution and finally washed for 1 h with relaxing solution. The reason why such a long treatment time was needed is probably ascribed to the slow diffusion of gelsolin molecules into a fibre. The solution was changed to a low salt contracting solution (20 mM KCl, 5 mM $MgCl_2$, 5 mM ATP, 4 mM EGTA, 4.1 mM $CaCl_2$ and 20 mM MOPS (pH 7.0)) to make sure that active tension was reduced upon the removal of thin filaments. To minimize the degradation of reconstituted fibres, active tension was measured between 2 and 15°C in a cold room. The active tension was measured at low ionic strength (~60 mM), as the muscle generated more force at low ionic strength than at physiological ionic strength (~200 mM) especially at low temperature. Active tension of a fibre could be reproducibly measured under our experimental conditions. After treatment with gelsolin, the sarcomere length was adjusted to 2.2 µm by monitoring diffraction lines from fibres illuminated by a He–Ne laser. To reconstitute actin filaments, the bathing solution was exchanged with KI solution (80 mM KI, 4 mM $MgCl_2$, 4 mM ATP, 4 mM EGTA, 20 mM BDM, and 10 mM K-phosphate (pH 7.0)) containing 1 mg ml^{-1} of purified G-actin which had been

mixed just prior to use. Preparations were incubated for 10 min. This procedure was repeated three times. Unbound actin molecules were washed out by BDM-relaxing solution. All the procedures for gelsolin treatment and reconstitution of actin were performed at 2°C. To reconstitute thin filaments, tropomyosin and troponin complexes (total protein concentration of 7 mg ml^{-1}), in BDM-relaxing solution, were further added to the actin filament-reconstituted fibres and incubated for 1 h at 15°C. Active tension of the reconstituted fibres was measured between 2 to 15°C in a solution with a low salt concentration. The concentration of free Ca^{2+}, which was controlled by changing the concentration of $CaCl_2$ in the presence of 4 mM EGTA, was determined using the published values for stability constants (Horiuti, 1986).

Electron microscopy

A muscle bundle composed of a few fibres was tied to a platinum wire and treated as described above. Control fibres in Ca rigor solution and gelsolin-treated fibres and actin filament-reconstituted fibres in relaxing solution were transferred into a solution containing 2.5% glutaraldehyde and 0.1 M Na-cacodylate (pH 7.2). They were fixed with the solution at 2°C overnight, and then with the solution containing 0.5% tannic acid for 30 min. After washing with 0.1 M Na-cacodylate (pH 7.2), the preparations were postfixed with 1% OsO_4 in the same buffer for 2 h at 2°C, dehydrated with ethanol and acetone and embedded in Poly/Bed 812 (Polysciences, Inc., Warrington, PA, U.S.A.). Thin sections were stained sequentially with saturated uranyl acetate and 2.6% lead citrate at 20°C. Electron micrographs were taken with a JEM 1200EX electron microscope (operating voltage, 100 kV; JEOL, Tokyo, Japan).

SDS-Gel electrophoresis and viscosity measurement

A bundle of four muscle fibres was dissolved in lysis solution (7.5% SDS, 10% glycerol, 1 mM DTT, and 10 mM Tris-HCl (pH 6.8)) and heated for 3 min at 90°C. SDS-PAGE was carried out according to the method of Laemmli (1970) with 13% polyacrylamide gel, and the protein was stained with Coomassie Brilliant Blue R. Images of gels were recorded by CCD camera (C3077; Hamamatsu Photonics, Hamamatsu, Japan) with input to a microcomputer. The densities of myosin heavy chain, myosin light chain 2, actin, α-tropomyosin and troponin C were determined by TV image processor (TVIP-4100 II; Nippon Avionics, Tokyo, Japan). Since the volume of muscle fibres differed from preparation to preparation, the amount of muscle proteins loaded was calibrated by using myosin heavy chain and myosin light chain 2 as a standard.

Viscosity was measured using an Ostwald capillary viscometer in a constant-temperature water bath at 2°C (flow time, 120 s).

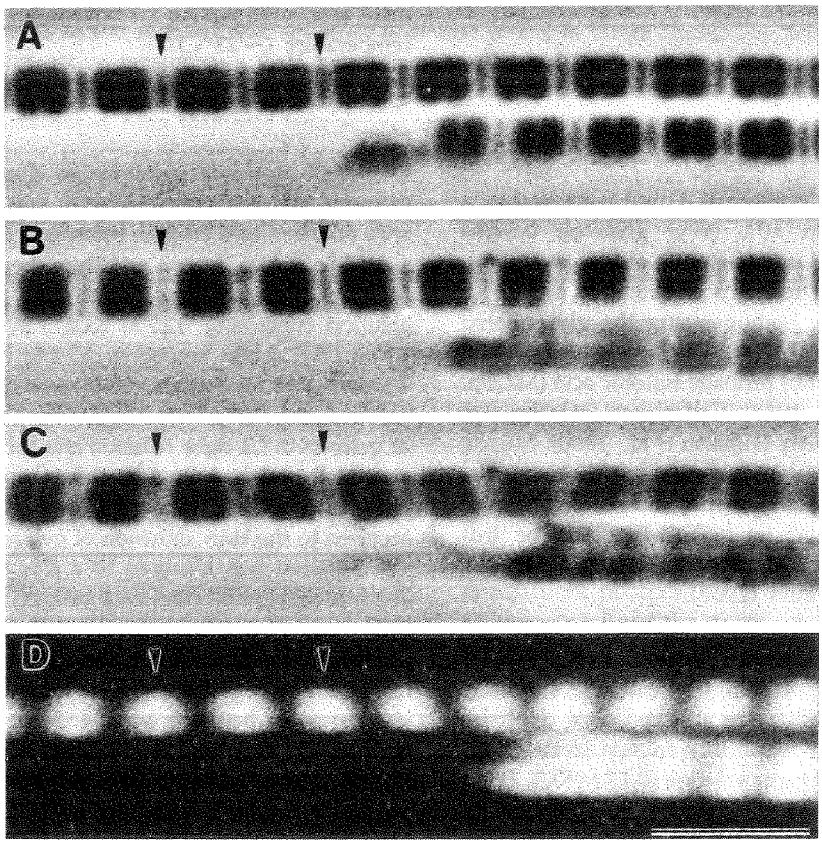

Fig. 1. Optical micrographs showing contraction of actin filament-reconstituted myofibrils. (A) Intact myofibrils. (B) Gelsolin-treated myofibrils; thin filaments in the myofibrils were removed by treatment with gelsolin (0.25 mg ml^{-1}) in a Ca rigor and in a contracting solution for 15 min each. (C, D) Actin filament-reconstituted myofibrils. Purified G-actin (0.5 mg ml^{-1}) which was mixed into BDM-relaxing solution just before use was added (for details, see Materials and Methods). Myofibrils shortened after removal of BDM. To visualize the location of reconstituted actin filaments, myofibrils were stained with rhodamine phalloidin in BDM-relaxing solution. (A, B, C) Phase-contrast micrographs; (D) fluorescence micrograph. Arrowheads indicate the positions of the Z lines. Scale bar = 5 μm.

Results

Reconstitution of actin filaments in myofibrils

To remove thin filaments from myofibrils adhered to a coverslip, myofibrils were treated with gelsolin (see Materials and Methods). The density of the I band decreased upon treatment with gelsolin under a phase-contrast microscope, indicating thin filaments had been removed (Fig. 1B; a small amount of shortening of the myofibrils occurred temporarily just after exchanging rigor solution with contracting solution containing gelsolin as observed in Fig. 1A, B). Removal of thin filaments except for short fragments located at the Z line was confirmed in other control experiments by staining myofibrils with rhodamine palloidin after formaldehyde fixation (data not shown,

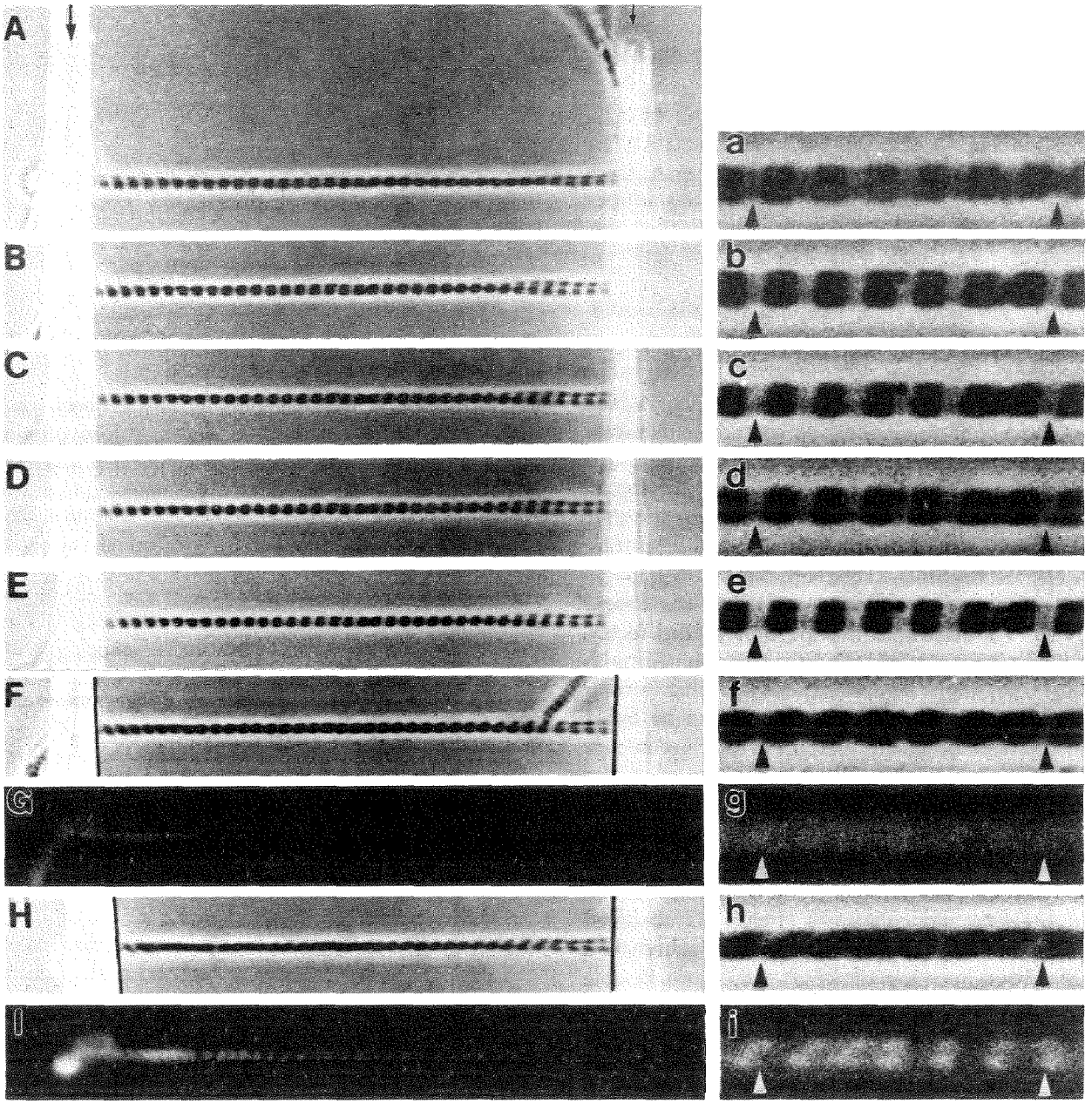

Fig. 2. Optical micrographs showing tension generation of an actin filament-reconstituted myofibril. Both ends of myofibril were attached to a pair of glass micro-needles (A large arrow indicates a stiff needle and a small arrow indicates a flexible needle). (A) Intact myofibril. (B, C) Gelsolin-treated myofibril; thin filaments were removed by treatment with gelsolin (0.25 mg ml^{-1}) in a Ca rigor (B) and in a contracting solution (C) for 15 min each. The solution was then exchanged with a relaxing solution (D) and a contracting solution (E). (F, G) Actin filaments were reconstituted in BDM-relaxing solution according to the same procedure as in Figs 1C, D. After the reconstituted actin filaments were labelled with rhodamine phalloidin, the solution was exchanged with relaxing solution (H, I). Solid lines in F, H indicate the inner edge of micro-needles. (A–F, H) phase-contrast micrographs; (G, I) fluorescence micrographs. (a–i) Higher magnification of (A–I), respectively. Arrowheads indicate the positions of the Z lines. Scale bars = 10 μm.

Table 1. Recovery of tension in actin filament-reconstituted myofibrils

	*Tension** (μg)	*Diameter* (μm)	*Tension per cross-sectional area‡* ($kg\ cm^{-2}$)
Control myofibril			
	37	1.19	3.33
	38	1.16	3.58
Average			3.46
Reconstituted myofibril			
	30	2.32	0.71
	16	1.80	0.63
	10	1.28	0.78
Average			0.71

*Tension of myofibrils was measured according to the method of Anazawa and colleagues (1992). Tension was undetectable in gelsolin-treated myofibrils.
‡Cross-sectioned area was assumed to be circular.

but the results were the same as those in Fig. 2 in Funatsu *et al.*, 1990).

To reconstitute actin filaments, purified G-actin which was in the process of polymerization was added (Ishiwata & Funatsu, 1985). Actin fragments remaining at the Z line were expected to function as nuclei for actin polymerization. The density of the I band increased again after polymerization of actin (Fig. 1C). When actin filaments were reconstituted, the myofibrils began to develop tension and shorten when BDM was absent (Fig. 1C, D). To determine the location of the reconstituted actin filaments, myofibrils were stained with rhodamine phalloidin. Figure 1D shows that strong fluorescence was observed at position where the intact thin filaments were originally located. Weak fluorescence was also observed at the H zone but this decreased after contraction.

The active tension of myofibrils was measured before the removal of and after the reconstitution of actin filaments with the microscopic method recently developed by Anazawa and colleagues (1992). As observed in Fig. 2, both ends of myofibrils were attached to a pair of micro-needles, one of which was more flexible than the other. The developed tension was measured from the displacement of the flexible needle. We confirmed that the thin filament-free myofibrils no longer generated tension (Fig. 2E). The actin filament-reconstituted myofibrils generated tension not only in contracting solution but also in relaxing solution (note that the distance between the two micro-needles in Fig. 2H is shorter than that in Fig. 2F). The tension was reversibly suppressed by the addition of 20 mM BDM to the relaxing solution. As summarized in Table 1, approximately 20% of the tension output was recovered by the reconstitution of actin filaments.

Optimal condition for reconstitution of actin filaments in muscle fibres

Reconstitution of thin filaments in muscle fibres was not successful with the method applied to the myofibrils. In the case of fibres, the following technical problems had

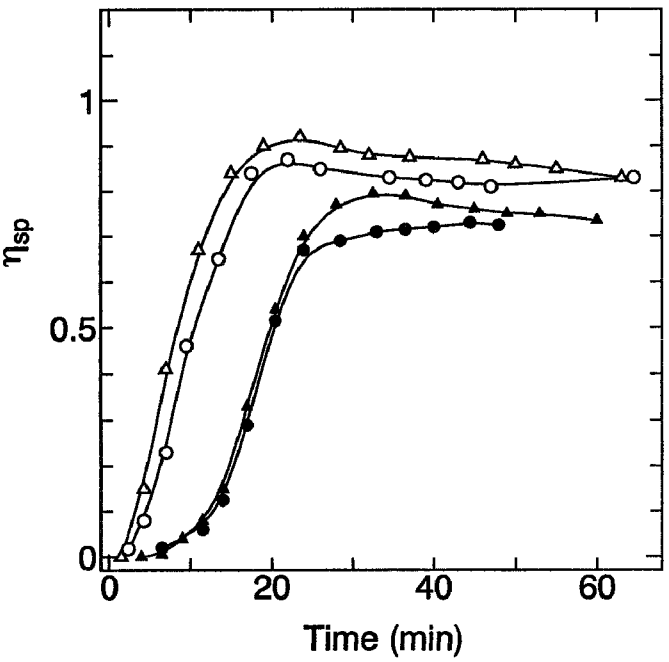

Fig. 3. Time course of polymerization of actin in solution. Polymerization of actin was induced by mixing G-actin and KCl (or KI) at time zero. The specific viscosity (η_{sp}) of the solution was measured by an Ostwald viscometer at 2°C. Flow time of solvent was approximately 120 s. Final concentrations, 1 mg ml^{-1} of actin, 80 mM KI (or KCl), 4 mM $MgCl_2$, 4 mM ATP, 4 mM, EGTA and 10 mM K-phosphate (pH 7); (○, ●) in the absence of BDM or (△, ▲) in the presence of 20 mM BDM; (●, ▲) polymerized by 80 mM KI or (○, △) 80 mM KCl.

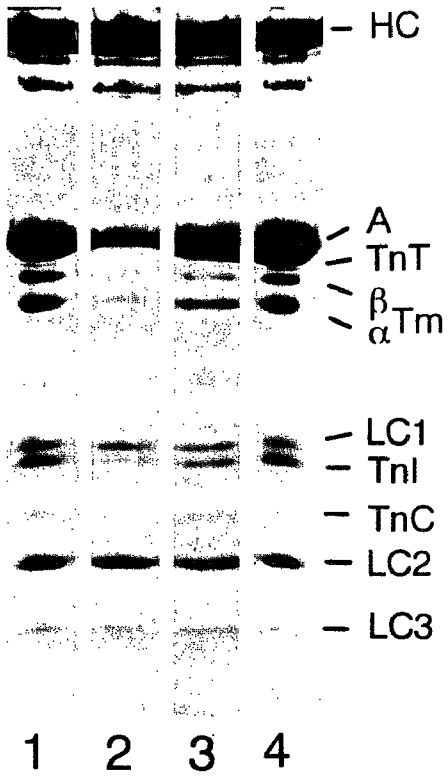

Fig. 4. SDS-PAGE patterns of rabbit psoas muscle fibres. (Lane 1) Control muscle fibres; (lane 2) muscle fibres treated with 0.5 mg ml^{-1} of gelsolin in Ca rigor solution and then in contracting solution at 2°C for 2 h each; (lane 3) after the gelsolin treatment, the muscle was incubated with 1 mg ml^{-1} of actin in the process of polymerization in 80 mM KI, 4 mM $MgCl_2$, 4 mM ATP, 4 mM EGTA, 20 mM BDM, and 10 mM K-phosphate (pH 7.0) for 10 min then repeated three times. Unbound actin molecules were washed out by relaxing solution containing 20 mM BDM. Tropomyosin and troponin complexes (total protein concentration 7 mg ml^{-1}) in the relaxing solution containing 20 mM BDM were then added for 1 h at 15°C. (Lane 4) Actin, tropomyosin and troponin were added to muscle fibres as in lane 3 without gelsolin treatment. HC, myosin heavy chain; LC1, myosin light chain 1; LC2, myosin light chain 2; LC3, myosin light chain 3; A, actin; Tm, tropomyosin; TnT, troponin T; TnI, troponin I; TnC, troponin C.

to be solved: (1) Spontaneous nucleation of actin polymerization had to be slowed as much as possible so that actin did not polymerize spontaneously before it diffused into the muscle fibres. (2) Active tension had to be suppressed during reconstitution to minimize the disorder of muscle fibres. To overcome these difficulties, actin was polymerized by KI at 2°C in the presence of BDM. As shown in Fig. 3, KI delayed the nucleus formation of actin polymerization with little effect on the final extent of polymerization. In the experimental condition used, spontaneous polymerization of actin was hardly observed within a 10 min period. The presence of 20 mM BDM had no significant effect on the polymerization of actin. KI was more advantageous than KCl because KI reduced the tension generation (data not shown) in addition to delaying polymerization of actin. Active tension disappeared in the presence of both 80 mM KI and 20 mM BDM. Thus it was possible to control the tension output of fibres without a regulatory system composed of tropomyosin-troponin complexes in the absence of Ca^{2+}.

We examined the degree of reconstitution by SDS-PAGE (Fig. 4). Approximately 90% of the actin, tropomyosin, and troponin were removed by gelsolin treatment (Fig. 4 lane 2). Figure 4 lane 3 showed that an additional 25% of actin and 20% of tropomyosin and troponin were incorporated into the fibre with the reconstitution of thin filaments (final content of actin, α-tropomyosin, and troponin C was 35%, 30%, and 30% of the original, respectively). The increase in quantity of actin, tropomyosin, and troponin did not appear to come from non-specific binding, since the amount of actin, tropomyosin, troponin incorporated into the fibre without gelsolin treatment under similar conditions was negligible (Fig. 4 lane 4).

Internal structure of muscle fibres before and after reconstitution of actin filaments

The internal structure of gelsolin-treated and actin filament-reconstituted muscle fibres was examined by thin section electron microscopy (Figs 5–7). Compared with intact fibres (Fig. 5), almost all thin filaments were removed by the gelsolin treatment (Fig. 6). The residual filaments observed at the I band were identified as connectin and nebulin (Funatsu *et al.*, 1990, 1993; Kruger *et al.*, 1991). On the addition of purified actin into the gelsolin-treated fibres, exogenous actin elongated from the Z line and finally penetrated into the A band (Fig. 7). Thick filaments appeared to be wavy by partial insertion of reconstituted actin filaments (Fig. 7A). The reconstituted actin filaments appeared to be thinner than thin filaments in an intact fibre (compare Figs 5C, D; 7C, D) owing to the lack of tropomyosin, troponin and nebulin. The numbers of thick filaments and thin filaments were counted on cross sections in the region of the A bands. The number ratio of thick and thin filaments in intact fibres was 1:2 (Fig. 5C, D). After the gelsolin treatment ~70 thin filaments remained for every ~4800 thick filaments (Fig. 6C) i.e. 0.7% of thin filaments remained. In Fig. 7C, ~1500 actin filaments were counted for every ~4800 thick filaments, indicating that 16% of the original number of thin filaments were reconstituted. The reconstituted actin filaments were located almost centrally in the hexagonal lattice of thick filaments where the thin filaments were originally located (Fig. 7C, D).

Cross sectional images showed that the spacing between thick filaments decreased after the removal of thin filaments (Figs 5C, D; 6C, D). The number densities of thick filaments in intact, gelsolin-treated and reconstituted fibres were, respectively, ~740, ~920 and ~820 μm^{-2} (Figs 5D, 6D & 7D). Thus, the corresponding lattice constants, i.e. the average distances between nearest-neighbour thick filaments, were, respectively, estimated

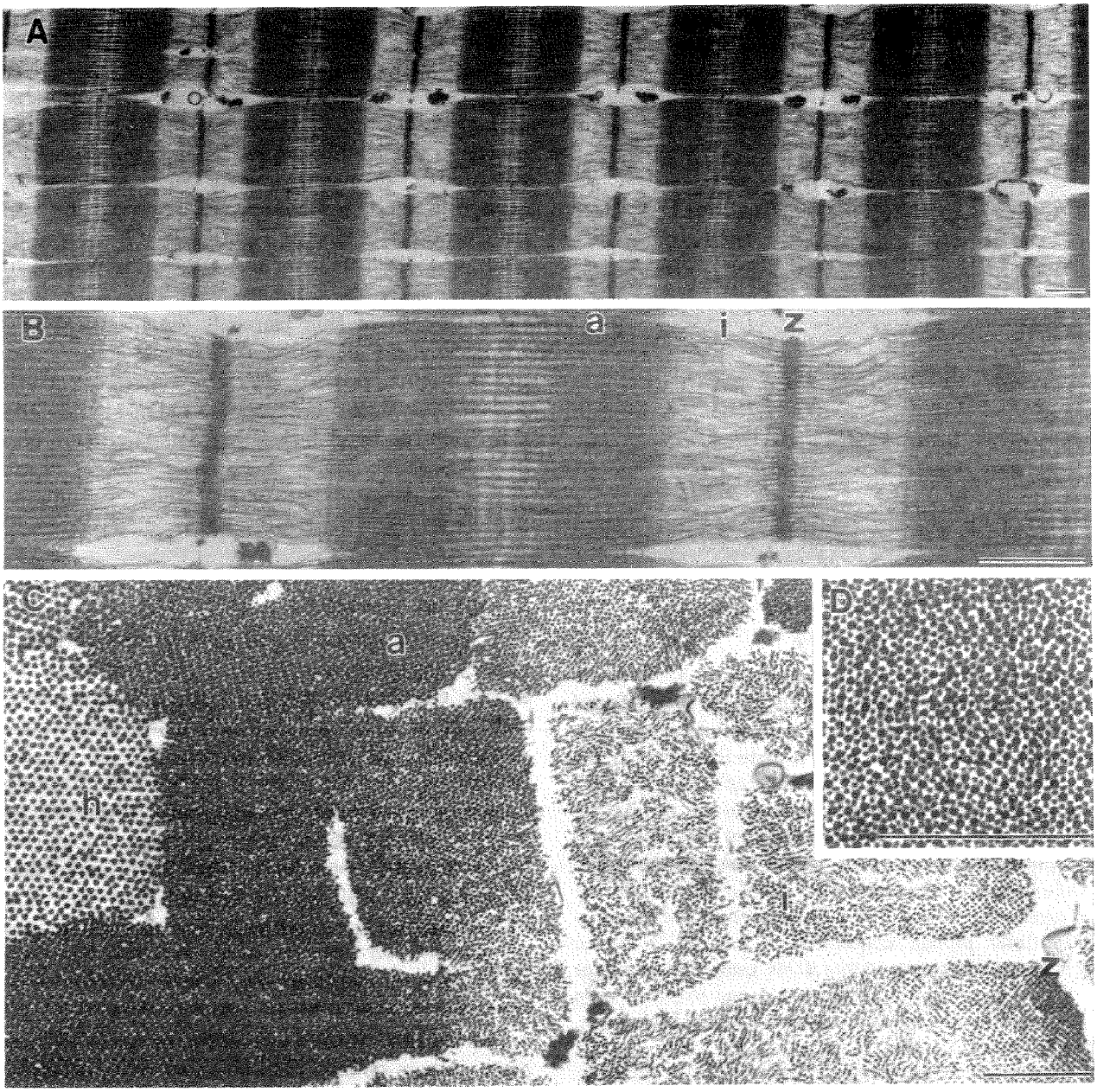

Fig. 5. Electron micrographs of glycerinated rabbit psoas muscle fibres. Longitudinal section views of the fibre at low (A) and high (B) magnification; cross section views of the fibre at low (C) and high (D) magnification. a, A band; i, I band; h, H zone; z, Z line. Scale bars = 0.5 μm.

to be 39.5, 35.4 and 37.5 nm. Moreover we explicitly measured the distance between nearest-neighbour thick filaments (Table 2). The distance was entirely dependent on whether adjacent actin filaments were present or not, i.e. 40 nm in the presence or 35 nm in the absence.

Tension recovery of reconstituted muscle fibres

Tension recovery after reconstitution of thin filaments in muscle fibres was examined. We measured the tension at low temperature (2–15°C) to minimize disorder of the fibres. Active tension could reproducibly be measured under our experimental conditions. Muscle fibres lost active tension after the gelsolin treatment (Fig. 8B). The active tension was recovered to ~20% of the original after the reconstitution of actin filaments (Fig. 8C). A characteristic feature of the actin filament-reconstituted fibres was that they generated tension in the presence of MgATP irrespective of whether Ca^{2+} was present or absent. The active tension could be reversibly inhibited by 20 mM BDM. After reconstitution of actin filaments in a muscle fibre of sarcomere length of 2.2 μm, the active tension of the reconstituted fibres at various sarcomere lengths was measured. Relative active tension has been plotted against a control fibre (Fig. 9). The magnitude of active tension decreased with increasing sarcomere length.

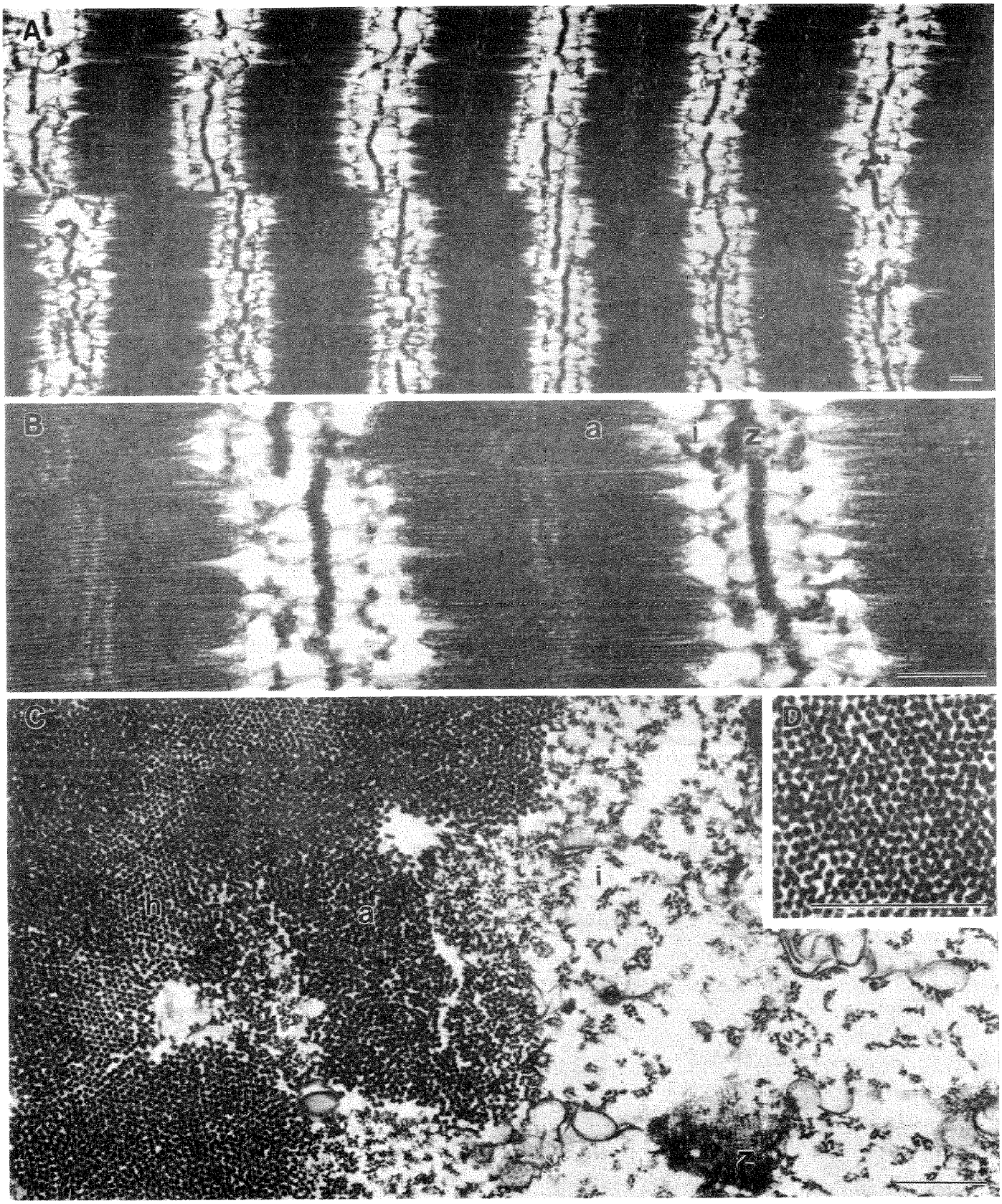

Fig. 6. Electron micrographs of gelsolin-treated muscle fibres. Longitudinal section views of the fibre at low (A) and high (B) magnification; cross section views of the fibre at low (C) and high (D) magnification. a, A band; i, I band; h, H zone; z, Z line. Scale bars = 0.5 μm.

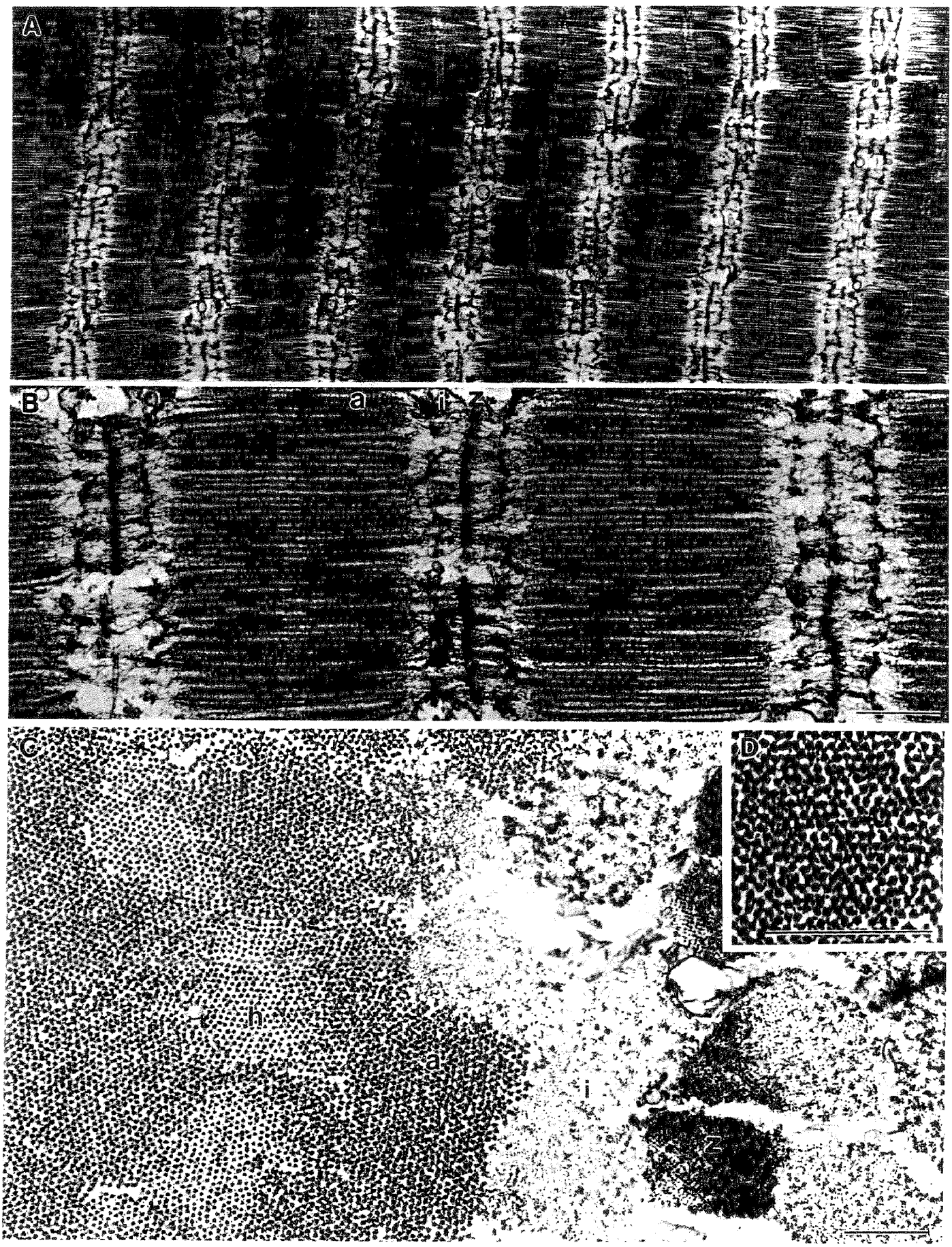

Fig. 7. Electron micrographs of actin filament-reconstituted muscle fibres. Longitudinal section views of the fibre at low (A) and high (B) magnification; cross section views of the fibre at low (C) and high (D) magnification. a, A band; i, I band; h, H zone; z, Z line. Scale bars = 0.5 μm.

Table 2. The distance between nearest-neighbour thick filaments

	Distance (nm)
Control fibre	40 ± 2.9 (n = 153)
Gelsolin-treated muscle	35 ± 4.1 (n = 159)
Reconstituted muscle	
(distance between thick filaments which are adjacent to actin filaments)	39 ± 4.9 (n = 107)
(distance between thick filaments which are not adjacent to actin filaments)	35 ± 4.3 (n = 109)

Reconstitution of thin filaments with tropomyosin and troponin in muscle fibres

Thin filaments were reconstituted by adding tropomyosin–troponin complexes into actin filament-reconstituted muscle fibres. The thin filament-reconstituted fibres regained sensitivity to Ca^{2+} (Fig. 8D). The magnitude of active tension hardly changed on the addition of regulatory proteins (Fig. 8C, D). In the reconstituted fibres, the cooperativity on the activation by Ca^{2+} was slightly reduced (Fig. 10); Hill coefficient of reconstituted fibres was 1.8, while that of intact muscle was 2.5

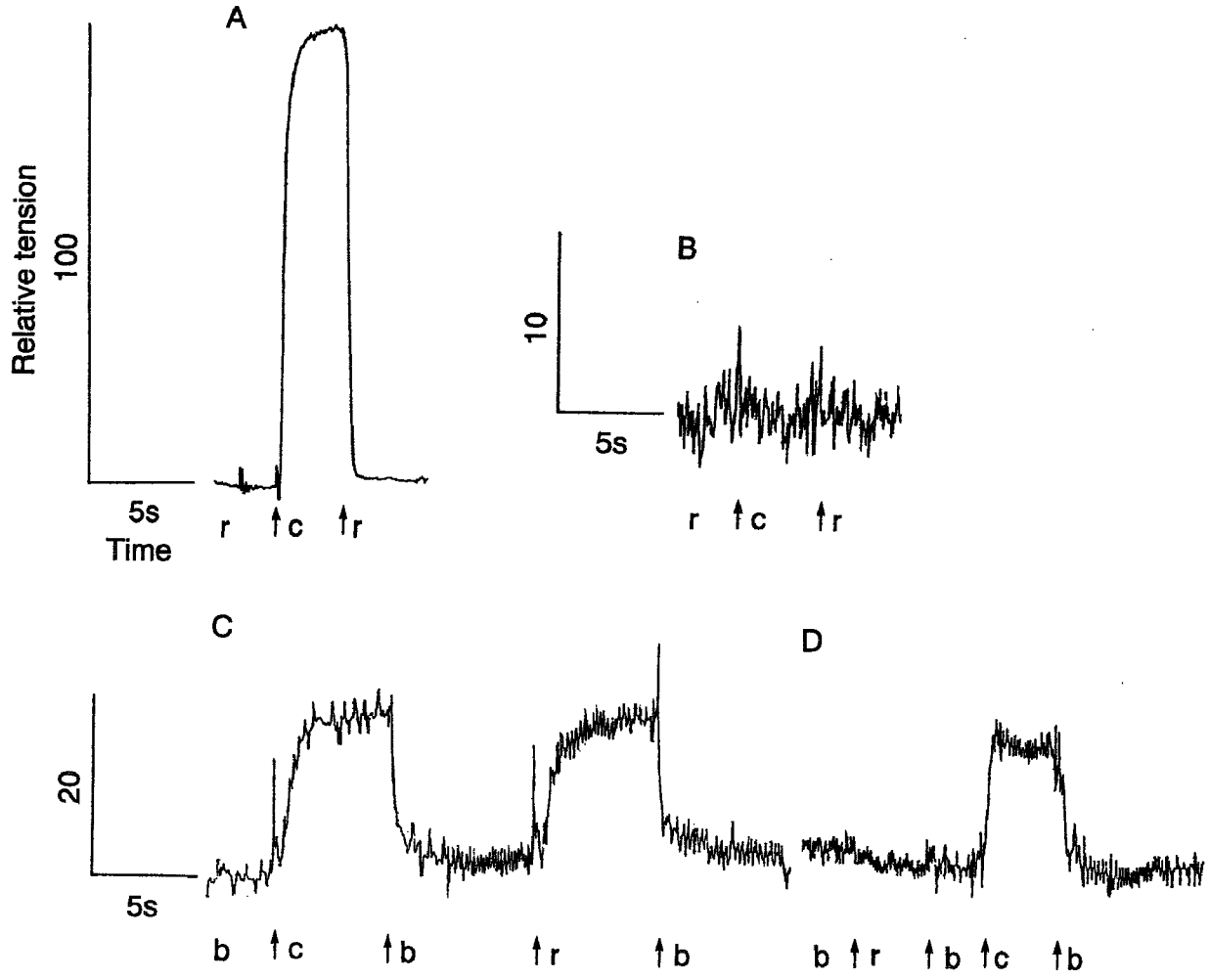

Fig. 8. Tension traces of a muscle fibre at various stages of reconstitution of thin filaments. (A) Initial intact fibre. (B) After thin filaments in the fibre had been removed by gelsolin treatment. (C) Actin filaments were reconstituted by adding exogenous actin (for details, see Materials and Methods). (D) Thin filaments were reconstituted by adding tropomyosin and troponin complexes. All traces were taken from the same fibre. Arrows indicate the time at which solution was exchanged. Active tension was measured at low ionic strength as muscle fibres generated more force than at physiological ionic strength. Noise came from the blow of a chiller in the cold room. Spikes were artifacts of solution changes. b, Low salt relaxing solution containing BDM ([25 mM KCl, 5 mM $MgCl_2$, 5 mM ATP, 4 mM EGTA, 20 mM BDM and 20 mM MOPS (pH 7.0)]). c, Low salt contracting solution (20 mM KCl, 5 mM $MgCl_2$, 5 mM ATP, 4 mM EGTA, 4.1 mM $CaCl_2$ and 20 mM MOPS (pH 7.0)). r, Low salt relaxing solution (25 mM KCl, 5 mM, $MgCl_2$, 5 mM ATP, 4 mM EGTA and 20 mM MOPS (pH 7.0)). Sarcomere length, 2.5 μm. Tension was measured at 15°C.

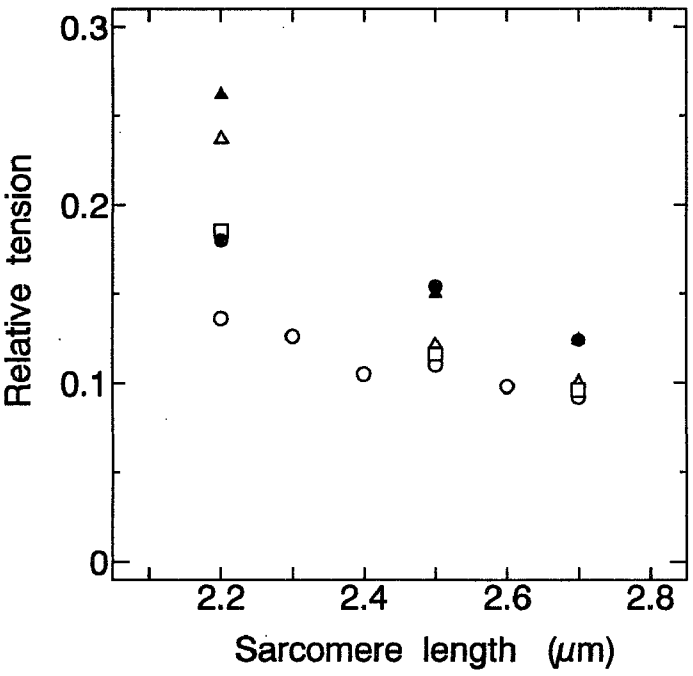

Fig. 9. Recovery of force generation of actin filament-reconstituted muscle fibres at various sarcomere lengths. Actin filaments in gelsolin-treated fibres were reconstituted at sarcomere length of 2.2 μm by adding exogenous actin in the presence of BDM (for details, see Materials and Methods). After reconstitution of actin, active tension was generated by changing solution to a contracting solution without BDM. The active tension of the reconstituted fibre relative to that in an intact fibre was plotted against the various sarcomere lengths. Results of five independent specimens (○,△,□,●,▲) are shown.

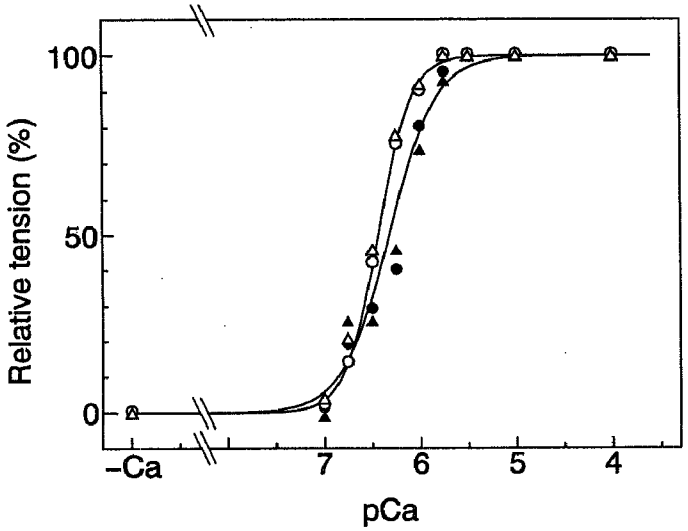

Fig. 10. The relationship between the isometric tension developed by muscle fibres and the free Ca^{2+} concentration. Open and closed symbols show intact and reconstituted fibres, respectively; circles and triangles show two independent experiments. Tension was normalized to that at pCa 4.0. Solid lines are curves fitted by Hill equations. Sarcomere length, 2.5 μm. Tension was measured at 15°C.

(average of two independent experiments). Also, the Ca^{2+}-sensitivity slightly decreased as the pCa value at half-maximum tension (pCa_{50}) was shifted to a lower level by approximately 0.3 pCa units.

Discussion

Structural and functional reconstitution of actin filaments

In the present work, reconstitution of actin filaments in gelsolin-treated muscle fibres and fibrils has been achieved for the first time. The reconstituted actin filaments were attached to the Z line at one end and oriented along the longitudinal axis of the myofibrils (Fig. 7A, B). We inferred that actin molecules were polymerized onto short fragments of actin filaments that remained at the Z line; the actin filaments must have functioned as nuclei for polymerization (Ishiwata & Funatsu, 1985). Some of reconstituted actin filaments were uniformly distributed along a myofibril (see diffuse fluorescence in Figs 2G & 2g), but they appeared to be dissociated during contraction of reconstituted fibrils (fluorescence was more localized in Figs 1D, 2I & 2i). This suggests that a part of reconstituted filaments were associated with thick filaments without attaching to the Z line, however these were released during contraction.

A decrease in the recovery ratio of relative tension at longer sarcomere lengths (Fig. 9) may be explained by the variation in length of the reconstituted actin filaments. The length distribution of reconstituted actin filaments, however, was not so broad as that *in vitro* judging from the fact that the shape of the fluorescent section was similar to the original I–Z–I brush (Figs 1D, 2I & 2i). Thus, the data showing the density of the reconstituted filaments in EM images, the quantity of incorporated actin determined by SDS-PAGE, and the recovery of active tension, i.e., about 20% of the intact, strongly suggest that the isometric tension borne by actin filaments is similar to that borne by native thin filaments.

Electron micrographs of cross sections of reconstituted fibres showed that the reconstituted actin filaments were located in a trigonal position in the hexagonal lattice formed by thick filaments (Fig. 7C, D), suggesting that this is a stable position for actin filaments (Hayashi *et al.*, 1977; Higuchi *et al.*, 1988). As shown in Table 2, the lattice constant decreased from 40 nm to 35 nm on removal of thin filaments (Figs 5C, D; 6C, D) and recovered to almost the original value after reconstitution of actin filaments (Fig. 7C, D). Such a large shrinkage of the filament lattice may be ascribed to artifact during preparation of specimen for electron microscopy. For a precise measurement of the lattice constant in the thin filament-free fibres, examination by X-ray diffraction is necessary.

Recently, it has been reported that nebulin is a component of the thin filaments in skeletal muscle (Wang & Wright, 1988) and a strong candidate for a length

regulator or a ruler of thin filaments (Wang & Wright, 1988; Kruger *et al.*, 1991; Labeit *et al.*, 1991). After treatment with gelsolin, a part of nebulin which located at a side of free end of the thin filament seems to be folded and entangled at the N2 line (Funatsu *et al.*, 1990; Kruger *et al.*, 1991). Another part of nebulin located between the N_2 line and the Z line may remain as an elongated form. Since it is known that nebulin associates with actin filaments *in vitro* (Jin & Wang, 1991), this part of nebulin may function as a guide for the polymerization of actin from the Z line. We are currently investigating the role that nebulin may play in the reconstitution of thin filaments by applying this same technique to bovine glycerinated cardiac muscle, as nebulin is absent in cardiac muscle (Locker & Wild, 1986; Hu *et al.*, 1986; Itoh *et al.*, 1988; Wang & Wright, 1988).

The key step in removal and reconstitution of thin filaments is how to maintain the Z line structure intact. Addition of proteinase inhibitors such as DFP and leupeptin improved the preservation of the structure, while longer treatment with gelsolin caused gradual disruption of the Z line even in the presence of higher concentrations of the proteinase inhibitors. Removal of actin at the Z line appeared to be a main reason for this disruption in structure.

In the present study, we tried to remove the majority of thin filaments to get a complete loss of active tension generation. When the fibres were vigorously treated with gelsolin, the partial disruption of the Z line structure was observed as shown in Figs 6 and 7. Figure 7 shows that thin filaments were not reconstituted in the region where the Z line was damaged. If the Z line is kept intact, a greater number of actin filaments would be expected to be present after reconstitution. If complete loss of active tension is not required and a smaller proportion of reconstitution is sufficient, a mild treatment with gelsolin is recommended. In this respect, cardiac muscle may be suitable for reconstituting thin filaments because the Z line structure appears to be more solid.

Reconstitution of thin filaments

We have shown that the Ca^{2+} sensitivity could be recovered by simply adding tropomyosin-troponin complexes to the actin filament-reconstituted fibres (Fig. 8). However, the tension versus pCa relation (Fig. 10) shows that both the cooperativity and the Ca^{2+} sensitivity were reduced slightly upon reconstitution. This may be ascribed to the incomplete binding of tropomyosin-troponin complexes to both grooves along a long helix of actin filaments or the change of the spacing within the filament lattice during preparation (Endo, 1972; Ishiwata & Oosawa, 1974). It is possible that better reconstitution of the thin filaments may be achieved by annealing the reconstituted fibres for a longer incubation time at a higher temperature in the presence of Ca^{2+}, for example, 1 h at 30°C (Ishiwata, 1973). In any case, the most appropriate conditions for reconstitution of thin filaments have yet to be fully elucidated.

The active tension generated by the actin filament-reconstituted fibres was not significantly affected by the addition of tropomyosin and troponin (Fig. 8). There are several reports showing that actomyosin ATPase activity is potentiated by the addition of tropomyosin (and troponin) *in vitro* (see Bremel *et al.*, 1972), but the present result suggests that the magnitude of active tension is not substantially increased. This may suggest that a tropomyosin–troponin complex simply functions as a switch for muscle activation. To elucidate this issue, better reconstitution of thin filaments and quantitative studies are required.

Mechanism of length determination of thin filaments

In intact skeletal muscle, the free end of the thin filaments corresponding to the pointed end of actin filaments is closed, so that additional polymerization of actin is inhibited (Sanger *et al.*, 1984; Ishiwata & Funatsu, 1985; Peng & Fischman, 1991). The free end becomes open by treatment with a high salt solution, that is, exogenous actin can polymerize onto the pointed ends after the high salt treatment, probably because the capping structure is removed (Ishiwata & Funatsu, 1985). In the present work, the capping structure was removed together with thin filaments by the gelsolin treatment, so that the pointed end of actin fragments remaining at the Z line must have been available for the polymerization of exogenous actin.

Recently, Fowler and colleagues (1993) reported that tropomodulin functions as a capping protein of thin filaments in skeletal muscle. Nebulin has been proposed to be a length determining ruler of thin filaments as mentioned above (Kruger *et al.*, 1991; Labeit *et al.*, 1991). The length distribution of reconstituted actin filaments was, however, not as broad as the exponential distribution observed in a solution at equilibrium (Fig. 1D). This suggests that the length of actin filaments may be regulated to some extent in the fibres and fibrils even without the interaction with nebulin, tropomyosin and tropomodulin. There is a possibility that the crystalline array of crossbridges distributed on thick filaments may regulate the polymerization of actin (Kawamura & Maruyama, 1970). Thin filament-free fibres will contribute to the study of the molecular mechanism for length determination of thin filaments.

Application of reconstituted fibres as a new experimental system

Until recently, the tension generation of the actomyosin complex was investigated by using so-called actomyosin thread. This thread was prepared by pushing out actomyosin complex dissolved in a high salt solution into a low salt solution through a thin syringe (see Crooks & Cooke, 1977). After the *in vitro* motility assay system was introduced several years ago, it has become possible to study the tension generation on a single actin filament

(Kishino & Yanagida, 1988). There is no doubt that these *in vitro* systems are powerful experimental tools for studying the structure and function of actin during contraction. However, in the *in vitro* motility system the myosin molecules will be randomly oriented. Our reconstituted system is superior to these previously used as the preparations have highly organized structure with the orientation of filaments and the periodic liquid-crystalline lattice structure resembling that of intact sarcomeres.

Reconstitution of actin using fluorescence- or spin-labelled proteins will make it possible to study the conformational change of thin filaments accompanying muscle contraction and its regulation; the present thin filament-reconstituted system is especially suitable for studying the orientation of actin, tropomyosin and troponin. Furthermore, our system will be useful for studying the structure and function of mutant proteins.

Acknowledgements

We would like to thank Dr Yoshiki Umazume (Jikei University) for sharing the apparatus for measuring tension of muscle fibres and Drs Hideo Higuchi, Yoshiharu Ishii (ERATO) and Jan M. West (Osaka University) for their advice and critical reading of the manuscript. We also wish to thank Mr Kiwamu Saito (ERATO) for analyses of polyacrylamide gel images. This work was partly supported by Grants-in-Aids for Scientific Research (No. 04402053 to S. Ishiwata) and for Scientific Research on Priority Areas (No. 04237228 to S. Ishiwata) from the Ministry of Education, Science and Culture of Japan.

References

ANAZAWA, T., YASUDA, K. & ISHIWATA, S. (1992) Spontaneous oscillation of tension and sarcomere length in skeletal myofibrils. Microscopic measurement and analysis. *Biophys. J.* **61**, 1099–108.

BREMEL, R. D., MURRAY, J. M. & WEBER, A. (1972) Manifestations of cooperative behavior in the regulated actin filament during actin-activated ATP hydrolysis in the presence of calcium. In *Cold Spring Harb. Symp. Quant. Biol.* **37**, 267–75.

CROOKS, R. & COOKE, R. (1977) Tension generation by threads of contractile proteins. *J. Gen. Physiol.* **69**, 37–55.

EBASHI, S., KODAMA, A. & EBASHI, F. (1968) Troponin. I. Preparation and physiological function. *J. Biochem.* **64**, 465–77.

ENDO, M. (1972) Stretch-induced increase in activation of skinned muscle fibres by calcium. *Nature New Biol.* **237**, 211–13.

FOWLER, V. M., SUSSMANN, M. A., MILLER, P. G., FLUCHER, B. E. & DANIELS, M. D. (1993) Tropomodulin is associated with the free (pointed) ends of the thin filaments in rat skeletal muscle. *J. Cell Biol.* **120**, 411–20.

FUNATSU, T. & ISHIWATA, S. (1989) Reconstitution of thin filaments and partial recovery of contractility in gelsolin-treated muscle fibers. *J. Muscle Res. Cell Motil.* **10**, 258–9 (Abstr.).

FUNATSU, T., HIGUCHI, H. & ISHIWATA, S. (1990) Elastic filaments in skeletal muscle revealed by selective removal of thin filaments with plasma gelsolin. *J. Cell Biol.* **110**, 53–62.

FUNATSU, T., KONO, E., HIGUCHI, H., KIMURA, S., ISHIWATA, S., YOSHIOKA, T., MARUYAMA, K. & TSUKITA, S. (1993) Elastic filaments *in situ* in cardiac muscle: deep-etch replica analysis in combination with selective removal of actin and myosin filaments. *J. Cell Biol.* **120**, 711–24.

HAYASHI, T., SILVER, R. B., IP, W., CAYER, M. L. & SMITH, D. S. (1977) Actin-myosin interaction. Self-assembly into a bipolar contractile unit. *J. Mol. Biol.* **111**, 159–71.

HIGUCHI, H., YOSHIOKA, T. & MARUYAMA, K. (1988) Positioning of actin filaments and tension generation in skinned muscle fibers released after stretch beyond overlap of the actin and myosin filaments. *J. Muscle Res. Cell Motil.* **9**, 491–8.

HIGUCHI, H. & TAKEMORI, S. (1989) Butanedione monoxime suppresses contraction and ATPase activity of rabbit skeletal muscle. *J. Biochem.* **105**, 638–43.

HORIUTI, K. (1986) Some properties of the contractile system and sarcoplasmic reticulum of skinned slow fibers from xenopus muscle. *J. Physiol.* **373**, 1–23.

HORIUTI, K., HIGUCHI, H., UMAZUME, Y., KONISHI, M., OKAZAKI, O. & KURIHARA, S. (1988) Mechanism of action of 2,3-butanedione 2-monoxime on contraction of frog skeletal muscle fibres. *J. Muscle Res. Cell Motil.* **9**, 156–64.

HU, D. H., KIMURA, S. & MARUYAMA, K. (1986) Sodium dodecyl sulfate gel electrophoretic studies of connectin-like high molecular weight proteins of various types of vertebrate and invertebrate muscle. *J. Biochem.* **99**, 1485–92.

HUXLEY, H. & HANSON, J. (1954) Changes in the cross-striations of muscle during contraction and stretch and their structural interpretation. *Nature* **173**, 973–7.

ISHIWATA, S. (1973) A study on the F-actin-tropomyosin-troponin complex. I. Gel-filament transformation. *Biochim. Biophys. Acta* **303**, 77–89.

ISHIWATA, S. & OOSAWA, F. (1974) A regulatory mechanism of muscle contraction based on the flexibility change of the thin filaments. *J. Mechanochem. Cell Motil.* **3**, 9–17.

ISHIWATA, S. & FUNATSU, T. (1985) Does actin bind to the ends of thin filaments in skeletal muscle? *J. Cell Biol.* **100**, 282–91.

ITOH, Y., MATSUURA, T., KIMURA, S. & MARUYAMA, K. (1988) Absence of nebulin in cardiac muscles of the chicken embryo. *Biomed. Res.* **9**, 331–3.

JIN, J. P. & WANG, K. (1991) Cloning, expression, and protein interaction of human nebulin fragments composed of varying numbers of sequence modules. *J. Biol. Chem.* **266**, 21215–23.

KATSURA, I. & NODA, H. (1973) Assembly of myosin molecules into the structure of thick filaments of muscle. *Adv. Biophys.* **5**, 177–202.

KAWAMURA, M. & MARUYAMA, K. (1970) Electron microscopic particle length of F-actin polymerized *in vitro*. *J. Biochem.* **67**, 437–57.

KISHINO, A. & YANAGIDA, T. (1988) Force measurements by micromanipulation of a single actin filament by glass needles. *Nature*, **334**, 74–6.

KRUGER, M., WRIGHT, J. & WANG, K. (1991) Nebulin as a length regulator of thin filaments of vertebrate skeletal muscles: correlation of thin filament length, nebulin size, and epitope profile. *J. Cell Biol.* **115**, 97–107.

LABEIT, S., GIBSON, T., LAKEY, A., LEONARD, K., ZEVIANI, M., KNIGHT,

P., WARDALE, J. & TRINICK, J. (1991) Evidence that nebulin is a protein-ruler in muscle thin filaments. *FEBS Lett.* **282,** 313–16.

LAEMMLI, U. K. (1970) Cleavage of structural proteins during the assembly of the head of bacteriophage T4. *Nature* **227,** 680–5.

LI, T., SPERELAKIS, N., TENEICK, R. E. & SOLARO, J. (1985) Effects of diacetyl monoxime on cardiac excitation-contraction coupling. *J. Pharmacol. Exp. Ther.* **232,** 688–95.

LOCKER, R. H. & WILD, D. J. C. (1986) A comparative study of high molecular weight proteins in various types of muscle across the animal kingdom. *J. Biochem.* **99,** 1473–84.

MAW, M. C. & ROWE, A. J. (1986) The reconstruction of myosin filaments in rabbit psoas muscle from solubilized myosin. *J. Muscle Res. Cell Motil.* **7,** 97–109.

PENG, I. & FISCHMAN, D. A. (1991) Post-translational incorporation of actin into myofibrils *in vivo*: evidence for isoform specificity. *Cell Motil. Cytoskeleton,* **20,** 158–68.

SANGER, J. W., MITTAL, B. & SANGER, J. M. (1984) Analysis of myofibrillar structure and assembly using fluorescently labeled contractile proteins. *J. Cell Biol.* **98,** 825–33.

SPUDICH, J. A. & WATT, S. (1971) The regulation of rabbit skeletal muscle contraction. I. Biochemical studies of the interaction of the tropomyosin-troponin complex with actin and the proteolytic fragments of myosin. *J. Biol. Chem.* **246,** 4866–71.

TANIGUCHI, M. & ISHIKAWA, H. (1982) *In situ* reconstitution of myosin filaments within the myosin extracted myofibril in cultured skeletal muscle cells. *J. Cell Biol.* **92,** 324–32.

TAWADA, K., YOSHIDA, A. & MORITA, K. (1976) Myosin-free ghosts of single fibers and an attempt to re-form myosin filaments in the ghost fibers. *J. Biochem.* **80,** 121–7.

WANG, K. & WRIGHT, J. (1988) Architecture of the sarcomere matrix of skeletal muscle: immunoelectron microscopic evidence that suggests a set of parallel inextensible nebulin filaments anchored at the Z line. *J. Cell Biol.* **107,** 2199–212.

Optical methods in biomedical and environmental sciences.
H. Ohzu and S. Komatsu, editors.

Microscopic measurement of the sliding and binding force between muscle proteins with optical tweezers

T. Nishizaka[a], H. Miyata[b], H. Yoshikawa[b], S. Ishiwata[a] and K. Kinosita Jr[b]

[a]Department of Physics, School of Science and Engineering, Waseda University, Okubo, Shinjuku-ku, Tokyo169

[b]Department of Physics, Faculty of Science and Technology, Keio University, Hiyoshi, Kohoku-ku, Yokohama 223, Japan

INTRODUCTION

The *in vitro* motile system recently developed has shown that myosin heads, a molecular motor of contractile system of muscle, are sufficient to generate a sliding force on a single actin filament [1,2]. We have examined the sliding and binding force between an actin filament and heavy-meromyosin (HMM, proteolytic fragment of myosin) molecules under various conditions by using a dual (fluorescence and phase-contrast) imaging microscope system and optical tweezers. The force produced on the actin filament was measured by trapping a polystyrene bead selectively attached to the rear end of the actin filament. First, the sliding force and its fluctuation generated on the actin filament were measured under various surface densities of HMM in the presence of ATP. Under low densities of HMM, the spike-like displacement of the actin filament was observed, reflecting the intrinsic properties of the sliding force generated by a few myosin heads. Second, the binding force between an actin filament and a single HMM molecule was measured in the absence of ATP.

MATERIALS AND METHODS

Optical tweezers is a technique to capture and manipulate a small particle of a micrometer size by means of a single beam of laser-light without direct contact [3]. A polystyrene bead, 1μm in diameter, was used as a trap particle. The optical trap force against the bead was proportional to the displacement from the center of the trap (the maximum slope, 0.4pN/nm at 150mW of laser power) for excursions of the bead out to 200nm, so that small biological forces mediated by motor proteins could be measured within the range of 0 to 80pN. The inverted microscope (TMD-300; Nikon, Tokyo) was equipped with a home-made optical apparatus and 1W Nd-YAG laser (1053-1000p; Amoco Laser Co., IL) as the optical tweezers system. A single actin filament labeled with fluorescent probe, rhodamine phalloidin, was visualized by using a CCD camera

equipped with an image intensifier [4,5]. The image of the bead was simultaneously observed by using another CCD camera equipped in a modified dual-view microscope as a phase-contrast image differing from fluorescence image in color and stored in a digital frame memory [6]. The position of the bead was determined by calculating the centroid of its intensity profile with a spatial resolution of nanometer scale. To apply the above method to the *in vitro* motile system, the bead was selectively attached to the rear end of an actin filament through an actin binding protein, gelsolin; HMM was attached to a glass surface precoated with nitrocellulose.

RESULTS AND DISCUSSION

In the presence of ATP, actin filaments slid on the glass surface and the bead attached to the filament was pulled by the sliding force generated by HMM molecules. Figure 1 shows the displacement of the bead at two different surface densities of HMM. In Fig. 1a, the actin filament undergoing the Brownian motion happened to come contact with the surface at 2sec and started to slide. The bead was pulled against the trapping force immediately after the filament was taut. In the case that the sliding force overcomes the trapping force, the bead escapes from the trapping area and the filament slides smoothly. In the case of Fig. 1, the maximum trapping force was stronger than the sliding force (the spring constant of the trapping force was adjusted to 0.04 (a) or 0.024pN/nm (b)), so that the bead was displaced up to the position where two forces acting in opposite directions were balanced. The bead fluctuated around the average position, i.e., 8pN (Fig. 1a) or 1pN (Fig. 1b). The relation between the sliding force and the number of interacting HMM molecules was studied by changing the concentrations of HMM

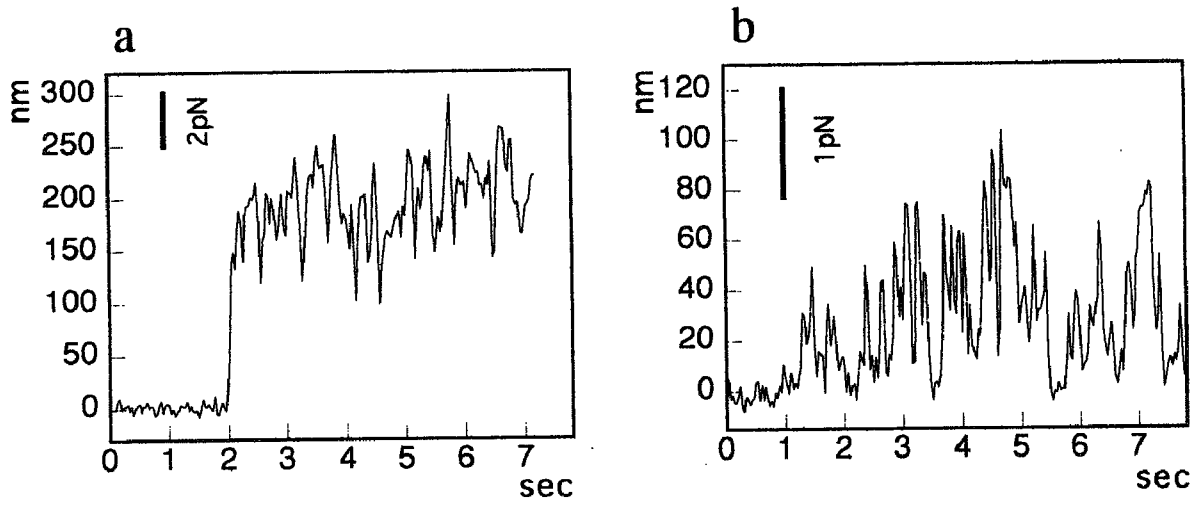

Figure 1. Displacement of the bead from the center of the trap. Condition, 1mM ATP (other solvent conditions, see [5]); HMM, 100 (a) or 30 (b) μg/ml; length of the actin filament, 6.1 (a) or 6.6 (b) μm.

perfused into a flow cell. We found that the average force was nearly proportional to the surface density of HMM. The slope of the linear relation showed about 1pN increase per 1μm of an actin filament every 100μg/ml of HMM. The HMM concentration of 25μg/ml was a lower limit to induce continuous sliding movement; all actin filaments were dissociated from the surface below this concentration. Around this critical concentration, the trapped filament frequently detached from the glass surface and the bead returned to the original position (Fig. 1b). The filament undergoing Brownian motion sometimes attached to the glass surface, slid for an instant and immediately detached, so that a spike-like force was produced. The height of the spike corresponded to 1-2 pN, but a part of these values may have been underestimated because of a low time resolution in our system (video rate, 1/30s). Judging from the fact that the bead returned to the center of the trapping force, there must be a moment that all of the interacting HMM molecules detached from the actin filament. On the other hand, such a moment may not exist for the filaments continuously sliding without load. It is inferred that a myosin head can not sustain the actin filament when the load largely fluctuates.

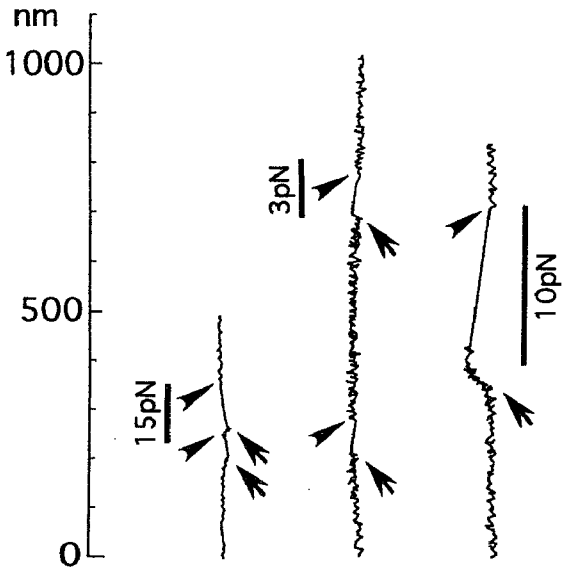

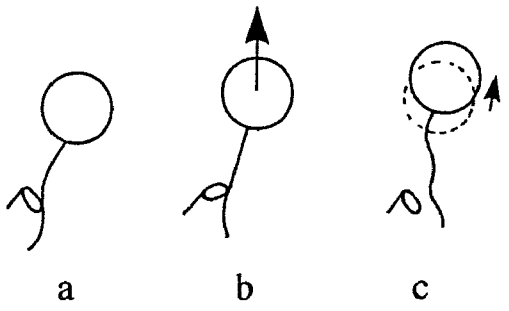

Figure 3. Schematic illustration of the process that the rigor bond between an actin filament and single HMM was broken. For a-c, see the text.

Figure 2. Examples of the trace of the bead which followed the center of the trap moving at a constant rate (100nm/s). The spring constant of the trapping force was changed at each sample. For arrows and arrowheads, see the text.

In the absence of ATP, myosin heads strongly bind to an actin filament. On the surface coated with very low concentrations of HMM, e.g., 1μg/ml, nodal points were observed along an actin filament; the filament was fixed at the nodal point but a part of the filament between the nodal points showed Brownian bending motion. Under high concentrations of HMM, such nodal points could not be observed and all parts of a filament attached to the surface, so that each nodal point is considered to correspond to an HMM molecule forming rigor bond. Using the

laser trap system movable at a constant rate, we imposed the external load on the acto-HMM complex, i.e., a crossbridge. Figure 2 shows the trace of the bead in the process that the short actin filament with only one or two nodal points was stretched (cf. Fig. 3). The center of the optical trap was moved upward at a constant rate, 100nm/sec. First, the bead followed the laser spot smoothly (see the trace below each arrow in Fig. 2; cf. Figs. 3a & b), but stopped when the actin filament was taut (see arrows in Fig. 2; cf. Fig. 3b). As the spot moved, the load imposed on the crossbridge increased in proportion to the distance between the bead and the trap center. As soon as the rigor bond was broken, the bead returned to the preceding trap center (see arrowheads in Fig. 2; cf. Fig. 3c). From this momentary displacement (see the straight part of the trace between arrow and arrowhead in Fig. 2), we could directly determine the force needed to break the rigor bond. The tensile strength thus estimated scattered between a few and 15 pN (Fig. 2). It appeared to be dependent on the direction of the imposed force, which may be ascribed to the asymmetrical structure of a myosin head. The mechanical work required for tearing off the rigor bond should be compared to the chemical energy derived from one ATP hydrolysis; the latter is 8.4×10^{-20} J, which is equivalent to the work required for the displacement of 8.4nm at 10pN. This is the first direct measurement of the binding force between actin and myosin and the first step to fully characterize the force produced by the motor proteins of muscle.

The number of HMM molecules interacting with a single actin filament was also estimated using the above method. When the long filament was loaded in the absence of ATP, the part of the filament was stretched straight from the nodal point and came off. These points were broken one after another, so that we could directly count the number of HMM molecules that had attached to the filament. Under 1μg/ml HMM, the number of HMM molecules that bound to the actin filament of 1μm long was about 1. This estimation suggests that 30 HMM molecules interact with the actin filament of 1μm long under 30μg/ml HMM (Fig. 2). If the fraction of myosin heads in the force-generating state is small, for example 5%, the average number of force-generating HMM molecules at one moment is estimated to be about 1.5 per 1μm of the filament. This number is plausible to generate the spike-like forces observed in this study.

The new methods used here enabled the measurement of the sliding and binding force exerted by muscle protein motors at a single motor level. The same method was successfully applied to the characterization of kinesin, a motor protein which transports organelles in the cell in collaboration with a microtubule. An 8nm stepwise motion was observed at very low concentrations of ATP [7]. Such stepwise motion has been also studied in the acto-myosin system [5]. The characterization of the sliding and binding force that induces the stepwise motion is crucial to elucidate the molecular mechanism of muscle contraction.

1 Kron S, Toyoshima YY, Uyeda TQP, Spudich JA. Methods Enzymol 1991; 196: 399-416
2 Ishijima A, Doi T, Sakurada K, Yanagida T. Nature 1991; 352: 301-306
3 Ashkin A, Dziedzic JM, Bjorkholm JE, Chu S. Optics Lett 1986; 11: 288-290
4 Nishizaka T, Yagi T, Tanaka Y, Ishiwata S. Nature 1993; 361: 269-271
5 Miyata H, Hakozaki H, Yoshikawa H, Suzuki N, Kinosita Jr K, Nishizaka T, Ishiwata S. J Biochem (in press).
6 Kinosita Jr K, Itoh H, Ishiwata S, Hirano K, Nishizaka T, Hayakawa T. J Cell Biol 1991; 115: 67-73
7 Svoboda K, Schmidt CF, Schnapp BJ, Block SM. Nature 1993; 365: 721-727

第３回 浜松医科大学
メディカルホトニクス ワークショップ
講演会要旨集

Life science における光学顕微鏡利用技術

日時：１９９４年　８月２７日（土）
１０：００～１７：３０

会場：浜松医科大学
〒４３１－３１ 静岡県 浜松市
半田町 ３６００番地

後援：浜松ホトニクス株式会社
株式会社ニコン
株式会社ニコン インステック

講演2

筋タンパク質モーターの構造と機能を探る新しい光学顕微鏡システム

石渡 信一（早稲田大学 理工学部 物理学科）

この数年ほどの間に，筋収縮運動や細胞運動などの生体運動を担っているタンパク質分子モーター１個の，ｎｍ（ナノメートル）オーダーの動きや，ｐＮ（ピコニュートン）オーダーの発生力が，実時間で計測されるようになってきた．計測には，レーザー光ピンセット[1]などの顕微操作装置を組み込んだ新しい光学顕微鏡システムが用いられている．

本講演では，分子モーター１個のレベルから，１０万個以上の分子モーターが規則的に集合した単一筋原線維のレベルに至るまでの，各階層構造における筋収縮系の運動特性・力学特性の研究が，新しい光学顕微鏡システムを用いてどのように行われているかについて，私の研究室での研究成果を中心に述べる．ところで，レーザー光ピンセットを中心とするビデオ顕微鏡システムの組立ては，慶應義塾大学・理工学部の木下一彦研との協同研究に負っており，その内容については，昨年の本ワークショップで，木下氏より詳しい説明があったことと思われる[1]．そこで私の講演は，光学顕微鏡システムそのものよりも，それを用いての研究成果の方に重点をおいたものにしたい（以下に掲載する図は，本年４月に開かれた計測連合シンポジウムの資料集で用いたものとほとんど同じです[2]）．

１　筋収縮系における分子モーターとその集合体について
－筋原線維・筋節・ミオシン・アクチン・分子モーターなどに関する基礎知識－

骨格筋の階層構造の模式図を図１に示す[3]．本講演では，直径約１μｍ，長さ数十μｍに調製した単一筋原線維（生体中のサイズは，直径は１μｍのオーダーだが，長さは１ｃｍ以上に達する）のレベルから，数μｍの大きさの筋節（サルコメア），多数のアクチン分子が繊維状に重合したアクチンフィラメント（約４００個で長さ１μｍ），分子モーターの駆動部と考えられているミオシン分子まで取り上げる．

ミオシン分子は図１のように，長さ２０ｎｍの頭部と，長さ１００ｎｍ以上の尾部からなる．２本の重鎖（ポリペプチド）が，ラセン構造を取りつつ尾部で絡み合い，頭部の部分で２つに分かれている．この他に，調節機能を持つと考えられる４本の軽鎖が２個の頭部にそれぞれ２本ずつ結合している．筋節中では，尾部同士が結合・重合してミオシン（太い）フィラメントを形成している．頭部の立体構造について，結晶構造解析の結果が昨年発表された[4]．モーター駆動部の

主要な部分は，この頭部に局在していると考えられている．ところで我々が実験で実際に取り扱うのは，ミオシン分子だけでなく，キモトリプシンなどのタンパク質分解酵素によって頭部の根元を切断して得られる頭部１個（Ｓ１）や，尾部の中程で切断して得られる２個の頭部を含む部分（ＨＭＭ）である．

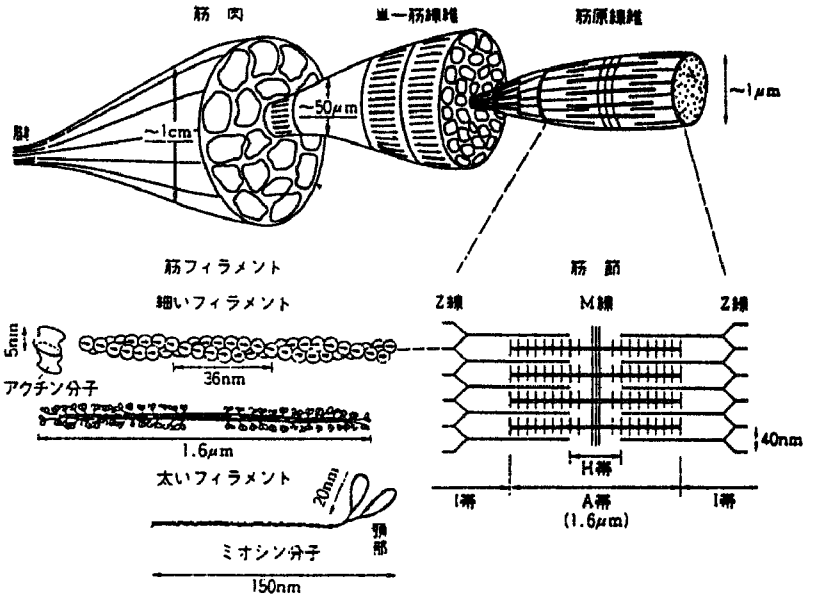

図１　筋収縮系の階層構造の模式図[3)]

さて，これらの階層構造を光学顕微鏡でどのように“見る”ことができるか．まず筋原線維の周期構造については，昔から知られているように，横紋構造として位相差顕微鏡下で比較的容易に観察することができる．従って，単一筋原線維の研究に特に新しい光学顕微鏡システムを必要とはしない．しかし，我々はガラス微小針を用いた顕微操作法と画像解析（ビデオ）システムを組み合わせることによって，これまで以上に簡便に単一筋原線維の運動特性・力学特性を計測できる顕微計測システムを組み上げた．単一筋原線維（厳密には半筋節）は，筋肉という運動器官を構成する収縮系としての最小機能単位であると考えられ，高次構造を備えた筋収縮系を理解する上で重要な実験系である．

ミオシン分子１個を“見る”ことは，新しい光学顕微鏡システムをもってしても未だ成功していない．一方アクチンフィラメントについては，アクチン分子１個に１個ずつ結合するファロイジン（茸毒；phallodin）分子に蛍光色素（例えばローダミン（rhodamine））を結合したローダミン・ファロイジン（Rd-Ph）を用いることによって，超高感度蛍光顕微鏡下でフィラメント１本の蛍光像として捉えることができる[5)]．一方，ガラス表面上に吸着したミオシン分子（あるいは，Ｓ１やＨＭＭ）の上をアクチンフィラメントが滑走する“*in vitro* 滑り運動系”と呼ばれる実験系が開発された[6,7)]．その結果，２種類の筋フィラメント相互の滑り運動をもたらす分子モーター，しかも１個の分子モーターの運動特性・力学特性を光学顕微鏡下で研究することが可能になった[8,9)]．

ところで，筋収縮滑り運動・力発生に必要な力学的エネルギーの源は，ＡＴＰ（アデノシン３燐酸）がＡＤＰ（アデノシン２燐酸）とＰｉ（無機燐酸）に加水分解される際に解放される化学エネルギーである（その５０％以上が力学的エネルギーに変換される）．ミオシン頭部がＡＴＰを結合し分解する本体であること

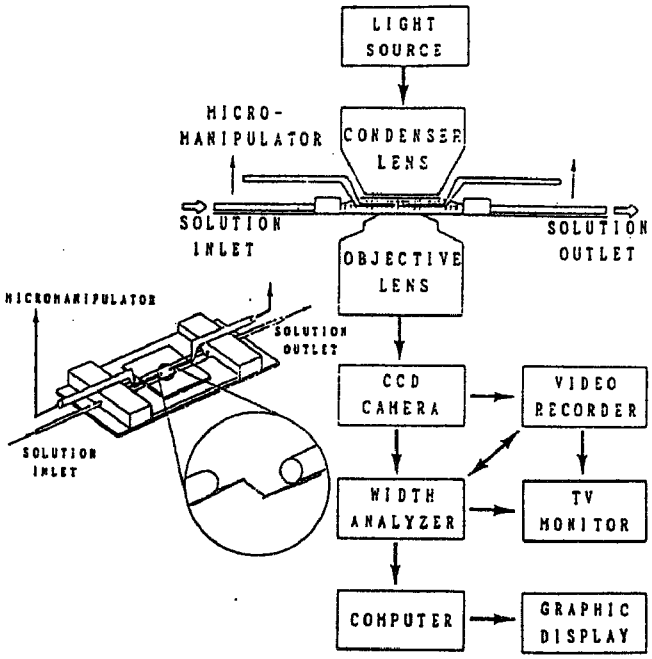

図２　筋原線維の顕微計測法[10)]

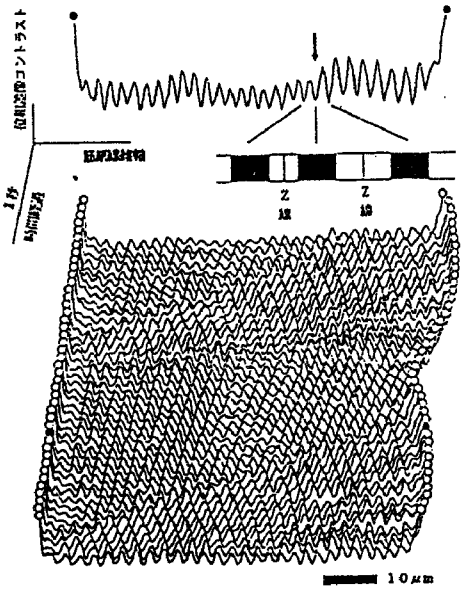

図３　筋原線維の自励振動波形[10)]

が，ミオシン分子が分子モーターと呼ばれる所以であるが，モーターとして機能するのに必要なＭｇＡＴＰの分解にはアクチンフィラメントとの相互作用が必須である．ミオシン頭部だけではＭｇＡＴＰを加水分解する能力（分解速度）が低い．

通常筋収縮系は，生理的な塩環境下に特にMg^{2+}とＡＴＰが共存する溶媒条件の元で弛緩（不活性）状態にある．この条件下に，内部膜系からμＭ以上のCa^{2+}が放出されると，Ca^{2+}が制御タンパク質に結合することによって分子モーターが活性化され，筋収縮系は収縮（活性）状態に転移する．このように，生体中では，膜系からのCa^{2+}の出し入れによって収縮系が弛緩と収縮の２状態のいずれを取るかが調節されている．

私の講演を理解する上での筋収縮系に関する予備知識は，これだけで十分だろう．

２　単一筋原線維の運動特性（自励振動）や力学特性（張力－長さ関係）の計測
－ガラス微小針による顕微操作・位相差顕微鏡・画像解析・ビデオシステム－

単一筋原線維を用いた筋収縮・力学特性の研究は，その重要性にもかかわらず，操作が困難なためにこれまでほとんど行われてこなかった．そこで私達は，筋原線維の両端を，マイクロマニピュレーターに装着した２本のガラス微小針に巻き付ける簡便な方法を編み出し，これを顕微画像解析系と組み合わせることによって，比較的容易に研究することのできる実験系を開発した[10)]．この実験系を用いて行った実験を紹介しよう（実験系の概念図は図２にある）．

筋収縮系は，上で述べたように，通常は収縮か弛緩かのいずれかをとるが，私達はこの２状態の中間状態として自励振動状態があることを１０年近く前に発見し，この状態をＳＰＯＣと呼ぶことにした[10]．遊離のCa^{2+}濃度がサブμM付近で発生するＳＰＯＣは以前から知られていたが，これをＣａ－ＳＰＯＣと呼び，我々の見いだしたＡＴＰにＡＤＰとＰｉが共存することによって生じるＳＰＯＣをＡＤＰ－ＳＰＯＣ（通常の収縮に必要なCa^{2+}は必要としない）と呼んで区別する．図３には，ＡＤＰ－ＳＰＯＣ条件下における筋節長振動の時間経過を示す自励振動波形の例を示す．各筋節の振動は素早い伸長相と緩やかな収縮相とからなる鋸波状で，周期は数秒（溶媒条件によって１～６秒の範囲で変化する）である．

このような自励振動が生じるメカニズムは非常に興味深いものだが，未だに解明できていない[10]．多数の分子モーターが働くことによって発生する協同的な性質がこの現象の本質であろうと考え，研究を進めている．またメカニズムの中には，化学過程→力学過程という順方向だけでなく，力学過程が逆に化学過程に影響を与えるというフィードバックが本質的な役割を演じているものと考えられる．そうであるならば，ＳＰＯＣ現象は，分子モーターがまさしく力学酵素(mechano-enzyme)であることを端的に示すものであるということができる．

一方，同じ顕微操作・解析法を用いて，私達は単一筋原線維の粘弾性特性の研究も行っている[11]．静的な長さ・張力関係，階段状の長さ変化に対する張力応答の時間経過を含む動的特性，伸長と短縮に伴う長さ・張力関係に見られるヒステリシス，その他これまで得られなかった様々な力学特性を得ることが出来るようになってきた．そして，この力学特性がネブリンやコネクチンなどの巨大弾性タンパク質由来のものであることを示すことも出来るようになった．

ところでＳＰＯＣ状態における筋原線維の長さと発生張力の振動波形は，両端のガラス針の位相差像の明るさを２値化することによって位置検出するという方法を用いて，変位については５０ｎｍ，張力については１ｎＮ（ナノニュートン），時間は１／３０秒の分解能で計測している[10]．これらの分解能はＣＣＤカメラービデオシステムによって制限されている．そこで今後は，ガラス針の位置検出を４（あるいは２）分割フォトダイオードで行うことによって，特に時間分解能を飛躍的に向上させる予定である．これが出来上がれば，筋原線維の長さのフィードバック制御を高精度で行うことが出来るようになる．

３　アクチンフィラメントの回転滑り運動と多重捻れ（スーパーコイル）形成
－アクチンフィラメントの可視化・*in vitro* 滑り運動系・超高感度蛍光顕微鏡－

分子モーターの滑り力ベクトルは，ほぼアクチンフィラメントの長軸方向を向いている．しかし，その正確な方向についてはほとんど分かっていない．そこで私達はこの点に注目し，滑り力ベクトルの方向を *in vitro* 滑り運動実験系を用いて明らかにしようと考えた．もし滑り力ベクトルの方向がアクチンフィラメントの長軸から少しでも傾いていれば，滑り力ベクトルは長軸と垂直な成分を持つ

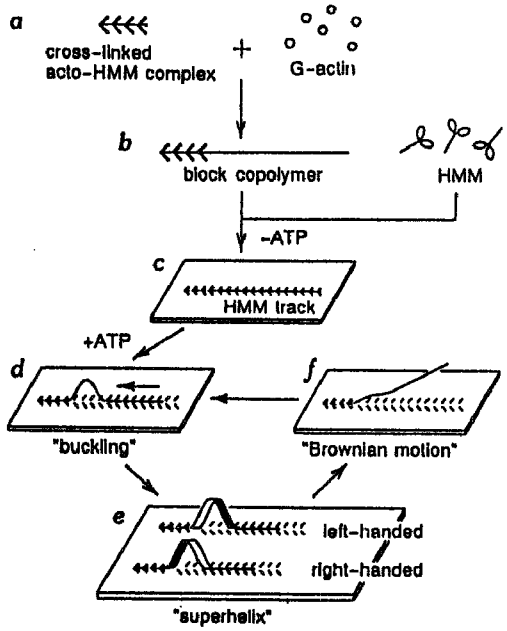

図４．アクチンフィラメントの回転滑り運動を示すための特殊な *in vitro* 滑り運動系[13)]

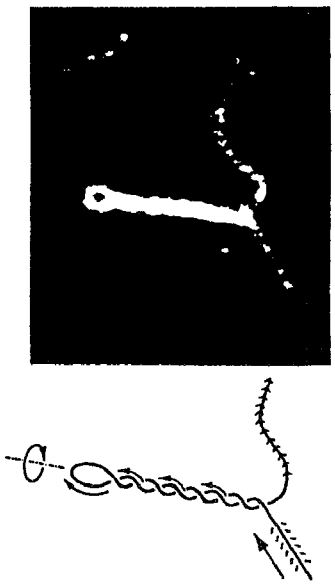

図５．アクチンフィラメントに見られた超ラセン構造[13)]

ことになり，フィラメントを回転させるようなトルクが存在することになる．そこで滑り運動中にアクチンフィラメントが回転運動するか否か，回転するならばどちら向きに回転するか，を検出できればよい．しかし回転運動を直接観察することは，フィラメントが柔らかくて曲がりやすいので難しい．そこで私達は，試行錯誤の末，図４に示すような，回転運動を間接的に証明することの出来る特殊な実験系を考案した[13)]．

図４に示した方法によってアクチンフィラメントの滑り運動の先端部を固定すると，後端部の滑り運動に押されてフィラメントの中程が座屈して横に膨らむ．もし滑り運動に回転が伴っていれば横に膨らんだ部分が捻れて超ラセン（supercoil）が形成されるはずである．この超ラセンが右巻きならば後端部の回転は左回転，左巻きならば右回転であると結論できる．得られた典型的な例を図５に示すが，形成された超ラセンはほとんど左巻きであった．即ち結論は，アクチンフィラメントの滑り運動は右ネジが進むように生じるというものである．

４　筋タンパク質モーター１個の動きと発生力の計測
－レーザー光ピンセット・画像解析－

in vitro 滑り運動系とレーザー光ピンセット・画像解析システムを組み合わせることによって，分子モーター１個の運動・力学特性を明らかにすることを目指している（この部分は全て慶應義塾大学・理工学部・木下一彦研究室との共同研

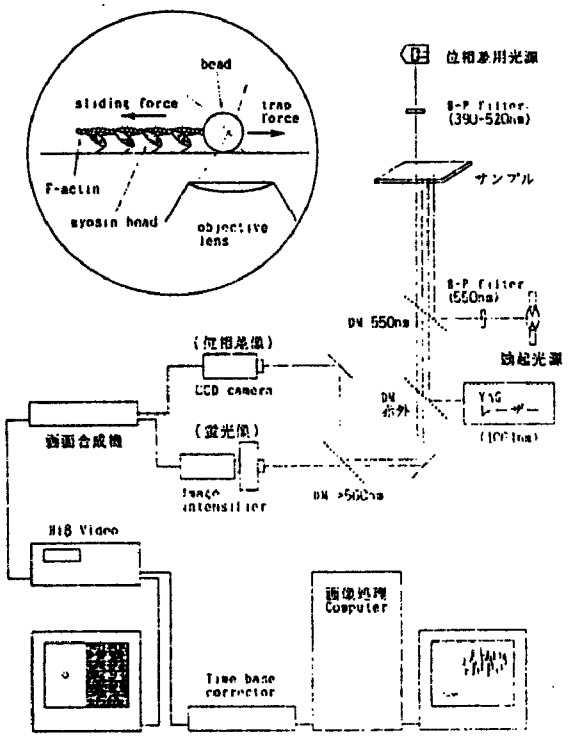

図６　分子モーターの動作特性を計測するための顕微解析装置

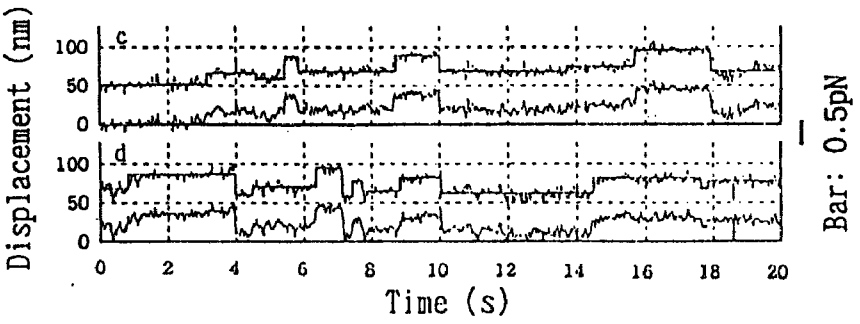

図７　分子モーターの動きの時間経過[9)]

究による）．実験系は，アクチンフィラメントの滑り運動の後端部に直径１μmのプラスチックビーズを結合し，このビーズを光ピンセットで捕捉・操作し滑り力を計測しようとするものである[9)]．ビーズの捕捉力は赤外レーザー光の強度によって決まるが，最大約１００ｐＮである．この範囲内では捕捉力はフックのバネと見なしてよい．この装置の概略を図６に示す．

この方法を用いて，私達は少数個の分子モーターによる滑り運動・滑り力の特性を検討した[9)]．その一例を図７に示す．図７は，ＡＴＰ１分子の加水分解に伴う運動を検出するために，ＡＴＰ濃度を１μＭと低く抑え，ミオシン（実際にはＨＭＭ）１分子当たり１秒間に約１個のＡＴＰ分子が結合・分解するような条件下におけるビーズの運動の時間経過を示している．所々にステップ状の変位が生じている．これらのステップの大きさは光ピンセットの捕捉力を大きくすると減少したが，この例の場合には，平均約９ｎｍであった．これは分子モーター１個のサイズにほぼ等しい．このステップに対応する発生力は０．１ｐＮであった．

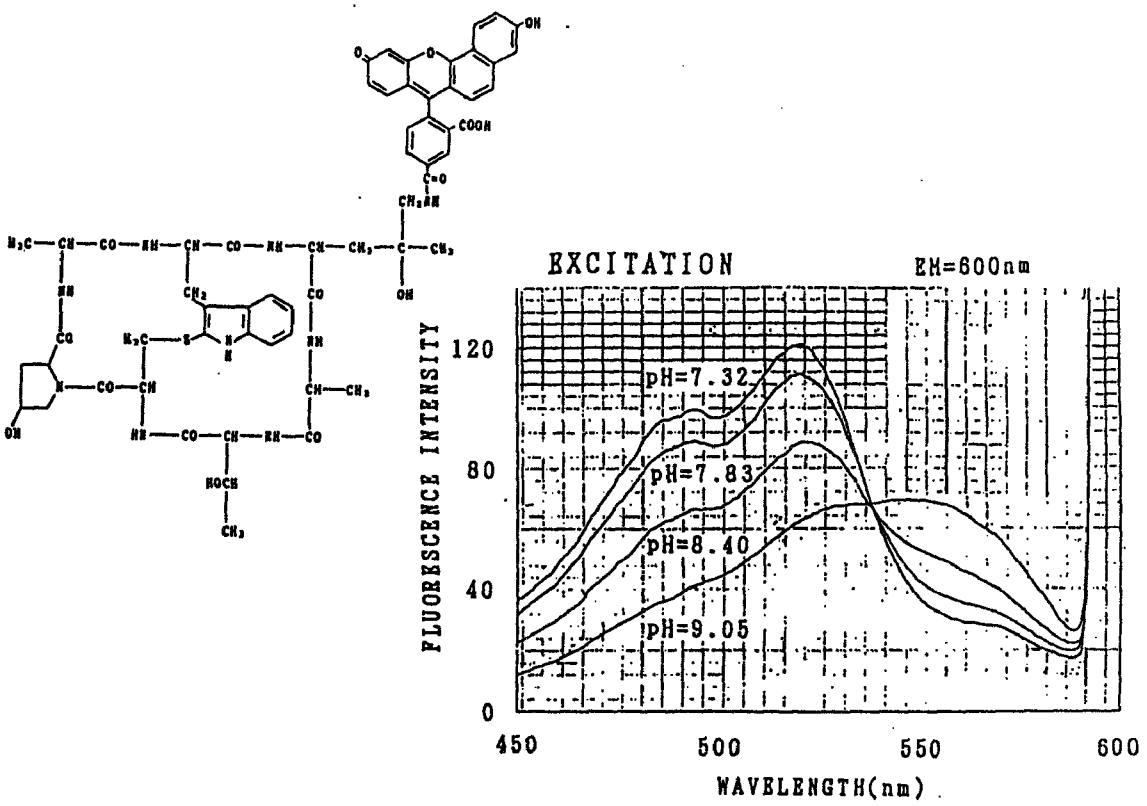

図８　ｐＨ感受性蛍光色素ＳＮＡＦＬ－Ｐｈａｌｌｏｉｄｉｎの構造とアクチンフィラメントに結合したときの励起スペクトルのｐＨ依存性

このように，少数個の分子モーターの動作特性を調べることができるようになってきた．そこでさらに，厳密に分子モーター１個を扱えるようにしたい．問題は，分子モーターの数をどのようにして数えるかである．私達は，ＡＴＰ非存在下（硬直条件下）でミオシン分子がアクチンフィラメントに強く結合することに着目し，硬直条件下でアクチンフィラメントをＨＭＭ分子から一つ一つ引き剥がすことで分子モーターの数を数えることにした．この方法で数えた分子モーターの数（ガラス表面上での数密度）と単位長さのアクチンフィラメントに発生する張力とが比例することなどが確認されている．１個の分子モーターの動作特性は，ＡＴＰ存在下におけるミオシン・アクチン間の結合力が弱い（結合時間が短い）ためにまだ得られていないが，今後さらに実験系を工夫することによって可能にしたい．

硬直条件下あるいは滑り運動を伴わない条件（例えば硬直条件にＡＤＰを添加）下で１個のＨＭＭ（あるいはＳ１）分子からアクチンフィラメントを引き剥がすのに必要な破断力を計測した．その結果，最大２０ｐＮ，平均８ｐＮという値が得られた．また，分子が引き剥がされるまでのビーズの変位計測を精度よく行うことによって，分子モーターの変形と張力関係を求めることが出来た．この変形・張力曲線の傾きから見積もったモーター分子１個の弾性率は平均０．４ｐＮ／ｎｍであった．またデータ収集の段階だが，今後はこのような顕微計測を

精度よくできる実験系をさらに工夫することによって，分子モーター１個の力学特性を明らかにしたい．

５　筋タンパク質モーターの力学過程と化学過程の同時計測
－ｐＨ感受性蛍光色素・Ｗ（Double-view）光学顕微鏡－

筋収縮系における化学過程を力学過程とともに同時画像化することによって，メカノケミカルカップリング（力学・化学共役）を時間的・空間的に明らかにする方法を，この数年来私達は模索している．問題なのはＡＴＰ分解をどのように画像化するかだが，私達はＡＴＰ分解反応に伴うｐＨの減少（ＡＴＰ分解に伴ってＨ$^{+}$が放出されることによる）をｐＨ感受性の蛍光色素で検出することを試みている．蛍光分子が溶液中に遊離することによって生じる蛍光の背景光をなくすための方策として，私達は２つ検討している．１つは，蛍光分子として図８のようなｐＨ感受性蛍光色素（ＳＮＡＦＬ）とファロイジンとを共有結合して得た物質ＳＮＡＦＬ－Ｐｈを用いることである．これによって，アクチンフィラメントだけを蛍光像として捉え，アクチン分子近傍のｐＨ変化だけを感度良く検出することが出来る．この色素については，２波長励起・１波長検出して蛍光像の蛍光強度比を求めることにより約０．１ｕｎｉｔの感度でｐＨ画像が得られることを確認している．ただ，２波長励起の場合には，装置上今のところ同時画像化できないという弱点がある．ｐＨ感受性蛍光色素としてＳＮＡＦＬの代わりにＳＮＡＲＦを用いることが出来れば，１波長励起・２波長検出に適しているので木下等の開発したＷ光学顕微鏡系[14]を装備することによって厳密に２波長同時画像化が出来，ｐＨ画像を少なくとも１／３０秒ごとに捉えることができるようになる．この目的のために，現在ＳＮＡＲＦ－Ｐｈの化学合成を試みている．

２つ目の方策は，蛍光色素は遊離したままであっても蛍光背景光をなくすことの出来るものとして，２光子吸収（励起）法を採用することである．赤外波長領域の強力なレーザー光源で励起することによって焦点面近傍だけを選択的に可視光励起することができる．分厚い試料であっても厚さ方向の背景光が混入しないので，共焦点走査型顕微鏡のような切片像が得られることになる．この方法の場合には，市販のＳＮＡＲＦを用いることが出来るので，Ｗ光学系を組み合わせることによって同時画像化が出来る．ただ難点は局所像しか得られないことであるが，非常に有望な方法であることに間違いはない．

参考文献

1) 昨年の本ワークショップにおける木下 一彦 氏の講演録と，鈴木 直哉，木下 一彦；“光ピンセット”，生体の科学，44，159-165 (1993)．斎藤 究，柳田 敏雄；“光ピンセット法による分子操作とナノ計測”，蛋白質核酸酵素，39，1344-1349 (1994)．

2) 石渡 信一；“生体運動システムにみる物理法則”，第５回計測連合シンポジウム先端計測 ’９４ 資料集，学術会議計測工学研連，pp. 61-68 (1994).
3) 石渡 信一；“筋フィラメントの構造と機能”，病態生理，10，437-444 (1991).
私の研究室における，１９８８年頃までの研究をまとめたものとして，石渡信一；“収縮構造を解剖する”，生物物理のフロンティア，日本物理学会編，培風館，東京，pp. 134-145 (1989).
4) I. Rayment, W. R. Rypniewski, K. Schmidt-Base, R. Smith, D. R. Tomchick, M. M. Benning, D. A. Winkelman, G. Wesenberg and H. M. Holden; "Three-dimensional structure of myosin subfragment-1: a molecular motor", *Science*, 261, 50-58 (1993).
これに関する総説としては，須藤 和夫；“蛋白質分子モーター”，蛋白質核酸酵素，39，1190-1201 (1994). I. Rayment and H. M. Holden; "The three-dimensional structure of a molecular motor", *Trends Biochem. Sci.*, 19, 129-134 (1994).
5) T. Yanagida, M. Nakase, K. Nishiyama and F. Oosawa;"Direct observation of motion of single F-actin filaments in the presence of myosin", *Nature*, 307, 58-60 (1984).
6) S. J. Kron and J. A. Spudich; "Fluorescent actin filaments move on myosin fixed to a glass surface", *Pro. Nat. Acad. Sci. USA*, 83, 6272-6276 (1986).
7) 最近の総説として，T. Yanagida, Y. Harada and A. Ishijima; "Nano-manipulation of actomyosin molecular motors *in vitro*: a new working principle", *Trends Biochem. Sci.*, 18, 319-324 (1993).
特に，ガラス微小針に変性ミオシン分子を吸着し，これを介してアクチンフィラメントをガラス針に保持するという技法を用いて，アクチンフィラメントに発生するｐＮオーダーの収縮力を初めて検出したものとして，A. Kishino and T. Yanagida; "Force measurements by micromanipulation of a single actin filament by glass needles", *Nature*, 334, 74-76 (1988).
この技法を発展させて，少数個の分子モーターによる発生力の揺らぎを検出したものして，A. Ishijima, T. Doi, K. Sakurada and T. Yanagida; "Subpiconewton force fluctuations of actomyosin in vitro"; *Nature*, 352, 301-306 (1991).
8) J. T. Finer, R. M. Simmons and J. A. Spudich; "Single myosin molecule mechanics: piconewton forces and nanometre steps", *Nature*, 368, 113-119 (1994).
キネシン・微小管系におけるキネシン分子のステップ状の滑り運動を定量的に示した例として，K. Svoboda, C. F. Schmidt, B. J. Schnapp and S. M. Block; "Direct observation of kinesin stepping by optical trapping interferometry", *Nature*, 365, 721-727 (1993).

9) H. Miyata, H. Hakozaki, H. Yoshikawa, N. Suzuki, K. Kinosita, Jr., T. Nishizaka and S. Ishiwata; "Stepwise motion of an actin filament over a small number of heavy meromyosin molecules is revealed in an *in vitro* motility assay", *J. Biochem.*, 115, 644-647 (1994).

10) T. Anazawa, K. Yasuda and S. Ishiwata; "Spontaneous oscillation of tension and sarcomere length in skeletal myofibrils. Microscopic measurement and analysis", *Biophys. J.*, 61, 1099-1108 (1992).
筋原線維の自励振動現象については，S. Ishiwata, N. Okamura, H. Shimizu, T. Anazawa and K. Yasuda; "Spontaneous oscillatory contraction (SPOC) of sarcomeres in skeletal muscle", *Adv. Biophys.*, 27, 227-235 (1991).
総説として，S. Ishiwata and K. Yasuda; "Mechano-chemical coupling in spontaneous oscillatory contraction of muscle", *Phase Transitions*, 45, 105-136 (1993).

11) K. Yasuda, T. Anazawa and S. Ishiwata; "Microscopic analysis of the elastic properties of nebulin in skeletal myofibrils", submitted to *Biophys. J.* (1994)

12) T. Funatsu, T. Anazawa and S. Ishiwata; "Structural and functional reconstitution of thin filaments in skeletal muscle", *J. Musc. Res. Cell Motil.*, 15, 158-171 (1994).

13) T. Nishizaka, T. Yagi, Y. Tanaka and S. Ishiwata; "Right-handed rotation of an actin filament in an *in vitro* motile system", *Nature*, 361, 269-271 (1993).

14) K. Kinosita, Jr., H. Itoh, S. Ishiwata, K. Hirano, T. Nishizaka and T. Hayakawa; "Dual-view microscopy with a single camera: Real-time imaging of molecular orientations and calcium", *J. Cell Biol.*, 115, 67-73 (1991).

31. *Length Regulation of Thin Filaments without Nebulin*

By Kenji YASUDA,*) Hideaki FUJITA,**) Yasutake FUJIKI,**) and Shin'ichi ISHIWATA**)

(Communicated by Setsuro EBASHI, M. J. A., Nov. 14, 1994)

Abstract: Recent work has suggested that the length of thin filaments in skeletal muscles is determined by a protein ruler, nebulin, located along the long axis of thin filaments. To examine the function of nebulin, the length distribution of the thin filaments was investigated by staining actin filaments with fluorescent rhodamine-phalloidin in rabbit cardiac muscles, which do not contain nebulin, and in skeletal muscles, which contain nebulin, by laser scanning confocal microscopy. The microscopic observation showed a difference in staining patterns between cardiac and skeletal muscle fibers when the staining was done without chemical fixation. This suggests that nebulin suppresses the attachment of phalloidin to actin filaments. Analysis of fluorescence distribution showed that the length deviation of thin filaments in the cardiac muscle was as small as that in the skeletal muscle. This indicates that the length of the thin filaments is regulated even without nebulin.

Key words: Cardiac muscle; skeletal muscle; thin filaments; rhodamine-phalloidin; nebulin; laser scanning confocal microscopy.

Introduction. Earlier studies on muscle structures using the electron microscope showed that both thin and thick filaments are of uniform lengths.[1),2)] Since then, there have appeared several reports showing that the thin filaments have broad length distribution in rat and frog cardiac muscles[3),4)] and even in rat skeletal muscles.[5)]

Recently, nebulin, a large protein being specifically present in vertebrate skeletal muscles, has been suggested to be a length regulator for thin filaments.[6)–11)] Wang's group reported a correlation between the molecular weight of nebulin and the thin filament length in several skeletal muscle tissues extracted from chickens, rabbits, humans and snakes in which the filament length was determined within the standard deviations of 0.05 μm.[7)]

However, nebulin is absent in the cardiac muscle;[6),12),13)] although nebulin-sized proteins exist, the amount present in the muscle is small and there is no cross-reactivity with anti-nebulin antibodies.[6)]

In this study, the length distribution of thin filaments is examined by observing actin filaments stained with fluorescent rhodamine-phalloidin (RhPh)[14)] under a confocal microscope to clarify the role of nebulin as a length determining ruler. The rabbit cardiac papillary and skeletal psoas muscle were chosen as examples suitable for comparison.

Materials and methods. *Solutions.* Solution A, 0.15 M KCl, 1mM $MgCl_2$, 10 mM 3-(N-morpholino) propanesulfonic acid (MOPS) (pH 7.0), 1 mM EGTA, 10 mM DTT, and 1 mM leupeptin; solution B, solution A containing 1% Triton-X100; solution C, solution A containing 33 μM RhPh; solution D, solution A containing 3% formaldehyde; solution E, 0.1 M KCl, 2 mM $MgCl_2$, 2 mM MOPS (pH 7.0), 1.5 mM NaN_3, and 3.3 μM RhPh; solution F, 25 mM KCl, 4 mM $MgCl_2$, 25 mM imidazole-HCl (pH 7.4), 1 mM EGTA, and 30 mM DTT.

*) Advanced Research Lab., HITACHI Ltd., Hatoyama, Saitama 350-03, Japan.
**) Dept. of Physics, School of Science and Engineering, Waseda Univ., Shinjuku-ku, Tokyo 169, Japan.

RhPh was purchased from Molecular Probe Inc. (Eugene OR, U.S.A.); catalase and glucose oxydase were from SIGMA Chemical Co. (St. Louis, Mo., U.S.A.); EGTA and MOPS were from Dojindo Laboratories (Kumamoto); DTT was from Wako Pure Chemical Industries, Ltd. (Osaka). Other chemicals were of reagent grade.

Cardiac and skeletal muscle fibers stained with rhodamine-phalloidin. Two types of preparation were examined for RhPh staining, i.e., staining without formaldehyde fixation (NF preparation) or staining after formaldehyde fixation (FF preparation) of rabbit cardiac papillary and skeletal psoas muscles glycerinated in 50% (v/v) glycerol containing 0.5 mM $NaHCO_3$, 5 mM EGTA, and 1 mM leupeptin for more than 3 weeks at −20°C. First, a single skeletal or a small bundle of cardiac glycerinated fibers were mounted on a glass slide; glycerol was washed out with solution A and the fibers were immersed in solution B for 30 min at 4°C to remove the membrane system. For NF preparation, solution B was substituted for solution C, and the fibers were stained with RhPh overnight at 4°C and then free RhPh was washed out with solution A so that the fibers could be microscopically observed. For FF preparation, solution B was substituted for solution D instead of solution C and the fibers were immersed for 30 min at 4°C. After formaldehyde fixation, the fibers were stained with RhPh in solution C overnight at 4°C and then free RhPh was washed out with solution A to allow microscopic observation.

Single actin filaments stained with rhodamine-phalloidin. Actin was prepared from acetone powder which had been obtained from a rabbit leg and a back white muscle according to a standard procedure.[15] For RhPh staining, 0.1 mg/ml G-actin was polymerized in solution E overnight at 4°C in the dark. Just before microscopic observation, 30 μg/ml heavy meromyosin in solution F was infused into the narrow space between a silanizing glass slide and a cover slip, and then 0.5 mg/ml bovine serum albumin in solution F was infused. Then F-actin (final concentration, 0.1 μg/ml) diluted in solution F containing 0.04 mg/ml catalase, 0.22 mg/ml glucose oxydase, and 4.5 mg/ml glucose was infused for microscopic observation.[16]

Laser scanning confocal microscopy. Both muscle fibers and actin filaments stained with RhPh were observed using a laser scanning confocal microscope system (LSM-GB200, OLYMPUS Co., Tokyo). The light source was a 25 mW Ar laser of 488 nm. A 550 nm long-pass filter was used to detect the fluorescence of RhPh. A PLAPO 60X WLSM [1.0 NA] objective lens was used. Scanning time to take one picture was 16 s. The fluorescence intensity was recorded in a 1024×768 frame memory with an intensity range of 256 steps. The intensity profile was obtained by scanning along a line with the width of 10 pixels on the X-Y plane; the depth of the X-Y plane was changed along the Z axis by moving the sample stage using a piezo actuator.

Data analysis of thin filament fluorescent images. The fluorescence intensity profiles of the thin filaments obtained from confocal images of the I-Z-I brush, a bundle of thin filaments, were compared with a model calculated using a convolution method. The intensity I(x) of the thin filaments at position x from the Z line was calculated using $I(x) = F^{-1}(F(T(x))\cdot F(A(x)))$, where F and F^{-1} are, respectively, the Fourier and Fourier inverse transformation functions; T(x) shows a relative proportion of existence of thin filaments ($T(x<L_0) = 1$ and $T(x>L_0) = 0$ when the length of the thin filaments is uniformly L_0); A(x) is a relative intensity profile of a point light source (in the present work RhPh-stained single actin filaments were selected as a point light source).

Results and discussion. *Confocal images of cardiac and skeletal muscle fibers.* First, the stained regions of NF and FF prepared cardiac and skeletal muscle fibers were compared with the use of a confocal microscope. In the cardiac muscle, the entire thin filament region was stained in both NF (Figs. 1a, 2a) and FF (Figs. 1b, 2b) preparations. In the skeletal muscle, only the ends of the thin filaments, i.e., the pointed end at the

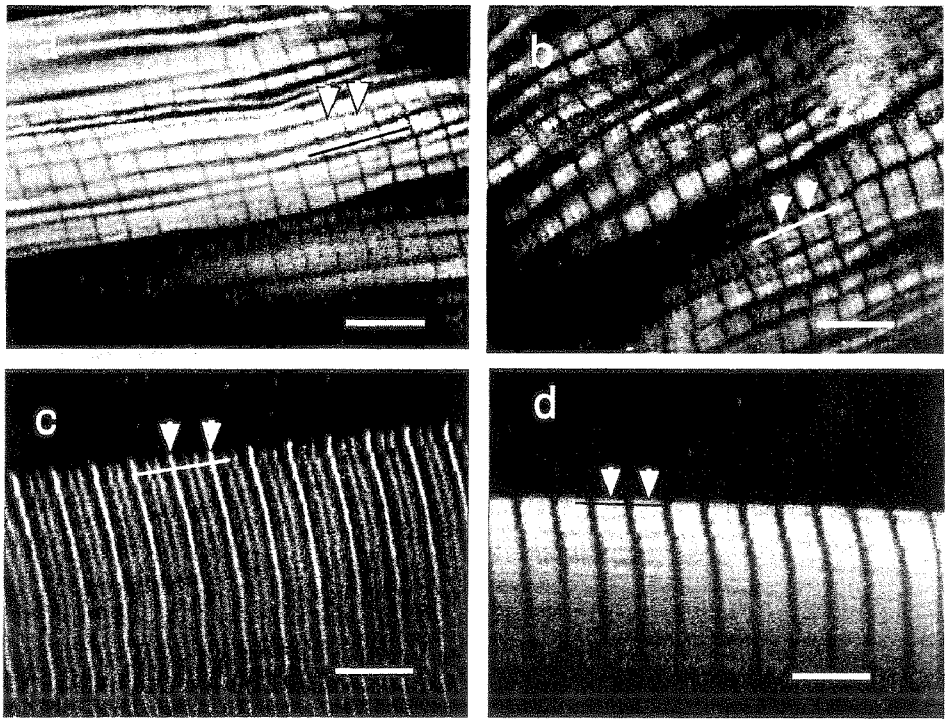

Fig. 1. Confocal fluorescence images of cardiac and skeletal muscle fibers. Actin filaments were made visible by rhodamine-phalloidin staining without (a and c) or after (b and d) formaldehyde fixation. Micrographs a and b are of the cardiac muscle and c and d are of the skeletal muscle. The fluorescence intensity differs depending on the gain of the photomultiplier. The intensity profile was obtained along a thin line of each fiber (cf. Fig. 2). Arrows indicate the position of the Z lines, and the scale bars are 5 μm.

center of each sarcomere and the barbed end at the Z line, were stained in the NF preparation (Figs. 1c, 2c), although the entire thin filament region was stained in the FF preparation (Figs. 1d, 2d). Szczesna and Lehrer[17] also reported that the staining pattern in skeletal myofibrils, which was initially an NF type, changed to an FF type after staining for 2–3 h in a rigor solution at low pH. These results suggest that nebulin inhibits RhPh staining on actin filaments by binding along the long axis. The accessibility of RhPh to its binding site on thin filaments, which is suppressed by nebulin, seems to be modified by the chemical fixation or solvent conditions.

Confocal images of actin filaments. The fluorescence intensity profiles were obtained for single actin filaments regarded as a point light source. Actin filaments were fixed on a glass surface through rigor bonds with heavy meromyosin molecules adsorbed on the glass surface. The intensity profiles were obtained along the X and Z axes (Figs. 3a, b). A half width of the former profile was 0.29 μm and that of the latter was 2.57 μm; these values indicate a spatial resolution of the microscopic system. The spatial resolution along the Z axis was sufficiently narrow to obtain the intensity profiles of the I-Z-I brush in muscle fibers.

Length distribution of thin filaments in muscle fibers. Fluorescence intensity profiles of FF prepared cardiac and skeletal muscles were analyzed using the convolution method described above. Data could be simulated by assuming a uniform length of 1.05 to 1.1 μm in the cardiac muscle (Fig. 5a), and 1.0 to 1.1 μm in the skeletal muscle (Fig. 5b). The latter

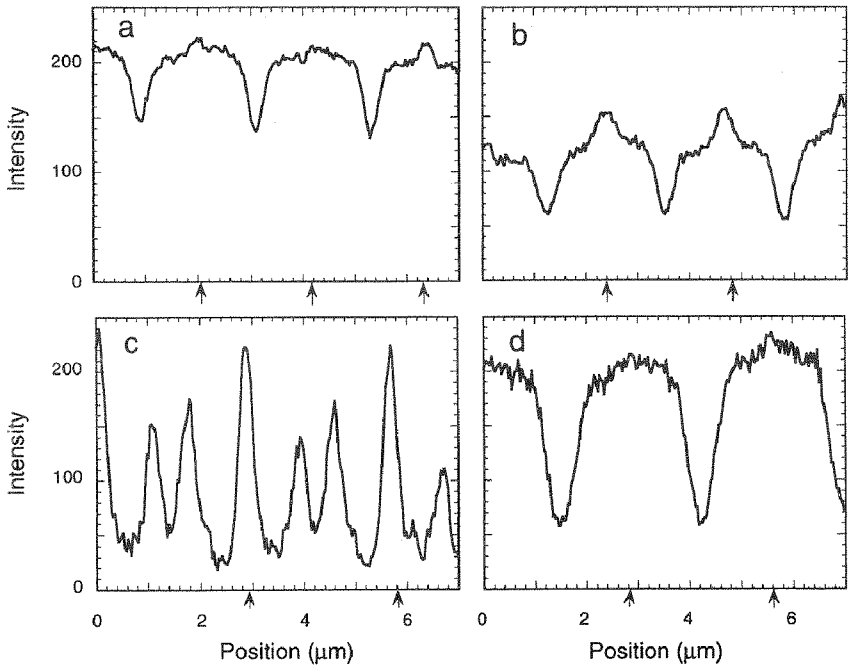

Fig. 2. Fluorescence intensity profiles of cardiac and skeletal muscle fibers stained with rhodamine-phalloidin. Intensity profiles in a to d were obtained along the thin lines indicated in Figs. 1a to d, respectively. Arrows indicate the position of the Z lines. The ordinate is the fluorescence intensity in arbitrary units (a. u.) and the abscissa represents the position along the long axis of the myofibrils.

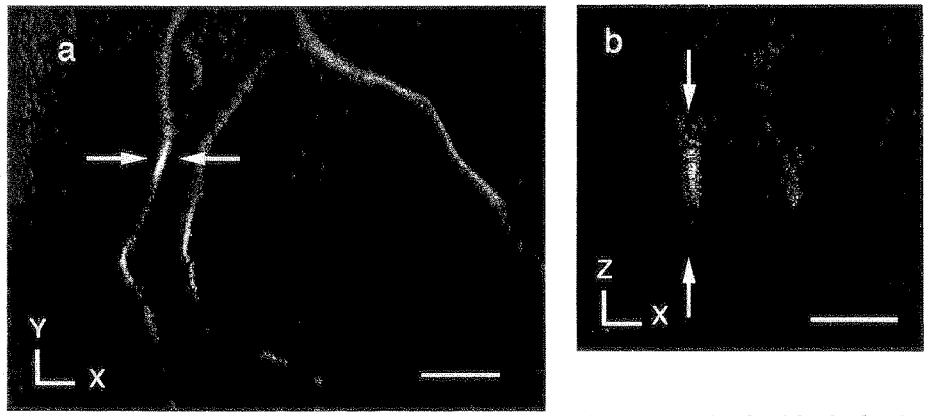

Fig. 3. Confocal fluorescence images of single actin filaments stained with rhodamine-phalloidin. Image a is on the X-Y plane; image b is on the X-Z plane constructed using image processing from a series of images on the X-Y plane obtained along the Z axis. Arrows, see Fig. 4. Scale bars are 5 μm in a and 2 μm in b.

deviation was within the same range as that reported previously.[7] Concerning the length distribution in the cardiac muscle, a previous electron microscopic observation showed a broad distribution ranging from 0.6 to 1.1 μm in rat atrial trabeculae and a somewhat narrower distribution ranging from 0.9 to longer than 1.1 μm in rat papillary muscles.[3),4)] Our results not only support the latter observation but, moreover, indicate that the width

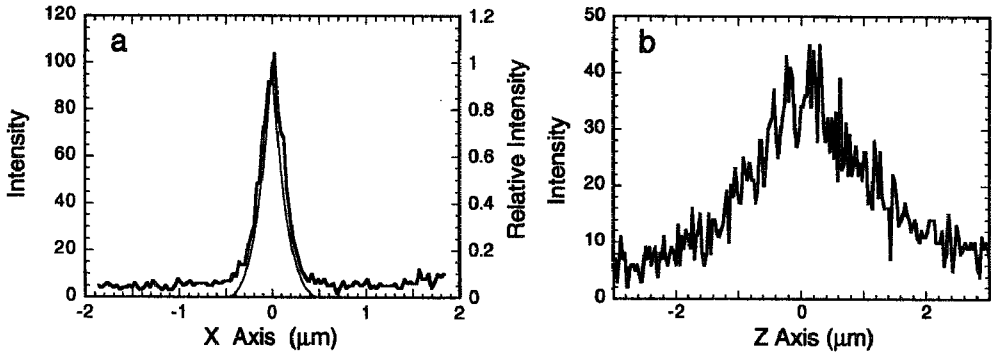

Fig. 4. Fluorescence intensity profiles of single actin filaments stained with rhodamine-phalloidin. Intensity profiles were obtained by measuring intensity (a. u.) between the two arrows indicated in Fig. 3. Graph a is the intensity profile along the X axis on the X-Y plane shown in Fig. 3a; the thin line was obtained by smoothing the data profile, which is used for convolution analysis in Fig. 5. Graph b is the intensity profile along the Z axis on the X-Z plane shown in Fig. 3b.

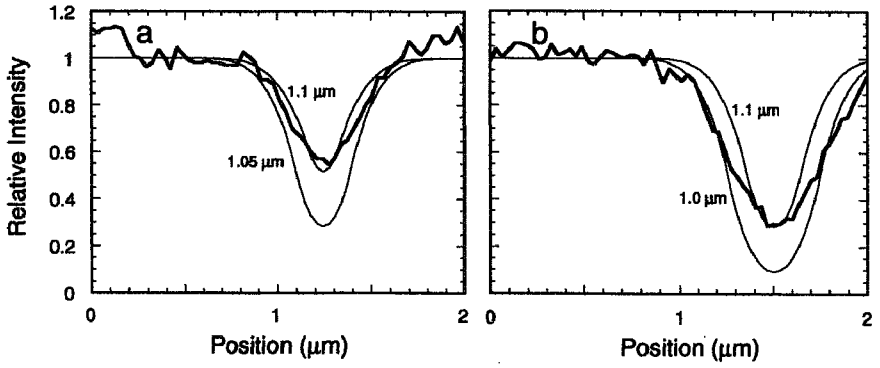

Fig. 5. Analysis of the thin filament length distribution in cardiac (a) and skeletal (b) muscles. Thick lines in a and b indicate the relative intensity profiles obtained from Figs. 2b and d, respectively. The thin lines indicate the intensity profiles calculated from the convolution method using the intensity profile of an actin filament shown by the thin line in Fig. 4a and assuming that the thin filaments are of uniform lengths of 1.0, 1.05, and 1.1 μm as shown in the figures.

of the distribution in the papillary muscle is similar to that in the skeletal muscle.

Nebulin is not a length regulator of thin filaments. The present work demonstrated that the length of the thin filaments in rabbit cardiac papillary muscles, which do not contain nebulin, is determined within the spatial resolution of the microscope as in the case of the skeletal psoas muscle, which contains nebulin. This result indicates that nebulin is not a main length regulator of the thin filaments, although we do not deny the possibility that nebulin plays an essential role for length determination within molecular precision in collaboration with a capping protein.[15] Finally, we should mention that it is desirable to examine whether the length distribution of the thin filaments in rat skeletal muscle is so broad as reported previously[5] by using the technique described here.

Acknowledgments. We thank Dr. Hideki Kanbara of Hitachi, Ltd. for giving us the opportunity to use a confocal microscope system, Dr. Kazuo Takeda of Hitachi, Ltd. for his

valuable suggestion of using the convolution method for estimating thin filament length, and Dr. Shin-ichiro Umemura of Hitachi, Ltd. for his continuous encouragement. This study was supported in part by Grants-in-Aids for Science Research and for Scientific Research on Priority Areas from the Ministry of Education, Science, and Culture of Japan.

References

1) Huxley, H. E.: J. Mol. Biol., **7**, 281–308 (1963).
2) Page, S. G., and Huxley, H. E.: J. Cell Biol., **19**, 369–390 (1963).
3) Robinson, T. F., and Winegrad, S.: Nature (Lond.), **267**, 74–75 (1977).
4) ——: J. Physiol., **286**, 607–619 (1979).
5) Traeger, L., and Goldstein, M. A.: J. Cell Biol., **96**, 100–103 (1983).
6) Wang, K., and Wright, J.: ibid., **107**, 2199–2212 (1988).
7) Kruger, M., Wright, J., and Wang, K.: ibid., **115**, 97–107 (1991).
8) Labeit, S. *et al.*: FEBS Lett., **282**, 313–316 (1991).
9) Trinick, J.: ibid., **307**, 44–48 (1992).
10) Wright, J., Huang, Q.-Q., and Wang, K.: J. Muscle Res. Cell Motil., **14**, 476–483 (1993).
11) Pfuhl, M., Winder, J., and Pastore, A.: EMBO J., **13**, 1782–1789 (1994).
12) Locker, R. H., and Wild, D. J. C.: J. Biochem., **99**, 1473–1484 (1986).
13) Hu, D. H., Kimura, S., and Maruyama, K.: ibid., **99**, 1485–1492 (1986).
14) Faulstich, H. *et al.*: J. Muscle Res. Cell Motil., **9**, 370–383 (1988).
15) Ishiwata, S., and Funatsu, T.: J. Cell Biol., **100**, 282–291 (1985).
16) Kron, S. J. *et al.*: Methods in Enzymology, **196**, 399–416 (1991).
17) Szczesna, D., and Lehrer, S. S.: J. Muscle Res. Cell Motil., **14**, 594–597 (1993).

Microscopic Analysis of the Elastic Properties of Nebulin in Skeletal Myofibrils

Kenji Yasuda,* Takashi Anazawa,‡ and Shin'ichi Ishiwata‡

*Advanced Research Laboratory, Hitachi Ltd., Hatoyama, Saitama 350-03, Japan, and ‡Department of Physics, School of Science and Engineering, Waseda University, 3-4-1 Okubo, Shinjuku-ku, Tokyo 169, Japan

ABSTRACT The elastic properties of nebulin were studied by measuring the elasticity of single skeletal myofibrils, from which the portion of the thin filament located at the I band had been selectively removed by treatment with plasma gelsolin under rigor conditions. In this myofibril model, a portion of each nebulin molecule at the I band was expected to be free of actin filaments and exposed. The length of the exposed portion of the nebulin molecule was controlled by performing the gelsolin treatment at various sarcomere lengths. The relation between the passive tension and extension of the exposed portion of the nebulin showed a convex curve starting from a slack length, apparently in a fashion similar to that of wool. The slack sarcomere length shifted depending on the length of the exposed portion of the nebulin, however, the relation being represented by a single master curve. The elastic modulus of nebulin was estimated to be two to three orders of magnitude smaller than that of an actin filament. Based on these results, we conclude that nebulin attaches to an actin filament in a side-by-side fashion and that it does not significantly contribute to the elastic modulus of thin filaments. The relation between the passive tension and extension of connectin (titin) was obtained for a myofibril from which thin filaments had been completely removed with gelsolin under contracting conditions; this showed a concave curve, consistent with the previous results obtained in single fibers.

INTRODUCTION

The contractile system of muscle requires an elastic framework to maintain its organized structure (for recent reviews, cf. Small et al., 1992; Ebashi, 1991). Recent studies have demonstrated that an exceptionally giant protein called connectin (titin) (Maruyama, 1986; Wang, 1985) is elastic so as to be responsible for the passive tension generation in stretched muscle fibers (Funatsu et al., 1990, 1993; Wang et al., 1993) and for positioning thick filaments at the center of each sarcomere (Horowits and Podolsky, 1987). As directly observed by electron microscopy after the selective removal of thin filaments from single skeletal muscle fibers (Funatsu et al., 1990) and a bundle of cardiac muscle (Funatsu et al., 1993), connectin (titin) filaments connect the ends of thick filaments and the Z line. Also, connectin (titin) has attracted attention because it is a candidate for the length-regulating ruler of thick filaments (Wang and Wright, 1988; Whiting et al., 1989; Trinick, 1992).

On the other hand, another giant protein called nebulin was recently found and suggested to be located along a thin filament (Wang and Wright, 1988). It has also attracted attention because it is a plausible candidate for the regulator of thin filament length (Kruger et al., 1991; Jin and Wang, 1991; Labeit et al., 1991; Wright et al., 1993; Pfuhl et al., 1994). In relation to its physiological function, it is interesting that nebulin is absent from cardiac muscle (Wang and Wright, 1988; Itoh et al., 1988); this seems to reflect the fact that the length of thin filaments is not strictly regulated (Robinson and Winegrad, 1977). It is important to examine the elastic properties of nebulin, because nebulin is considered to be a scaffold, as well as a template protein, that is responsible for stabilization and length determination of the filaments (Wang and Wright, 1988; Trinick, 1992; Wright et al., 1993; Pfuhl et al., 1994). From a physiological point of view, the extent to which nebulin contributes to the elastic modulus of thin filaments is also an important issue.

Viscoelastic properties of the elastic elements such as connectin (titin) in muscle fibers have been extensively studied using single fibers, skinned mechanically (Natori, 1954) or chemically (cf. Magid and Law, 1985). Recently, we have succeeded in manipulating single myofibrils under an optical microscope and measuring the tension development on the order of nanonewtons (Anazawa et al., 1992). The present study was designed to examine the structure and function of nebulin, using the above system.

To study the mechanical properties of these giant myofibrillar proteins, we used plasma gelsolin (brevin), an actin-binding protein possessing the ability to sever an actin filament, as a molecular tool for selectively removing thin filaments (cf. Funatsu et al., 1990, 1993). New types of contractile systems have been obtained with gelsolin treatment under rigor conditions and subsequently under contracting conditions; the models thus obtained appeared to be suitable for studying the mechanical properties of nebulin and connectin (titin) separately. A preliminary report of this work was presented previously (Yasuda et al., 1992).

Received for publication 11 May 1994 and in final form 29 July 1994.

Address reprint requests to Dr. Shin'ichi Ishiwata, Department of Physics, School of Science and Engineering, Waseda University, 3-4-1 Okubo, Shinjuku-ku, Tokyo 169, Japan. Tel.: 81-3-3203-4141; Fax: 81-3-3200-2567; E-mail: ishiwata@cfi.waseda.ac.jp.

Abbreviations used: BDM, 2,3-butanedione 2-monoxime; DFP, diisopropyl fluorophosphate; MOPS, 3-(*N*-morpholino) propanesulfonic acid.

Mr. Anazawa's current address: Central Research Laboratory, Hitachi Ltd., Kokubunji, Tokyo 185, Japan.

0006-3495/95/02/598/11 $2.00

MATERIALS AND METHODS

Solutions

Solution A: 60 mM KCl, 5 mM $MgCl_2$, 10 mM Tris-maleate (pH 6.8), and 1 mM EGTA; rigor (−Ca) solution: 0.15 M KCl, 1 mM $MgCl_2$, 10 mM 3-(*N*-morpholino)propanesulfonic acid (MOPS) (pH 7.0), 1 mM EGTA, 2 mM diisopropyl fluorophosphate (DFP), and 2 mM leupeptin; rigor (+Ca) solution: the above rigor (−Ca) solution containing 0.1 mM $CaCl_2$ instead of 1 mM EGTA; relaxing solution, 0.12 M KCl, 4 mM $MgCl_2$, 4 mM ATP, 20 mM MOPS (pH 7.0), 2 mM EGTA, 2 mM DFP, and 2 mM leupeptin with or without 20 mM 2,3-butanedione 2-monoxime (BDM); rigor-gelsolin (RG-) solution, 0.15 M KCl, 1 mM $MgCl_2$, 10 mM MOPS (pH 7.0), 0.1 mM $CaCl_2$, 2 mM DFP, 2 mM leupeptin, and 0.1 mg/ml gelsolin; contraction-gelsolin (CG-) solution: 0.15 M KCl, 5 mM $MgCl_2$, 4 mM ATP, 10 mM MOPS (pH 7.0), 0.1 mM $CaCl_2$, 2 mM DFP, 2 mM leupeptin, and 0.1 mg/ml gelsolin. ATP was purchased from Boehringer Mannheim GmbH (Mannheim, Germany), MOPS from Dojindo (Kumamoto, Japan), DFP and BDM from Wako Pure Chemical Industries Ltd. (Osaka, Japan), leupeptin from Peptide Institute Inc. (Osaka, Japan). Other chemicals were of reagent grade.

Preparation of myofibrils

Single or a small bundle of skeletal myofibril was prepared by homogenizing rabbit psoas glycerinated muscle fibers as described previously (1 mM leupeptin was added to the glycerol solution); the homogenization was done in solution A using a homogenizer (IKA-WERK T-18 type, 8G, Staufen, Germany) (Ishiwata and Funatsu, 1985; for further detail, see Ishiwata et al., 1993). The diameter of the single or the small bundle of skeletal myofibril used in the present work ranged from 1.5 to 3.7 μm. The number of sarcomeres between a pair of glass micro-needles (cf. Figs. 1, 3, and 9) was 25–40. Cardiac myofibrils (used in Fig. 2 only) were prepared from bovine papillary glycerinated muscle using a similar procedure (for further detail, see N. Fukuda, T. Fujita, and S. Ishiwata, unpublished data). Myofibrils thus prepared were stored in solution A at 0°C and used on the same day.

Preparation of plasma gelsolin

Plasma gelsolin (brevin), a calcium-dependent, actin-binding, and actin-severing protein (Yin and Stossel, 1979; Harris and Weeds, 1984), was purified from bovine plasma using a rapid, simple procedure developed by Kurokawa et al. (1990); bovine plasma was fractionated with 35–50% $(NH_4)_2SO_4$ in the presence of 50 mM Tris-HCl (pH 8. 0) and 0.1 mM DFP (E-64 was omitted), and then dialyzed against a Ca^{2+}-free solution. Plasma gelsolin was bound to a DE-52 (Whatman Biosystems Inc., Maidstone Kent, U.K.) column in the Ca^{2+}-free solution and eluted by increasing the concentration of Ca^{2+}. The purification procedure was repeated once more, using the same column. Plasma gelsolin thus obtained showed a single band corresponding to a molecular weight of about 90 kDa on SDS-PAGE.

Microscopic system for tension measurement and structure analysis

The microscopic system used for measuring tension development and for analyzing the internal structure of myofibrils was essentially the same as described previously (Anazawa et al., 1992), except that a piezo element was used for stretching a myofibril by controlling displacement of a stiffer glass micro-needle. In brief, the system consists of the following parts: (1) temperature-controlled cell (about 200 μl) in which a myofibril is fixed to a pair of glass micro-needles, one of which is flexible (Hooke's elastic constant, 0.22–1.06 μg/μm) and the other is rigid (~300 μg/μm); (2) micromanipulators with a piezoelectric element (PSt 150/50/5, Dr. Lutz Pickelmann, Munich, Germany); (3) an inverted phase-contrast microscope (DIAPHOT-TMD; Plan Apo 60 X oil DM objective lens [1.40 NA] for measuring tension and for taking the micrographs and density profiles shown in Figs. 1, 3, and 9; Nikon Co., Ltd., Tokyo) equipped with a CCD-camera (C3077H, Hamamatsu Photonics K. K., Hamamatsu, Japan); and (4) a video-computer system for image analysis. The developed tension and the average sarcomere length were estimated by measuring the deflection of the flexible needle and the separation between the inner edges of the two micro-needles by using a double-channel position detector (Width analyzer C3161, Hamamatsu Photonics K. K.). The developed tension of myofibrils and the fine structure of sarcomeres were determined simultaneously and recorded on a video tape recorder; a density profile of the recorded image of a myofibril was analyzed afterward by an image processor (Slot vision, Mitani Shouji K. K., Tokyo). The entire system was controlled by a personal computer (PC9801, NEC Co., Ltd., Tokyo). Space and time resolutions (spatial resolution, 50 nm; time resolution, 1/30 s) were limited mainly by the recording system. The binding of fluorescence dye-labeled actin to myofibrils was examined under an optical microscope (Fluophoto VFD-R; CF Plan 100 X oil DM objective lens [1.25 NA] for Fig. 2; Nikon Co., Ltd.). Tri-X films (Eastman Kodak Co., Rochester, NY) were used for taking phase-contrast and fluorescence micrographs (Microdol-X developer diluted 1:3; Eastman Kodak Co.).

Preparation of several models of myofibrils

We prepared the following two types of artificial models of myofibrils. First, a myofibril in which the portion of the thin filament located at the I band was selectively removed with gelsolin treatment for 10 min in an RG-solution (we call this model an *RG-treated* myofibril). Second, a myofibril from which thin filaments, other than the short fragments located at the Z line, were selectively removed by a two-step gelsolin treatment in an RG-solution and then in a CG-solution for 5 min (we call this model a *CG-treated* myofibril). This two-step procedure is essentially the same as that used in the previous study on muscle fibers (Funatsu et al., 1990). These models of myofibrils, both ends of which had been held by a pair of glass micro-needles, were observed under phase-contrast and fluorescence microscopes (Fig. 1).

The selective removal of thin filaments was confirmed by staining with 0.33 μM rhodamine phalloidin (Molecular Probes Inc., Eugene, OR) after chemical fixation in each solution containing 3% formaldehyde for 30 min (cf. Figs. 1 and 2; Funatsu et al., 1990). To identify the thin filaments without damaging mechanical and contractile properties of myofibrils, staining with 0.33 μM rhodamine phalloidin was done in each solution without chemical fixation (cf. Fig. 3). In this case, only the free (pointed) ends of thin filaments and the Z line were labeled (cf. Funatsu et al., 1990). In case of skeletal myofibrils, the staining was done after holding the myofibrils with a pair of glass micro-needles. All procedures were done in the cell at room temperature (about 25°C).

Preparation of labeled actin

Actin was prepared from acetone powder that had been prepared from rabbit leg and back white muscle according to a standard procedure (cf. Ishiwata and Funatsu, 1985). For actin labeling, F-actin (2.0 mg/ml; 0.1 M KCl, 0.6 mM ATP and 20 mM $NaHCO_3$) was mixed with 250 μM tetramethylrhodamine-5(and-6)-iodoacetoamide (Molecular Probes) and stored over night at 0°C. The solution was ultracentrifuged at 100,000 × *g* for 90 min, and the pellet was dissolved in 0.1 mM ATP, 10 mM MOPS (pH 7.0), 1.5 mM NaN_3, 1 mM DTT and 50 μM $CaCl_2$; the resulting solution was dialyzed against the same solvent at 2°C. After sufficiently depolymerizing the actin, the solution was ultracentrifuged again. Sephadex G25 (fine) was used for final removal of a trace amount of free dye. About 55% of actin was labeled. The critical concentration for polymerization of labeled actin was slightly higher than that of unlabeled actin.

Examination of actin binding to nebulin in myofibrils

To examine the binding of actin to the portion of nebulin that had been dissociated from actin filaments as a result of the gelsolin treatment of

myofibrils, fluorescence dye-labeled F-actin (0.5 mg/ml) was added to skeletal and cardiac myofibrils in a rigor (−Ca) solution containing 4 mM ADP. Free ATP in the F-actin solution was removed as much as possible by hydrolyzing it with 0.2 mg/ml hexokinase (Sigma Chemical Co., St. Louis, MO) in the presence of 1 mM glucose. Within 10 s to 10 min after the addition of actin to the myofibrils, unbound actin was washed out with a rigor (−Ca) solution and the region into which labeled F-actin had been incorporated was examined by fluorescence and phase-contrast microscopy.

RESULTS

Sarcomere structure in RG-treated and CG-treated myofibrils

First, we examined how thin filaments were removed in the RG-treated and CG-treated myofibrils. Thin filaments of about 1 μm in length were present at both sides of the Z line in an untreated myofibril (Fig. 1 *a*). After the gelsolin treatment in an RG-solution, only the portion of the thin filament located at the I band had been removed (note the dark I band in Fig. 1 *b*), whereas the portion of the thin filament located at the A band remained intact (note the width of each fluorescent band in the doublet located at the center of each sarcomere in Fig. 1 *b*; see also Discussion; cf. Funatsu et al., 1990); in addition, short fragments remained at the Z line. To examine this myofibril model, the solution was finally exchanged for a rigor (−Ca) solution and then for a relaxing solution for each purpose. The RG-treated myofibril was further treated with gelsolin in a CG-solution. As a result, thin filaments other than the fragments at the Z line were removed (note that only the Z line in the I-Z-I brush is fluorescent in Fig. 1 *c*). The solution was finally exchanged for a relaxing solution.

Second, we examined whether nebulin was exposed at the I band in the RG-treated myofibril. If exposed nebulin is present at the I band, exogenous F-actin may bind to that exposed portion, because *in vitro* experiments have shown that a part of nebulin molecule binds to F-actin (Jin and Wang, 1991; Chen et al., 1993; Pfuhl et al., 1994). Fig. 2 demonstrates the binding of rhodamine-labeled F-actin to the I band region of the RG-treated skeletal myofibril (Fig. 2 *a*). This binding did not occur in the RG-treated cardiac myofibril (Fig. 2 *b*). Fig. 2 *c* confirms that the portion of the thin filament located at the I band was selectively removed from cardiac myofibrils, as is essentially the case in skeletal myofibrils (cf. Fig. 1 *b*). Rhodamine-labeled G-actin did not bind to the RG-treated myofibrils under low salt, nonpolymerizable conditions (data not shown). On the other hand, such binding of F-actin was not observed in untreated myofibrils for either skeletal or cardiac muscles (data not shown; for skeletal myofibrils see Ishiwata and Funatsu, 1985). These results suggest that exposed nebulin is present in skeletal muscle after RG-treatment.

Third, we examined whether nebulin connects the Z line and the portion of the thin filament remaining as fragments at the A band in the RG-treated myofibril. If nebulin does form a connection, the thin filament fragments at the A band should move with extension of the sarcomere under relaxing conditions, whereas it would not be expected to move under rigor conditions. Fig. 3 *a–c* show that under rigor conditions, the bright doublets corresponding to the free ends of thin filaments observed on a fluorescence micrograph (Fig. 3, *b* and *c*) did not change their position when sarcomere length was extended from 2.76 μm (Fig. 3 *b*) to 3.06 μm

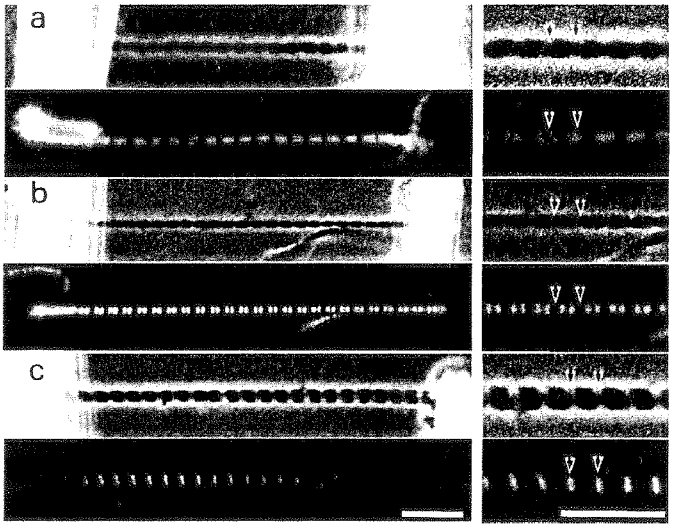

FIGURE 1 Optical micrographs of myofibrils before and after gelsolin treatment. Actin filaments were visualized by rhodamine-phalloidin staining after formaldehyde fixation. (*a*) Untreated myofibril; (*b*) myofibril treated with gelsolin in an RG-solution; (*c*) myofibril further treated with gelsolin in a CG-solution. All procedures were done at room temperature. The upper and lower parts of each figure are phase-contrast and fluorescence micrographs, respectively. Enlarged figures are shown on the right. The reason why the fluorescence intensity of the Z line in *c* looks much greater than that in *b* is that the exposure time to take the photograph of *c* was longer than that of *b*. Also, it is to be noted that the appearance of the A band in phase-contrast micrograph differs depending on the position of focal plane (cf. *b* and *c*). Arrows indicate the positions of the Z lines. Uniform sarcomere length (L) were maintained even after the gelsolin treatment and stretching of myofibrils (SD of L was less than 1% of the average L in the examples shown here). Scale bars, 10 μm.

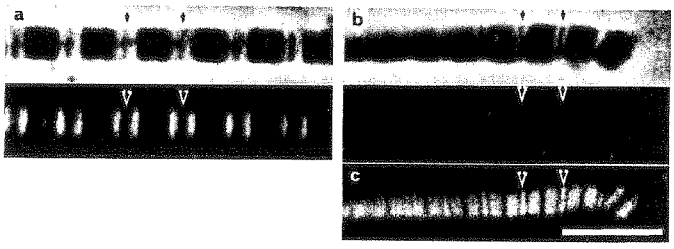

FIGURE 2 Optical micrographs of RG-treated myofibrils of skeletal and cardiac muscle. Rhodamine-labeled F-actin (0.5 mg/ml, without ATP) was added to an RG-treated myofibril of skeletal muscle (*a*) or cardiac muscle (*b*) in a rigor (−Ca) solution. As a reference, the RG-treated cardiac myofibril was stained with rhodamine phalloidin after formaldehyde fixation (*c*, the same myofibril as in *b*). The upper and lower parts of *a* and *b* are phase-contrast and fluorescence micrographs, respectively, and *c* is a fluorescence micrograph. All procedures were done under a microscope, without holding the ends of myofibrils, at room temperature. The I band width in the cardiac myofibril is small because the slack sarcomere length is short. The fluorescence pattern obtained in *a* was essentially the same even at shorter I band width. Arrows indicate the positions of the Z lines. Scale bar, 5 μm.

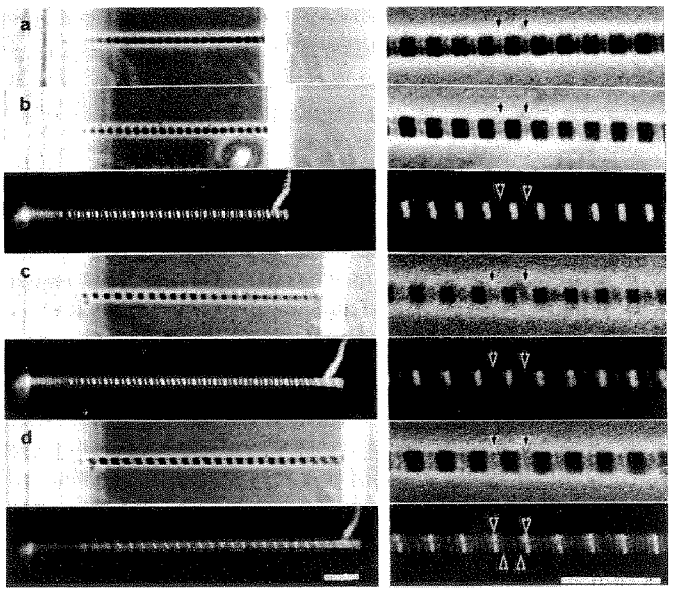

FIGURE 3 Optical micrographs showing the effects of extension on RG-treated myofibrils under rigor and relaxing conditions. The free ends of thin filaments and the Z line were visualized by rhodamine-phalloidin staining without formaldehyde fixation. (*a*) Untreated myofibril (average sarcomere length (*L*), 2.65 μm); (*b*) myofibril of *a* after gelsolin treatment in an RG-solution (*L*, 2.76 μm); (*c*) myofibril of *b* that had been stretched to an *L* of 3.06 μm in a rigor (−Ca) solution and then (*d*), the rigor (−Ca) solution was exchanged for a relaxing solution containing BDM (*L*, 3.14 μm). All procedures were done at room temperature. The upper and lower parts of each figure are phase-contrast and fluorescence micrographs, respectively. The fluorescence micrograph of *a* was omitted because it was essentially the same as that of *b*. Enlarged figures are shown on the right. Arrows pointing from the upper sides of myofibrils indicate the positions of the Z lines. Both the central fluorescent doublet (*b* and *c*) and the quartet (*d*) in each sarcomere correspond to the free ends of thin filaments. Arrows pointing from the lower side of the myofibril in *d* indicate the outer pair of quartet bands originating from the central doublet of *c*. Scale bars, 10 μm.

(Fig. 3 *c*). That is, the free ends of thin filaments did not move and only the I band was elongated.

The average separation between a pair of doublets across the Z line, i.e., the apparent length of the I-Z-I brush, increased from 2. 24 to 2.55 μm, suggesting that the I band had been elongated by 0.16 (=(2.55 − 2.24)/2)μm. On the other hand, the I band width was 0. 58 (=(2.76 − 1.6)/2) μm before extension and 0.73 (=(3.06 − 1.6)/2) μm after extension, where the A band width was assumed to be 1.6 μm. From these values, the extent of elongation of the I band was calculated to be 0.15 (= 0.73 − 0.58) μm, consistent with the above value, i.e., 0.16 μm. Because the sarcomere length was 2.65 μm and the I band width was 0.52 μm before RG-treatment (Fig. 3 *a*), the I band was stretched by about 40% (=(0.73 − 0.52)/0.52) all together after the RG-treatment.

Accompanying the exchange of the rigor solution for a relaxing one, the doublet bands (Fig. 3 *c*) were split into four, i.e., a quartet (Fig. 3 *d*); an inner pair of bands was located in the central portion, and an outer pair was located near the Z line (cf. *bottom arrows* in Fig. 3 *d*) in each sarcomere. The fluorescence intensity showed that the proportion of inner and outer bands was about 1. Fig. 3 *d* illustrates the attained sarcomere length of 3.14 μm, slightly longer than that shown in Fig. 3 *c*; the average separation between the inner bands across the Z line was 2.55 μm, nearly the same as that shown in Fig. 3 *c*, whereas the average separation between the outer bands across the Z line was 1.43 μm, much shorter than the above. The latter result strongly suggests that at least about half of the thin filament fragments remaining at the A band are connected to the Z line through an elastic body, probably nebulin, and that nebulin shrinks as cross-bridges are detached in a relaxed state in the presence of BDM. We noticed that the outer pair of bands could not be observed in the relaxing solution without BDM, suggesting that at room temperature a small number of cross-bridges were still attached.

We interpret the above results as summarized schematically in Fig. 4. The fine structures of sarcomeres in RG-treated (cf. Figs. 1 *b* and 3, *b* and *c*) and CG-treated (Fig. 1 *c*) myofibrils correspond to those shown in Fig. 4, *b*, *c*, and *e*, respectively (for further detail, see Discussion). Under rigor conditions, the portions of thin filaments located at the A band remain intact as fragments maintaining rigor cross-bridges (Fig. 4 *b*). On stretching of the RG-treated myofibril, only the I band is elongated (Fig. 4 *c*). Accompanying re-

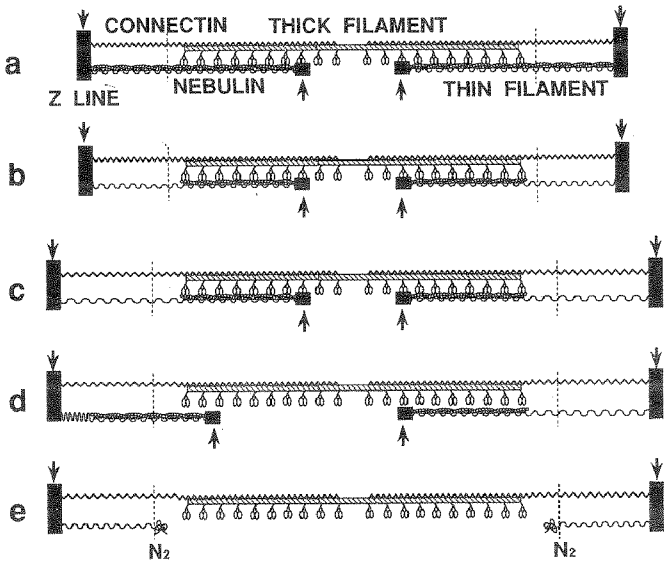

FIGURE 4 Schematic illustration showing the assumed filament structure of a sarcomere before and after gelsolin treatment. (*a*) Untreated sarcomere before gelsolin treatment; the fine structures of thick and thin filaments together with connectin (titin) and nebulin are depicted schematically. (*b* and *c*) RG-treated sarcomere under rigor conditions; because of the gelsolin treatment in an RG-solution, the portions of thin filaments located at the I band have been removed, so that a portion of each nebulin molecule is expected to be exposed (*b*) and with sarcomere stretching (*c*) only the I band is elongated without movement of the thin filament fragments remaining at the A band. (*d*) RG-treated sarcomere under relaxing conditions; the remaining fragments of thin filaments move to the Z line (*left* half) or stay as in *c* (*right* half) depending on whether the exposed portion of the nebulin molecule shinks. (*e*) CG-treated sarcomere; thin filaments are removed by further treatment of *c* with gelsolin under contracting conditions, so that the nebulin is free of actin filaments. Portions of the free ends of nebulin appear to be folded and have become entangled at the N_2 line (cf. Funatsu et al., 1990). Dashed lines indicate the approximate position of the N_2 line. Arrows indicate the position at which rhodamine-phalloidin staining occurs without chemical fixation.

laxation, as illustrated in the left half of Fig. 4 *d*, a portion of the thin filament fragments moves to the Z line, forming the outer pair of fluorescent bands (cf. Fig. 3 *d*); another portion barely moves at all, as illustrated in the right half of Fig. 4 *d*, forming the inner pair of fluorescent bands (cf. Fig. 3 *d*).

Here we present another piece of data consistent with the above structure of the gelsolin-treated sarcomere illustrated in Fig. 4. Fig. 5 is an example showing the time course of the tension development in an RG-treated myofibril that occurred as a result of CG-treatment. The active tension developed at the initial peak was nearly one-tenth of the tension developed under normal contracting condition with Ca^{2+}. This degree of active tension could not be eliminated even when the RG-treatment was prolonged; the exposed nebulin connecting the thin filament fragment and the Z line is considered to be responsible for the transmission of this active tension generation.

Time course of tension development with the extension of RG-treated myofibrils and viscoelastic analysis

We measured the tension passively developed accompanying the extension of myofibrils under various conditions. Fig. 6 shows an example of the time course for development of the passive tension in an RG-treated myofibril under rigor (−Ca) conditions. Tension increased abruptly with extension, decayed in an exponential manner with a relaxation time of about 10 s, and reached a steady state within about 60 s. Such properties were unchanged in CG-treated and untreated myofibrils under relaxing conditions, although the relaxation times were different. On the other hand, the tension response in an untreated myofibril under rigor conditions immediately reached a steady state without decay (data not shown).

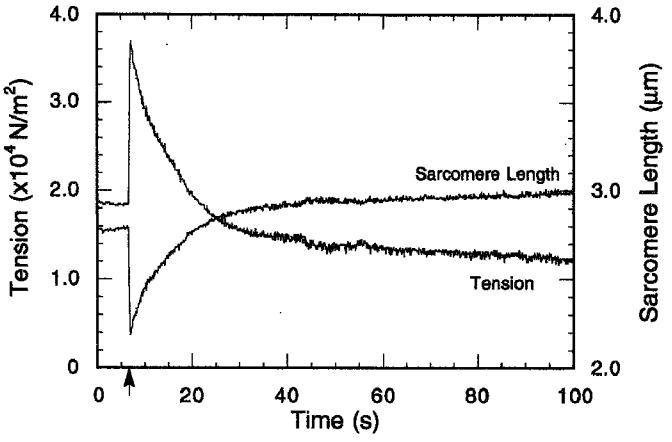

FIGURE 5 Time course of active tension development and sarcomere length change in an RG-treated myofibril accompanying CG-treatment. First, the myofibril treated with RG-solution at an average sarcomere length of 2.47 μm was stretched to 2.79 μm, so that the rigor tension was developed. Then, the solution was exchanged for CG-solution (see *arrow*). Active tension developed quickly increasing from 1.86×10^4 N/m² to a peak of 3.71×10^4 N/m²(sarcomere length, 2.2 μm) within 0.6 s. After the tension had risen to the peak level, it decreased exponentially to a level of 1.4×10^4 N/m² (sarcomere length, 3.0 μm). The myofibril used here is the same as that shown in Fig. 7. In this case, no feedback control was used, so that the myofibril length changed in accordance with the tension change. Hooke's elastic constant of the flexible glass micro-needle was 0.57 μg/μm.

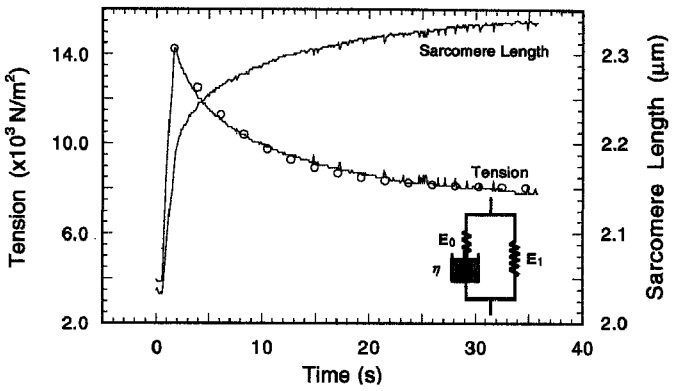

FIGURE 6 Time course of passive tension development with extension of an RG-treated myofibril in a rigor (−Ca) solution. In this example, an RG-treated myofibril was stretched so that the average sarcomere length quickly changed from 2.03 μm to 2.19 μm together with a tension change from 3.8×10^3 N/m² to 14.3×10^3 N/m². When the tension had decreased to a steady level, the average sarcomere length was 2.33 μm; the steady tension at this sarcomere length, 7.8×10^3 N/m², has been plotted in Fig. 7. The ordinate, tension (N) per unit cross section (m²) of myofibrils of which the cross sectional area (1.8×10^{-12} m²) was estimated from the average width of a myofibril assuming a circular cross section. Hooke's elastic constant of the flexible glass micro-needle was 0.22 μg/μm. (*inset*) Visco-elastic model representing each half sarcomere used for describing the time course of tension decay, which is composed of two Hookean springs (E_0 and E_1) connected in parallel and a viscous element (η) connected to a spring (E_0) in series. A best-fit result is superimposed on the experimental result with open circles.

We estimated the elastic modulus of nebulin based on the assumption that a viscoelastic model composed of viscous and elastic elements shown in the insert of Fig. 6 represents each half sarcomere; at this sarcomere length, shorter than 2.5 μm, the contribution of connectin (titin) is considered to be negligible (see Discussion). The time course of tension decay after stretch is described as follows:

$$\frac{(\text{passive tension})}{S}\ (\text{in units of N/m}^2) = \frac{\frac{E_1 \cdot X_0}{n}}{1+\frac{E_1 \cdot S}{n \cdot k}} + \frac{\frac{E_0 \cdot X_0}{n}}{\left(1+\frac{(E_0+E_1)\cdot S}{n \cdot k}\right)\cdot\left(1+\frac{E_1 \cdot S}{n \cdot k}\right)} \cdot \exp\left[-\frac{1+\frac{E_1 \cdot S}{n \cdot k}}{1+\frac{(E_0+E_1)\cdot S}{n \cdot k}} \cdot \frac{E_0}{\eta} \cdot t\right], \quad (1)$$

where S is the cross sectional area of myofibril, X_0 is the displacement of the rigid micro-needle, E_0 and E_1 are (elastic moduli)/S, η is (a viscous coefficient of dashpot)/S, n is a number of half-sarcomeres connecting in series in the myofibril, and k is Hooke's elastic constant of the flexible micro-

needle. The values of E_1 and E_0 were estimated from the final plateau level and initial peak of tension, respectively, whereas the value of η was estimated from the decay rate (cf. Fig. 6). The best result was obtained in Fig. 6 by setting the values of E_0, E_1, and η at 2.8×10^4 N/m^2, 5.7×10^3 N/m^2, and 2.3×10^5 N · s/m^2, respectively.

If the cross sectional area per a single thin filament of a myofibril is assumed to be 7×10^{-16} m^2 (center-to-center distance between thick filaments, 40 nm), the E_0, E_1, and η values per thin filament are estimated to be 20 pN, 4.0 pN, and 17 pN · s, respectively. If two nebulin molecules are bound to one thin filament (this is still speculative), the values of these parameters for a single nebulin molecule become half of the above values.

Tension versus extension relation of myofibrils under various conditions

Passive tension development was examined with stepwise stretching of myofibrils under various conditions. Fig. 7 depicts typical examples of tension versus extension relations for an untreated myofibril under rigor (−Ca) and relaxing conditions (±BDM), for an RG-treated myofibril under rigor (−Ca) conditions and for a CG-treated myofibril under relaxing conditions (−BDM). A steady level of tension was measured after stepwise stretching of myofibrils starting from a slack sarcomere length to longer sarcomere lengths

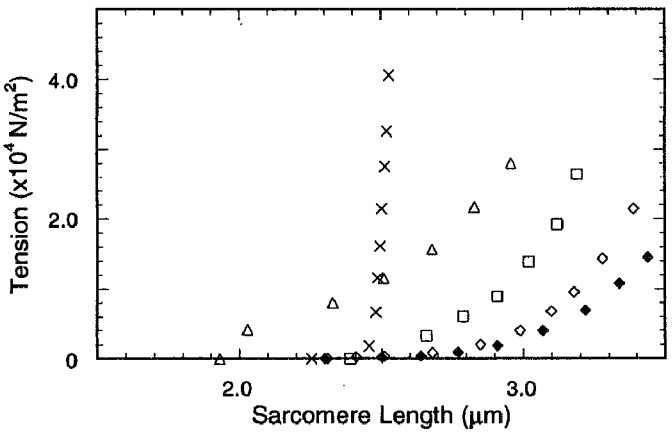

FIGURE 7 Passive tension versus extension relation of myofibrils under various conditions before and after gelsolin treatment (cf. Figs. 1, 3, and 4). First, an untreated myofibril at an average sarcomere length of 2.47 μm (L_0) was gradually extended in a rigor (−Ca) solution, and the tension was measured (×); after returning to the initial sarcomere length (L_0), it was treated with gelsolin in a rigor (+Ca) solution (RG-treated myofibril; cf. Figs. 1, 3, and 4), and the passive tension was measured stepwise (△) in a rigor (−Ca) solution starting from a slack length at which there was no tension, L_R (about 1.93 μm in this case); the RG-treated myofibril was further treated with gelsolin in a contracting solution after returning to L_0 (CG-treated myofibril; cf. Figs. 1, 3, and 4) and the passive tension was measured stepwise (□) in a relaxing solution without BDM starting from a slack length, L_S (about 2.38 μm in this case). As a control, the passive tension of an untreated myofibril was also measured in a relaxing solution without (◇) and with (◆) BDM by using a different specimen. The tension at a steady state (cf. Fig. 6) was plotted at each sarcomere length (L) after the extension.

plotted on the abscissa. As shown in Fig. 7, the developed passive tension of untreated myofibrils in a relaxing solution containing 20 mM BDM was smaller than that observed in the absence of BDM. This suggests that some fraction of the cross-bridges were still attached in the relaxing solution without BDM at room temperature.

The shape of almost all curves was concave except in RG-treated myofibrils, for which the curve was convex at shorter sarcomere length. The slack sarcomere length, at which the tension disappears, was shortest in an RG-treated myofibril (L_R). Tension developed spontaneously as a consequence of RG-treatment, suggesting that an elastic body, probably nebulin, shrinks in response to removal of the portion of the thin filament located at the I band. This is consistent with the formation of the outer fluorescent doublet in the quartet, as described in Fig. 3 *d* (see Discussion).

After complete removal of the thin filaments by CG-treatment, the tension versus extension relation became concave and resembled that of an intact myofibril under relaxing conditions. This result is consistent with a previous result obtained using a single muscle fiber (Funatsu et al., 1990). A slight difference between the present and previous results is that greater tension development was observed in this study, although the extent of the shift in slack length (L_S) to the left (from about 2.5 to 2.4 μm in this example) was similar. The difference became larger as the transient tension development and the shortening of sarcomeres were increased with CG-treatment (cf. Fig. 5). To minimize this effect, shortening of myofibrils was suppressed to some extent by feedback control with a piezo element when the solution was exchanged from an RG-solution to a CG-solution.

Tension versus extension relation of an RG-treated myofibril

To study the elastic properties of nebulin of various lengths, RG-treated myofibrils were prepared under different conditions of sarcomere length (L_0). The use of this procedure allows the length of the exposed portion of nebulin to be controlled according to the assumed filament structure of the RG-treated myofibril (cf. Fig. 4, *b* and *c*). The length of the exposed portion of nebulin was estimated by $(L_0 - L_A)/2$, where L_A is an A band width (cf. Fig. 4). Fig. 8 *a* shows five examples thus obtained, corresponding to five different L_0 (indicated by *arrows*), i.e., 2.25, 2.31, 2.47 (the same as in Fig. 7), 2.47, and 2.72 μm, and the slack lengths (L_R) were 1.76, 1.90, 1.93 (the same as in Fig. 7), 1.98, and 2.11 μm, respectively. The data were reproducible within this range of sarcomere lengths (L) less than 3.2 μm.

The relative tension versus extension relation was replotted against the assumed natural length of the exposed portion of nebulin, i.e., $(L_R - L_A)/2$, at which length the stress of nebulin is expected to disappear. The results summarized in Fig. 8 *b* show that all relations, except at large λ, overlap with each other; the overlapping region was extended if the contribution of resting tension, which appeared at $L > 2.5$ μm (cf. Fig. 7), was simply subtracted.

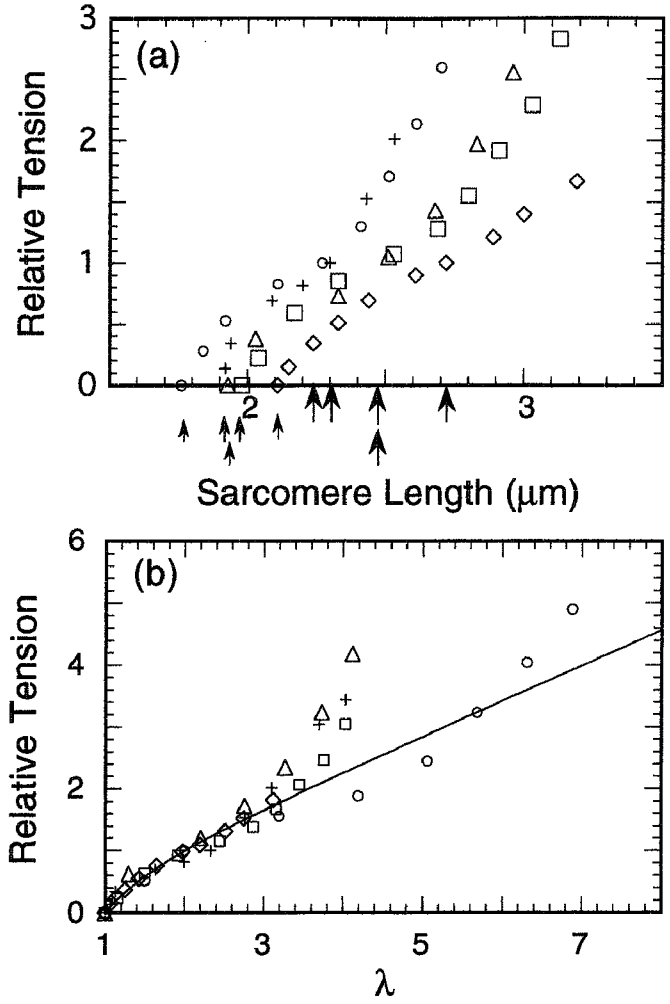

FIGURE 8 Passive tension versus extension relation of RG-treated myofibrils in a rigor (−Ca) solution. (*a*) RG-treated myofibrils (cf. Figs. 1, 3, and 4) were prepared at average sarcomere length (L_0) of 2.25 (○), 2.31 (+), 2.47 (△, □), and 2.72 (◇) μm, as indicated by the large arrows. (△) A replot of Fig. 7. Relative tension was obtained by normalizing the tension against that developed at the initial sarcomere length (L_0) at which the gelsolin treatment was done. Measurement procedures, the same as in Fig. 7. (*b*), in the relative tension versus extension relation obtained in *a*, the sarcomere length was first replotted against $(L - L_A)/(L_R - L_A) = \lambda$, where L is a variable sarcomere length, L_A a thick filament length (assumed to be 1.6 μm) and L_R is the slack sarcomere length, which differs among myofibrils as indicated by small arrows (1.76 (○), 1.90 (+), 1.93 (△), 1.98 (□), and 2.11 (◇) μm); each tension curve was further normalized by the relative tension at $\lambda = 2$. A thin line represents $(4/7)(\lambda - 1/\lambda^2)$, a normalized equation describing rubber elasticity.

Homogeneity and constancy of sarcomeres during extension

Fig. 9 is an example of an image profile from phase-contrast micrograph of an untreated myofibril (Fig. 9 *a*), an RG-treated myofibril (Fig. 9 *b–d*), and a CG-treated myofibril (Fig. 9 *e*). Neither over-stretched nor over-shortened sarcomeres could be observed. In this example, the SD of sarcomere lengths in each myofibril was about 2% of the average sarcomere length (cf. in an example shown in Fig. 1, SD was less than 1%). This sarcomere homogeneity was maintained throughout the present experiments.

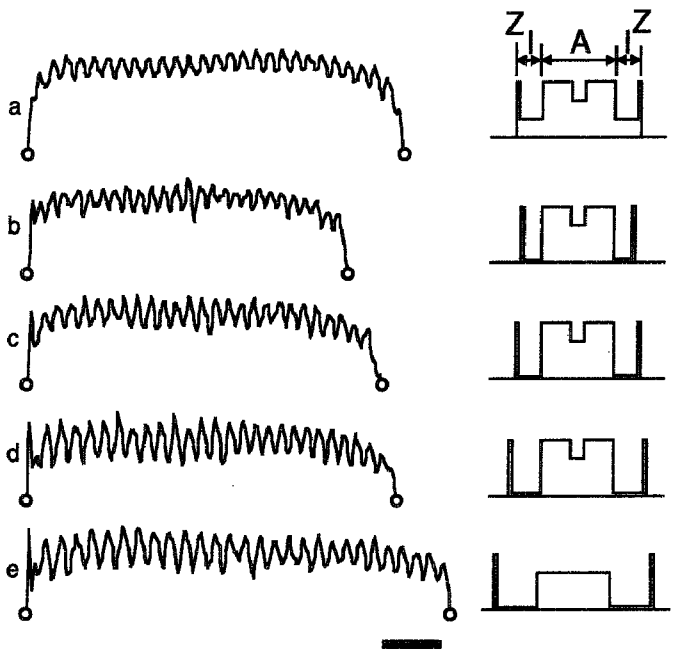

FIGURE 9 Image profile of a myofibril obtained by phase-contrast microscopy. The horizontal and vertical axes represent the position along a myofibril and darkness of the phase-contrast image, respectively. The two circles on either side correspond to the inner edges of the micro-needles. A peak and a valley of the image profile correspond to the center of the A band and the Z line, respectively (the Z line is not clear because of the low resolving power of the objective lens used here (Plan 60 × DM, Nikon)); the density profile of each sarcomere is schematically illustrated at the right-hand side. (*a*) Untreated myofibril in a rigor (−Ca) solution (L (average sarcomere length) = 2.50 μm); (*b–d*), the RG-treated myofibril was stretched stepwise in a rigor (−Ca) solution (L = 2.24 (*b*), 2.46 (*c*), and 2.69 (*d*) μm; SD of L was at most 2% of L); (*e*) the CG-treated myofibril in a relaxing solution (L = 3.16 μm; the number of sarcomeres, 29). Here, we have shown an example in which the number of sarcomeres between the inner edges of micro-needles increased from 25 to 27 on extension of a myofibril; when firmly adhering to a glass surface, the number of sarcomeres did not change. For phase-contrast images and conditions, see Figs. 1 and 3. Scale bar, 10 μm.

DISCUSSION

Have we really succeeded in measuring the elastic modulus of nebulin?

The validity of the present work, especially the estimation of elastic modulus of nebulin, relies upon the assumption that a certain portion of nebulin is exposed in a manner such as that illustrated in Fig. 4 *b* after RG-treatment and that this exposed portion of nebulin is most compliant in the RG-treated myofibril. Our results provide evidence supporting this assumption. First, as Fig. 1 *b* demonstrates, the portion of the thin filament located at the I band was selectively removed; on the other hand, the portion of the thin filament located at the A band remained as fragment. Judging from the fluorescence intensity of the rhodamine phalloidin-labeled RG-treated myofibril (Fig. 1), actin filaments remaining at the I band were negligibly few in number. Even if actin filaments remained after the gelsolin treatment, they would have been destroyed by such massive extension, i.e.,

by several tens of % (cf. Figs. 3 and 7–9) because actin filaments are not sufficiently extensible so as to be capable of enduring a stretch of more than 10% (cf. Kishino and Yanagida, 1988). The possibility of persisting tropomyosin threads is also small, because tropomyosin and troponin actually diffuse out of muscle fibers (cf. Funatsu et al., 1990).

Furthermore, exogenous F-actin attached to the I band in skeletal muscle after RG-treatment, whereas it did not in cardiac muscle in which nebulin is absent (Fig. 2). We confirmed as previously reported, as a control, that in an untreated muscle exogenous F-actin did not bind to the I band (cf. Ishiwata and Funatsu, 1985). The nebulin molecule is now considered to be located along an actin filament, in a side-by-side fashion, over its entire region from the free end of a thin filament to the Z line (cf. Wang and Wright, 1988; Wright et al., 1993). It is thus probable that the portion of nebulin located at the I band was dissociated from an actin filament and thereby exposed.

A third piece of evidence supporting our assumption that the actual elasticity of nebulin was measured is that only the I band was uniformly elongated on stretching RG-treated myofibrils (cf. Figs. 3 *c* and 9 *b–d*). This indicates that the I band is the most extensible (compliant) component of a gelsolin-treated sarcomere structure, such that the elastic modulus estimated herein can be ascribed primarily to the elastic structure located at the I band.

Fourth, the mechanical connection between the thin filament fragments that remained at the A band and the Z line was demonstrated by the following results. (1) An atypical tension versus extension relation, especially in regards to tension development, was obtained under rigor conditions for RG-treated myofibrils at the sarcomere lengths at which the gelsolin treatment was done and, in addition, where the contribution of connectin (titin) was negligibly small because of the reason discussed below and judging from the fact that the slack sarcomere length of untreated and CG-treated myofibrils is about 2.5 μm (Fig. 7) longer than that of RG-treated ones (Fig. 8 *a*). (2) Active tension, nearly one-tenth of the tension obtained under normal contracting condition, was produced transiently in association with CG-treatment of RG-treated myofibrils (Fig. 5). There is no possibility that 10% of the thin filaments were intact at that point because the I band was elongated by 40% under rigor conditions before the CG-treatment as described above.

Fifth, as shown in Fig. 3, although the fluorescent doublets that represent the free ends of the thin filament fragments did not move with stretching of the sarcomere in a rigor solution, about a half of them did move to the Z line as soon as the solution was exchanged for a relaxing one containing BDM. The distance between the outer fluorescent band and the Z line observed in Fig. 3 *d* (1. 43/2 μm) just corresponded to (the length of the thin filament fragments remaining at the A band (about 0.5 μm)) + (the assumed natural length of the exposed portion of the nebulin (about 0.2 μm; cf. Fig. 8) at a sarcomere length of 2.65 μm). This correspondence strongly suggests that the exposed portion of the nebulin shrinks to its assumed natural length.

Sixth and finally, we should examine a possibility that the exposed portion of nebulin is entangled with the elastic filaments in the RG-treated myofibrils. The passive tension versus extension relation shown in Figs. 7 and 8 may be explained by assuming that the exposed portion of nebulin is collapsed onto a portion of connectin (titin) filaments so as to make it shorter and nonextensible. As a result of the shortened length of the extensible segment, the slack sarcomere length may shift toward the shorter one. But, because the entanglement is not considered to be released by the CG-treatment, the shortened slack length should remain unchanged after the CG-treatment. Fig. 7 shows that this is not the case.

Alternatively, there remains a possibility that the exposed portions of nebulin themselves are entangled with each other in the RG-treated myofibrils. In this case, the shortened slack length may be reversibly returned to the original length after the CG-treatment, because all of the thin filament fragments remaining at the A band are removed by the CG-treatment (cf. Fig. 4 *e*). If such entanglement occurs, the value we estimated puts an upper limit on the elastic modulus of nebulin.

Thus, we conclude that the elastic properties of the exposed portion of nebulin could be studied under a situation such as that illustrated in Fig. 4 *b*.

At present, it is important to ascertain what proportion of nebulin was preserved intact after the gelsolin treatment. First, we can point out that our previous SDS-PAGE studies on single muscle fibers showed that at most 25% of nebulin was removed, probably by proteolysis, leaving more than 75% of nebulin intact, after the CG-treatment (see Fig. 1 in Funatsu et al., 1990, 1993). The duration of gelsolin treatment was much shorter in the present study than that utilized in the previous studies, although the temperature was higher. There is a report showing that nebulin is fragmented by 0.1 mM Ca^{2+} (Tatsumi and Takahashi, 1992), but this effect can be neglected, because nebulin from the rabbit psoas muscle is reported to be stable for up to one day of incubation and the duration of Ca^{2+} incubation in the present study was short (less than 1 h in total).

Even if nebulin was not digested by proteolysis, the possibility remains that one end of the nebulin molecule was detached from the Z line. We estimate that at least half of the thin filament fragments located at the A band are mechanically attached to the Z line through the exposed portion of nebulin, based on the fluorescence intensity distribution of the quartet shown in Fig. 3 *d*.

Thus, although there is a possibility that the elastic modulus of nebulin given in Results is an underestimate, the extent of underestimation being within a 10-fold limit even when two to three factors of overestimation of the cross sectional area of a myofibril are taken into account.

Contribution of nebulin to the elasticity of thin filaments

If nebulin attaches to a thin filament only at the free end of the thin filament and the Z line, the entire length of nebulin will be extended even in RG-treated myofibrils irrespective of the extent of thin filament removal, so that the slack length (L_R) should be independent of the length of the portion of the thin filaments removed. The fact that L_R decreased with the decrease in L_0 (Fig. 8 *a*) suggests that nebulin is attached to an actin filament in a side-by-side fashion between about 0.3 and 0.6 μm from the Z line. Also, the fact that the convex curves obtained at different L_0 overlapped each other after normalization (Fig. 8 *b*) suggests that the exposed portion of nebulin is mechanically uniform, at least, at the I band region we examined (up to 0.6 μm from the Z line).

The static elastic modulus, E_1, of the exposed portion of nebulin, i.e., E_1 per thin filament, was also estimated from the slope of the tension versus extension relation at L_0 (before normalization in Fig. 8 *a*) to be 10.3 ± 7.6 (SD for $n = 5$) pN (=(10.3 ± 7.6) × 10^{-3} pN/nm for the 1 μm long exposed portion of nebulin); this value was essentially the same as the E_1 (4.0 pN) obtained in Fig. 6. Thus, the static elastic modulus of the exposed portion of nebulin is apparently 2 × 10^3 times smaller than that of an actin filament, which is estimated to be about 2 × 10^4 pN (=20 pN/nm for an actin filament 1 μm long and 2 nm in the effective radius of cross section) (cf. Fujime, 1987; Higuchi et al., 1993). If we take into account the possibility that the elastic modulus of nebulin thus obtained is a 10-fold underestimate, as considered above, the actual elastic modulus of nebulin should be 10 times larger than that estimated here. It is still, however, 2 × 10^2 times smaller than that of an actin filament. Thus, we conclude that nebulin, at least the portion of the molecule located within about 0.6 μm of the Z line, does not contribute to the static elastic modulus of thin filaments in muscle.

This conclusion may raise questions because the amino acid sequence suggests that nebulin is composed of an α-helix (Labeit et al., 1991; Pfuhl et al., 1994) and the elastic modulus of a single α-helix is estimated to be 2 × 10^3 pN (=2 pN/nm for α-helix (PBLG) 1 μm long; cf. Higuchi et al., 1993), several tens times larger than that estimated for nebulin in the present work. If nebulin is composed entirely of α-helix, such a low stiffness would not be expected. Our results suggest that nebulin is not composed entirely of α-helix.

Possible reasons for the convex relation between tension and extension in RG-treated myofibrils

There are at least two plausible quantitative explanations for the convex tension (K) versus extension relation obtained in RG-treated myofibrils (Figs. 7 and 8): (1) rubber elasticity due to cross-link formation among elastic filaments, and (2) a conformational change of nebulin between two states having different equilibrium length.

First, the curve can be partly simulated by an equation describing the rubber elasticity: $K = C(\lambda - 1/\lambda^2)$, where C is a constant containing an absolute temperature and λ is the relative degree of extension defined in Fig. 8. As shown by the master curve depicted in Fig. 8 *b*, the initial monotonous rising phase of the curves ($\lambda < 3$) can be simulated by the above equation taking C as 1.0 × 10^3 (*open circles*), 6.3 × 10^3 (*crosses*), 4.3 × 10^3 (*triangles*), 2.9 × 10^3 (*squares*), and 1.3 × 10^4 (*diamonds*) (N/m^2). The rubber elasticity requires cross-linking among elastic filaments and a constant myofibril volume. This appears to be analogous to a model of connectin (titin) configuration in cardiac muscle suggested by Funatsu et al. (1993). However, in the above discussion, we have excluded a possibility that exposed portion of nebulin gets entangled in connectin (titin) in the RG-treated myofibrils. Therefore, in the future, we should examine another possibility that the exposed portions of nebulin themselves are entangled with each other.

Second, the convex curve was similar to that obtained for wool (Speakman, 1927). Therefore, an alternative explanation would be that nebulin is composed of many structural units, each of which can exist in two states having different equilibrium lengths. When released from actin filaments, a structural unit with a shorter equilibrium length is assumed to be more stable than a longer one, so that extra tension appears spontaneously at L_0. A comparable idea was successfully applied to keratin molecules (for experimental work, cf. Astbury and Woods, 1933; for a theoretical model, cf. Kubo, 1965). The theoretical model was recently adopted by Oda and Go to explain the elastic properties of connectin (titin) (Oda and Go, 1992). It can simulate exactly the curve obtained for an RG-treated myofibril (Fig. 8) over its entire length (even $\lambda > 3$) if appropriate parameter values are selected (cf. Fig. 7 in Oda (1993)). This explanation is consistent with the assumed filament structure illustrated in Fig. 4, *c* and *d*. To clarify this problem, the fine structure of exposed nebulin at its natural and slack length should be determined in the future.

Resting tension and elastic properties of connectin (titin)

In the present study, we confirmed a previous result indicating that the tension versus extension relation of CG-treated single fibers is similar to the resting tension versus extension relation of intact fibers (Funatsu et al., 1990). The absolute value of resting tension itself was similar to that obtained in previous studies; e.g., 1.4 × 10^4 N/m^2 at $L = 3.4$ μm in an example shown in Fig. 7 (cf. Moss and Halpern, 1977; Magid et al., 1984; Magid and Law, 1985; Bartoo et al., 1993). Compared with our previous results (compare Fig. 7 with Fig. 7 in Funatsu et al., 1990), the curve shifted to the upper left-hand side in the CG-treated myofibrils. This can probably be ascribed to a certain degree of damage, e.g., entanglement of the filaments produced in the lattice structure due to the shortening of, or active tension development in, sarcomeres during CG-treatment. Preliminary experiments showed that this transient shortening could be partially suppressed by the addition of BDM maintaining the isomet-

ric length of myofibrils, but it was difficult to suppress contraction completely at room temperature (lowering the temperature, however, is effective). Such damage may have been minimized in the fiber, because the gelsolin treatment was done at 2°C. In this respect, Takemori's (1991) observation that the resting tension of a skinned semitendinosus frog muscle increased gradually with contraction may be relevant, although he did not indicate clearly why this occurred.

The above situation may be clarified if we use cardiac muscle in which nebulin is absent; but, unfortunately, we have not yet succeeded in manipulating a cardiac myofibril using the same technique as that applied to a skeletal myofibril. In any case, however, we can conclude that resting tension is attributable primarily to connectin (titin) filaments, as previously reported (Funatsu et al., 1990).

We thank Prof. S. Fujime of Yokohama City University for valuable advice and critical reading of an early version of this article.
This work was supported in part by grants-in Aid for Scientific Research (No. 04402053 to S. Ishiwata) and for Scientific Research on Priority Areas (No. 04237228 and 05221234 to S. Ishiwata) from the Ministry of Education, Science and Culture of Japan.

REFERENCES

Anazawa, T., K. Yasuda, and S. Ishiwata. 1992. Spontaneous oscillation of tension and sarcomere length in skeletal myofibrils. Microscopic measurement and analysis. *Biophys. J.* 61:1099–1108.

Astbury, W. T., and H. J. Woods. 1993. X-ray studies of the structure of hair, wool, and related fibers. II. The molecular structure and elastic properties of hair keratin. *Phil. Trans.* 232:333–394.

Bartoo, M. L., V. I. Popov, L. A. Fearn, and G. H. Pollack. 1993. Active tension generation in isolated skeletal myofibrils. *J. Muscle Res. Cell Motil.* 14:498–510.

Chen, M.-J. G., Shih C.-L., and K. Wang. 1993. Nebulin as an Actin Zipper. A two-module nebulin fragment promotes actin nucleation and stabilizes actin filaments. *J. Biol. Chem.* 268:20327–20334.

Ebashi, S. 1991. Excitation-contraction coupling and the mechanism of muscle contraction. *Annu. Rev. Physiol.* 53:1–16.

Fujime, S. 1987. Sarcomeric element flexibility. *In* Optical Studies of Muscle Cross-bridges. R. J. Baskin and Y. Yeh, editors. CRC Press, FL. 149–188.

Funatsu, T., H. Higuchi, and S. Ishiwata. 1990. Elastic filament in skeletal muscle revealed by selective removal of thin filaments with plasma gelsolin. *J. Cell Biol.* 110:53–62.

Funatsu, T., E. Kono, H. Higuchi, S. Kimura, S. Ishiwata, T. Yoshioka, K. Maruyama, and S. Tsukita. 1993. Elastic filaments in situ in cardiac muscle: deep-etch replica analysis in combination with selective removal of actin and myosin filaments. *J. Cell Biol.* 120:711–724.

Granzier, H. L. M., and K. Wang. 1993. Passive tension and stiffness of vertebrate skeletal and insect flight muscles: the contribution of weak cross-bridges and elastic filaments. *Biophys. J.* 65:2141–2159.

Harris, H. E., and A. G. Weeds. 1984. Plasma gelsolin caps and severs actin filaments. *FEBS Lett.* 177:184–188.

Higuchi, H., Y. Nakauchi, K. Maruyama, and S. Fujime. 1993. Characterization of β-connectin (titin 2) from striated muscle by dynamic light scattering. *Biophys. J.* 65:1906–1915.

Horowits, R., and R. J. Podolsky. 1987. The positional stability of thick filaments in activated skeletal muscle depends on sarcomere length: evidence for the role of titin filaments. *J. Cell Biol.* 105:2217–2223.

Ishiwata, S., T. Anazawa, T. Fujita, N. Fukuda, H. Shimizu, and K. Yasuda. 1993. Spontaneous tension oscillation (SPOC) of muscle fibers and myofibrils. Minimum requirements for SPOC. *In* Mechanism of Myofilament Sliding in Muscle Contraction. H. Sugi and G. H. Pollack, editors. Plenum Publishing Corp., New York. 545–556.

Ishiwata, S., and T. Funatsu. 1985. Does actin bind to the ends of thin filaments in skeletal muscle? *J. Cell Biol.* 100:282–291.

Jin, J.-P., and K. Wang. 1991. Nebulin as a giant actin-binding template protein in skeletal muscle sarcomere: interaction of actin and cloned human nebulin fragments. *FEBS Lett.* 281:93–96.

Kishino, A., and T. Yanagida. 1988. Force measurements by micromanipulation of a single actin filament by glass needles. *Nature.* 334:74–76.

Kruger, M., J. Wright, and K. Wang. 1991. Nebulin as a length regulator of thin filaments of vertebrate skeletal muscles: correlation of thin filament length, nebulin size, and epitope profile. *J. Cell Biol.* 115:97–107.

Kubo, R. 1965. Statistical mechanics. An Advanced Course with Problems and Solutions. North-Holland, Amsterdam. 134 and 153–155.

Kurokawa, H., W. Fujii, K. Ohmi, T. Sakurai, and Y. Nonomura. 1990. Simple and rapid purification of brevin. *Biochem. Biophys. Res. Commun.* 168:451–457.

Labeit, S., T. Gibson, A. Kakey, K. Leonard, M. Zeviani, P. Knight, J. Wardale, and J. Trinick. 1991. Evidence that nebulin is a protein-ruler in muscle thin filaments. *FEBS Lett.* 282:313–316.

Magid, A., and D. J. Law. 1985. Myofibrils bear most of the resting tension in frog skeletal muscle. *Science.* 230:1280–1282.

Magid, A., H. P. Ting-Beall, M. Carvell, T. Kontis, and C. Lucaveche. 1984. Connecting filaments, core filaments, and side-struts: a proposal to add thee new load-bearing structures to the sliding filament model. *In* Contractile Mechanics in Muscle. G. Pollack and H. Sugi, editors. Plenum Publishing Corp., New York. 307–328.

Maruyama, K. 1986. Connectin, an elastic filamentous protein of striated muscle. *Int. Rev. Cytol.* 104:81–114.

Maruyama K., A. Matsuno, H. Higuchi, S. Shimaoka, S. Kimura, and T.Shimizu.1989. Behavior of connectin (titin) and nebulin in skinned muscle fibers released after extreme stretch as revealed by immunoelectron microscopy. *J. Muscle Res. Cell Motil.* 10: 350–359.

Moss, R. L., and W. Halpern. 1977. Elastic and viscous properties of resting frog skeletal muscle. *Biophys. J.* 17:213–228.

Natori, R. 1954. The property and contraction process of isolated myofibrils. *Jikeikai Med. J.* 1:119–126.

Nave, R., D. O. Fürst, and K. Weber. 1990. Interaction of α-actinin and nebulin in vitro: support for the existence of a fourth filament system in skeletal muscle. *FEBS Lett.* 269:163–166.

Oda, K. 1993. A model for generation of resting tension in connectin. Master's dissertation. Kyoto University, Kyoto, Japan.

Oda, K., and N. Go. 1992. A model on the mechanism of tension development in an elastic muscle protein, connectin. *Biophys. Suppl. (Jpn.).* 32:S197*a*. (Abstr.)

Pfuhl, M., S. J. Winder, and A. Pastore. 1994. Nebulin, a helical actin binding protein. *EMBO J.* 13:1782–1789.

Pieronbon-Bormioli, S., R. Betto, and G. Salviati. 1989. The organization of titin (connectin) and nebulin in the sarcomeres: an immunocytolocalization study. *J. Muscle Res. Cell Motil.* 10:446–456.

Ridgway, E. B., A. M. Gordon, and D. A. Martyn. 1983. Hysteresis in the force-calcium relation in muscle. *Science.* 219:1075–1077.

Robinson, T. F., and S. Winegrad. 1977. Variation in thin filament length in heart muscle. *Nature.* 267:74–75.

Small, J. V., D. O. Fürst, and L.-E. Thornell. 1992. The cytoskeletal lattice of muscle cells. *Eur. J. Biochem.* 208:559–572.

Speakman, J. B. 1927. The intracellular structure of the wool fiber. *J. Textile Inst.* 18:T431–T453.

Takahashi, K., A. Hattori, R. Tatsumi, and K. Takai. 1992. Calcium-induced splitting of connectin filaments into α-connectin and a 1,200-kDa subfragment. *J. Biochem. (Tokyo).* 111:778–782.

Takemori, S. 1991. Relaxation of resting tension after stretch of skeletal muscle fibers. *Biophys. Suppl. (Jpn.).* 31:S247*a*. (Abstr.)

Tatsumi, R., and K. Takahashi. 1992. Calcium-induced fragmentation of skeletal muscle nebulin filaments. *J. Biochem. (Tokyo).* 112: 775–779.

Trinick, J. 1992. Understanding the functions of titin and nebulin. *FEBS Lett.* 307:44–48.

Wang, K. 1985. Sarcomere-associated cytoskeletal lattices in striated muscle: reviews and hypothesis. *In* Cell and Muscle Motility, Vol. 6. J. W. Shay, editor. Plenum Publishing Corp., New York. 315–369.

Wang, K., R. McCarter, J. Wright, J. Beverly, and R. Ramirez-Mitchell. 1991. Regulation of skeletal muscle stiffness and elasticity by titin isomers: a test of the segmental extension model of resting tension. *Proc. Natl. Acad. Sci. USA.* 88:7101–7105.

Wang, K., R. McCarter, J. Wright, J. Beverly, and R. Ramirez-Mitchell. 1993. Viscoelasticity of the sarcomere matrix of skeletal muscles. The titin-myosin composite filament is a dual-stage molecular spring. *Biophys. J.* 64:1161–1177.

Wang, K., and J. Wright. 1988. Architecture of the sarcomere matrix of skeletal muscle: immunoelectron microscopic evidence that suggests a set of parallel inextensible nebulin filaments anchored at the Z line. *J. Cell Biol.* 107:2199–2212.

Whiting, A., J. Wardale, and J. Trinick. 1989. Does titin regulate the length of muscle thick filaments? *J. Mol. Biol.* 205:263–268.

Wright, J., Q.-Q. Huang, and K. Wang. 1993. Nebulin is a full-length template of actin filaments in the skeletal muscle sarcomere: an immunoelectron microscopic study of its orientation and span with site-specific monoclonal antibodies. *J. Muscle Res. Cell Motil.* 14:476–483.

Yasuda, K., T. Anazawa, and S. Ishiwata. 1992. Elastic properties of myofibrils studied by a microscopic system newly developed for tension analysis. *J. Muscle Res. Cell Motil.* 13:478*a*. (Abstr.)

Yin, H. L., and T. P. Stossel. 1979. Control of cytoplasmic actin gel-sol transformation by gelsolin, a calcium-dependent regulatory protein. *Nature.* 281:583–586.

Journal of Muscle Research Cell Motility
Vol. 16, 337-338 (1995) Abstr.

Imaging of mechanochemical coupling of muscle contractile system by pH-sensitive fluorescent dyes

H. KATO[1], M. KAWASE[1], T. NISHIZAKA[1], K. SOMEYA[1], G. MARRIOTT[2], K. KINOSITA JR[3] and S. ISHIWATA[1]

[1]*Department of Physics, School of Science and Engineering, Waseda University, Shinjuku-ku, Tokyo 169, Japan,* [2]*Abteilung Zellbiologie, Max Planck Institut für Biochemie, 8033 Martinsried bei München, Germany and* [3]*Department of Physics, Faculty of Science and Technology, Keio University, Kohoku-ku, Yokohama 233, Japan*

Study of mechanochemical coupling, i.e., the relation between chemical process of ATP hydrolysis and mechanical process such as sliding movement and tension development, is important for elucidating molecular mechanism of muscle contraction. In the present work, we tried to image ATPase activity under an optical microscope by using proper pH-sensitive fluorescent dyes which detect H^+ released accompanying ATP hydrolysis. The developed tension of single myofibrils was measured by using a microscopic technique manipulating single myofibrils prepared from glycerinated rabbit skeletal muscle fibres (Shimizu *et al., Biophys. J.* 61, 1087–98, 1992). First, by using SNAFL-phalloidin(Ph) which was synthesized in our laboratory, we attempted to measure and image local pH around actin filaments. The fluorescence intensity obtained at two different excitation wave lengths of SNAFL-Ph that was attached to thin filaments in myofibrils, changed in parallel with the change in pH of solvent. Second, we tried to synthesize and apply SNARF-Ph which seems to be suitable for so-called Double-View (W) microscopy (Kinosita *et al., J. Cell Biol.* 115, 67–73, 1991), because SNARF-Ph can be imaged at two different emission wave lengths. Finally, we found that free carboxy SNARF-1 (Molecular Probes Inc.) could be excited and imaged under the W-microscope by continuous excitation with YLF laser (wave length, 1053 nm) in two photon absorption manner. This technique has the advantage of detecting local fluorescence intensity even if free dyes exist in solvent. Now, we are trying to image both ATPase activity (local pH change) and mechanical properties of myofibrils under isometric and SPOC (cf. Ishiwata *et al., Adv. Biophys.* 27, 227–35, 1991) conditions with high space and time resolution by combining the above techniques.